Modulation of hERG Potassium Channels as Potential Therapeutic Targets in Breast Cancer

Submitted by Sara Al-Rawi
Bachelor Applied Science with Honours, Master of Science (Pharmacy)

A thesis submitted in total fulfilment
of the requirements for the degree of Doctor of Philosophy

July 2019

Department of Pharmacy and Applied Science
School of Molecular Sciences
College of Science, Health and Engineering
La Trobe University
Victoria
Australia

Contents

Acknowledgement

Statement of Authorship

Except where reference is made in the text of this thesis, this thesis contains no material published elsewhere or extracted in whole or in part from a thesis submitted for the award of any other degree or diploma.

This thesis includes work by the author that has been published or accepted for publication as described in the text. Except where reference is made in the text of the thesis, this thesis contains no other material published elsewhere or extracted in whole or in part from a thesis accepted for the award of any other degree or diploma.

No other person's work has been used without due acknowledgment in the main text of the thesis. This thesis has not been submitted for the award of any degree or diploma in any other tertiary institution.

_____

Sara Al-Rawi

05 July 2019

Abstract

Targeting hERG potassium channels in cancer therapy is an important avenue in cancer research since they are more highly expressed in many cancers. Two breast adenocarcinoma cell lines MCF-7 and MDA-MB-231 were used to investigate how NS1643 and six structurally similar, previously untested, urea and thio urea quinazolin-4-one compounds, altered hERG channel function and cancer progression.

Expression of hERG channels was confirmed in both lines with the KCNH2 antibody to be located on the mitochondrial, nuclear and endoplasmic reticulum membranes. All the compounds affected the membrane potential of both cancer cell lines, being largely antagonists in MCF-7 cells and largely agonists in MDA-MD-231 cells. In cardiomyocytes, NS1643 and the six quinazolin-4-ones were all agonists with specificity for hERG channels confirmed by successfully antagonizing them with 1 µM Terfenadine except for LTUJH28B and LTUJH37B.

In MCF-7 cells, NS1643 decreased proliferation, inhibited the cell cycle with cells accumulated in G1 phase, induced apoptosis and reduced necrosis. In MDA-MB-231 cells NS1643 decreased proliferation but did not affect the cell cycle, yet increased apoptosis and reduced necrosis. All the quinazolin-4-one compounds reduced proliferation in MCF-7 cells, less potently than NS1643, while in MDA-MB-231 cells only LTUJH28B and LTUJH37B inhibited proliferation, again less potently than NS1643.

Compounds LTUJH18B, LTUJH28B and LTUJH37B caused accumulation of cells at G2/M phase in MCF-7 cells, while none of the quinazolin-4-one compounds affected the cell cycle in MDA-MB-231 cells. Compounds LTUJH28B and LTUJH51B increased apoptosis in MCF-7 cells, while in MDA-MB-231 cells all the quinazolin-4-ones significantly increased apoptosis, with LTUJH37B being more potent than NS1643. In MCF-7 cells, LTJH37B, LTUJH47B and LTUJH51B increased necrosis only, while in MDA-MB-231 cells apart from compounds LTUJH18B and LTUJH47B necrosis was decreased by LTUJH06B, LTUJH28B, LTUJH37B and LTUJH51B. Finally, none of the quinazoline-4-one compounds were toxic to cardiomyocytes, however all completely inhibited cytochrome P450 isozymes 2E1 and 3A4. Previously untested compounds deserve further investigation to better understand their mechanism of action as hERG channel modulators in breast cancer and how they can be used as potential anti-cancer agents.

Abbreviations

Akt/PKB- Protein kinase B

Apaf-1- Apoptotic protease activating factor 1

Bad- Bcl-2 antagonist of cell death

Bid- BH3 interacting domain death agonist

Bim- Bcl-2 interacting mediator of cell death

BRAC1 and 2- Breast cancer 1

CHK2- Checkpoint kinase 2

cIAP2- Cellular inhibitors of apoptosis proteins

CKI- Cyclin-dependent kinase inhibitor

c-Myc- proto-oncogene

DABLO- IAP-binding protein with low pI

DISC- Death-inducing signalling complex

DMSO- Dimethyl sulfoxide

EGFR- epidermal growth factor receptor.

EIF-4E- Eukaryotic translation Initiation Factor 4E

G1- Gap phase 1

G2-Gap phase 2

GA- Gambogic Acid

HEK293- Human embryonic kidney 293 cells

Her2- human epidermal growth factor receptor 2

IAP- Inhibitors of apoptosis proteins

IUPHAR- International Union of Basic and Clinical Pharmacology

MAP-Mitogen activated protein

ORAI1- Calcium release-activated calcium channel protein 1

p53- Tumour protein p53

PI3K- Phosphoinositide 3-kinases

PM- Plasma membrane

PTEN- Phosphatase and tensin homolog

TRAAK- TWIK related arachidonic acid stimulated K^+ channel

TREK- TWIK-related channel

TWIK- Two Pore Domain Weak Inward Rectifying K^+ channel 1

TRP-Transient receptor potential channel

XIAP- X-Linked inhibitor of apoptosis protein.

Chapter One: Literature Review

Cancer is a major world health concern, both in terms of individual morbidity and mortality as well as a major cost burden. According to the Australian Institute of Health and Welfare, an estimated 48,586 deaths occurred due to various cancers with 138,321 new cancer cases diagnosed in 2018 (Welfare 2018). Although there are numerous treatment options, not all are successful and if so the incidence of relapse is common. To improve and develop new, more effective treatments, better understanding of how cancer develops, and progresses is needed. Recently the expression of ion channels in various cancer types was identified, and strongly linked to cancer progression. These channels are normally associated with membrane potentials in electrically excitable cells. Their function in cancer cells, however, is unclear, but has an impact on cell proliferation and apoptosis.

1.1   Neoplastic Transformation

Neoplastic cells arise from genetic mutations of several genes that enhances the survival capabilities of normal cells. It is a complex process that can transform cells over short or long periods of time into very heterogeneous populations. Normal cells exposed to stressful environments will initially undergo adaptive changes. This may be by metaplasia, where one epithelial cell transforms into another that is better able to survive the stress; hyperplasia where cell proliferation increases; or dysplasia were genetic mutations result in cells of different size, shape and capabilities. If the stress continues, changes become more permanent and the transformed cells begin to display common enhanced survival characteristics (Vogelstein and Kinzler 1993). Classified as the hallmarks of cancer (Hanahan and Weinberg 2000), these changes allow the cells to proliferate at an increased rate regardless of growth signals (both inhibitory and stimulatory), with inhibition of apoptotic responses (increasing survival of dysfunctional cells), increased angiogenesis (to deliver nutrients and oxygen to the increasing tumour mass), enhanced ability to invade surrounding tissue (utilising blood and lymphatic vessels to metastasize throughout the body) and seed tumours at distance sites, and unlimited replicative potential. Additional hallmarks have since been proposed, including evasion of immune surveillance, metabolic stress (Seyfried and Shelton 2010), genomic instability (Negrini, Gorgoulis, and Halazonetis 2010), mitotic stress and DNA damage and replication stress (Macheret and Halazonetis 2015).

Under normal conditions, cells have many regulatory processes that ensure these cancerous changes do not occur, but when mutated can initiate and stimulate cancer progression. The regulatory processes involve two important groups of genes / proteins, the proto-oncogenes and the tumour suppressor genes (Foster 2008). The proto-oncogenes, including Her2/neu (human epidermal growth factor receptor 2 derived from rodent glioblastoma cell line), Ras, c-Myc, are genes that normally regulate cell proliferation and differentiation. However, when a proto-oncogene mutates due to chromosomal rearrangement or gene amplification, it

becomes permanently activated and is then referred to as an oncogene. Mechanisms of oncogene activation including HER-2 oncogene is present in 20% of primary breast cancers. Another mode of oncogene activation is point mutation in the Ras oncogene which enhances its downstream effects which produces the cancer malignancy characteristics such enhanced cell proliferation as well as the alteration in migration and angiogenesis (Downward 2003). This is seen commonly in solid cancers such as lung, colorectal and pancreatic but not breast cancers. Other modes of oncogene activation include the transcription of new fusion gene into protein with better function via chromosomal translocation. Oncogenic components may also work together to produce its effect, for example in breast cancer the HER-2/Neu cascade (Nahta, Hortobágyi, and Esteva 2003).

In primary breast cancer, HER-2 gene amplification and overexpression is found in cancer with lobular origin and has been found to be associated with enhanced aggressiveness (Slamon et al. 1987), while it is rarely overexpressed in benign breast tissue (Osborne, Wilson, and Tripathy 2004). HER-2 encodes for the 185-kDa transmembrane tyrosine kinase growth factor receptor. The activation of this receptor leads to the initiation of the downstream activation of signalling pathways such as mitogen-activated protein (MAP) kinase and 3-kinase (PI3K)/Akt. This activation impacts proliferation and angiogenesis, with altered cell-cell interactions, increased motility, metastases and resistance to apoptosis (Oved and Yarden 2002). Other HER family members including EGFR (also known as HER-1) are also highly expressed in lung, head and neck cancer and to a lesser extent in breast cancer. Some studies have shown that expression of EGFR is associated with a worse prognosis in oestrogen negative cells (Witton et al. 2003).

The p53 oncogene is the most studied tumour suppressor gene, normally being responsible for the regulating cell division. Any DNA damage due to chemotherapy or irradiation activates the p53 oncogene. The activation may lead to enhanced transcription of CKIp21 which causes temporary cell cycle arrest in G1 or G2/M phase prior to mitosis and it is also capable of triggering apoptosis (Zou et al. 2000). Overexpression of p53 is believed to occur in 20-30% of breast cancers, and is associated with worse prognoses in breast cancer (Thor et al. 1992). The oncogenes and tumour suppressor genes functions are summarised in Table 1.

Oncogene	Function
HER-2	Tyrosine kinase receptor
Ras	G-protein
PI3K	Kinase
Akt	Kinase
EIF-4E	Initiator of protein translation
Cyclin D1	Cell-cycle mediator
Cyclin E	Cell-cycle mediator
c-myc	Transcription factor
Tumour suppressor gene	**Function**
p53	Induces cell-cycle arrest, cell-cycle checkpoint activation Triggers/facilitates apoptosis
p27	Inhibits cyclin-dependent protein kinases; arrests cell cycle in G1 phase
BRCA-1	Regulates DNA transcription; acts to repair damage DNA
BRAC-2	Repairs damaged DNA
CHK2	Cell cycle checkpoint kinase activates p53 after DNA damage
ATM	Checkpoint kinase activates CHK2
PTEN	Phosphatase, negative regulator or Akt kinase
Rb	Retinoblastoma gene, repressor of cell cycle and protein translation

Table 1. Oncogenes and tumour suppressor genes and their functions, adapted from (Osborne, Wilson, and Tripathy 2004)

1.2 Cell Cycle

As any cell grows and proliferates, changes can be observed throughout the 'Cell Cycle'. The cell cycle can be divided into four phases: G1, S, G2 and M phases (Figure 1). When cells are not cycling, they are classified as being in the G0 phase, in which cells are quiescent. Cells in the G1 phase (Gap) of the cell cycle are in a pre-synthesis state during which cells grow and carry out their normal function. Cells then transition into the S phase (Synthesis) of the cell cycle, during which DNA is replicated in preparation for cell division. During the G2 phase (Gap) of the cell cycle, cells produce proteins and other factors in preparation for mitosis. Cells then transition into the M phase (Mitosis) of the cell cycle. During mitosis, cells undergo sequential changes – prophase, metaphase, anaphase and telophase - to produce two 'daughter' cells with identical copies of the DNA. The daughter cells may either continue to cycle or may leave (or may arrest in G0/G1 phase of the cell cycle), where they may form into differentiated cells with specialized functions or become temporarily or permanently non-proliferative (senescent).
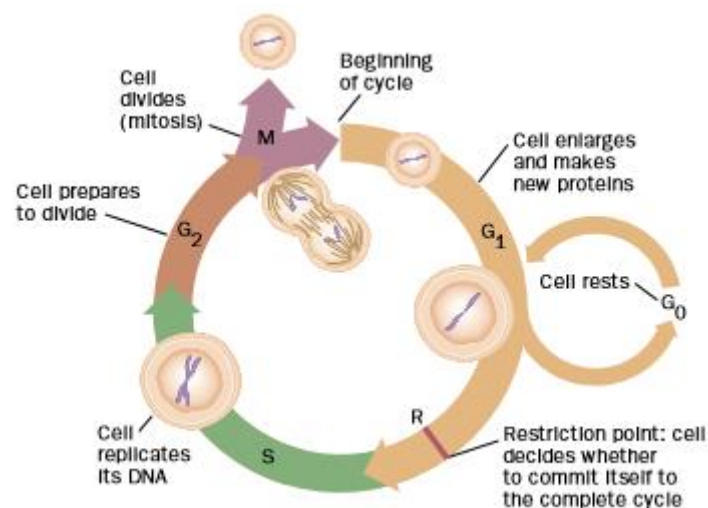
Figure 1.The summary of events in the cell cycle and the checkpoints that regulate the balance between cell growth and arrest or apoptosis (Weinberg 1996).

1.2.1 Cyclin-Dependent Kinase Regulation of Cell Cycle Progression

To maintain the genomic integrity of cells, the transition of cells from one phase of the cell cycle to the next (or within each phase) is tightly regulated by different cellular proteins at what are referred to as 'checkpoints'. A key family of proteins that regulate these checkpoints are the cyclin-dependent kinases (CDKs) (Hartwell and Kastan 1994). The CDKs are a family of serine/threonine protein kinases that are activated at specific points of the cell cycle by cyclins (summarized in Table 2). Binding of a cyclin to a CDK creating a cyclin/CDK complex, induces a conformational change that allows phosphorylation of the conserved threonine residues, and thus CDK activation.

Cell cycle phase	CDK	Cyclin
G$_1$ Phase	CDK4	Cyclin D1, D2, D3
	CDK6	Cyclin D1, D2, D3
G$_1$/S Phase Transition	CDK2	Cyclin E
S phase	CDK2	Cyclin A
G$_2$/M phase transition	CDK1(cdc2)	Cyclin A
Mitosis	CDK1(cdc2)	Cyclin B
	CDK7	Cyclin H

Table 2.Cyclin-CDK activation at different cell cycle phases (Vermeulen, Van Bockstaele, and Berneman 2003).

CDK activity can also be regulated by CDK inhibitors (CKIs). There are two families of CKIs; the INK4 family including p16[Ink4A], p15[Ink4B], p18[Ink4C] and p19[Ink4D] that exerts its inhibitory effects on CDK4 or CDK6 during the G1 phase, and the Cip/Kip family including p21 (Cip1), p27 (Kip1) and p57 (Kip2) that generally inactivate the cyclin/CDK complexes. CKIs act via the G1 cyclin/CDK as forced expression of each CKI leads to G1 cell cycle arrest. CKIs are also involved in G1 checkpoint control, while their effects on G2/M cyclin/CDK complex remains unclear (Nakayama and Nakayama 1998).

1.2.2 Transition from G$_1$ to S phase - Checkpoint

Daughter cells arising from mitotic division during M phase, re-enter the cell cycle at G1 phase. Initiation of the Ras dependent kinase pathway stimulates the release of Cyclin D early in G1-phase, that interacts with CDK4 and CDK6, followed by Cyclin E later in G1 phase. Some cells may stop cycling early in G1 phase, becoming quiescent or entering G0 phase, while others continue past the Retinoblastoma (Rb) gene restriction checkpoint in late G1. The cells passing the Rb restriction checkpoint enter S phase where DNA replication occurs (Laskey, Fairman, and Blow 1989; Bartek and Lukas 2001).

The Rb restriction point in G1 phase can also stop DNA replication, acting as a gate keeper, determining if cells can enter S phase to complete the cell cycle or not enter and cause cell cycle arrest (Vermeulen, Berneman, and Van Bockstaele 2003; Weinberg 1996). For cells progressing through the rest of the cell cycle, phosphorylation of Rb by the combination of CDK and cyclin forming cyclin-cdk complex is required. In its non-phosphorylated state Rb binds and inhibits transcription factor E2, which is needed to activate the transcription of genes required for cells to enter the S phase. Once Rb is phosphorylated, this releases the bound E2F transcription factor for S phase to proceed (Fearon 1997; Devita Jr, Lawrence, and Rosenberg 2015)

1.2.3 Transition from G2 to M phase and Cytokinesis - Checkpoint

The G2 phase is a checkpoint that monitors reorganization of cell synthesis as well as regulation of unrepaired DNA damage. Any damaged cells coming from S phase are eliminated at the checkpoint through the cyclin-CDK-CKI system. This checkpoint also prevents segregation of chromosomes that are not intact (Ruddon 2007).

There are several events required for cells to progress from the G2 phase into mitosis .Firstly, the inactive cdc2 is phosphorylated by cdc25b and cdc25c protein phosphatase (Hattori et al. 2004), promoting cdc2-cyclin B complex formation (known as mitosis promoting factor, MPF). Cdc25b levels subsequently increase in response to cdc2-cyclin B complex activation, which further activates the complex in a positive feedback loop (Molinari 2000). This leads the cells to undergo premature mitosis that can cause damage, which is controlled by nuclear protein wee1 and myt1 maintaining cdc2 in a phosphorylated state during interphase. To prevent damage in the cells undergoing G2-M phase transition, p21 and p53 prevent a second round of DNA replication by inhibiting the action of cdks. p53 increases transcription of the 14-3-3σ gene which inhibits entry into G2 phase. The combination of 14-3-3σ with cdc25c phosphatase in the cytoplasm forms a 14-3-3σ – cdc25c complex which inhibits the entry of cdc25c into the nucleus, blocking DNA replication, leading to cell cycle arrest (Foster 2008; Evan and Littlewood 1998). The spindle assembly checkpoints ensure accurate alignment of chromatids before the division of the cell into daughter cells in the M phase (Ruddon 2007).

1.3 Apoptotic Cell Death

Apoptosis is a highly regulated form of cell death, where the cell's own proteins participate in cellular destruction and removal. It is essential for normal tissue development and maintenance but is frequently disrupted in many diseases and cancer types. Alternatively, the less desired form of cell death, necrosis, is also strongly associated with disease, and is unregulated, stimulating an inflammatory response.

1.3.1 Apoptosis versus Necrosis

Apoptosis is an intracellular suicide mechanism leading to the internal breakdown of cells that are subsequently eliminated by phagocytosis. As the cell undergoes apoptosis, characteristic physiological changes can be observed including dismantling of the cell's cytoskeleton causing the cell to shrink and the development of membrane blebbing. Activation of specialised enzymes break down chromatin and internal cell organelles as shown in Figure 2 (Duprez et al. 2009). During apoptosis cells do not lose their plasma membrane integrity, confining cellular debris and toxins within the membrane package. During the later stages of apoptosis, cells display phosphatidylserines (PS) which are signalling molecules for phagocytic cells. Due to the precise and highly regulated nature of these events, it is

immunologically silent and does not stimulate an inflammatory response (Krysko and Vandenabeele 2008).

In necrosis, a less regulated process, cells undergo cytoplasmic organelle swelling, followed by the loss of membrane integrity and release of toxic cellular contents into the surrounding extracellular space which does cause inflammation (Figure 2). This is in contrast to apoptosis which does not trigger inflammation since cells undergoing apoptotic cell death maintain their membrane integrity and do not lose their cellular content before disintegrating and being ingested by phagocytes (Rock and Kono 2008). Previously the inflammatory process was believed to occur due to changes in the inflamed tissues. However, it has now been proven that inflammation triggered by necrosis is activated by the induction of factors such as tumour necrosis factor (TNF) or lipopolysaccharide (LPS) whose signalling causes the release of cellular components capable of inducing inflammation (Wallach et al. 2016).
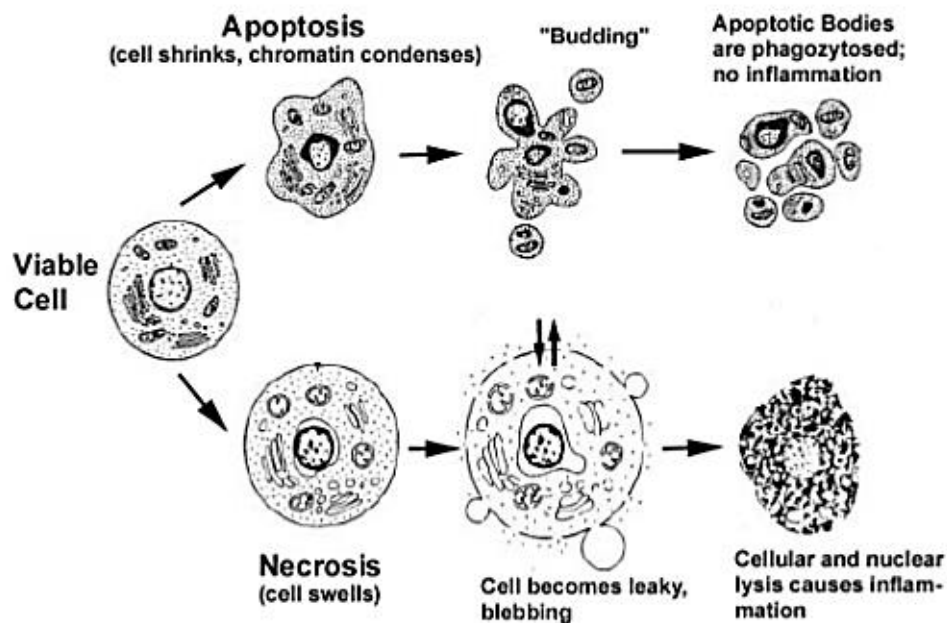
Figure 2. Morphological hallmarks of the apoptotic and necrotic cell death process (Gewies 2003).

1.3.2 Regulation of Apoptosis

Apoptosis is a highly regulated process, and the proteins involved are highly conserved among species. There are two protein families that are important in regulating apoptotic events within the cell; the bcl-2 (B cell lymphoma-2) family of proteins that control mitochondrial integrity (Youle and Strasser 2008), and the caspases (cysteinyl aspartate-specific protease) that are specialised enzymes (Fuentes-Prior and Salvesen 2004). Apoptosis may be initiated by one of two pathways, either the intrinsic (mitochondrial) or the extrinsic (death receptor) pathway, that converge on activation of executioner caspases (see Figure 3).

1.3.3 Intrinsic Apoptotic Pathway

The intrinsic pathway (see Figure 3) is controlled by the Bcl-2 family of proteins. Bcl-2 family members can be divided into 2 distinct groups, pro- and anti-apoptotic, and their interactions, forming heterodimeric complexes, determine the cell's fate. Anti-apoptotic proteins, including Bcl-2, Bcl-xl and Bcl-w, bind to and inactivate certain pro-apoptotic proteins. Pro-apoptotic proteins can be further divided into two subgroups; Bcl-2 associated X protein (Bax) that interacts with the mitochondrial membrane, and the BH3-only proteins including BH3 interacting domain death agonist (Bid), Bcl-2 interacting mediator of cell death (Bim) and Bcl-2 antagonist of cell death (Bad) that bind to and inhibit the function of anti-apoptotic proteins (Shin et al. 2001). The tumour suppressor p53 is a key regulator of apoptosis that in turn regulates the transcription of target genes involved in the regulation of cell cycle arrest, cell death mechanisms (including apoptosis and senescence) as well as DNA repair; have also been directly linked to the mitochondria and induction of the intrinsic apoptosis pathway (Parrales and Iwakuma 2015).

Following activation of the death signal BH3-only proteins, bind to and neutralise anti-apoptotic Bcl-2 proteins allowing pro-apoptotic proteins such as Bax to interact with the mitochondrial membrane, forming pores. This results in mitochondrial outer membrane permeabilization (MOMP) and changes to the mitochondrial membrane potential ($\Delta\psi m$). This membrane potential change allows the release of several proteins normally contained within the mitochondrial inter-membrane space (IMS), including cytochrome c (Cyto c) into the cytosol. Cyto C complexes with Apaf-1 and procaspase, resulting in the activation of the initiator caspase 9 (Riedl and Salvesen 2007).

Other pro-apoptotic proteins released from the mitochondria include SMAC (second mitochondria-derived activator of caspases), DIABLO (direct IAP binding protein with low pI) and Omi/HTRA. The Smac/DIABLO is an important signalling protein released from the mitochondria and acts by blocking the anti-apoptotic effect of proteins known as inhibitor of apoptosis proteins (IAPs) (Loreto et al. 2014; Salvesen and Duckett 2002). High temperature

requirement A (HTRA) family of proteins regulate mitochondrial function and are known to act as tumour suppressors that promote cell death. HTRA expression is downregulated in cancer cells which allows tumour growth and metastasis (Zurawa-Janicka, Skorko-Glonek, and Lipinska 2010).

Once released, SMAC / DIABLO inhibit the action of the inhibitor of apoptosis proteins (IAPs) including XIAP, cIAP and cIAP2, found in the cytosol that inhibit caspase 9, caspase 3 and caspase 7 (LaCasse et al. 2008). Downstream activation of caspase 9 is essential in apoptotic cell death which is cleaved into the active effectors caspase 3, caspase 6 and caspase 7 that allow the release of mitochondrial apoptotic factors (Youle and Strasser 2008).

1.3.4 Extrinsic Apoptotic Pathway

The extrinsic pathway of apoptosis, also referred to as the death receptor pathway is activated when death receptors TNFR (tumour necrosis factor receptor) and another member of the TNF receptor superfamily known as death receptor 6 (DR6) (Shi et al. 2018), Fas or TRAIL-R (TNF-related apoptosis-inducing ligand receptor) bind to specific receptors TNF, FasL and TRAIL, respectively (see Figure 3).

Signalling via TNFR1 leads to the formation of two complexes. Complex I is formed at the plasma membrane and is important in the downstream activation of NF-κB and mitogen activated protein kinases (MAPKs). It consists of TNFR1, TNFR-associated death domain, TRAF2, RIPI, cIAP1 and cIAP (Wilson, Dixit, and Ashkenazi 2009). The endocytosis of TNFR1 leads to the formation of complex II, which is similar to the receptor-proximal death inducing signalling complex (DISC) that is recruited by FasL and TRAIL (including tumour necrosis factor receptor type 1-associated death domain (TRADD), and FADD (Fas-associated protein with death domain). These complexes subsequently recruit and activate initiator caspase-8 or caspase-10 (Peter and Krammer 2003).

1.3.5 The Caspase Cascade

Regardless of how apoptosis is stimulated, intrinsically or extrinsically, both pathways converge at the activation of initiator caspases (8, 9 and 10), which then initiates the 'caspase cascade'. Caspases, a family of cysteinyl aspartate-specific proteases, are considered central regulators of apoptosis. Once activated the initiator caspases, cleave and activate downstream effector caspases including caspase 3, which ultimately execute apoptosis.
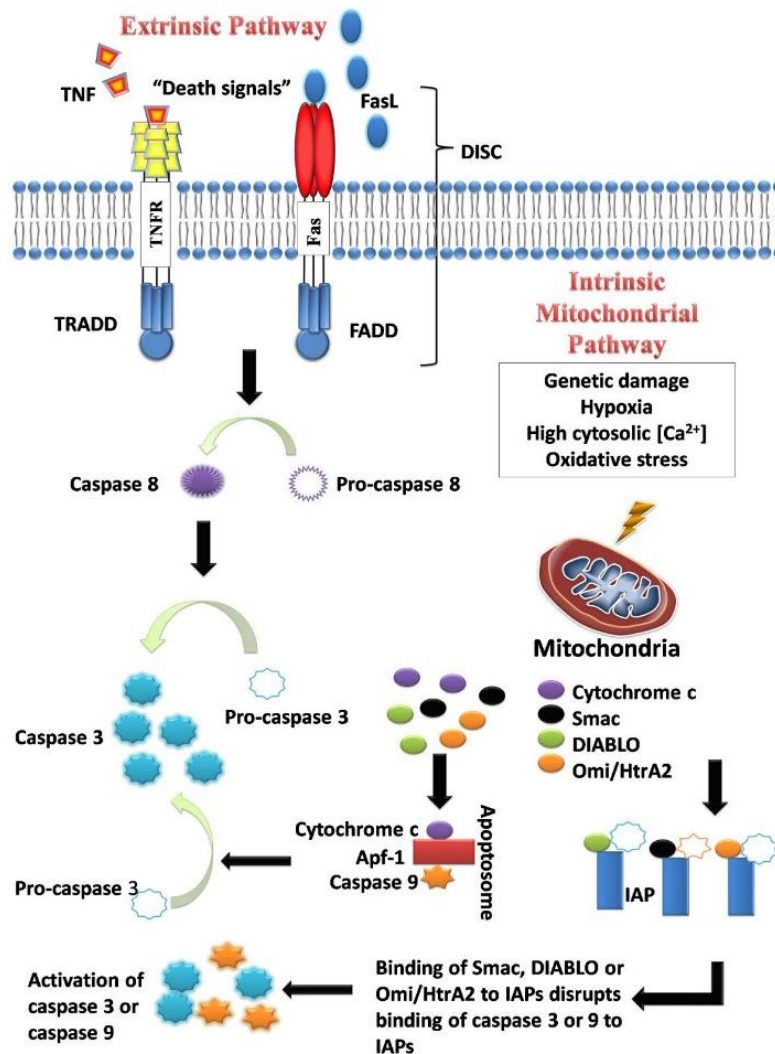
Figure 3. The intrinsic and extrinsic apoptotic pathways leading to cell death via caspase activation (Wong 2011).

1.4   Breast Cancer

Breast cancer accounts for 29 per cent of all cancers diagnosed in 2019, and it is the most commonly diagnosed cancer in Australian women. It is estimated that 19,535 Australians will be diagnosed with breast cancer, with an average of 53 people diagnosed with breast cancer every day. The risk of an individual being diagnosed with breast cancer by their 85th birthday being 1 in 675 males and 1 in 7 females (B.C.NAustralia 2019) .

Breast cancer, as with all types of cancers, is a very heterogeneous disease, with cells present at varying stages of cancerous progression within the one tumour. Due to this variability, breast cancer can be classified according to several features including: histopathological type, grade of the tumour, stage of the tumour, and expression of proteins and genes (Weigelt and Reis-Filho 2009).

1.4.1   Histopathological type

Although breast cancer has many different histology's, most breast cancers are derived from the epithelium lining of the ducts or lobules and are classified as mammary ductal carcinoma. Based on analyses of biopsy samples, 3 common histopathology's have been identified; ductal carcinoma *in situ*, invasive ductal carcinoma and invasive lobular carcinoma (Weigelt, Geyer, and Reis-Filho 2010).

Ductal carcinoma *in situ* (DCIS) is a preinvasive cancer with cells that are restricted to the duct lobular system of the breast (Bane 2013). It is usually unilateral and may interrupt the structure of the duct as it spreads (Wong E. 2018). Invasive ductal carcinoma (IDC) is an invasive breast cancer that attacks the ducts and resides in stroma (Goh et al. 2019), producing a palpable mass following a fibrous response. Due to its invasive nature IDC can metastasize to the lymph and blood (Wong E. 2018). Another major population of breast cancer is the invasive lobular carcinoma (ILC) which occurs in the lobular units of the breast (Reed et al. 2015). It is highly invasive often metastasizing to the abdominal viscera, GI, ovaries and uterus (Wong E. 2018).

1.4.2   Grade of the Tumour

Grading focuses on anaplastic type changes, or dedifferentiated appearance of the breast cancer cells compared with normal breast tissue. As normal breast cells differentiate, they display specific shapes and orientate themselves along the basement membrane in an orderly fashion. Anaplastic cancerous cells lose this organised pattern, becoming 'disorganised', along with proliferating uncontrollably. Cells become more variable in size and shape, the nuclei become less uniform and the organised alignment along the basement membrane is reduced. As cells progressively dedifferentiate and lose these features, pathologists classify cells as; well differentiated (low-grade), moderately differentiated (intermediate grade), and

poorly differentiated (high-grade). Poorly differentiated cancers have a worse prognosis (Rakha et al. 2010).

1.4.3 Expression of receptors and proteins

Breast cancer cells are reliant on hormonal stimuli to grow and develop. Reduction in the expression of oestrogen (ER) and progesterone (PR) receptors, or both, occurs over time as the tumour progresses. Breast cancer cells vary in their expression of receptors and are commonly referred as being ER positive (ER+) or ER negative (ER-) and PR positive (PR+) or PR negative (PR-). Cells with none of these receptors are called triple negative and are generally associated with a poorer patient prognosis than those expressing at least some of the receptors (Parise et al. 2009).

The oncogene, human epidermal growth factor receptor (HER2) is implicated in 15-30% of mammary carcinogenesis (Burstein 2005) and has an important role in the development and progression of certain aggressive types of breast cancer. HER2 is an important marker, with breast cancer cells being characterized as either HER2 positive (HER2+) or HER2 negative (HER2-) (Malhotra et al. 2010). Breast cancers often over express the human epidermal growth factor gene (25-50 copies) with a 40-100-fold increase in HER2 protein (Burstein 2005). HER2 has also been found to be activated in oestrogen positive breast cancer since oestrogen activates HER2 signalling (Shou et al. 2004) and overexpression increases the risk of invasion and metastasis (Park, Kim, Park, et al. 2005) as well as relapse (Slamon et al. 1987).

Breast cancer cells can be further classified in accordance to their intrinsic molecular subtypes including; basal like breast cancer, HER2-enriched, luminal A and luminal B. Molecular expression studies have identified luminal A cells to be estrogen and/or PR positive and HER2 negative , luminal B cells are similar with the only difference being that they are HER2 positive. While the molecular subtype of triple negative breast cancer cells is identified as basal like breast cancer. Prognosis of patient with luminal A subtypes is best while basal like cancer is associated with worst prognosis (Hon et al. 2016).

1.5 Treatment Options

There are currently many treatment options available for breast cancer depending on the classification; including surgery, chemotherapy, radiation, hormone therapy, immunotherapy or a combination of these. A mainstay treatment for breast cancer, hormone therapy, is reliant on the presence of oestrogen receptors, which becomes less effective as the tumour progresses. Surgery is beneficial as it can result in the total removal of tumour, however it is a very intrusive form of treatment that does not always result in complete removal. Treatments such as chemotherapy and radiation elicit their effects by causing cellular damage and increasing apoptosis. Although effective such treatment has many off-target effects and uncomfortable side effects.

1.5.1 Hormone Therapy - Tamoxifen

Tamoxifen is a selective oestrogen receptor modulator (SERM) with anti-oestrogenic activity in breast tissues (Manna and Holz 2016). It is the main treatment of choice with oestrogen receptor (ER) positive early breast cancer (An 2016). The anti-oestrogenic activity of tamoxifen includes the competitive inhibition of oestrogen binding to oestrogen receptors leading to the reduction in oestrogen related gene expression (Osborne 1998). This modification in oestrogen signalling results in G1 cell cycle arrest, and induces apoptosis in cells (Ellis et al. 1997).

1.5.2 Surgery

One of the traditional treatments of breast cancer, is to surgically remove the entire breast (mastectomy) or the primary lesion and the affected axillary lymph nodes through a process known as wide local excision (WLE). Prior to surgery, the primary lesion is treated with either radiation, chemotherapy or tamoxifen to reduce the tumor size making it easier to remove (Davies 2016).

1.5.3 Chemotherapy

There are numerous types of chemotherapy drugs, or chemicals used to target or treat cancers. Chemotherapeutic drugs are categorized based on how they work, whether they directly target DNA, inhibit the cell cycle and other types of cellular damage. The main classes of anticancer chemotherapeutic agents include the anthracyclines, mitotic inhibitors, antimetabolites, alkylating agents, and more targeted drugs including Herceptin. Many of these are used as neoadjuvant therapy to reduce the size of a tumour prior to surgery while others are used as adjuvant therapy to minimize relapse of the cancer (Thompson and Moulder-Thompson 2012).

1.5.3.1 Action and side effects of commonly used cancer chemotherapeutics

Among the anthracyclines (e.g. epirubicin (Pharmorubicin®), doxorubicin (Adriamycin®)) are commonly and effectively used to treat many cancers including breast adenocarcinoma. All of them intercalate DNA strands and inhibit topoisomerase II preventing relaxation of supercoiled DNA. This results in cells being unable to progress to mitosis and apoptosis is triggered (Fornari et al. 1994; Pommier et al. 2010). Taxanes are mitotic inhibitors (e.g. paclitaxel (Taxol®), docetaxel (Taxotere®)) which also arrest the cell cycle by stabilizing the microtubules (binding to β tubulin). With the microtubules accumulating inside the cells again apoptosis is triggered (Lyseng-Williamson and Fenton 2005; Brito, Yang, and Rieder 2008). Antimetabolites (e.g. capecitabine, 5-fluorouracil (5-FU), gemcitabine (Gemzar®)) inhibit the enzyme thymidylate synthase preventing the production of thymidine nucleoside needed for DNA repair and replication (Longley, Harkin, and Johnston 2003). Gemcitabine also acts as

a cytidine masquerade inserting into DNA strands allowing bases to be added to it and producing a "masked chain termination" (Mini et al. 2006) again preventing DNA repair or replication. Alkylating agents such as cyclophosphamide cause DNA cross linkages of guanine nucleotides so the DNA cannot be repaired or replicated (Hall and Tilby 1992). While the more targeted therapies such as trastuzumab (Herceptin®), lapatinib (Tykerb®) and bevacizumab (Avastin®) are monoclonal antibodies used to treat HER2 receptor positive breast cancer but not directly disrupt other tissues. However, they do cause immunological reactions in some patients (Le, Pruefer, and Bast 2005; Shih and Lindley 2006) Lapatinib (Tykerb®) works slightly differently inhibiting tyrosine kinase which interrupts the HER2/neu and EGPR pathways (Nelson and Dolder 2006).

Since dysregulated proliferation signalling pathways are commonly recognized as the cause of cell transformation in cancer, unfortunately during anti-cancer treatment, it is the attack of these pathways that inadvertently affects other normal, rapidly proliferating cells. Hence the anticancer efficacy of these agents comes at a cost of normal tissue toxicity among which anthracycline is a frequent offender. So, while chemotherapies have proven their efficacy in many cases, patients often experience debilitating side effects that significantly reduce their quality of life. Moreover, cancer relapse with treatment resistance underscores the urgent need to identify novel molecular targets for the development of alternative therapies (Litan and Langhans 2015).

Most chemotherapeutic drugs exert their anti-cancer effect by targeting rapidly proliferating cancer cell populations. Other rapidly proliferating non-cancerous cells are inadvertently targeted; including intestinal cells, hair follicles and bone marrow cells (Pérez-Herrero and Fernández-Medarde 2015). Damage to these normal tissue cells leads to the common side effects associated with chemotherapies, including mucositis, inflammation and ulceration of the GI tract lining (Kwon 2016), bone marrow abnormalities such as leukopenia and pancytopenia (Weinzierl and Arber 2013) and hair loss (alopecia) when treatments damage growth of hair follicles (Yoon et al. 2016). More serious side effects that are less common but limit chemotherapy use include cardiotoxicity, lung toxicity, renal toxicity and neuropathy (Plenderleith 1990). Finally, since the human body recognizes these toxic medicines in the chemical trigger zone, nausea and vomiting as they stimulated via activation of the vomiting centre in the medulla (Andrews and Rudd 2016).

1.5.3.2 Cardiac side effects

Chemotherapy induced cardiotoxicity can be divided into four broad categories: 1) directed cytotoxic effects with a range of cardiac dysfunctions, such as heart failure and reduced left ventricular ejection fraction, 2) cardiac ischemia, 3) cardiac arrythmia and 4) pericarditis (Csapo and Lazar 2014; Thomas 2017). Many chemotherapeutic agents are known to induce such cardiovascular abnormalities including in order of cardiotoxic category above: 1) alkylating agents, anthracyclines and tyrosine kinase inhibitors, 2) antitumor antibiotics and topoisomerase inhibitors, 3) anthracyclines and 4) cyclophosphamide and cytarabine, to name a few (Thomas 2017; Tromp et al. 2017). The investigation of any new novel compounds for their potential to modulate hERG channels in the treatment of breast adenocarcinoma must also address the potential for cardiotoxic side effects.

1.6 Cardiac Electrical Activity

Cardiotoxicity is one of the most deleterious effects arising from cancer therapeutics and is a major factor contributing to mortality (McGowan et al. 2017) . All current and potential drug treatments need to be assessed for their potential impact on cardiac function. All cardiac cells, and nerve cells, have an electrochemical and voltage gradient (potential difference) across the plasma membrane, due to an uneven distribution of electrolytes (e.g. sodium, potassium, chloride) either side of the cell membrane. This distribution is regulated by specific ion channels, creating a more negative charge inside cells compared with outside. Appropriate and rapid movement of various ions is important in initiating changes in the potential difference across the membrane resulting in rhythmic cardiac contractions (McCormick 2014). In between heart beats, the membrane is referred to as resting and the potential difference across the membrane is known as the resting membrane potential (V_m). When an appropriate signal is initiated in the cardiac pacemaker, precise movement of different ions across the cell membrane occurs resulting in the action potential. The electrochemical changes that occur across the entire heart are important for the precise regulation of cardiac contractility and are typically represented by an electrocardiogram (ECG) (Wulff, Castle, and Pardo 2009).
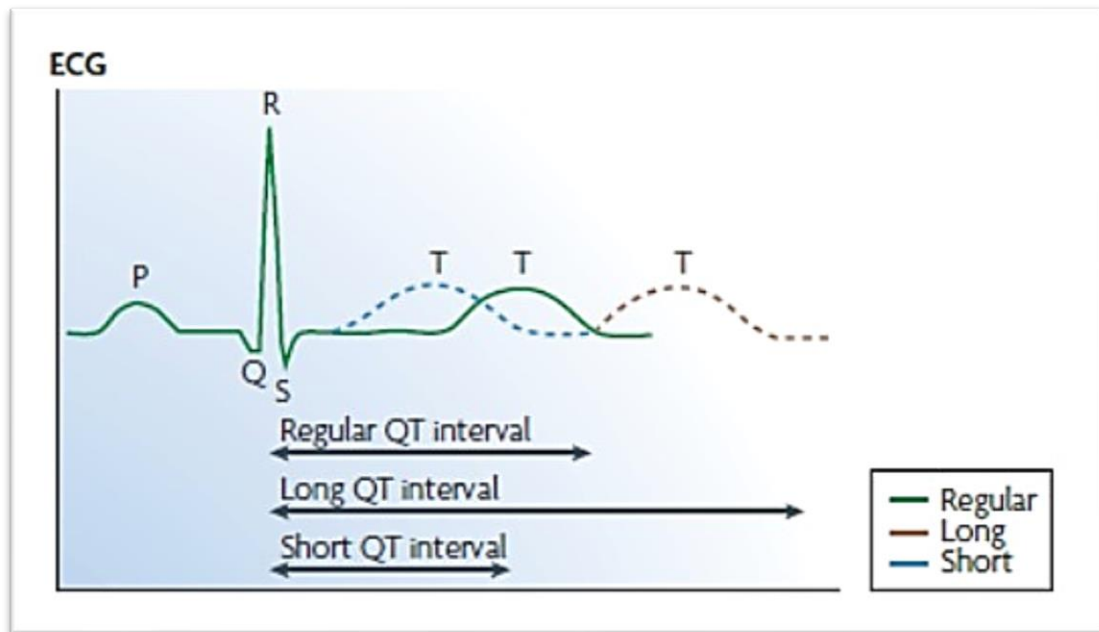
Figure 4. Representative ECG trace showing the different components of depolarization and repolarization in the ventricular myocardium adapted from (Wulff, Castle, and Pardo 2009).

A typical ECG trace is shown in Figure 4, where the P wave represents depolarisation of the atria and the QRS complex represents both repolarization of the atria and depolarization of the ventricles. The T wave represents repolarization of the ventricles and the QT interval is the duration between depolarization and repolarization of ventricles (Klabunde 2011). Many changes in the ECG have clinical significance and all demonstrate changes in the ionic currents associated with the electrical activation of the heart. More recently focus has been centred on changes in the QT interval because it is strongly associated with the development of fatal cardiac arrhythmias (Vandenberg et al. 2012). Figure 4 shows how the ECG is altered when the QT interval is lengthened (long QT syndrome) or shortened (short QT syndrome) caused by malfunctioning/inhibited hERG potassium channel, either of which can result in cardiac arrhythmia.

1.6.1 Resting Membrane Potential

Resting membrane potentials vary in different cell types, ranging from -50mV in epithelial cells and -70 mV in neurons, to -90mV in skeletal muscle and ventricular myocardium (see Figure 5), but the overall range tends to be between -100 and -20mV (Yang and Brackenbury 2013a).
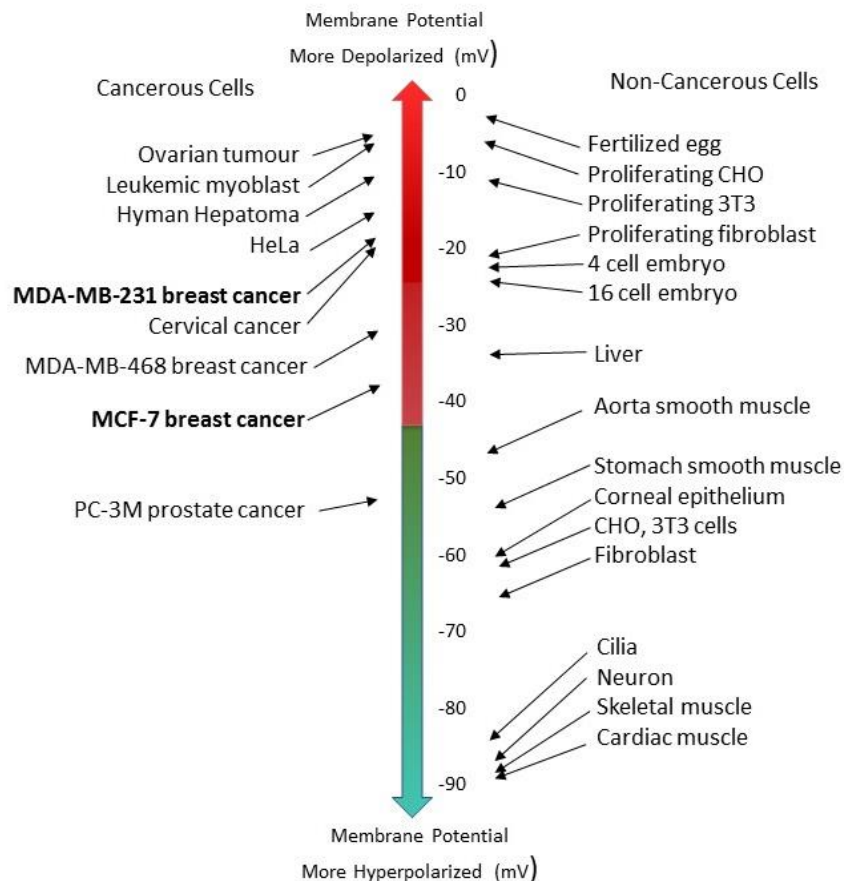
Figure 5. Range of membrane potentials recorded in a selection of cancerous cells and non-cancerous cells adapted from (Yang and Brackenbury 2013a).

The principle regulators of the resting membrane potential are potassium ion channels, but there are significant contributions from the other cationic channels (e.g. Na^+ and Ca^{2+}) and anionic channels (i.e. Cl^-). Activation of these channels may be voltage-dependent, ligand-gated or store-operated and the signals may be external or via intracellular mediators. The activity of channels may also be altered by metabotropic receptors (e.g. G protein coupled receptors, GPCR), pH, inflammatory mediators, second messengers, osmotic fluctuations, volume changes and temperature variations (Alexander, Mathie, and Peters 2011). Among the family of potassium channels, the hERG (human ether-a-go-go) are of interest because they have been identified not only in the development of long QT syndrome in the heart (Vandenberg et al 2012), but they play an important role in transformed malignant cells with respect to proliferation, migration and metastasis (Yang and Brackenbury 2013a).

1.6.2 Action Potential

In excitable cells (i.e. muscle and nerve), the resting membrane potential can undergo a transient reversal in potential known as the action potential. In nerve and skeletal muscle, the action potential relies on Na^+ influx (inward current) and K^+ efflux (outward current) to cause the depolarization and repolarization of the plasma membrane, respectively (Katz 2010). In smooth and cardiac muscle, however, an influx of Ca^{2+} is also required for the action potential to trigger contraction (Viola et al. 2014).

An action potential (Figure 6) for ventricular cardiac cells is initiated by a depolarising current from cells in the sino-atrial node which reduces the electrical potential from -70mV to -60 mV, opening fast sodium channels resulting in an influx of Na^+ (which moves the membrane potential to towards the sodium equilibrium potential of +20 mV). Further, Ca^{2+} channels (T-type and L-type) also open during the upstroke further bringing in positive charge to assist in reversing the Vm and moving it towards +20mV. The depolarising phase is fast (lasts milliseconds) and is known as the upstroke of the action potential (**phase 0**). Sodium channels close rapidly following the upstroke, and T-type Ca^{2+} channels have already closed by -30mV, but the L-type Ca^{2+} channels remain open. **Phase 1** is defined by the first step in repolarisation which begins with transient outward current potassium channels opening (I_{to}) while slow calcium channels (L-type Ca^{2+}, I_{Ca}) remain open. **Phase 2** is the plateau phase that generates a depolarising Ca^{2+} influx (inward Ca^{2+} current) that is balanced by a repolarising K^+ efflux (outward K^+ current). **Phase 3** is the repolarising phase of the action potential, caused by the inhibition of depolarising currents (i.e. closure of L type Ca^{2+} channels) due to the opening of K^+ channels which enhances the repolarising current. In this phase, the membrane potential returns to its initial resting value of -90 mV. Finally **Phase 4,** is the resting state of the action potential and it is maintained by the ligand-gated outward rectifiers and the ionic balance across the membrane is restored by a variety of pumps and exchangers (i.e., Na^+-K^+ ATPase, Ca^{2+}-ATPases and the Na^+-Ca^{2+} exchanger) (de Bakker and van Rijen 2010).
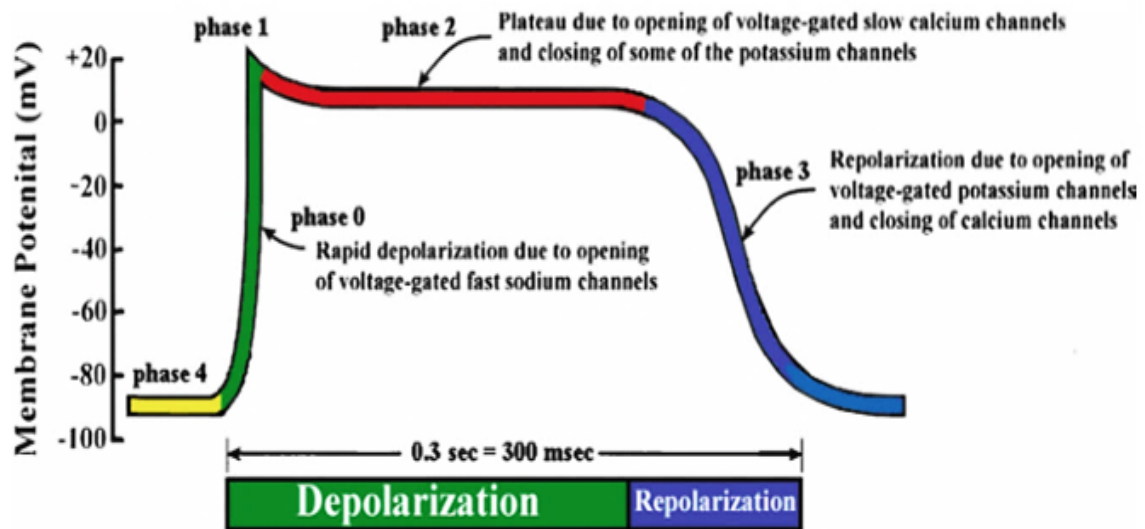
Figure 6. Phases of the ventricular cardiac action potential (de Bakker and van Rijen 2010).

1.6.3 Ion channels

Ion channels are pore-forming integral membrane proteins present both on plasma membrane and intracellular organelle membranes that undergo conformational changes to open and close (Jentsch, Hübner, and Fuhrmann 2004). Opening and closing of ion channels allows specific ions to move across the membrane by passive diffusion, from high concentration to low concentration (Hille 2001). Mechanisms that stimulate opening and closing of ion channels can include changes in membrane potential (most of Na^+, K^+, Ca^{2+} and some Cl^- channels), while others are relatively voltage insensitive and are ligand gated by a variety of first and second messengers or other intracellular and extracellular mediators (e.g. some K^+ and Cl^- channels, TRP channel, ryanodine receptors and IP_3 receptors) (Alexander, Mathie, and Peters 2011).

1.6.3.1 Ligand Gated Ion channels

Ligand gated ion channels are affected by receptors that include excitatory cation selective nicotinic acetylcholine receptors (Millar and Gotti 2009; Changeux 2010), 5-HT_3 (Barnes et al. 2009), (Walstab, Rappold, and Niesler 2010) ionotropic glutamate (Lodge 2009; Traynelis et al. 2010) and P_{2X} receptors (Jarvis and Khakh 2009; Surprenant and North 2009) as well as inhibitory anion selective receptors such as $GABA_A$ (Olsen and Sieghart 2008; Belelli et al. 2009) and glycine receptors (Lynch 2009; Yevenes and Zeilhofer 2011). The activation of these channels is dependent on the binding of a ligand or endogenous/exogenous modulator such as a neurotransmitter to the receptor which in turn causes a conformational change, generating an altered conducting state of the channel. These channels are predominately

expressed in the nervous system and the somatic neuromuscular junction as they mediate fast (millisecond) synaptic transmission (Alexander, Mathie, and Peters 2011).

1.6.3.2 Voltage Gated ion channels

Voltage gated ion channels undergo conformational changes following a change in the membrane potential (Nekouzadeh and Rudy 2016). Voltage gated ion channels include; sodium, calcium, chloride and potassium channels (Alexander et al. 2017).

1.6.3.3 Sodium channels

Voltage gated sodium (Na_v) channels are essential in the initiation and propagation of the action potential in excitable cells such as neurons, cardiomyocytes and skeletal muscle. The Na_v channels are made up of nine subtypes (Na_v 1.1-1.9) which are classified in accordance to the alpha subunit of the channel as it is pore forming, to mediate the transport of Na^+ ions through the membrane.   The expression and gating of Na_v channels is predominately controlled by the beta subunits (β_1 - β_4) of the channel (Yu and Catterall 2003).

1.6.3.4 Calcium channels

Voltage gated calcium channels (Ca_v) share a similar structure to voltage gated sodium channels (Na_v) with each protein is formed of four modules and six transmembrane domains, with each domain presenting a pore loop that when facing each other create the loop. In contrast voltage gated potassium channels (K^+) are mostly tetramers (four distinct proteins), each protein forms one module of six transmembrane domains with a pore loop . Voltage gated calcium channels are inward conducting channels (Ca^{2+} influx) that activate when the membrane is depolarised (Rao et al. 2015). In excitable cells, voltage gated calcium channels (Ca_v) are responsible for various physiological functions which includes the release of neurotransmitters, secretion of hormones, gene expression, intracellular signalling and muscle contraction among many other functions. Of the calcium channels, L-type and T-type are the most important in the cardiovascular system (Katz 2010).

There are also other highly Calcium selective channels including TRPV5 and TRPV6 as well as ORAI 1. The Transient receptor potential channel (TRPV5) regulates calcium transport in the kidney, while TRPV6 channel regulates calcium influx in the small intestine (van de Graaf, Hoenderop, and Bindels 2006). Overexpression of TRPV6 has been associated with solid cancers such as prostate and breast (Monteith, Davis, and Robert-Thomson 2012).Calcium release-activated calcium channel protein (ORAI 1), enhanced calcium influx when internal calcium stores are depleted within the cell. The ORAI 1 channel expression has been shown to be upregulated in breast cancer cells T-47D, MCF-7 and MDA-MB-231 when compared to normal cell lines. This upregulation of ORAI1 in basal like breast cancer has been shown to lead to poor prognosis (Azimi, Robert-Thomson, and Monteith 2014).

1.6.3.5 Chloride channels

Chloride channels regulate chloride transport across cell membranes either passively or actively. There are 10 subtypes of chloride channels identified by their mode of activation. The CLC family are voltage gated, while the CFTR group are cAMP regulated and calcium activated. The other 8 CLC types include CLC 1-7 and CLCk (which includes subtypes CLCka and CLCkb) (Rao et al. 2015). The flow of organic solutes and anions through the chloride channels is influenced by volume-sensitive organic osmolyte/anion channels (VSOAC). These organic solutes can modify cell volume and play an important role in various physiological functions including pH regulation, cell volume regulation, proliferation, trans-epithelial secretion and membrane potential stabilization (Mindell and Maduke 2001).

1.6.3.6 Potassium channels

Voltage gated K^+ channels (VGKC, K_v) are made up of 12 subtypes (K_v1- K_v12) divided into 3 categories, that allow the flow of K^+ ions across the plasma membrane and some of them are listed in Table. 3. Firstly, voltage-gated K^+ channels (6 transmembrane helices, 1 pore domain, voltage sensor) include the transient outward current (I_{to}), the outward rapid rectifier (I_{Kr}), the outward slow rectifier (I_{Ks}), the ultra-rapid outward rectifier (I_{Kur}) and the calcium-activated K^+ channel (I_{KCa}). Secondly, the ligand-gated K^+ channels (2 transmembrane helices, 1 pore domain) are the ATP-sensitive K^+ channels (I_{KATP}), acetylcholine-activated K^+ channel (I_{KAch}) (Snyders 1999; Tamargo et al. 2004; Wulff, Castle, and Pardo 2009; Schmitt, Grunnet, and Olesen 2014) and the inward rectifier (I_{K1}). Thirdly, other outward rectifiers (4 transmembrane helices, 2 pore domain) that are not listed here and are not well characterized are known as TWIK, TRAAK, TRASK, TREK , and they contribute to the resting K^+ conductance in many cells (Huang et al. 2017). Of interest in this study is the class of voltage-gated K^+ channels known as I_{Kr} (hERG channels) since they are responsible for repolarization of the cardiac action potential but are also implicated in regulating the cell cycle in both normal tissue cells and cancerous cells (Blackiston, McLaughlin, and Levin 2009).

Channel subtypes	Functional Role
Voltage gated	
Ultra-rapid outward (delayed) rectifier (I_{Kur})	Opens very early during the plateau (atrial myocytes), initiates repolarization
Rapid Outward (delayed) rectifier (I_{kr})	Opens early during the plateau, initiates repolarization
Slow outward (delayed) rectifier (I_{Ks})	Opens late during the plateau, initiates repolarization
Transient outward current (I_{to1})	Opens briefly immediately after depolarization, regulates action potential duration.
Calcium-activated potassium ($I_{K.Ca}$)	Activated by high cytosolic calcium, accelerates repolarization in calcium-overload
Ligand gated	
ATP-sensitive potassium ($I_{K.ATP}$)	Normally inhibited by ATP, opens in energy starved hearts
Acetylcholine-activated potassium ($I_{K.Ach}$)	Activated by $G_{\alpha i}$ in response to vagal stimulation and adenosine; hyperpolarize resting cells, slows SA node pacemaker, shortens the atrial action potential
Inward (anomalous) rectifier (IK_1) and two pore domain (I_{leak})	Maintains resting potential, closes with depolarization to prolong the plateau

Table 3. Potassium channel subtypes and their functions (Wulff, Castle, and Pardo 2009).

1.6.4 Human ether-a-go-go (hERG) Channel

The human ether-a-go-go (hERG) channels are responsible for the rapid (IKr) rectifier potassium current, chiefly responsible for membrane repolarisation in phase 3 of the cardiac action potential. The hERG channels belong to the ether à-go-go (EAG) family (Vandenberg et al. 2012) and generate an outward rectifying, voltage-dependent, potassium current in ventricular cardiomyocytes. There are two subunits that determine the properties of hERG channels; the α subunit $K_V11.1$ which is coded for by the KCNH2 gene, and the β-subunit MiRP1, which is coded for by the KCNE2 gene. Functional hERG channels are formed by the aggregation of four identical α-subunits encoded by the KCNH2 gene. Each α-subunit consists of six transmembrane domains (S1–S6) and intracellular amino- and carboxy-termini (Figure 7). The voltage sensor domain resides in the first four transmembrane domains, while the S5 and S6 helices form the potassium selectivity filter (Sanguinetti and Tristani-Firouzi 2006).
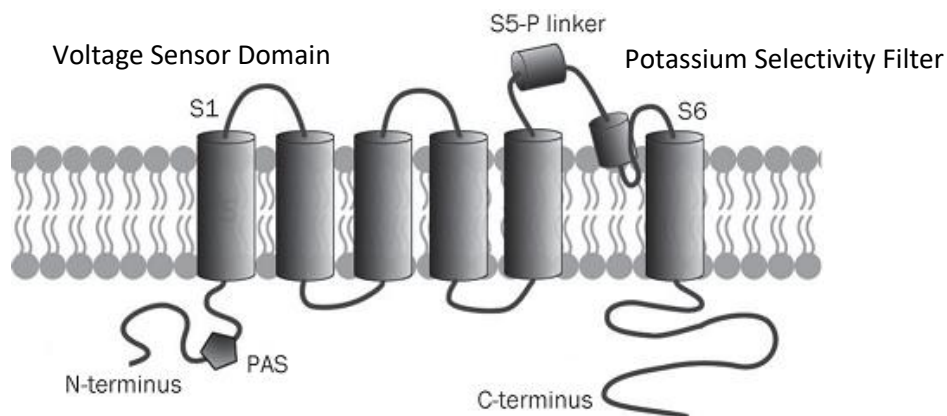
Figure 7. HERG channel subunits (Zhou et al. 2011).

hERG channels have rather distinctive gating kinetics particularly with respect to their inactivation properties (Figure 8). At the resting membrane potential (-80mV) the activation gate is closed and the channel is in a stable, non-conducting state (Perry, Sanguinetti, and Mitcheson 2010). As the membrane depolarizes, the activation gates open slowly, but as depolarization proceeds the channel enters an inactivated non-conducting state. Inactivation is strongly voltage- and time-dependent and occurs in the late depolarisation phase of the cardiac action potential. Once repolarization begins, this causes the channels to recover from the inactivated state within a few milliseconds leading to a large current tail which decays as the activation gate closes and membrane potential returns to rest (Sanguinetti and Tristani-Firouzi 2006). Therefore, hERG channels are involved in the repolarization of the cardiac action potential after the L type Ca^{2+} channels have closed.
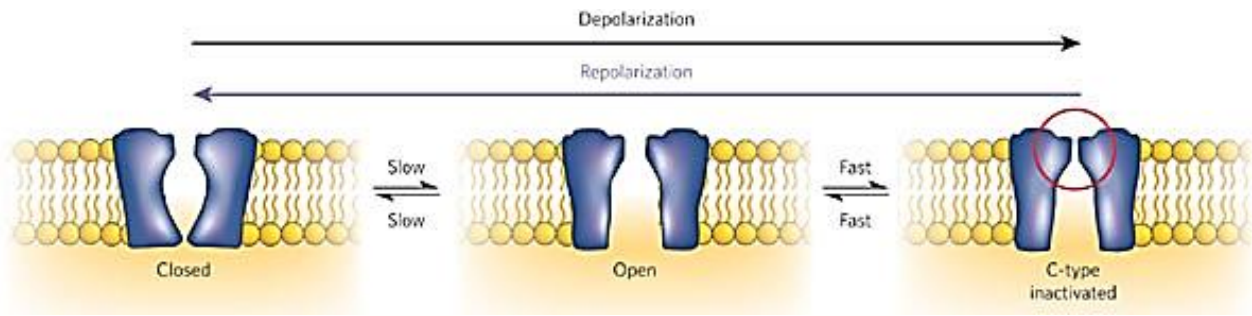
Figure 8. Illustration of the activation properties of the hERG channel (Sanguinetti and Tristani-Firouzi 2006).

1.7 Ion Channels and Cancer

Over the last two decades there has been significant research undertaken to understand the link between ion channel transporter mechanisms and cancer. Expression of voltage gated ion channels has been reported in all of stages of cancer progression in many cancer types (Pedersen and Stock 2013). Increased activity of voltage gated sodium, calcium and potassium channels has been associated with cancer malignancy due to their role in increasing proliferation, migration and survival of cancer cells (Table 4). The regulation of ion channel expression by hormones and growth factors responsible for cancer growth further links ion channels with cancer progression (Djamgoz, Coombes, and Schwab 2014).

With ion channel activity recognised as part of tumour generation and progression, cancer is now classified as a channelopathy, which is defined as a disease that is brought about by dysregulation in the function of ion channels either through alteration in the channel expression (known as transcriptional channelopathy) or through other disruptions (e.g. drug induced) which modify the function of these channels (Litan and Langhans 2015). Having been implicated in cancer progression, ion channels are now being explored as target therapies.

Voltage gated channels (Na^+, K^+, $Ca2^+$ and Cl^-) including the Kv 11.1 voltage gated potassium channels serve an important role in all stages of cancer progression from proliferation and cell cycle control to migration and metastasis (Table 4).
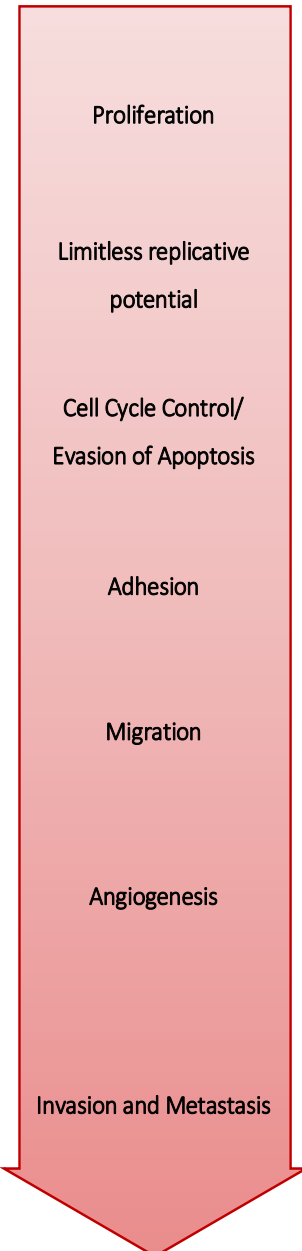
Cancer Stage	Family of Membrane Channels	Class of Channels
Proliferation	Cys loop cationic Ca^{2+} permeable Voltage gated Ca^{2+} (Ca_v) Voltage gated K^+ (K_v) Ca^{2+} activated K^+ (K_{Ca}) Inward rectifying K^+ (Kir) Background K^+ (K_{2P}) Transient receptor potential (TRP)	nAChR α7 Ca_v1 (L type), $Ca_v2.3$ (R type), $Ca_v3.2$ (T type) $K_v10.1$, $K_v11.1$, $K_v1.3$ $K_{Ca}3.1$ Kir3.1, Kir6.1 $K_{2P}2.1$, $K_{2P}9.1$ TRPC6, TRPV6, TRPM7
Limitless replicative potential	Voltage gated Ca^{2+} (Ca_v)	Ca_v1 (L type)
Cell Cycle Control/ Evasion of Apoptosis	Voltage gated K^+ (K_v) ATP dependent K^+ (K_{ATP}) Inward rectifying K^+ (Kir) Background K^+ (K_{2P}) Transient receptor potential (TRP) SOC, Ca^{2+} selective Cl^- (CLC)	$K_v10.1$, $K_v11.1$, $K_v1.3$ K_{ATP} Kir4.1 $K_{2P}9.1$ TRPV6, TRPM2 Orai1 CLC-3
Adhesion	Voltage gated Ca^{2+} (Ca_v) G protein inwardly rectifying K^+ (GIRK)	$Ca_v3.2$ (T type) GIRK1, GIRK2, GIRK4
Migration	Voltage gated Na^+ (Na_v) Voltage gated K^+ (K_v) Ca^{2+} activated K^+ (K_{Ca}) Inward rectifying K^+ (Kir) Transient receptor potential (TRP) Cl^- (CLC)	$Na_v1.5$, $Na_v1.6$, $Na_v1.7$ ASIC1 $K_v1.1$, $K_v1.3$, $K_v10.1$, $K_v11.1$ $K_{Ca}3.1$ Kir4.1 TRPM7 CLC-3
Angiogenesis	Voltage gated K^+ (K_v) Ca^{2+} activated K^+ (K_{Ca}) SOC, Ca^{2+} selective Transient receptor potential (TRP)	$K_v10.1$, $K_v11.1$ $K_{Ca}1.1$, $K_{Ca}3.1$ Orai1 TRPC3, TRPC4, TRPC6
Invasion and Metastasis	Voltage gated Na^+ (Na_v) Voltage gated Ca^{2+} (Ca_v) Voltage gated K^+ (K_v) Ca^{2+} activated K^+ (K_{Ca}) Inward rectifying K^+ (Kir) SOC, Ca^{2+} selective Transient receptor potential (TRP) Cl^- (CLC) Na^+ non-voltage gated, DEG regulated	$Na_v1.5$, $Na_v1.7$ $Ca_v3.1$ $K_v11.1$ $K_{Ca}1.1$, $K_{Ca}2.3$, $K_{Ca}3.1$ $K_{ir}3.1$ Orai1 TRPC1, TRPM1 CLC-3 ENaCα, ENaCγ, ASIC1, ASIC2

Table 4. Ion channels involved in the various stages of cancer progression. Data compiled from (Kale, Amin, and Pandey 2015), (Litan and Langhans 2015). Channels in IUPHAR format.

In non-excitable cells the resting membrane potential (Vm) tends to be relatively stable, but it is not static. The Vm fluctuates in a cyclic manner but the changes are much less dramatic than those reported in excitable cells. Membrane potential is varied locally within tissue cells in response to extracellular and intracellular signals, that may cause opening and closing of a range of plasma membrane channels. Further, Vm differs when cells progress through the cell cycle and is known to be more depolarized (less negative) in proliferating cells than nonproliferating cells (see reviews (Blackiston, McLaughlin, and Levin 2009; Yang and Brackenbury 2013a)). For example, mesenchymal cells (Sundelacruz, Levin, and Kaplan 2013), You et al, 2013), cardiomyocytes, and vascular smooth muscle (Jia et al. 2013). Controlled variations in Vm are also recognized for appropriate embryonic tissue development, such as nerves and cardiac muscle (van Kerrebroeck et al. 2003; Uriu-Adams and Keen 2010; van Vliet et al. 2010; Kleger and Liebau 2011; Ring et al. 2012; Podda et al. 2013).

1.7.1 Ion Channels - Regulation of Cell Cycle Phases

Cancerous cells in general have a less negative (more depolarized) Vm than non-proliferating cells which is due to elevations in intracellular Na^+, K^+, and may be associated with reduced intracellular Cl^- concentrations. Any alteration in channel conductance that affects the rhythmic cycle in cancerous cells (alternating hyperpolarized and depolarized Vm states) will likely disrupt proliferation (as in tumour formation) or induce cell cycle arrest (leading to apoptosis and necrosis).

Since the landmark work of Clarence D. Cone in the 1960's who identified that the membrane potential (Vm) of sarcoma cells was directly related to progression through the cell cycle (Cone 1969) , it is now recognize that during G1/S transition Vm becomes hyperpolarized, while the transition through the G2/M phase requires a more depolarized Vm (Blackiston, McLaughlin, and Levin 2009; Freedman, Price, and Deutsch 1992). Many of the ionic currents and channels responsible for these variations in Vm during the cell cycle have been identified (see Figure 9 below). There are many different potassium channels involved in regulation of the cell cycle, some of which promote a more negative Vm (e.g. Kv1.3, Kv1.5 Kv10.1 and Kv11.1 or hERG channels), while others reduce the Vm to more positive values (e.g. $K_{Ca}3.1$). Among the many K^+ channel types involved in Vm regulation, hERG channels that normally allow K^+ efflux (moving Vm towards more hyperpolarizing values) appear to have a significant role in cell cycle regulation. There is increased hERG conductance between G1 and S phases, but the channels are inactive during G2 and M phases (Becchetti 2011; Rao et al. 2015).
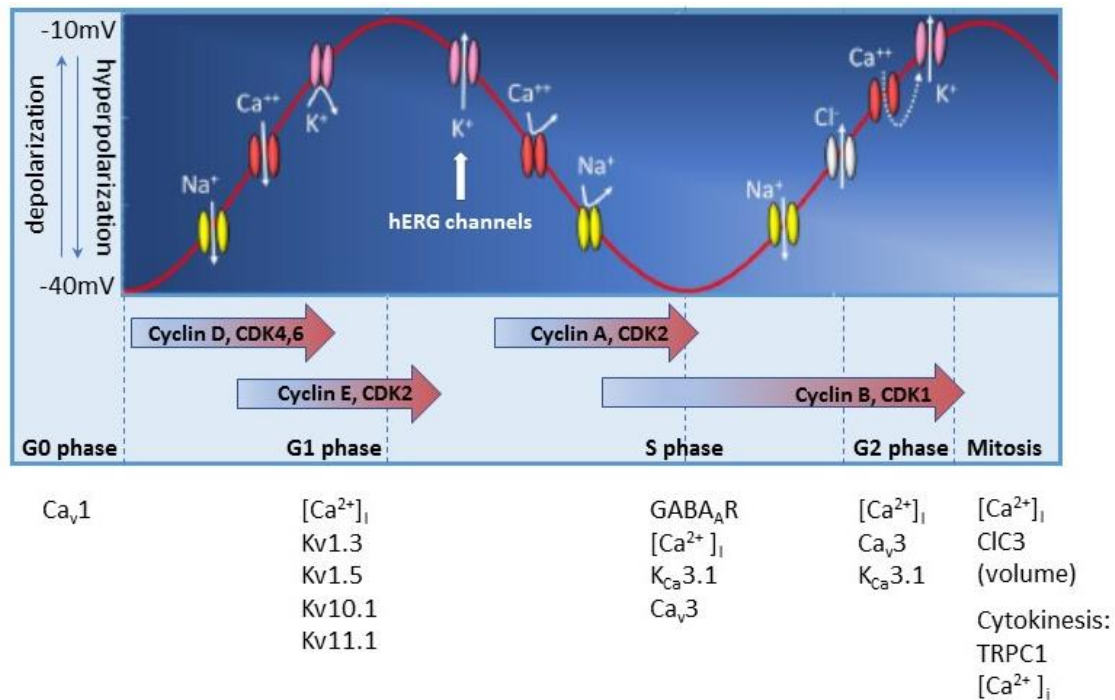
Figure 9 Diagram illustrating phases of the cell cycle and changes in membrane potential (Vm). Known ion channels and ionic conditions are listed below as well as the Cyclins for each phase. ↑Current,⌐|No current adapted from (Becchetti 2011; Rao et al. 2015) .

1.7.2 Ion Channels - Regulation of Apoptosis

Apoptosis is a type of programmed cell death that is fundamental to normal embryonic development, morphogenesis and normal tissue repair, but when dysregulated has an integral role in tumour development and progression (Kondratskyi et al. 2015).   Regulation of apoptosis is highly complex with a multitude of signalling pathways, receptors, enzyme systems and molecules involved often with feed forward and feedback loops (Kondratskyi et al. 2015; Rao et al. 2015).   Ion channels are also members of this complex system providing influx and efflux of cations and anions that activate many intracellular steps in both the extrinsic and intrinsic apoptosis pathways.   Among their important roles, ion channels provide the ions for changes in membrane potential, cell volume and as docking stations for intracellular systems (e.g. MAP kinase pathway) (Rao et al. 2015).   There are members of the 4 key classes of ion channels indicated in the regulation of apoptosis; Na^+, K^+, Ca^{2+} and Cl^- channels. Ion channels involved in apoptosis are not restricted to the plasma membrane (PM), there are several important ion channels found on the mitochondrial membrane (MM) and associated with the endoplasmic reticulum (ER) as can be seen in Figure 10 (below).

Among the huge family of K^+ channels found in cancer cells, some have been identified as key modulators of the cell cycle (e.g. $K_v1.3$, $K_v1.5$, $K_v10.3$, $K_v11.1$, $K_{Ca}3.1$), so inhibition of these channels often induces apoptosis (Becchetti 2011; Rao et al. 2015) . A characteristic

feature of apoptosis is cell shrinkage, and this is strongly linked to K$^+$ loss since cytoplasmic water leaves the cells when these channels are opened (Bortner and Cidlowski 2007).

Considering that K$^+$ efflux is proposed to be a pro-apoptotic factor, modulation of K$^+$ channels may be an excellent candidate for apoptosis regulation (Kondratskyi et al. 2015). However, knowledge of the K$^+$ channels in different cell types is important since their expression is so varied. For example, inhibition of Kv11.1 (hERG channels) has been shown to reduce proliferation and activate apoptosis (Wang et al. 2002; Jehle et al. 2011) resulting in cell death in human small cell lung cancer (Glassmeier et al. 2012) and human glioblastoma cells (Staudacher et al. 2014). Another PM channel, Kv10.1 is inhibited by imipramine (an antidepressant) inhibiting proliferation by apoptosis in ovarian cancer (Asher et al. 2011), osteosarcoma (Wu et al. 2013) and small cell lung carcinoma (Jahchan et al. 2013), but in melanoma cells apoptosis is not induced (Gavrilova-Ruch et al. 2002). On the mitochondrial membrane, Kv1.3 inhibition using cell permeant compounds mediates apoptosis and inhibits tumour growth *in vivo* via both the extrinsic and the intrinsic pathways (Szabò et al. 2005). Also, Kv1.5 activity and expression are suppressed in various cancer lines, including breast cancer cell lines, which when returned to normal activity inhibits cell growth via apoptosis (Bonnet, Archer, Allalunis-Turner, Haromy, Beaulieu, Thompson, Lee, Lopaschuk, Puttagunta, and Bonnet 2007).
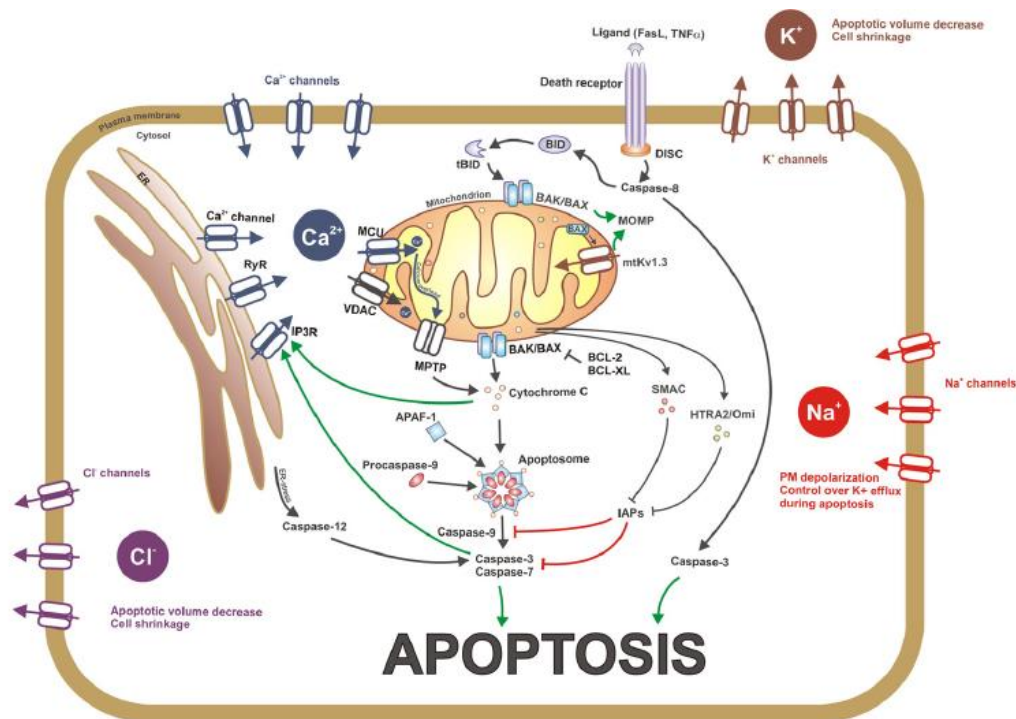
Figure 10. Ion channels involved in the regulation of cellular apoptosis (Kondratskyi et al. 2015).

There have been several studies indicating that Ca^{2+} is an important regulator of apoptosis at all stages, from initiation to final phagocytosis of apoptotic bodies (Orrenius, Zhivotovsky, and Nicotera 2003; Pinton et al. 2008). Cytoplasmic Ca^{2+} overload is known to stimulate mitochondrial Ca^{2+} uptake triggering the intrinsic apoptotic pathway (Hajnóczky et al. 2006; Kroemer, Galluzzi, and Brenner 2007; Giorgi et al. 2012). Rise in intracellular Ca^{2+} also activates calpains (cysteine proteases) which mediate cleavage of many BCL-2 family members (BID, BCL-2 and BCL-XL), and promotes MOMP and Cyto C release (Chen et al. 2001; Gil-Parrado et al. 2002).

A variety of Ca^{2+} channels on the PM (e.g.Ca_v1, Ca_v3), the MM (e.g. Mitochondrial Ca^{2+} uniporter, MCU and voltage-dependent anion channel, VDAC) and ER (ryanodine receptor, RyR, and IP_3 receptor, IP_3R) regulate calcium homeostasis in cells (Berridge, Bootman, and Roderick 2003; Rizzuto et al. 2012). Since Ca^{2+} is an important intracellular messenger involved in the activation of many biochemical pathways, it is not surprising that one of them is apoptosis. Among the PM Ca^{2+} channels (Ca_v1, Ca_v2 and Ca_v3), overexpression of $Ca_v3.1$ suppressed cell proliferation and increased apoptosis in MCF-7 breast adenocarcinoma cell line, but overexpression of $Ca_v3.2$ did not (Rostovtseva and Bezrukov 2008). Further, there was a differential distribution of $Ca_v3.1$ and $Ca_v3.2$ channels on PM of apoptotic and non-apoptotic cells. Blocking of Ca_v3 channels with mibefradil and pimozide reduced cell viability and induced apoptosis (Tan and Colombini 2007) in part by decreasing phosphorylation of Akt, Rictor and activating caspases (Vander Heiden et al. 2000). Genetic knock down of Ca_v1 channels however, had no effect on proliferation or apoptosis (Vander Heiden et al. 2000).

The MCU on the inner mitochondrial membrane is a selective Ca^{2+} pore for influx, while the VDAC on the outer mitochondrial membrane carries many anionic species but is more permeable to Ca^{2+} in its closed state (Vander Heiden et al. 2000; Tan and Colombini 2007). Both transporters can induce mitochondrial Ca^{2+} overload which triggers the mitochondrial permeability transition pore (MPTP) or activates the pore-forming activity of pro-apoptotic members of the BCL-2 protein family (Tait and Green 2010; Leanza et al. 2014). The resulting mitochondrial outer membrane permeabilization (MOMP) causes loss of the mitochondrial transmembrane potential ($\Delta\Psi_m$), arrest of mitochondrial ATP synthesis and release of pro-apoptotic proteins from the intermembrane space into the cytoplasm (Kondratskyi et al. 2015). Decreased expression of MCU has been associated with human colon cancer and prostate cancer cells protecting themselves from induction of apoptosis (Marchi et al. 2013) but in oestrogen receptive negative (MDA-MB-231) and basal-like breast cancers it is over expressed, and knockout did not affect apoptosis (Curry et al. 2013). It appears that Ca^{2+} influx may not be as important for triggering apoptosis in these breast cancer cells. The contribution of VDAC to apoptosis appears to be isoform specific with $VDAC_1$ regarded as pro-

apoptotic and VDAC$_2$ as anti-apoptotic (Cheng et al. 2003; Tajeddine et al. 2008). VDAC$_1$ is physically liked to the IP$_3$R on the ER via the molecular chaperone glucose-regulated protein 75 (GRP75) providing a direct pathway for Ca^{2+} transfer from ER to mitochondria (Szabadkai et al. 2006). VDAC$_2$ does not form complexes with IP$_3$R which suggests it is not involved in Ca^{2+} transmission (De Stefani et al 2012) and is less involved in apoptosis induction.

Multiple PM voltage-gated Na$^+$ channels (Na$_v$) are expressed in many cancers with Na$_v$1.5 being most abundant in breast and colon cancer cell lines (Fraser et al. 2005) while Na$_v$1.6 in cervical cancer and Na$_v$1.7 in prostate cancer (Roger et al. 2006). Some cancers alternatively express neonatal isoforms such as neonatal Na$_v$1.5, Na$_v$1.7 and Na$_v$1.9 (Brackenbury et al. 2007). Of importance is that Na$_v$ expression and activity is enhanced in strongly metastatic breast cancer cell lines (i.e. MDA-MB-231) compared with the weakly metastatic MCF-7 cell lines (Roger, Besson, and Le Guennec 2003). Further, reducing the expression or conductance (e.g. tetrodotoxin blockade) of Nav channels does not alter proliferation (Anderson et al. 2003; Nakajima et al. 2009; Davis et al. 2012) in MDA-MB-231 cells nor androgen-independent prostate cancer (Fraser et al. 2005; Fraser et al. 2014; Nelson et al. 2015). Indeed, phenytoin (an anti-convulsing drug) which is known to block Nav is very effective in reducing not only invasion and metastasis in MDA-MB-231 breast cancer cells, but also proliferation (Fraser et al. 2005; Fraser et al. 2014; Nelson et al. 2015) but this may not be by Nav blockade *per se.*

The chloride channels (CLC 1-7, CLCka and CLCkb) are also involved in cell cycle regulation, particularly CLC2 and CLC3 (Habela et al. 2009; Hong et al. 2015) being involved in the accurate control of cell volume and pre-mitotic condensation (PMC) that occurs prior to mitosis (Habela and Sontheimer 2007). Cl$^-$ conductance increases in the M phase and expression of CLC3 is increased in the PMC phase to further enhance its actions (Rao et al. 2015). Knockout of CLC3 caused increased length of the cell cycle via disrupted volume control in nasopharyngeal, endometrial and ovarian cancer (Li, Wang, and Lin 2008; Xu et al. 2010; Li, Wu, and Wang 2013). If the cell cycle is stalled, this may lead to induction of apoptosis. There may be a role of targeting the inhibition of chloride channels in the treatment of some cancers.

1.8 hERG Channels in Cancer

Among the voltage gated K^+ channels, hERG channels were one of the first voltage gated potassium channels discovered to play a role in the survival and progression of tumours (Hemmerlein et al. 2006). Studies have shown that hERG channels are expressed in a variety of cancer cell lines and tissues with expression indicative of the aggressiveness and metastasis of tumours. In electrically excitable cells, hERG channels are involved in membrane potential changes, but in cancer cells hERG channels appear to be also involved in proliferation, cell cycle control and apoptosis (Wulff, Castle, and Pardo 2009).

1.8.1 Expression of hERG Channels in Cancer

The overexpression of hERG channels, has been associated with worse prognoses and considered a marker for cancer diagnosis in several solid and haematological cancers (Lastraioli et al. 2004; Shao et al. 2008; Smith et al. 2002; Ding et al. 2010). hERG channel expression has been reported in early stage cancers, with more variable expression as the neoplasia develops, while there is either little or no hERG expression in the non-cancerous comparable tissue. hERG channel expression has been assessed in various cancer types, in cell lines, *in vivo* models and primary tumour biopsies.

1.8.2 mRNA and Protein Expression Assessed in Cell Lines

Quantitative analysis has been conducted at both the mRNA and protein levels. At the mRNA level, normal rat brain and heart express an mRNA transcript of about 4.4kb, representing the full-size transcript for hERG (Bianchi et al. 1998). However, in various cancer cell lines, multiple mRNA transcripts exist ranging in size from 2.2kb to the full size 4.4kb, suggesting alternative splicing of the hERG mRNA may occur in cancer phenotypes. The smaller transcripts generally lack parts of or most of the NH_2 terminus of the hERG channel and generally have faster deactivation kinetics (Bianchi et al. 1998). The different bands were also expressed at different concentrations depending on the cell line. In two neuroblastoma cell lines (SH-SY5Y) three bands were obvious, 4.4, 2.9 and 2.4, with the 4.4kb size the most dominant (Zhao et al. 2008). While in SK-NBE the same three bands were apparent, but the 2.9kb was the most dominant suggesting a possible functional difference in activation kinetics (Bianchi et al. 1998). Other non-nervous tumours were also assessed resulting in mRNA bands of similar size, rhabdomyosarcoma (TE671), breast adenocarcinoma (SK-BR3) (Bianchi et al. 1998) and cellosaurus cell line (NCI-N592) all expressing the 4.4, 2.9 and 2.4kb mRNA with the 4.4 and 2.9kb transcripts being most dominant (Bianchi et al. 1998). In monoblastic leukaemia (FLG29) a different transcript expression was documented, 4.0 and 2.2kb, with the smaller transcript being the most dominant (Bianchi et al. 1998).

Western blot analysis was typically used to assess hERG protein size and abundance in many cancer cell lines. Most studies identified 2 dominant bands, one at about 150kDa corresponding to the mature, fully glycosylated hERG protein, while the smaller band of about 135kDa represented the partially glycosylated, immature hERG protein. Normal tissue cell lines, including ovarian (CHO) and fibroblasts, did not express any hERG protein. However, hERG protein was found in several types of cancer cell lines, including breast adenomas (MCF-7), breast adenocarcinomas (SKBr3 and MDA-MD-231) (Lansu and Gentile 2013) and pancreatic cancers (PANC-1, MIAPaCa-2 and BxPc-3) (Lastraioli et al. 2015). There was variability in expression in pancreatic cancers, high levels expressed in PANC-1 cells (85%), with moderate protein expression seen in MIAPaCa-2 cells (76%) and the lowest level of expression observed in BxPC-3 cells (5%), with minimal expression detected in normal pancreatic tissues (Lastraioli et al. 2015), showing that hERG expression is higher in the early stage PANC-1 and MIAPaCa-2 cells than the later stage BxPC-3 cells. The 155kDa hERG channel protein was expressed in human colon carcinoma cell lines HCT116 and HT-29. While in gastric cancer, western blot analysis showed a significant upregulated expression of hERG protein in several cancer cell lines (SGC7901, AGS, MGC803 and MKN45) (Shao et al. 2008), compared with the immortalised epithelial cell line (GES).

1.8.3   hERG Expression Assessed in Patient Biopsies

hERG channel expression has also been assessed in biopsies taken directly from cancer patients. Biopsies from patients with oesophageal squamous cell carcinomas (ESCC), showed negative expression of hERG mRNA in 11 non-cancerous tissues using PCR, while it was highly expressed in ESCC. Protein expression using pathologist assessment of immunohistochemistry staining of hERG channels revealed that of the 68 patients examined hERG protein expression was observed in 53 patients (77.9%) and negative in 15 (22.1%), compared with no expression in the tissue matched control group (Ding et al. 2008).

hERG channel expression has also been identified as an indicator of worse of prognosis in several types of cancers including oesophageal adenocarcinoma (Ding et al. 2008), colorectal cancer (Lastraioli et al. 2012), pancreatic ductal adenocarcinoma (Feng et al. 2014), and endometrial cancer (Cherubini, Taddei, Crociani, Paglierani, Buccoliero, Fontana, Noci, Borri, Borrani, and Giachi 2000). Opposing this, hERG channel expression in breast adenocarcinomas (Bianchi et al. 1998; Lansu and Gentile 2013; Iorio et al. 2018) and gastric tumours (Shao et al. 2008) indicate high expression early in cancer progression, decreasing as the malignancy develops.

Oesophageal biopsies from 90 patients with varying diagnoses was obtained, including normal tissue, patients suffering from gastroesophageal reflux both with and without esophagitis, and

samples from patients diagnosed with Barrett's oesophagus (BE a precursor to cancer) and oesophagus adenocarcinomas (ADKs). Samples were assessed using immunohistochemistry (protein) and RT-PCR (mRNA). No expression was identified in normal tissue or patients with gastro-oesophageal reflux symptoms. However, results indicated that 69% of patients with BE expressed increased protein levels of hERG channels. When 6 samples of patients diagnosed with oesophagus adenocarcinomas (ADKs), that had been previously diagnosed with BE were analysed for hERG protein expression, results showed 89% of those patients displayed higher expression (Lastraioli, Taddei, Messerini, Comin, Festini, Giannelli, Tomezzoli, Paglierani, Mugnai, De Manzoni, et al. 2006). Results indicated, expression of hERG channels increased as the malignancy developed and progressed in oesophagus adenocarcinomas.

Analysis of samples from 135 patients diagnosed with stage I to stage III colorectal cancer (CRC) for hERG channel expression confirmed it to be an indicator of progression and worse prognosis. hERG channels were expressed in the cytoplasm of the cells and the tumour stroma in 23% of samples tested. Furthermore, hERG positivity and Glut-1 negativity was shown to be an indicator or worse prognosis of CRC in patients suffering from stage I and II (Lastraioli et al. 2012).

There are some types of cancers that display the opposite effect, initially high levels expressed during early stages decreasing as the cancer progresses. This could also be reflective of the changing type or size of the hERG expressed. Tissue Biopsies from 40 patients diagnosed with different molecular subtypes of breast cancer. There were 4 subtypes involved; Luminal A (ER+ and/or PgR+,HER2-, Low Ki67),which is an early stage slow growing tumour subtype, the faster growing tumour subtype of Luminal A (ER+ and/or PgR+, HER2-, high Ki67 or ER+ and/or PgR+, HER2+, any Ki67). There were also fast-growing luminal cancer HER2-enriched tumours (ER-,PgR-, HER2+) and basal-like tumours also known as triple negative (ER-,PgR- and HER2-). Immunohistochemical staining showed hERG expression in all samples, with the highest being in Luminal A samples with favourable prognosis and the lowest being in basal-like samples that has worse prognosis (Iorio et al. 2018).

1.9 Function of hERG Channels in Cancer

One of the methods used in the assessment of hERG channel activity and its subsequent impact in cancer cells is through the manipulation of hERG activation kinetics using either commercially available hERG channel modulators or siRNA technology that silences protein expression. Results indicate that modulating the activity of hERG channels alters several cell characteristics that promote survival, including proliferation and apoptosis (summarised in Table 5 below).

1.9.1 hERG Channel Modulation of Proliferation in Cancer

Inhibition of hERG channels, causing voltage changes due to the blockage of K^+ efflux, has been linked to the slowing of cell growth as it stops the cells from undergoing transient hyperpolarisation (resulting in continuous depolarization) and arrests the cell cycle (Pardo 2004).

The action of the macrolide antibiotic, erythromycin as a chemo sensitizing, agent used in conjunction with chemotherapeutic drugs vincristine, paclitaxel and 10-Hydroxycamptothecin (HCPT) has been extensively studied previously (Chen, Jiang, and Zhen 2005).

Cancer Type	Cell Line	hERG channel modulator	Proliferation	Cell Cycle phase (Accumulation)	Cell Death	Reference
Lung cancer	SW2, OHI, OH3 and H83	E-4031	Nil	NR	NR	Glassmeier et al. 2012
	Highly metastatic human lung giant cell carcinoma	Erythromycin + Vincristine	+	++ (G1)	NR	Chen et al. 2005
Human colon cancer cell lines	HT29	Erythromycin + Vincristine	++	Nil	NR	Chen et al. 2005
	H630, DLD1, HCT116	Way 123,398 and E-4031	NR	NR	NR	Lastraioli et al. 2004
	HCT116, HCT8, HT29		NR	NR	NR	Crociani et al. 2013
Human leukaemia cell line	K562	Gambogic acid	+	++ (G0/G1)	++	Cui et al. 2009
	K562, CEM, U937, HL60	E-4031	+ - (HL60)	Nil	Nil	Smith et al. 2002
	FLG 29.1	CsCl, E4031 and Way 123,398	++	+ (G1)	Nil	Pillozzi et al. 2002
Human gastric cancer	SGC7901, AGS, MGC803, MKN45	Cisapride	++	++ (G1/S)	++	Shao et al 2005
Melanoma	MDA-MB-435S	E-4031	++	-	NR	Afrasiabi et al. 2010
	A375	NS1643	++	++	++	Perez-Neut et al.2016
Human neuroblastoma	LNT-229 U87MG	Doxazosin	++ +	++ (G0/G1)	++ ++	Staudacher et al. 2014
Human embryonic kidney cells	HEK-293	Cisapride	++	-	NR	Afrasiabi et al. 2010
	HEK-293	Doxazosin	NR	NR	++	Thomas et al. 2008
Human mammary adenocarcinoma	MCF-7	Erythromycin	++	-	NR	Chen et al. 2005
	MCF-7	Astemizole E-4031 Imipramine	++ - -	NR	NR	Roy et al. 2008
	SKBR3 MDA-MB-231	NS1643	++ ++	++ (G1)	- Nil	Lansui et al. 2013
	MDA-MB-231	NS1643	++	NR	NR	Fukushiro-Lopes et al. 2018

Key: NR- not reported; Nil – no effect; + some inhibition; ++ strong inhibition

Table 5. Summary of varous hERG channel modulators on different cancer cell lines.

The influence of erythromycin on hERG channel activity, directly impacting proliferation in various cancer cell lines including HT-29, T84, MCF-7, PG and A549 was assessed using MTT cell proliferation assay. Results of the assay showed inhibition of proliferation in all the cancer cell lines.

Cisapride, a serotonin $5HT_4$ agonist, has been shown to have antiproliferative effect in MDA-MB-435S cells, siRNA also caused downregulation of hERG, leading to decreased proliferation in MDA-MB-435S cells (Afrasiabi et al. 2010). An MTT proliferation assay was conducted in gastric cell lines SGC7901, AGS, MGC803 and MKN45 following exposure to Cisapride, showed that it inhibited proliferation in a progressive manner such that with longer exposure, there was more retardation of cell growth (Shao et al. 2005).

Gambogic acid (GA), a natural compound, is an anti-tumour agent used to activate caspase and induce apoptosis in T47D breast cancer cells (Zhang et al. 2004). In human leukaemia K562 cells, gambogic acid inhibited hERG channels with a subsequent decline in proliferation. This growth inhibition was attributed to the irreversible cell cycle arrest at the G0/G1 phase (Cui et al. 2009). Inhibition of hERG channels using various repurposed cardiovascular drugs known to modulate hERG channel activity indicate an effect on cellular proliferation, arresting most cell lines in G1 phase of the cell cycle, but appears to be cancer cell specific.

E-4031 an experimental class III antiarrhythmic drug that blocks potassium channels of the hERG type (Kurokawa et al. 2008), was first used to assess the function of hERG channels in cancers. In lung cancer cells lines, SW2, OH1, OH3 and H82, E-4301 inhibited hERG channel activity, detected using the whole cell patch clamp, but failed to show an impact on proliferation, assessed using the colorimetric XTT assay (Glassmeier et al. 2012). However, in the neuroblastoma cell line SHSY5Y, inhibition of hERG channels by E-4301 reduced proliferation (Crociani et al. 2003). Both studies demonstrated the presence of hERG channels in these cancer cell models but failed to confirm their effect on proliferation.

Given the therapeutic potential in cancer cells, other antiarrhythmic and cardiovascular medications were also assessed, including E-4031, caesium chloride (CsCl) and the antiarrhythmic drug, Way 123,398. In leukaemia cell lines, FLG 29.1, K562, HL60, CEM and U937, hERG channel inhibition had anti-proliferative activity, arresting their cell cycle in G1 phase (Pillozzi et al. 2002; Smith et al. 2002). In these studies, hERG channel modulators with quite distinct chemical structures were all successful in reducing hERG channel current.

The inhibition of hERG channels by quinazoline compound doxazosin, an α_1 receptor antagonist, traditionally used in the treatment of high blood pressure, was assessed in a human glioblastoma cell line, LNT-299 using the colorimetric cell proliferation assay (XTT).

Results showed inhibition of proliferation which was due to the inhibition of hERG channels in these cells (Staudacher et al. 2014).

In another study the histamine receptor (H_1 receptor) antagonist astemizole was investigated since it was withdrawn from the market in 1999 due to HERG channel inhibition in cardiomyocytes (Rampe and Brown 2013). Astemizole inhibited hERG channels in MCF-7 cells leading to reduced proliferation, but E-4031 had no effect (Roy et al. 2008).

Gene silencing is advanced technology used to explore hERG channels as a target in cancer therapy, where siRNA is used to inhibit the expression of hERG proteins. In human metastatic gastric carcinoma cells SGC7901 knocking out hERG protein expression using siRNA led to inhibition of proliferation (Shao et al. 2008).   Silencing the hERG gene in human neuroblastoma SHSY5Y cell line through shRNA-hERG1 and shRNA-hERG1/1b plasmid vector construction caused inhibition in the proliferation of these cells both *in vitro* and *in vivo* (Zhao et al. 2008).

Research is now focusing on the use of hERG channel activator agents such as the diphenyl urea derivate, NS1643, which appears to enhance the action of hERG channels in cardiomyocytes; but there has been little research conducted in cancer cell lines (Hansen, Diness, et al. 2006a; Rao et al. 2015). The effect of NS1643 on cell growth (using the trypan blue assay) was conducted on human melanoma and cell growth was inhibited (Perez-Neut et al. 2016), even though the hERG channels were now being stimulated. In breast cancer cell lines NS1643 inhibited SKBR3 cells more than MDA-MB-231 cells (Lansu and Gentile 2013). The variability in the response was attributed, in part, to the differences in hERG channel expression. In the MDA-MB-231 xenograft model, injected intraperitoneally with NS1643, led to a significant reduction in tumour growth compared with the control group (Fukushiro-Lopes et al. 2018).

1.10 hERG channel role in Apoptosis

Studies have shown that sodium, calcium, chloride and potassium ion channels are involved in regulation of apoptosis (1.7.2 Ion Channels – Regulation of Apoptosis).   The pharmacological manipulation of potassium channels, including hERG channels, has been shown to increase tumour cell apoptosis which is also reviewed in Table 5 (Pillozzi et al. 2011; Suzuki et al. 2012; Gong et al. 2010; Ganapathi, Kester, and Elmslie 2009).

Different methods have been employed in the investigation of hERG channel induction of apoptosis. siRNA technology where specific protein expression is inhibited is one of the methods used to assess induction of apoptosis. When used in the human gastric cancer cell

line SGC7901, apoptosis Annexin V/PI staining showed an increase in the apoptotic cell population when compared to control cells (Shao et al. 2008).

Direct exposure to test compounds with anti-tumour drugs and hERG channel antagonist gambogic acid (GA) has been used to investigate its potential to induce apoptosis in the leukemic cell line, K562. Annexin V staining used to evaluate the induction of apoptosis showed that GA did significantly increase the apoptotic cell population (Cui et al. 2009).

More established pharmaceutical tools such as the hERG antagonists, Cisapride and doxazosin, have been used in to investigate hERG channel activity causing induction of apoptosis. When human gastric cancer cell line SGC7901 was exposed to Cisapride, Annexin V/PI analysis showed increased apoptotic cell population. Exposing human glioblastoma cell line LNT-229 and U87MG and human embryonic kidney cells transfected to express hERG (HEK-293) to doxazosin also enhanced the apoptotic population in those cells (Staudacher et al. 2014; Thomas et al. 2008), indicating that both of these hERG channel antagonists can induce apoptosis leading to reduction in tumour cells. Not all hERG channel antagonists induce apoptosis. When human leukemic cell lines FLG 29.1, K562 and HL60 were exposed to E-4031, Way 123,398 and CsCl both in combination and individually, cytofluorimetric analysis showed no increase in the number of apoptotic cells (Pillozzi et al. 2002).

hERG channel agonists have also been assessed for the induction of apoptosis in breast cancer cells. Breast cancer cell lines SKBR3 and MDA-MB-231 were exposed to NS1643, but no apoptosis was recorded (Lansu and Gentile 2013). In melanoma cell line A375, NS1643 caused significant G2/M cell cycle arrest due to the activation of senescent programming by increasing p21Waf and p16INK4A (Perez-Neut et al. 2016). In the melanoma cell lines, upregulating hERG channels activated a senescence pathway.

1.11 Aims of this research project

Several studies have indicated an important role for hERG channels in various cancers, with respect to cancer development and progression. But with the differing expression patterns and truncated forms of hERG channels in different cancers, it is unclear the true impact they have in breast cancer. This study will investigate the role of hERG channels in two different cell lines representing hormone positive and hormone negative subtypes of breast cancer cells (MCF-7 and MDA-MD-231).   Using immunohistochemistry, the cellular location of hERG channels in these breast cancer cell lines will be confirmed, while several proliferative and apoptotic assays will explore the functional role of hERG channels in breast cancer.

To confirm hERG channels have a role in these two breast cancer models, a known agonist, NS1643, which has been reported to be of potential therapeutic benefit in breast cancer, will be used to identify how its presence alters proliferation, cell cycle progression, apoptosis and necrosis.

Building on current research opinion that modulation of hERG channels may be therapeutically beneficial in breast cancer, a selection of structurally related compounds (urea or thiourea containing quinazolin-4-one) to NS1643 (a diphenyl urea) will be tested for the first time to determine whether they modulate hERG channels and how they compare with NS1643 in altering proliferation, cell cycle progression, apoptosis and necrosis. From these initial results some simple structure-activity relationships regarding their effect on the breast cancer cell lines will be explored.

Finally, during drug discovery, the off-target side effects always need to be considered and since blocking hERG channels in the heart (resulting in long QT syndrome) is recognized as a significant cancer therapy side effect, some initial investigation into cardiac cytotoxicity and hERG channel modulation by NS1643 and the quinazoline-4-one derivatives will be conducted on cardiomyocytes.

Chapter 2 - Materials and Methods

2.1 Cell Lines

2.1.1 Breast adenocarcinoma cell lines

Human breast cancer cell lines, MCF-7 and MDA-MB-231, were obtained from the American Type Culture Collection (ATCC, Victoria, Australia) in freeze media vials and stored in liquid nitrogen (-80°C) until used.

MCF-7 cells were originally isolated from a pleural effusion sample from a 69 year old female patient with breast adenocarcinoma, at the Michigan Cancer Foundation in 1973 (Welsh 2013). It is a non-invasive cell line, of an advanced tumour with a doubling time of 29 hours. It is a hormone positive cell line for breast cancer due to the presence of functional oestrogen receptors and its requirement for oestrogen for growth both *in vitro* and *in vivo*.

A hormone negative cell line for breast cancer is MDA-MB-231. It originated from a pleural effusion sample from a 51-year-old Caucasian female patient with invasive ductal carcinoma and was extracted at M D Anderson Cancer Centre (Welsh 2013), with population doubling time of 38 hours. It is a cell line that is oestrogen, progesterone and growth factor receptor (HER2) negative. These characteristics are responsible for the invasive nature of the cell line *in vivo* causing it to spontaneously metastasize to lymph nodes when grown as a xenograft model (Welsh 2013).

2.2 Cell Culture

The cells were cultured in a sterile cell culture media (DMEM/F12 (HEPES), Thermofisher Scientific, Australia) completed with 10% foetal bovine serum (FBS, Focus Bioscience, Australia) in accordance with the guidelines supplied by ATCC.

2.2.1 Establishing the cell line

After removal of the primary culture vial from the liquid nitrogen and thawing in a sterile manner, the contents of the vial were added to a 15 mL centrifuge tube (Greiner, Interpath, Australia) containing 5 mL of sterile cell culture media. The tube was centrifuged for 5 minutes at 200g (Heraeus Biofuge Primo centrifuge, K.I. Scientific, Australia). The supernatant was discarded, and the pellet resuspended in 1 mL of sterile cell culture media.

The cell suspension was then added to a 75 mL sterile flask (Greiner, Interpath, Australia) containing 20 mL of cell culture media. Then the flask was placed in a Heracell 150i CO_2 incubator to allow cell growth at 37°C and 5% CO_2, until 80% confluent. To obtain the best results, in accordance with the supplier's recommendations both MDA-MB-231 and MCF-7 cells were sub cultured to passage 25 only.

2.2.2 Passaging or trypsinisation of cells

Once cells reached 80% confluence, or following any treatment, cells were washed with 10mL of sterile 0.01M phosphate buffer solution (PBS) to remove any traces of cell culture media. Sterile Trypsin-EDTA 0.05% (5 mL - 0.5g/500mL trypsin and 0.2g/500mL EDTA, Sigma-Aldrich, Australia) was then added to the culture flask to detach adherent cells. To optimize trypsin activity, the flask was placed back in the incubator at $37^{\circ}C$ and 5% CO_2 for 2-5 minutes. The subsequent cell suspension was transferred to a centrifuge tube containing 5 mL of cell culture media to inactivate the trypsin. Finally, the suspension was centrifuged at 200g (Heraeus Biofuge Primo centrifuge, K.I. Scientific, Australia) for 5 minutes to obtain a cell pellet from which cells were cultured again for the individual experiments.

2.2.3 Primary Cardiomyocytes

In cardiovascular research, sheep cardiomyocytes are commonly used as an inexpensive model for investigating calcium dynamics (Walweel and Laver 2015). Sheep hearts were obtained from Hardwick's abattoir in Kyneton, Victoria, from freshly killed animals. The heart was immediately flushed in ice cold Krebs-Henseleit mammalian Ringer (KHMR) to remove all traces of blood and transported on ice back to the laboratory. The KHMR comprised (mmol L^{-1}): NaCl (118), KCl (4.75), KH_2PO_4 (1.18), $MgSO_4$ (1.18), $NaHCO_3$ (24.80) and D-glucose (10). Prior to use, the KHMR was carbogenated (95% O_2, 5% CO_2) for 45 minutes and the pH was adjusted to 7.4 with 4M KOH. The KHMR was calcium free to mimic a cardioplegic solution and enhance cell survival in transit.

Once in the laboratory the heart was flushed again with ice cold KHMR as above and the right ventricular tissue was removed. Sheep cardiomyocytes were prepared according to the method of (Fabiato 1985). Briefly, the ventricular tissue was minced into 1-2 mm size pieces and placed into 50 mL centrifuge tubes in calcium free KHMR at room temperature ($22^{\circ}C$). Preparation of isolated myocytes involved a series of incubations in a mixture of digestive enzymes (2.5% Trypsin, Sigma-Aldrich, Australia), 4.02 U/mg collagenase (Worthington Biochemicals Corporation, Australia) in varying proportions to remove the connective tissue between myocytes. Cells were sequentially incubated in the enzyme cocktail for 30 minutes on a shaker bath (Ratek orbital mixer, Australia), centrifuged for 5 minutes at 450g (Heraeus Biofuge Primo centrifuge, K.I. Scientific, Australia) and the supernatant discarded. Each time the pellet was resuspended in KHMR. In the final 3 steps of this process, the calcium concentration was gradually increased to 2.5 mmol L^{-1} final concentration.

Finally, the heart digest was gently homogenised in a tissue glass Dounce homogeniser (Sigma-Aldrich, Australia) to produce a cell suspension. The tissue homogenate was then centrifuged for 5 minutes at 450g (Heraeus Biofuge Primo centrifuge, K.I. Scientific, Australia)

before being resuspended in freeze media (10% DMSO (Sigma Aldrich, Australia), 45% foetal bovine serum (FBS, Focus Bioscience, Australia), 45% Prepared media (DMEM with 10% FBS, Life Technologies, Australia) and aliquoted into cryovials (Interpath Services, Australia) before placing into a -80℃ freezer until required.

2.3 Preparation of hERG channel modulators and quinazolin-4-one compounds

Two commercially available hERG channel modulators were used in this study. NS1643 (Sigma-Aldrich, Australia) is a known hERG channel agonist (Hansen, Diness, et al. 2006) and terfenadine (Sigma- Aldrich, Australia) a known hERG antagonist (Rampe et al. 1998). Before use in experiments, both compounds were made up to 1mM stock solutions in DMSO (Sigma-Aldrich, Australia) and stored at 4^0C.

Six l urea and thiourea containing quinazolin-4-one compounds were synthesized (LTUJH06B, LTUJH18B, LTUJH28B, LTUJH37B, LTUJH47B and LTUJH51B) and kindly donated by the chemistry team led by Dr. Jasim Al-Rawi (La Trobe University, Bendigo, Australia). Each compound was initially made up as a 1mM stock solution in dimethyl sulfoxide (DMSO, Sigma-Aldrich, Australia). Depending on the experimental protocol, a range of concentrations were prepared by serial dilution (typically varying between 10^{-9} M to 10^{-4} M). In all cases, care was taken to ensure that the final concentration of DMSO did not exceed 0.5% (v/v) since it is known to increase cell death and interfere with many fluorescent assays (Mastyugin et al. 2004). Once the compounds were prepared in DMSO stored at 4^oC, prepared compounds were generally stable for at least 5 years when stored correctly.

2.4 hERG channel expression

The expression of hERG channels in breast cancer cell lines, MCF-7 and MDA-MB-231 was investigated using the fluorescent tagged KCNH2 (hERG gene) primary polyclonal antibody (Thermofisher, Australia). To identify different organelles cells were also counterstained with Hoechst blue and Mitotracker red, for the nucleus and mitochondria, respectively.

Cells were seeded to a concentration of 10^5 cells/well in a 6 well plate containing a sterile coverslip and placed in an incubator at 37^oC and 5% CO_2 overnight. Following overnight incubation media was removed from wells and cells were washed twice with PBS. Following washes cells were fixed with 100 µL of 0.05% paraformaldehyde in PBS and incubated in the dark for 1 hour at room temperature. After 1 hour, the 0.05% paraformaldehyde was removed and replaced with 100 µL 70% methanol and incubated for 1 hour at 4^oC. The cells were then washed twice in 0.05% Triton X-100 in PBS (100 µL/well) following incubation. The cells were further incubated in 10% FBS in PBS (100 µL/well) for 35 minutes at room temperature. Cells were then incubated with 100 µL KCNH2 primary polyclonal antibody (Thermofisher, Australia) overnight at 4^oC.

Following overnight incubation, cells were washed 3 times in cold PBS, then incubated with 100 µL FITC conjugated anti-rabbit secondary antibody (diluted with Milli-Q water) for 45 minutes at room temperature (22°C). Washes in cold PBS followed incubation. Cells were then counter stained with 3 µl Mitotracker red (10 mg/mL, Thermofisher, Australia) and 3 µl Hoechst blue (20 mM, Thermofisher, Australia) in PBS for 15 minutes. Finally, cells were washed with Milli-Q water and the coverslip with cells was mounted with dibutylphthalate polystyrene xylene (DPX) on a glass microscope slide. The coverslip was viewed using an Olympus FV10i confocal (Olympus, Australia).

2.5 Sulforhodamine B Assay

This is one of the commonly used assays in cytotoxicity screening. The principle of this assay is based on the capability of the bright pink anionic aminoxanthene SRB dye to stoichiometrically bind to protein components of cells that have been fixed by trichloroacetic acid (TCA). The amount of dye extracted from stained cells is directly proportional to the cell mass (Vichai and Kirtikara 2006).

The Sulforhodamine B (SRB) assay was used to test the effect of both, the commercial hERG channel modulators and the quinazolin-4-one derivatives on the breast adenocarcinoma cell lines (MDA-MB-231 and MCF-7). Using 24 well plates, cells were seeded at a concentration of 10^4 cells/well and left to adhere overnight in an incubator at 37°C and 5% CO_2. Following incubation, media was aspirated from the wells and replaced with media containing test compounds at various concentrations (1, 5 and 10µM) and the plates were returned to the incubator for a further 72 hours.

After 72 hours, the test media was discarded. Cells were fixed in cold 10% trichloroacetic acid (TCA, 300 µL/well) at 4°C for 30 minutes. Following fixing, cells were washed 5 times in running water and left to air dry. Once dry, 200µL of 0.1% SRB (Sigma-Aldrich, Australia) in 1% acetic acid (prepared with Milli-Q water) was added to each well to stain cells for 15 minutes. After 15 minutes, cells were washed 4 times with 1% acetic acid to remove any excess stain, then left to air dry. Once dry the stain was then dissolved in 200µL/well 10 mM unbuffered Tris, during which the plate was shaken for 10 minutes using an orbital shaker to ensure homogeneity. Finally, 150µL aliquots of the stain was transferred to a 96 well plate (black clear bottom, Greiner, Interpath, Australia), that was then placed in a FlexStation 3 (Molecular Devices, Bio-strategy, Australia) and absorbance was measured at 540 nm. Decreased absorbance was indicative of enhanced cell death. Data were analyzed using Graphpad Prism, by one-way ANOVA followed by a Newman-Keuls multiple comparison test, where $P < 0.05$ was regarded as significantly different.

2.6 Cell Cycle Analysis - Propidium Iodide (PI) Assay

The easiest way to measure and monitor the progression of cells through the cell cycle is by measuring their DNA content, as this is one factor that changes consistently depending on the phase of the cell cycle. Propidium iodide (PI) is the most widely used fluorescent dye for staining DNA in whole cells (or isolated nuclei). PI intercalates into the DNA helix of fixed and permeabilized cells. The intensity of PI staining corresponds with DNA content resulting in defined G1 and G2 peaks with an intervening S phase. Events to the left of the G1 peak are referred to as sub G1 and can be an indicator of cell death. An example of a cell cycle histogram is shown in Figure 11.
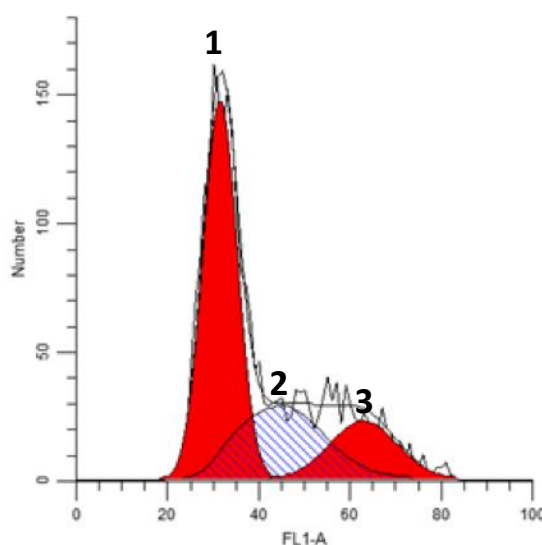
Figure 11. An example of a cell cycle histogram following data analysis using Modfit. The peaks are indicative of the different stages of the cell cycle where 1= % cells in G1 phase, 2=% of cells in S phase and 3=% cells in G2/M phase.

The effect of NS1643 and quinazolin-4-one compounds on progression through the cell cycle was assessed for both breast adenocarcinoma cell lines, MDA-MB-231 and MCF-7. Cells were seeded in 12 well plates at 10^4 cells/well for 24 hours. After 24 hours cells were treated with test compounds at 10µM.

To repeat cell passaging and detaching after treatment, cells were trypsinised to detach from the flask and washed in 500µL PBS. After inversion, tubes were centrifuged for 5 minutes. After removing the supernatant, cells were fixed in 500µL, 70% ethanol and refrigerated (4°C) for 30 minutes. After fixation with 70% ethanol, cells were washed with PBS twice and centrifuged for 5 minutes at 200g. Cell pellets were collected and 250µL of 25µg/mL propidium iodide and 100µg/mL RNase in PBS mixture was added, then covered and placed in an incubator for 30 minutes. Samples were analysed in an Accuri CFlow Plus flow cytometer.

Histograms were analysed using the cell cycle analysis program Modfit (Verity software house, USA), where the percentage of cells accumulated in each cell cycle phase was calculated. Data were pooled and tested using a one-way ANOVA and Newman-Keuls multiple comparison test in Graphpad Prism, with $P<0.05$ being regarded as statistically significant.

2.7 Annexin V/PI Assay

In cells undergoing apoptosis, the membrane phospholipid phosphatidylserine (PS) flips from the inner to the outer leaflet of the plasma membrane exposing it to the extracellular environment (Biosciences 2011). The Annexin V stain is a 35-36 kDa Ca^{2+} - dependent phospholipid-binding protein with high affinity for PS and binds to exposed PS on the apoptotic cell surface. Annexin V conjugates to fluorochromes, while retaining its high affinity for PS, hence it is used as a probe for flow cytometric analysis of cells undergoing apoptosis (Biosciences 2011). Propidium iodide (PI) is used to assess plasma membrane integrity during Annexin V apoptotic assays. PI is a fluorescent vital dye that stains DNA. It does not cross the membrane of viable cells or cells in the early stages of apoptosis because of their membrane integrity (Biolegends 2018). A typical example of the scatter plot is given in Figure 12, where the percentage of cells undergoing apoptosis or necrosis can be ascertained.
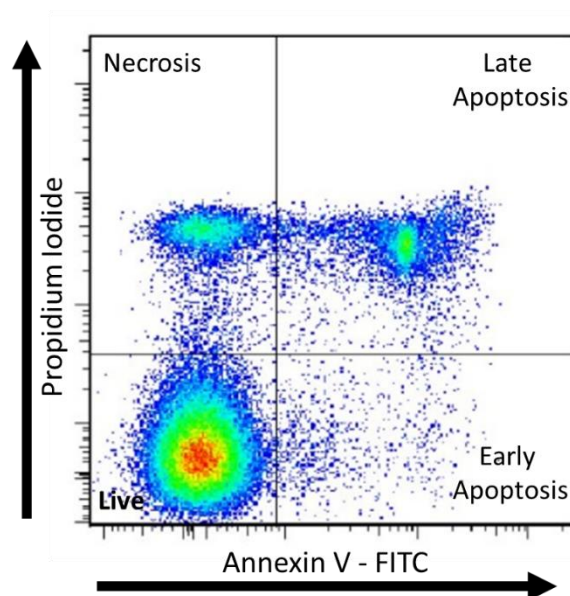

Figure 12. An example of light scatter plot following data collection using CFlow plus of breast cancer cells stained with Annexin V and propidium iodide. The light scatter plot is divided to 4 sections; bottom left=live cells, top left=necrotic cells, top right =early apoptosis and bottom right=late apoptosis.

The ability of hERG agonist NS1643 and the quinazolin-4-one derivatives to induce apoptosis or necrosis in the MDA-MB-231 and MCF-7 cell lines was assessed using Annexin V and propidium iodide staining. Cells were seeded in 12 well plates (10^4 cells/well) and placed in an incubator at 37° C, and 5% CO_2 for 24 hours. After incubation, media was replaced with test media containing 10µM of each test compound for 72 hours. Following treatment, cells were washed twice with cold PBS and then resuspended in 100µL of 1x binding buffer (0.1M HEPES/NaOH, pH 7.4; 1.4mM NaCl; 25mM $CaCl_2$). Both 1µL Annexin V (90 µg/mL, Thermofisher, Australia) and 10µL of PI stain (1 mg/mL, Sigma-Aldrich, Australia) was added to the cell suspension containing binding buffer. The cell suspension was gently vortexed, and the cells were incubated for 15 minutes in the dark at room temperature. After incubation, an additional 400µL of 1x binding buffer was added to each tube. The cell suspension was read immediately using Accuri CFlow Plus flow cytometry. Excitation and emission wavelengths for Annexin V were 488 nm and 518 nm; while for PI they were 488-540 nm and 617 nm, respectively. Data were pooled and tested using a one-way ANOVA and Newman-Keuls multiple comparison test in Graphpad Prism, with $P < 0.05$ being regarded as statistically significant.

2.8 Human Membrane Apoptosis Array

To test the effect of NS1643 and the quinazolin-4-one derivatives on the apoptotic pathways in cell lines MDA-MB-231 and MCF-7, the Human Apoptosis Antibody Array (43 targets, Abcam) was used.

2.8.1　Protein lysate

Once cells were confluent, culture media was removed and replaced with media containing 10µM NS1643, LTUJH18B, LTUJH28B or LTUJH37B with a negative control containing media only. Cells were incubated in the presence of the compounds for 24 hours. After 24 hours, cells were detached with trypsin and the cell pellet was washed twice in PBS. After treatment, cells were washed with PBS containing 1 mM phenylmethylsulfonylfluoride (PMSF) and centrifuged at 200g for 5 minutes at 4°C. Pelleted cells were suspended with 100µL lysis buffer (Abcam, VIC, Australia), 1 mM PMSF and 10 mg mL^{-1} aprotinin and incubated on ice for 30 minutes. Samples were then centrifuged at 15,000g for 20 minutes at 4°C. The supernatant containing the protein extracts was transferred to pre-chilled Eppendorf tubes.

To determine the total protein concentration in the lysate, a bicinchoninic acid assay (BCA) was completed using the BioRad DC Protein Assay Kit II (BioRad Laboratories, Philadelphia) along with a standard curve of known protein concentration. Solutions for the protein determination standard curve were prepared as follows. Reagent A was prepared by the addition of 20 µL reagent S to 1 mL of reagent A. BSA standards were made to final

concentrations (mg/mL) of 1.5, 1.25, 1.0, 0.5 and 0 by diluting BSA standard in Milli-Q water. Reagent A was prepared fresh for every assay by mixing 30µL reagent S for every 1mL of reagent A. Five microliters of each diluted standard and samples was pipetted in duplicate into wells of a 96 well plate and 25µL of working Reagent A was added. This was followed by the addition 200µL of reagent B to each of the wells. The plate was gently agitated and left to incubate at room temperature for 15 minutes. After 15 minutes, the absorbance (750 nm) was read using a Flexstation 3 (Molecular Devices, Bio-strategy, Australia).

2.8.2 Human apoptosis array assay

Once the total protein concentrate of lysate was determined, the human apoptosis array assay was conducted in accordance with the manufacturer's instructions. The membranes were placed (on the side containing the various markers to be tested) into the 8 well tray provided in the kit. Membranes were blocked by being incubated in 2 mL of 1x blocking buffer on a rocking platform. At the completion of the incubation, blocking buffer was decanted and the membranes were incubated overnight at 4°C on a rocking platform with protein samples from cells treated with NS1643 or selected quinazolin-4-one derivatives. A separate membrane was used for each test compound.

Following overnight incubation, protein samples were aspirated out of the wells and membranes were washed 3 times with 2mL of fresh wash buffer 1 for 5 minutes at room temperature. An extra wash was also performed where each membrane was placed in a clean container with 20 mL wash buffer 1 at room temperature while on a rocking platform for 45 minutes. Membranes were then returned to the 8 well tray. Membranes were then washed twice with wash buffer II for 5 minutes at room temperature with each wash using fresh buffer.

After the removal of wash buffer II, 1 mL of 1x Biotin-conjugated anti-cytokines was added to each membrane and incubated overnight at 4°C on a rocking platform. Following incubation, anti-cytokine reagent was aspirated and washes with buffers I and II was repeated. Membranes were then incubated at room temperature for 2 hours with 1.5 mL of 1x streptavidin-HRP. After 2 hours, membranes were washed with wash buffer I and II as described above.

Each membrane was placed with markers side placed on a plastic sheet and excess fluid was drained by blotting the edge of the membrane. Equal volumes (1.25 mL each) of detection buffer C and D (made up fresh for each experiment) was added into a 15 mL centrifuge tube. The detection buffer mixture (250µL) was added to each membrane and left to incubate for 2 minutes. Excess liquid was removed, and another plastic sheet was placed on top of the membranes ensuring no bubbles were present. Chemiluminescent images were captured using Syngene G-BOX (G: BOX-CHEMI-XL1.4, USA) and dot blot intensity was analyzed

using GeneTools Syngene software. Further analysis of the dot blots was completed according to the Abcam protocol, where the blank and negative control was subtracted from each antibody spot and then the chemiluminescence was normalized to the positive control (relative response). Since these experiments were conducted only once (in duplicate) for each test compound, no statistical analyses could be performed. Relative changes in marker chemiluminescence that was at least twice the values under control conditions for each cell line were reported.

2.9 Membrane Potential Assay

The Cellular Membrane Potential Assay kit (Abcam, Australia) uses the long wavelength red fluorometric membrane potential indicator (10x MP dye), to show any change in the membrane potential (Vm) due to the opening of ion channels. When channels are opened the MP dye enters, and fluorescence is increased.

The assay was conducted in black, clear bottom 96 well plates (Corning, Interpath, Australia). MCF-7 and MDA-MB-231 cells were seeded at a concentration of $2x10^4$ cells/well in 100 µL in sterile cell culture media (DMEM/F12 (HEPES), Thermofisher Scientific, Australia) completed with 10% foetal bovine serum (FBS, Focus Bioscience, Australia) and placed in the incubator at 37^oC and 5% CO_2 overnight. The 10x MP sensor red fluorescent dye was diluted to 1xMP using 1 mL Hank's Buffer with HEPES (HHBS) immediately prior to use. Following 1-hour incubation, 100µL diluted MP sensor dye solution was added to each well and returned to the incubator for another hour. A 96 well black compound plate containing; 10µM NS1643 and 10µM of respective quinazolin-4-one compounds (i.e. LTUJH18B, LTUJH28B and LTUJH37B) were prepared. A positive control solution at 50 mM KCl final concentration, was used to stimulate opening of hERG potassium channels (by providing a voltage step to the cell membrane).

Following the 1-hour incubation, both assay and compound plates were placed into the Flexstation 3 (Molecular Devices, Bio-strategy, Australia). The Flexstation 3 was programmed (SoftMax pro 5.4) to add 70µL per well of compounds to cells and membrane potential changes were recorded 17 secs following compound addition. Fluorescence was excited at 620 nm and emission was read at 650 nm.

Relative fluorescence units (RFU) were normalized to the control response (cells in media only) since this assay cannot read the actual membrane potential, only the difference in Vm under different conditions. To standardize the results, the average RFU for control conditions was set to 1.0. Any changes above or below 1.0 would indicate potassium channels opening or being inhibited, respectively. Data were pooled and tested using a one-way ANOVA and

Newman-Keuls multiple comparison test in GraphPad Prism, with $P<0.05$ being regarded as significantly different.

2.10   FluxOR Potassium Ion Channel Assay

hERG agonist NS1643 and novel quinazoline derivatives were investigated for their potential effect on voltage gated potassium channels using the FluxOR™ Potassium Ion Channel Assay (Life Technologies, Australia). The principle of the assay (shown in Figure 13) is to use thallium (Tl+) permeability to potassium channels. A thallium solution outside the cells will move down its concentration gradient (into the cell) when potassium channels are stimulated to open. Once inside the cell, thallium binds with a preloaded dye increasing fluorescence.
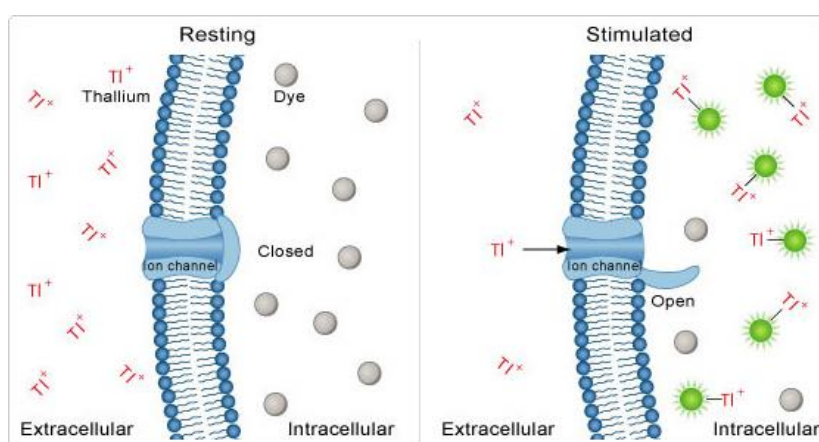
Figure 13. Stimulated potassium channels open causing the binding of thallium to indicator dye resulting in fluorescence (LifeTechnologies 2014).

This assay can measure the activity of many classes of potassium channels (voltage gated, and ligand gated) so it is necessary to set up the stimulating conditions appropriate for the channel type being investigated. In this study the focus was hERG potassium channels which only open at positive membrane potentials of +20mV by using an appropriate KCl stimulating solution (Zhang, Liu, and Tseng 2004).

The commercial protocol was followed, with some optimization. The Loading Buffer (containing the Tl+ flux dye) was prepared by the addition of power load concentrate (100x dilution, component C), FluxOR reagent (1000x dilution, component A), distilled/deionised water, FluxOR assay buffer (10x dilution, component B) and probenecid (2.5mM, component D), respectively. The Assay Buffer was prepared by mixing distilled/deionized water, FluxOR assay buffer (Hank's balanced salt solution, 20mM HEPES, component B) and probenecid (2.5mM, component D), respectively.

A vial of sheep cardiomyocytes was removed from the -80°C freezer, thawed and the contents of vial placed in a centrifuge tube containing 5mL growth media (DMEM/F12 (HEPES), Thermofisher Scientific, Australia). Cells were centrifuged at 200g for 5 minutes and resuspended with Loading Buffer at a concentration of 5×10^3 cells per well. The cell suspension was placed into a 25 cm³ tissue culture flask and incubated at room temperature, in the dark for 4 hours. Prior to the assay, sheep cardiomyocytes were loaded with FluxOR dye in the Loading Buffer for 4 hours in the dark at room temperature. After this, cells were centrifuged (200g) for 5 minutes and resuspended in Assay Buffer. The cardiomyocyte/assay buffer suspension was then dispensed (70µL/well) into a black, clear bottom, poly-lysine coated 96 well plate (Interpath, Australia) which became the Assay Plate. Stimulus buffers were prepared containing no added potassium (K- buffer) to serve as the negative control and a potassium containing positive control (K+ buffer) with a final concentration of 100mM K^+ to stimulate opening of hERG channels. The Stimulation Buffer (K+ buffer) comprised: 2.5 mL deionized water, 1 mL FluxOR chloride-free buffer (5 mM stock, Component E), 1mL K_2SO_4 stock (125 mM, Component F), and 0.5 mL Tl_2SO_4 (50 mM, Component G). The final K^+ and Tl^+ concentrations in the Stimulation Buffer were 100mM and 10 mM, respectively. The K- buffer contained no K_2SO_4 but was otherwise identical to that described above. All solutions were at pH 7.4. The plate containing the Stimulus Buffer plus compounds (10 µM final) was prepared and placed into the FlexStation 3 (Molecular Devices, Bio-Strategy, Australia).

Reading Plates were prepared by the addition of 80 µL aliquots of cell suspension, and cells were allowed to settle for a few minutes, before the experiment at room temperature (22°C). The FlexStation 3 was programmed (SoftMax Pro 5.4) to add 20µL of Stimulus Buffer (either K- or K+) after 20 seconds. The Reading Plate was read every 2 secs for a total of 3 minutes. The assay uses an excitation wavelength of 460 to 490 nm and an emission wavelength of 520 to 540 nm.

The FluxOR assay was used to confirm the response of sheep cardiomyocytes to K+ stimulation designed to activate hERG channels. This was tested by also using the known agonist NS1643. The hERG channels were also blocked by the known antagonist, terfenadine, (1µM) which would inhibit any agonism of hERG channels in the presence of K^+ and in the presence of the quinazolin-4-one derivatives. Relative fluorescence units (RFU) were recorded from each well and normalized to the initial RFU recorded using the expression $\Delta F/F_0$, where ΔF is the difference between the recorded RFU for each time interval and the initial RFU at time = 0 seconds, and F_0 is the RFU recorded at time = 0 seconds. This way any variation in absolute RFU was standardized for comparison between experiments. Differences in the final amplitude of each trace was the average of the last 20 seconds of recording. Data were pooled and differences in the responses were tested using the unpaired

Student's t-test (after a normality Tukey test) with P<0.05 being regarded as statistically significant.

To further evaluate how the novel compounds were affecting hERG channel activation, each trace was normalized to the respective B_{max} so that the rate of rise (Hill coefficient, η) and the binding affinity (K_D) for each could be determined after fitting the data with a one-site binding hyperbola with the equation, $y = (B_{max} \times X^{\eta}) / (K_D^{\eta} + X^{\eta})$. The data were then subjected to an unpaired Student's t-test between 2 groups with unequal variances (determined by F-test): (a) positive control versus K^+ in the presence of novel compound, (b) positive control versus K^- in the presence of novel compound, and finally (c) between K^+ and K^- in the presence of the novel compound. Data were considered significantly different when $P < 0.05$ (two-tailed).

2.11   CellTox Green Cytotoxicity Assay

General toxicity assessment of novel quinazoline compounds was conducted using the CellTox Green Cytotoxicity Assay (Promega, Australia). The assay is based on cyanine dye interacting with DNA in nonviable cells but being excluded from viable cells. As demonstrated in Figure 14, when the dye binds DNA in damaged cells, fluorescence is increased. Viable cells produce no appreciable increases in fluorescence. The fluorescent signal produced is proportional to cell death. The more toxic a compound, the more cell death is expected compared with normal cell death under ideal survival conditions (negative control).
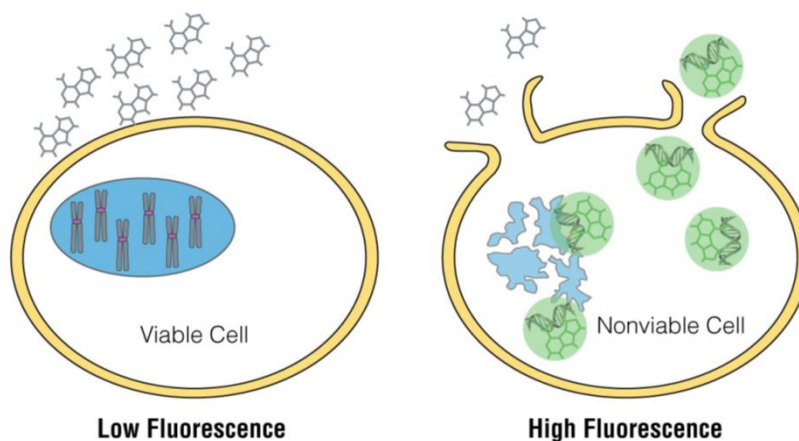
Figure 14. CellTox™ Green Dye binds DNA of cells with impaired membrane integrity increasing fluorescence (Promega 2016).

The CellTox assay was conducted following the manufacturer's protocol (CellTox™ Green Cytotoxicity Assay, Promega). A 4.8 mL aliquot of sheep cardiomyocyte suspension was prepared in growth media at a concentration of $1x10^6$ cells/mL and added to each well of a black clear bottom, poly-lysine coated 96 well plates (Interpath, Australia). Ten microliters of gentamycin and 10μL cyanine dye was then added to each sample and incubated at 37°C and 5% CO_2 for 24 hours. After 24 hours, concentrations ranging from 10^{-9} to 10^{-4} M of the various quinazolin-4-one derivatives was added in triplicate to wells in the plate containing cells. Two controls were also added, a lysis buffer that would show maximum cell death, and a negative control containing media only to show normal cell death. Plates were returned to the incubator at 37°C and 5% CO_2 for a further 24 hours. After 24 hours, fluorescence was measured (excitation wavelength 485 nm and emission wavelength 520nm) using the FlexStation 3 (Molecular Devices, Bio-Strategy, Australia). Cytotoxicity was assessed as percent cell death with respect to the negative control. Data were tested using a Student's unpaired t test in GraphPad Prism, with $P<0.05$ being regarded as statistically significant.

2.11.1 Vivid CYP450 Screening Assay

Vivid CYP450 screening is a high-throughput fluorescence-based assay designed for the detection of enzyme-drug interactions and CYP450 inhibition through Vivid Substrates and CYP450 BACULOSOMES Plus reagent. The CYP450 BACULOSOMES® Plus Reagents consist of insect cell microsomes that express a specific human CYP450 enzyme. When the Vivid Substrates are metabolized by the CYP450 enzymes, the resulting metabolites are highly fluorescent due to the release of the fluorescent dye from the substrate (as shown in Figure 15 below). If a compound inhibits a CYP450 enzyme, there will be a decrease in fluorescence. Conversely, if the compound does not inhibit the activity of the CYP450

enzyme, then the substrate will be broken down emitting high fluorescence (LifeTechnologies 2012).
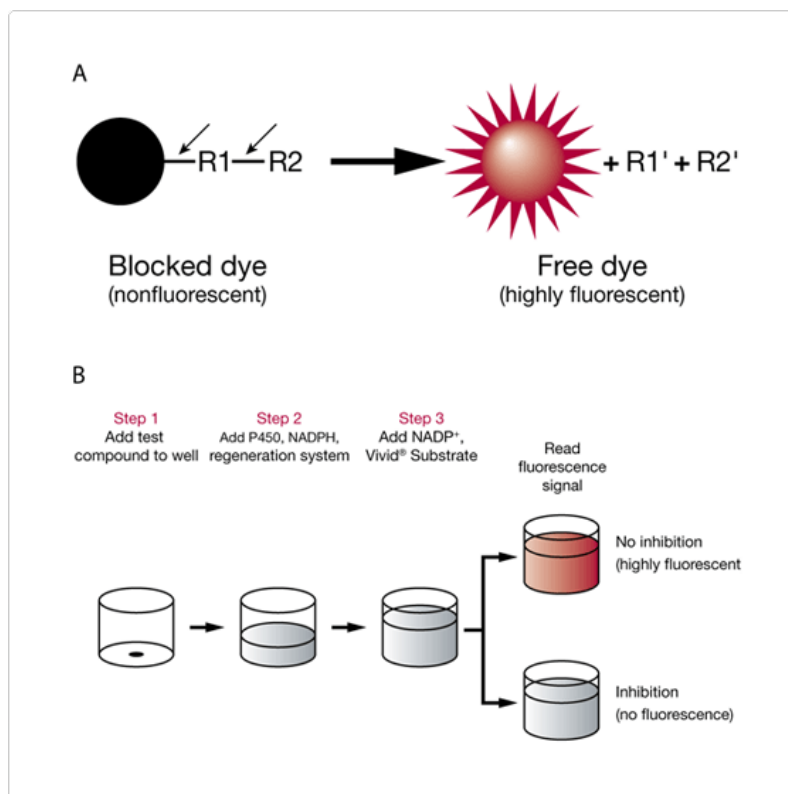
Figure 15. The principle of drug-dye interaction via Vivid® CYP450 Screening(LifeTechnologies 2012).

This protocol was conducted in accordance to the manufacturer's instructions for two CYP450 enzymes: CYP2E1 and CYP3A4. Prior to experimentation, the buffer stock for each assay was diluted to 1:1 concentration with Milli-Q water. Powder substrates for CYP2E1 and CYP3A4 were reconstituted with acetonitrile. From a 1 mM stock, all quinazolin-4-one derivatives to be tested including the appropriate known inhibitors were made up to 0.25 mM using the diluted assay buffer.

Using black clear bottom poly-lysine coated 96 well plates (Interpath, Australia), 50µL of each test compound as well as the known inhibitor (Cupral for CYP2E1 and Ketaconazole for CYP3A4) was added to wells in the first lane. To another test lane, 40µL of the assay buffer was added. Serial dilutions of the Quinazolin-4-one compounds were completed by aspirating 10µL from respective wells in the first lane and adding them to the following well containing 40 µL of assay buffer. At the end of the serial dilution each well contained 40µL of compound/ buffer mixture. The concentration range was 1 to 124 µM (or $-\log_{10}$ 6 to $-\log_{10}$ 3.91). The master mix containing a mixture of the assay buffer, the CYP450 enzyme as well as a regeneration system was then prepared. A 50µL aliquot was added to each of the test wells. A negative control of the assay buffer alone was also added, along with known inhibitors

Cupral (for CYP2E1) and Ketoconazole (for CYP3A4) as positive control for inhibition. The plate was incubated in the dark for 10 minutes to allow the enzyme to interact with the compounds.

At the end of the 10-minute incubation, 10µL of the reaction starter was added to each test well. The reaction starter was prepared by the addition of assay buffer to the appropriate substrate and mixed with $NADP^+$ for the regeneration system. The plate was then analysed in the Flexstation 3 (Molecular Devices, Bio-Strategy, Australia). Fluorescence was detected in the blue light range for both enzymes CYP2E1 and CYP3A4 (Excitation wavelength, 415nm, Emission wavelength, 460nm).
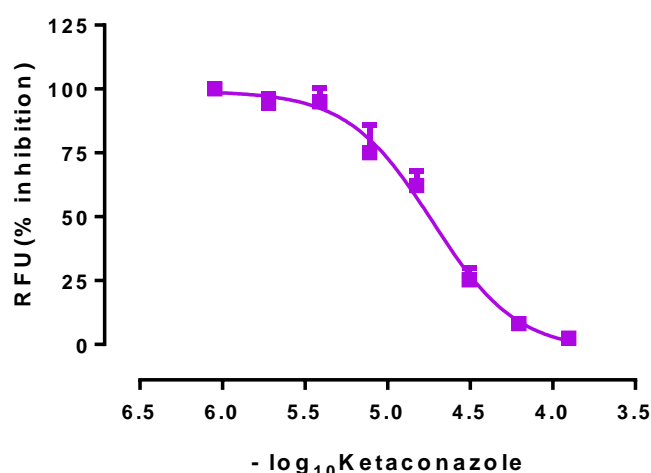
Figure 16. Sample inhibition curve showing the changes in fluorescence in the presence of Ketoconazole, the standard inhibitor of CYP3A4, using the vivid CYP450 screening kit.

Relative fluorescence units were recorded at 1-minute intervals, from the wells in the plate for a period of 1 hour. Changes in the relative fluorescence was normalized to the positive control response (maximum fluorescence) and plotted for each concentration of compound as a dose-response curve as shown in Figure 16. This curve was fitted in Graphpad Prism with an inhibitory Hill equation, $Y = 100/(1 + 10^{(X-logIC_{50})^* \eta})$ with variable Hill coefficient (η). Results for each test compound were compared with the response of the known inhibitor in each case. It was noted whether the compound inhibited the CYP450 enzyme and whether it altered the Hill coefficient (η), being the slope of the relation, and the shift in $log_{10} IC_{50}$ of the curve, which indicates any difference in the relative potency of the compound to inhibit the enzyme compared with the response of the known inhibitor. Data were pooled and the differences in the means were tested using an unpaired Student's t-test with $p < 0.05$ being regarded as significant.

Chapter 3 - Functional hERG channel expression in hormone positive and hormone negative breast cancer cells, MCF-7 and MDA-MB-231, assessed using the hERG channel modulator, NS1643

3.1 Introduction

Potassium channels are a diverse group of pore-forming transmembrane proteins that selectively facilitate potassium flow through an electrochemical gradient, normally in electrically excitable cells including cardiac cells and neurones. They participate in the control of membrane potential and cell excitability but more recently a functional role in cancer cells has been identified, including impact on cell volume, proliferation, cell migration, angiogenesis and apoptosis (Wulff, Castle, and Pardo 2009). Potassium ion channel hyperpolarising of membrane potential in cancer cells is highly linked to cancer progression (Djamgoz, Coombes, and Schwab 2014; Pedersen and Stock 2013).

The potassium channels most commonly investigated in relation to cancer are the human ether-a-go-go related gene or hERG channels. The hERG channels are voltage-gated potassium channels (also known as Kv11.1 and encoded by KCNH2) belonging to the EAG family. Expression of hERG voltage gated potassium channels is most common in conducting cells, including cardiac and neurons. The role of hERG channels is not exclusive to that of electrical transmission, with hERG channels being one of the first voltage gated potassium channels identified to play a role in the survival and progression of tumours (Hemmerlein et al. 2006). The modulation of hERG channels is an area of great interest, as the hyperpolarising action of these channels is involved in regulation of the membrane potential throughout the cell cycle in cancer cells (Lastraioli, Iorio, and Arcangeli 2015). Their action also drives proliferation and migration of cells by regulating Ca^{2+} signalling and cell volume (Kunzelmann 2005). The expression of hERG channels differs between tumour cells and heart cells in at least 3 different transcripts, which facilitates the idea of selectively modulating the activity of hERG channels in neoplastic cells while maintaining their function in cardiomyocytes (Crociani et al. 2003; Guasti et al. 2008).

Increased expression of potassium channels, specifically hERG channels, has been associated with worse prognoses and considered an indication of the advancement of solid cancers such as human endometrial, colorectal, gastric as well as haematological cancers such as leukemia (Cherubini, Taddei, Crociani, Paglierani, Buccoliero, Fontana, Noci, Borri, Borrani, Giachi, et al. 2000; Smith et al. 2002; Pillozzi et al. 2002; Wang et al. 2002; Crociani et al. 2003; Lastraioli et al. 2004; Zhao et al. 2008; Afrasiabi et al. 2010). It has been reported that hERG channel expression is upregulated mostly in the early cancer stages (Crociani, Lastraioli, Boni, Pillozzi, Romoli, D'Amico, Stefanini, Crescioli, Taddei, Bencini, et al. 2014), while hERG channel expression is more variable in later phases of the cancer as the needs of neoplastic cells differ from one cancer type to another (Smith et al. 2002; Comes et al. 2015). hERG channels are expressed in a variety of tumour cell lines of different histogenesis but are not present in the corresponding healthy cells from which the respective tumour cells

were derived. Quantitative analysis has been determined at both the mRNA and protein levels. At the mRNA level, the normal mRNA transcript of about 4.4kb, representing the full-size transcript for hERG, has been detected in normal heart and brain. However, in various cancer cell lines, multiple mRNA transcripts exist ranging in size from 2.2kb to the full size 4.4kb, suggesting alternative splicing of hERG mRNA may occur in cancer phenotypes. The smaller transcripts confirmed by Western blot analysis, generally lack part of or most of the NH2 terminus of the HERG channel, and functionally have faster deactivation kinetics (Bianchi et al. 1998). Most studies identified 2 dominant bands, one at about 150kDa corresponding to the mature, fully glycosylated hERG protein, with the smaller band of about 135kDa representing the partially glycosylated, immature hERG protein.   Analyses in breast adenocarcinomas suggest the normal hERG channel, 155kDa in size, is expressed in all cell lines while the more aggressive triple negative types additionally express the 135kDa truncated protein. In MCF-7 cells a luminal A subtype positive for both oestrogen and progesterone receptors, appears to only express the 155kDa protein (Roy et al. 2008). While SKBr3 and MDA-MB-231 cells, representing basal subtypes lacking both the oestrogen and progesterone receptors (Subik et al. 2010), expressed both protein forms with the 155kDa size protein being dominant in both cell types (Lansu and Gentile 2013). hERG channel expression has also been assessed in biopsies taken directly from cancer patients and identified as an indicator of worse prognosis in several types of cancers including oesophageal adenocarcinoma (Ding et al. 2008), colorectal cancer (Lastraioli et al. 2012), pancreatic ductal adenocarcinoma (Lastraioli et al. 2015), and endometrial cancer (Cherubini, Taddei, Crociani, Paglierani, Buccoliero, Fontana, Noci, Borri, Borrani, Giachi, et al. 2000). In contrast, hERG channel expression in breast adenocarcinomas and gastric tumours indicates high expression early in cancer progression but decreasing as the malignancy develops.

While the presence of hERG channels on the cell membrane is well recognized, it has been suggested that they may also be present on intracellular membranes in cancer cells (Blackiston, McLaughlin, and Levin 2009). Few studies have used higher magnification to determine the location of hERG channels intracellularly which could provide more information regarding their function in cancer progression. Lastraoli and colleagues using laser confocal microscopy identified hERG expression within discrete packages in the cytoplasm of pancreatic cancer cell lines (PDAC) and the description was not conclusive (Lastraioli, Iorio, and Arcangeli 2015). Another study exploring hERG expression in melanoma cell lines (MDA-MB-4355), also using confocal microscopy, described hERG channel expression 'distributed throughout the cells'(Afrasiabi et al. 2010). Neither study gave a thorough description nor utilised a counterstain for the plasma membrane or other cytoplasmic organelles, which would have provided crucial localisation information.

The function of hERG channels in cancer has been ascertained using either hERG channel agonists or antagonists. The resulting alteration in membrane potential inhibited cell proliferation, caused cell cycle arrest at G1 phase and increased apoptosis in a range of cancer cell lines. NS1643 opened hERG channels and reduced cell proliferation in SKBR3 and MDA-MB-231 breast cancer cell line lines (Lansu and Gentile 2013). Studies conducted in the xenograft model of MDA-MB-231 breast cancer also showed that NS1643 caused significant reduction in tumour growth (Fukushiro-Lopes et al. 2018). Further studies have identified that NS1643 significantly induced cell cycle arrest in G1 phase with a further decrease in cells in S and G2/M phases in breast cancer cell lines SKBR3 and MDA-MB-231 while induction of cell death assessed using Annexin V/PI stains showed no distinction between apoptosis and necrosis (Lansu and Gentile 2013). The function of hERG channels in breast cancers is not clear, although studies have alluded to its role in proliferation and apoptosis, no study has clearly defined their intracellular expression, nor compared their function in MCF-7 versus MDA-MD-231 breast cancer cell lines.

In this study, NS1643 action on hormone positive MCF-7 cells and hormone negative MDA-MB-231 cells were utilised to decipher the role of hERG channels on proliferation, cell cycle progression and apoptosis.

3.2 Results

3.2.1 HERG channel expression

Previous studies have identified hERG channel expression in both MCF-7 and MDA-MB-231 using western blot analysis. This confirms expression, but localisation using immunofluorescence could provide a better insight into its function. Antibodies to the synthetic peptide corresponding to human hERG channel aa1145-1159 (C terminal) encoded by the KCNH2 gene, was utilised, in conjunction with Hoechst blue and Mitotracker red, to counterstain the nucleus and mitochondria, respectively.

In MCF-7 cells (Figure 17d), green fluorescence was observed surrounding the nucleus corresponding to localization of the hERG channels in the endoplasmic reticulum (ER). There is also co-localization of hERG channels with the mitochondria (orange staining), and with the nucleus (light blue staining). Immunofluorescence for hERG channels was also observed in MDA-MB-231 cells (Figure 18d) but was more diffuse compared with MCF-7 cells. The protein was localized within the mitochondria and the nucleus, but less obvious regarding the endoplasmic reticulum. This staining pattern indicates hERG channel expression, and thus its function in association with the ER, mitochondria and nucleus. Note, there was no attempt to stain hERG protein on the plasma membrane of these cells which would have been removed after the Triton X100 treatment to allow the KCNH2 antibody access to the cytosol.

Figure 17. Localisation of hERG channels in MCF-7 breast cancer cells using primary anti-KCHN2 antibodies in the presence of counter stain Hoescht blue and Mitotracker red staining the nucleus and mitochondria respectively. (a-Hoechst Blue=Nucleus, b-Immunofluorescence for hERG protein expression, c-Mitotracker red=mitochondria, d- all staining tags combined to determine co-expression).
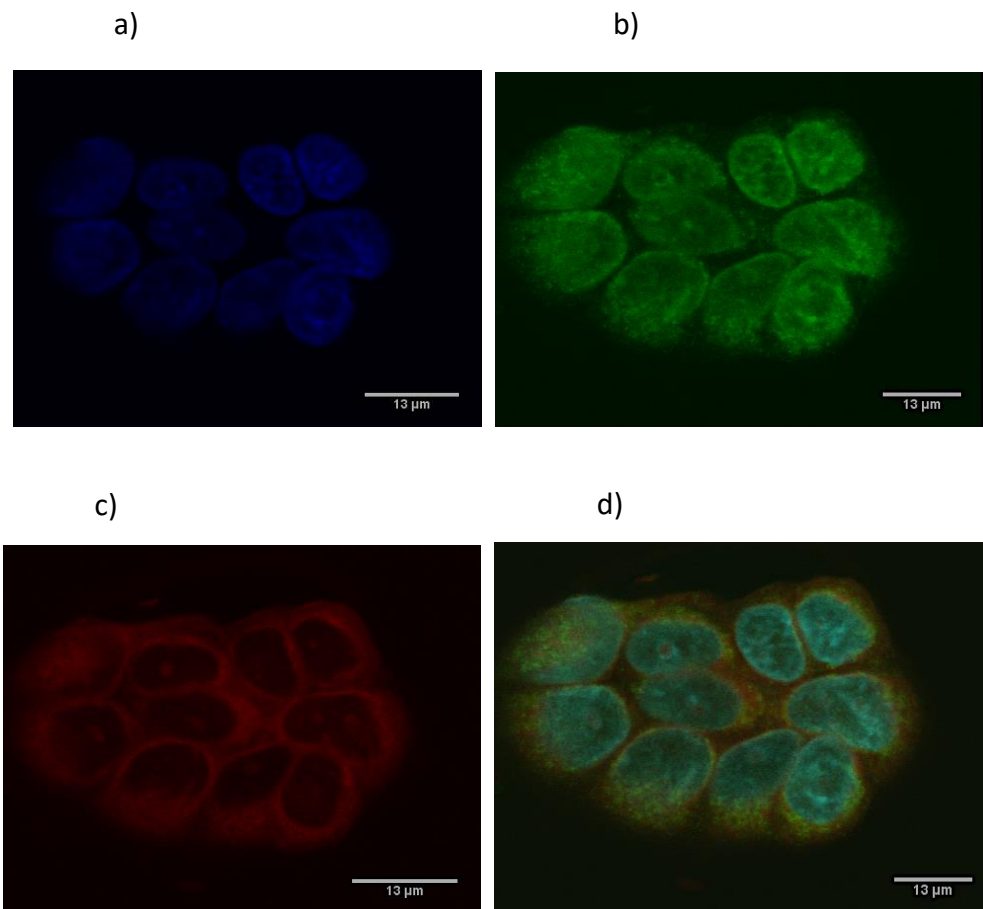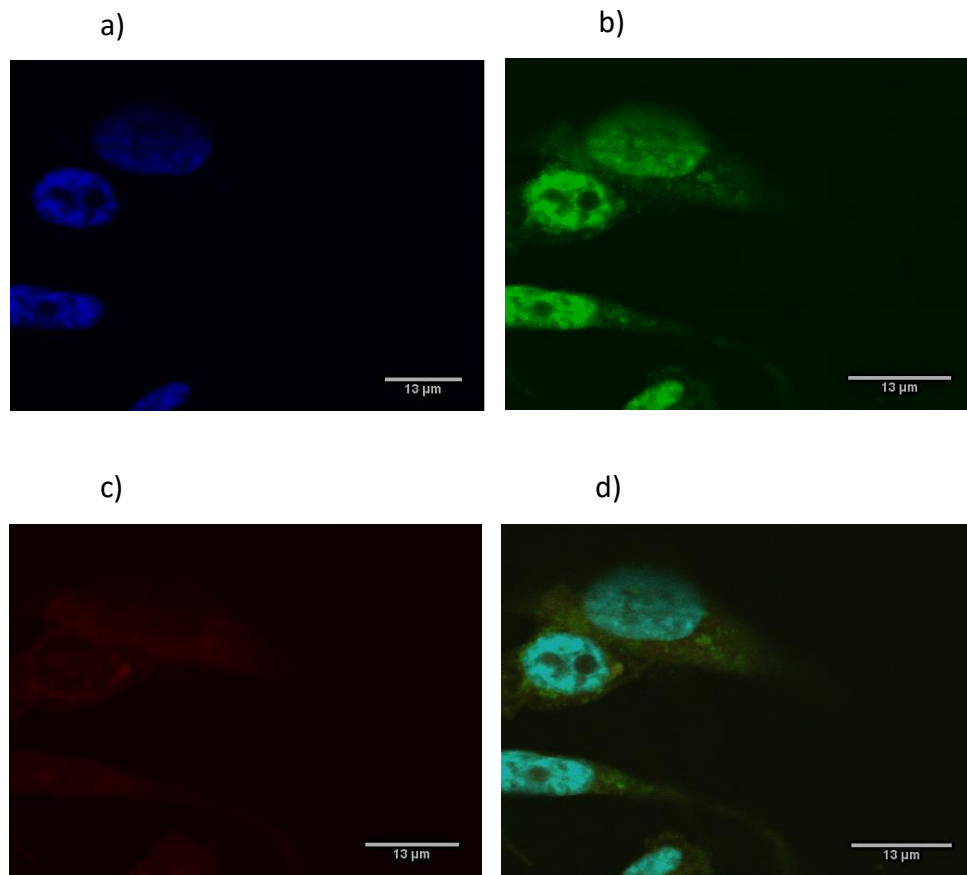
Figure 18. Localisation of hERG channels in MDA-MB-231 breast cancer cells using primary anti-KCHN2 antibodies in the presence of counter stain Hoescht blue and Mitotracker red staining the nucleus and mitochondria respectively. (a-Hoechst Blue=Nucleus, b-Immunofluorescence for hERG protein expression, c-Mitotracker red=mitochondria, d- all staining tags combined to determine co-expression).

3.2.2 Inhibitory effect of hERG channel modulator NS1643 – concentration range

The impact of hERG channel activation was assessed using the hERG channel modulator, NS1643 on the number of MCF-7 and MDA-MB-231 cells. An initial experiment was conducted to determine the optimum concentration of NS1643 that would exert the most effect in both cell lines. The Sulforhodamine B (SRB) assay was used to determine cell number following exposure to NS1643 for 72 hours.

When cells were exposed to increasing concentrations of NS1643 (1, 5 and 10µM), there was a corresponding decrease in cell number which was cell line dependent. MCF-7 cells showed a significant decrease in cell number as the concentration of NS1643 increased, from 1µM (98.35 ± 0.64, $p<0.01$), 5µM (95.83 ± 0.23, $p<0.001$) to 10µM (87.66 ± 0.88, $p<0.001$) when compared with the control (Figure 19a). In contrast to the progressive decrease observed in the MCF-7 cells, the MDA-MB-231 cells (Figure 19b) did not respond to hERG channel modulation until 10µM NS1643. After 72 hours exposure cell number decreased significantly less than for media only control (85.09 ± 3.243, $p<0.001$). Since 10µM NS1643 was the most effective concentration in inhibiting cell number in both cell lines, this concentration was used for the rest of experimentation.
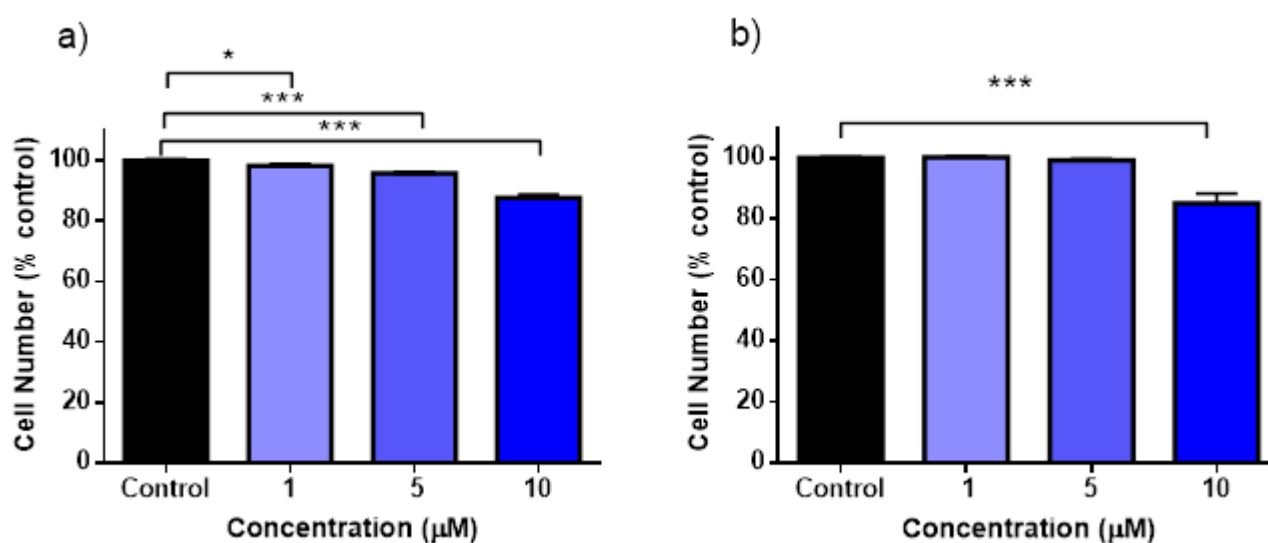
Figure 19. Sulforhodamine B analysis (cell number), shown as relative cell number (% control) for breast cancer cell lines, a) MCF-7 and b) MDA-MB-231 following treatment with increasing concentrations of the hERG channel agonist NS1643. Data expressed as mean ± SEM, number of replicates = 12, from 3 individual experiments. Statistical analysis; one way ANOVA (Newman-Keuls) *$p<0.05$, *** $p< 0.001$.

3.2.3 Investigating the specificity of hERG channels NS1643 dependent inhibition of cell proliferation in the presence of hERG channel inhibitor terfenadine

It is expected that NS1643 will activate hERG channels in breast cancer cell lines as it does in cardiomyocytes (Hansen, Diness, et al. 2006). To check that NS1643 was acting in the same way in the two breast cancer cell lines used in this study, a Sulforhodamine B (SRB) assay was conducted firstly only in the presence of 10µM NS1643. This was repeated by the addition of 2µM terfenadine, a known hERG channel antagonist. Cell growth inhibition was also tested in the presence of both 10µM NS1643 and 2µM terfenadine together to test whether their independent effects were additive or cancelled each other out. By combining NS1643 with terfenadine, one being an agonist and the other an antagonist, their independent effects should cancel out.

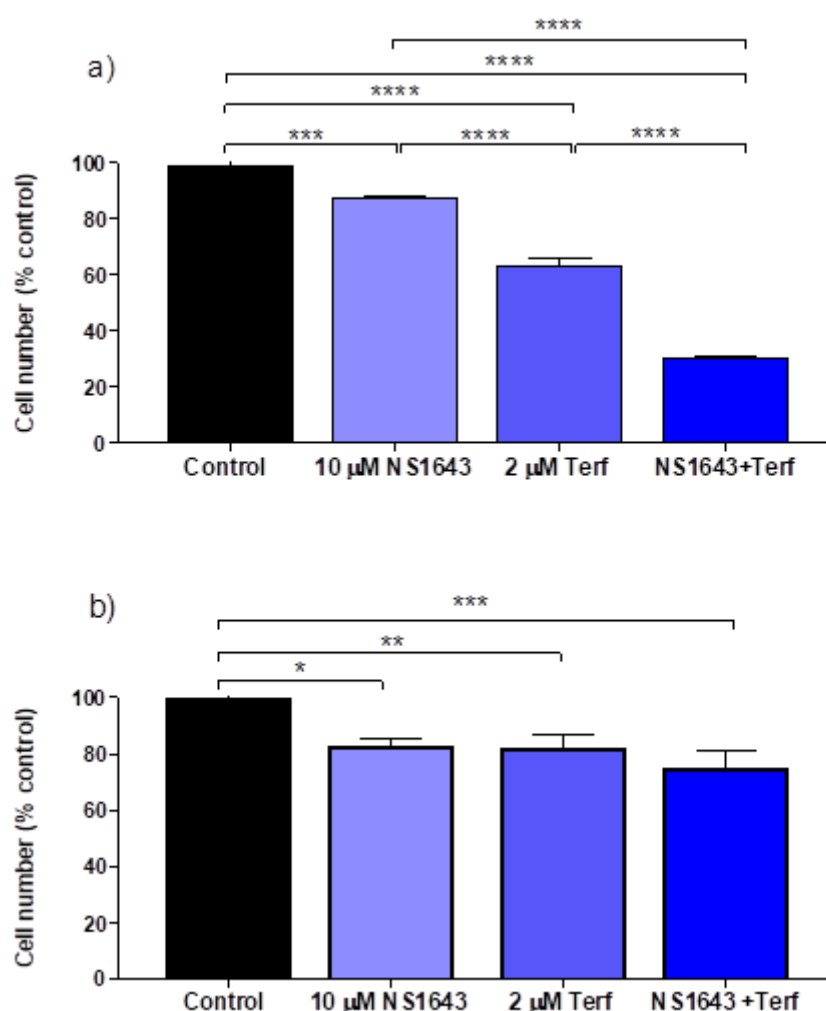Figure 20.Sulforhodamine B analysis of cell number, of breast cancer cell lines, a) MCF-7 and b) MDA-MB-231 following treatment with NS1643, terfenadine or a combination of both compounds to assess any impact on cell number. Data expressed as mean ± SEM, No. of replicates = 12, from 2 individual experiments. Statistical analysis; one-way ANOVA (Newman-Keuls) *p<0.05, **p<0.01, *** p< 0.001,****p<0.0001

Exposure of MCF-7 cells to 10µM NS1643 for 72 hours resulted in inhibition of cell number (87.66 ± 0.88, p<0.001, Figure 20a) compared with the control conditions. In the presence of 2 µM terfenadine alone, cell number decreased significantly (63.40 ± 2.77, p<0.0001) compared with the control, which was also significantly more inhibitory than for NS1643 (p<0.0001). Cells exposed to the combination of hERG agonist NS1643, and hERG antagonist terfenadine, showed further inhibition of cell number (30.54 ± 0.73, p<0.0001) compared with the control and to either NS1643 or terfenadine alone. These results were surprising since they suggest that in MCF-7 cells NS1643 appears to be acting as an antagonist rather than an agonist under these experimental conditions

Exposing MDA-MB-231 to 10µM NS1643 alone caused significant inhibition of cell number (82.48 ± 3.30, p<0.01) compared with the control conditions, and 2µM terfenadine alone also reduced cell number (81.62 ± 4.91, p<0.01) significantly from control (Figure 20b). The presence of NS1643 and terfenadine together also caused significant inhibition of cell number (74.57 ± 6.21, P< 0.001) from the control, but this was not significantly different from NS1643 or terfenadine on their own. These results indicate suggest that in the MDA-MB-231 cells, terfenadine is still acting as an antagonist, but NS1643 is behaving as an agonist.

3.2.4 Functional hERG channels-membrane potential in cancer cells

Considering the results in the previous assay it was decided to investigate further whether NS1643 was behaving differently in each cell line with respect to modulating hERG channels. Since the fundamental role of hERG potassium channels is to control membrane potential in excitable cells by the efflux of potassium ions in a voltage-dependent manner, a commercially available membrane potential kit was used to determine whether NS1643 would increase potassium permeability in both MCF-7 and MDA-MD-231 cell lines.

The membrane potential assay reflects channel opening but does not distinguish between the channel types. Therefore, if the channels are stimulated to open, there is an increase in fluorescence. Further, if some of the channels are blocked, there will be a decrease in fluorescence (since less dye can move into the cells). To compare membrane potential changes, cells growing in growth media only was used as a negative control, 50mM KCl was added to the media to stimulate the movement of potassium ions altering the membrane potential as a positive control, and 10µM NS1643 was added to cells to modulate hERG channels and record any membrane potential change, after 72 hours of treatment.

The negative control values were used as the reference for cells in normal media. Since this assay does not measure membrane potential *per se,* only an increase or decrease in membrane potential relative to the negative control could be recorded. In MCF-7 cells (Figure 21a), the addition of 50 mM KCl, which provided a depolarising step to open channels,

significantly increased the relative response (1.12 ± 0.03, P<0.01) compared with control. However, when 10µM NS1643 was added to the media, the relative response, and thus open channels, decreased significantly (0.88 ± 0.02, P<0.0001) compared with the media only, suggesting the channels are being closed or blocked.

In contrast, in MDA-MB-231 cells (Figure 21b) the addition of 50mM KCl to the media, increased the relative response (1.06 ± 0.02) but this was not statistically significant from the control. From Figure 18 (above) hERG channel staining was more diffuse and less intense suggesting that expression is less than in MCF-7 cells. Interestingly, when 10µM NS1643 was added to the media, relative fluorescence increased, indicating hERG channels opening (1.13 ± 0.02, P<0.0001). These results confirm that NS1643 is acting as an antagonist in MCF-7 cells and an agonist in MDA-MB-231 cells under these experimental conditions.
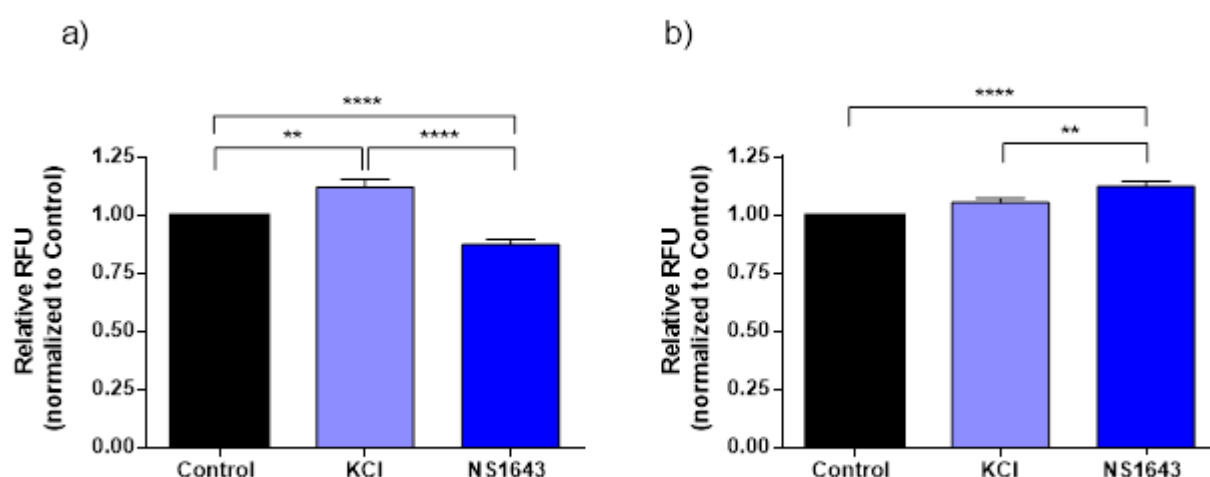
Figure 21. Changes in membrane potential in a) MCF-7 and b) MDA-MB-231 cells, following exposure to variable conditions including; in the presence of media only (negative control), 50mM KCl (positive control) and 10µM NS1643. Statistical analysis; Newman-Keuls one-way analysis of variance, **P<0.01,**** P< 0.0001. Data expressed as mean ± SEM, no. of replicates = 4.

3.2.5 NS1643 impacts on cell cycle progression in a cell dependent manner

NS1643 modulation of the hERG channels alters the membrane potential and impacts on cell number. To assess the impact of NS1643 on cell cycle progression in MCF-7 and MDA-MB-231 cell lines, a cell cycle assay was conducted using DNA specific dye propidium iodide (PI) to determine the percentage of cells in each phase of the cell cycle (G1, S and G2/M).

The percentage of MCF-7 cells (Figure 22) in each phase of the cell cycle cultured in media only was 51.94 ± 3.66 (G1), 35.32 ± 3.45 (S) and 12.74 ± 2.03 (G2/M), respectively. When exposed to 10μM NS1643 this caused a significant increase in cells in the G1 phase (76.67 ± 9.03, $p < 0.05$), with a corresponding decrease in the S phase (18.95 ± 6.43) and G2/M phase (4.37 ± 3.60) when compared to the control.

In contrast, there was no impact on the cell cycle profile in MDA-MB-231 cells (Figure 22) following 72 hours exposure to 10μM NS1643. With cells in growth media only, the percentage of cells in each phase was 47.72 ± 2.92 in G1, 45.48 ± 3.15 in S and 11.83 ± 1.62 in G2/M phases, respectively. The percentage of cells exposed to 10μM NS1643 in each phase was 48.12 ± 6.79 in G1, 41.69 ± 8.19 in S and 10.19 ± 4.06 in the G2/M phases, respectively.
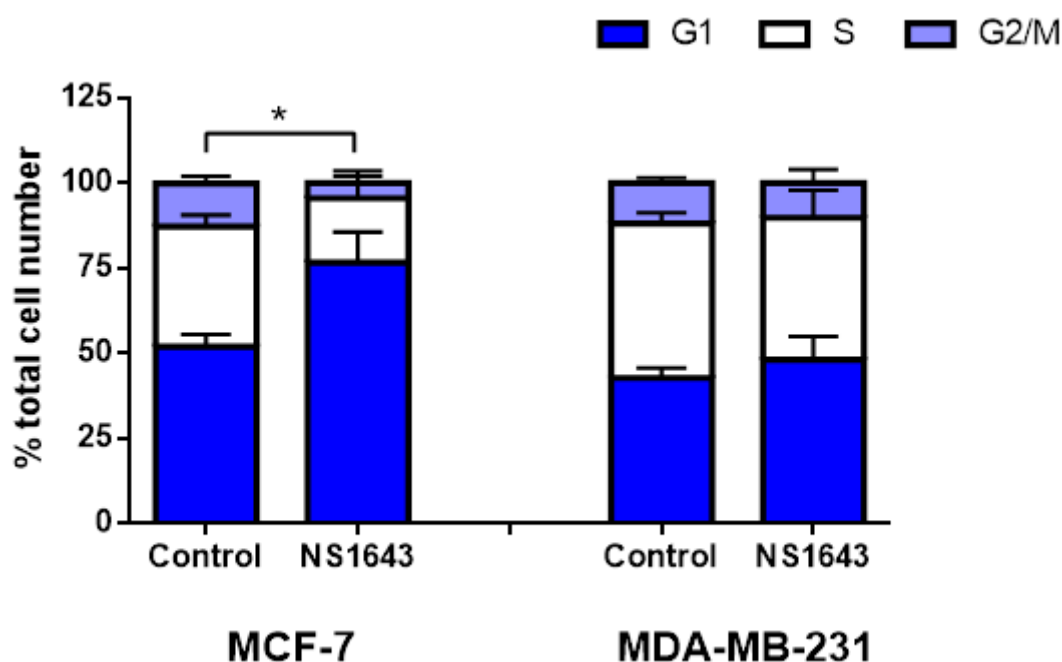
Figure 22. Cell cycle assay involving the DNA specific dye propidium iodide (PI) to determine cell cycle progression by assaying the percentage of cells in each phase of the cell cycle (G1, S and G2/M) following 72 hours exposure to 10μM NS1643 in MCF-7 and MDA-MB-231. Data expressed as mean ± SEM, number of replicates = 12 from 3 individual experiments. Statistical analysis: One-way ANOVA (Newman-Keuls) *$p < 0.05$.

3.2.6 Annexin V Assay-Apoptosis vs Necrosis

In this study the effects of the hERG channel modulation by NS1643 has reduced cell number in both cell lines, but only MCF-7 cells displayed a change in the cell cycle profile, suggesting changes in cell number is not necessarily due to a change in proliferation, but could reflect an increase in cell death.

To assess changes in apoptosis in MCF-7 and MDA-MB-231 cells following treatment with 10µM NS1643, the Annexin V/propidium iodide assay was utilised. In this assay, flow cytometry is used to distinguish between cells in apoptosis (regulated cell death) from those in necrosis (unregulated, less desired form of cell death). Apoptosis is a regulated form of cell death, reliant on the mitochondrial membrane potential; whereas necrosis, in contrast, is unregulated and the result of more toxic effects on the cells. An example of the flow cytometry indicating cells in different stages of apoptosis or necrosis is shown in Figure 23.
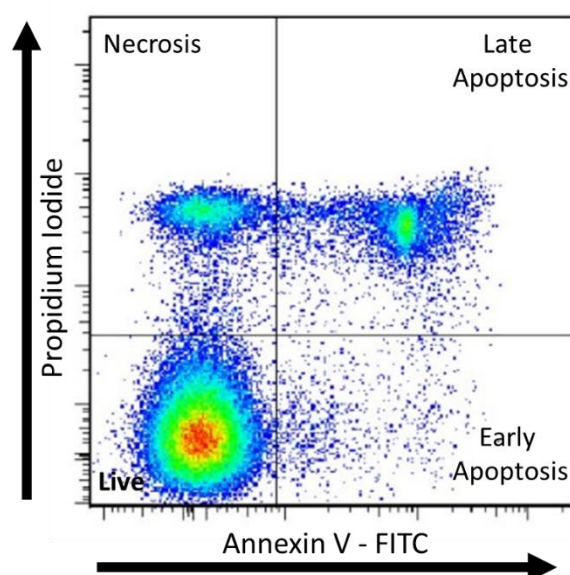
Figure 23. An example of light scatter plot following data collection using CFlow plus of breast cancer cells stained with Annexin V and Propidium iodide. The light scatter plot is divided to 4 sections; bottom left=live cells, top left=necrotic cells, top right = cells in late apoptosis and bottom right= cells in early apoptosis.

Exposing MCF-7 cells to 10µM NS1643 for 72 hours (Figure 24a), caused significantly increased apoptotic events (3.83 ± 0.33) compared with control conditions (2.36 ± 0.19, $p<0.01$). In MDA-MB-231 cells (Figure 24a), exposure to 10µM NS1643 for 72 hours also caused a significant increase in apoptotic events (10.21 ± 0.76) when compared to the control (6.02 ± 0.71, $p<0.01$).

Exposure to 10µM NS1643 for 72 hours (Figure 24b) caused a significant decrease in necrotic events in MCF-7 cells (9.86 ± 0.89) compared with control conditions (13.70 ± 1.39, p<0.05). Similarly, there was a significant decrease in necrotic events observed after 72 hours exposure to 10µM NS1643 (2.88 ± 0.48) in MDA-MB-231 cells compared to the control (4.88 ± 0.37, p<0.001. Figure 24b).
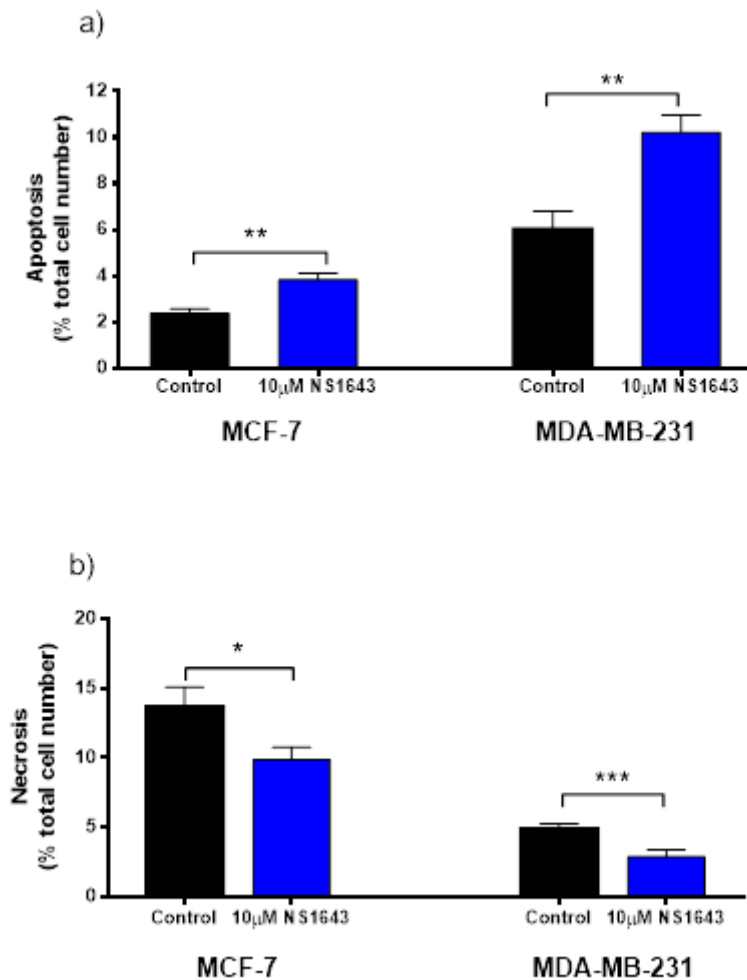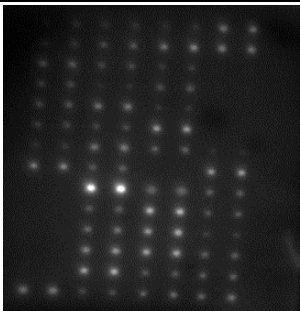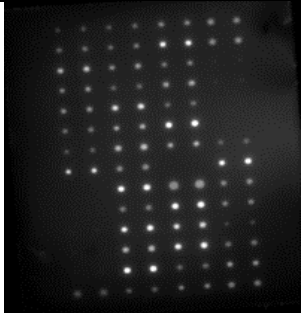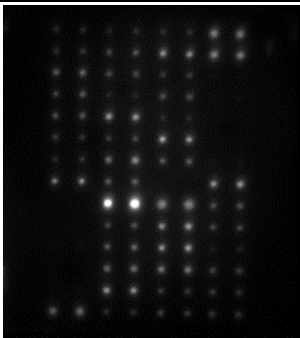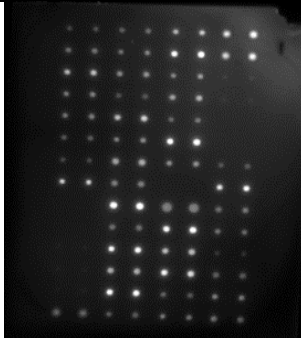
Figure 24. Annexin V analysis of cell death induction via (a) Apoptosis, (b) Necrosis following exposure to 10µM NS1643 for 72 hours. Data expressed as mean ± SEM, No. of replicates = 12 from 3 individual experiments. Statistical analysis; Unpaired Student's t-test *p<0.05, **p<0.01, *** p<0.001.

3.2.7 Human Apoptosis Antibody Membrane Array

To decipher the apoptotic pathway, intrinsic or extrinsic, utilised by each of the cell lines MCF-7 and MDA-MD-231. following treatment with 10µM NS1643, the Abcam Human Apoptosis Antibody Array was utilised. This array allowed investigation into the effect treatment had on the protein levels of 43 known apoptosis markers involved in both apoptotic pathways. Changes were assessed after 18 hours treatment with 10µM NS1643. Only select proteins involved in the intrinsic or extrinsic pathways were analysed. Examples of the array membranes are presented in Figure 25a, and the corresponding map of apoptosis markers are in Figure 25b. The results compare the relative intensity of the markers (normalized to positive control in each case) between control conditions and in the presence of 10µM NS1643 for each breast cancer cell line.

a)

Treatment	MCF-7	MDA-MB-231
Control (no treatment)		
Cells treated with NS1643		

b)

sTNF-R2	sTNF-R2	IGFBP-1	IGFBP-1	CD40	CD40	Pos	Pos
TNF-α	TNF-α	IGFBP-2	IGFBP-2	CD40L	CD40L	Pos	Pos
TNF-β	TNF-β	IGFBP-3	IGFBP-3	cIAP-2	cIAP-2	Neg	Neg
TRAILR-1	TRAILR-1	IGFBP-4	IGFBP-4	cytoC	cytoC	Neg	Neg
TRAILR-2	TRAILR-2	IGFBP-5	IGFBP-5	DR6	DR6	BLANK	
TRAILR-3	TRAILR-3	IGFBP-6	IGFBP-6	Fas	Fas	BLANK	
TRAILR-4	TRAILR-4	IGF-1sR	IGF-1sR	FasL	FasL	Bad	Bad
XIAP	XIAP	Livin	Livin	BLANK		Bax	Bax
BLANK	BLANK	P21	P21	HSP27	HSP27	Bcl-2	Bcl-2
BLANK	BLANK	P27	P27	HSP60	HSP60	Bcl-w	Bcl-w
Neg	Neg	P53	P53	HSP70	HSP70	BID	BID
Neg	Neg	SMAC	SMAC	HTRA	HTRA	BIM	BIM
Neg	Neg	Survivin	Survivin	IGF-I	IGF-I	Caspase 3	Caspase 3
Pos	Pos	sTNF-R1	sTNF-R1	IGF-II	IGF-II	Caspase 8	Caspase 8

Figure 25. a) A representation of Chemiluminescence detection of Abcam Human Apoptosis Antibody Array membranes in cell lines MCF-7 and MDA-MB-231 exposed to 10 µM NS1643 and without treatment (control), and b) is the corresponding map of apoptosis markers.

The impact of exposing MCF-7 and MDA-MB-231 cells to 10µM NS1643 for 18 hours on a selection of apoptotic markers is represented in Table 6. Generally, there was no change in the expression of the extrinsic apoptotic markers in MCF-7 cells but there was a 2-fold decrease in DR6 and Fas in MDA-MB-231 cells.   Further, there was no change in the expression of the extrinsic apoptotic markers in MCF-7 cells except for a 2-fold decrease in HTRA, while in MDA-MB-231 cells there was 2-fold decrease in apoptotic markers Bad, Bax, HTRA as well as the anti-apoptosis markers Bcl-2 and Bcl-w.

Apoptosis Marker		NS1643	
		MCF-7	MDA-MB-231
Extrinsic	TNF-α	-	-
	FasL	-	-
	TRAILR-1	-	-
	TRAILR-2	-	-
	TRAILR-3	-	-
	TRAILR-4	-	-
	DR6	-	↓
	Fas	-	↓
	sTNF-R1	-	-
	sTNF-R2	-	-
Intrinsic	p53	-	-
	Bad	-	↓
	Bax	-	↓
	BID	-	-
	BIM	-	-
	SMAC	-	-
	HTRA	↓	↓
	CytoC	-	-
	XIAP	-	-
	Bcl-2	-	↓
	Bcl-w	-	↓
	Caspase 8	-	-
	Caspase 3	-	-

Table 6. Impact of the hERG channel modulator NS1643 on the apoptotic pathway markers in breast cancer cell lines MCF-7 and MDA-MB-231 (arrows are indicative of 2 or more-fold increase/decrease in the expression of apoptotic marker).

3.3 Discussion

Using immunohistochemistry to identify expression patterns and NS1643 to modulate channel function, this study has shed more light on the role of hERG channels in breast cancer. The different protein localisation in MCF-7 and MDA-MB-231 cell lines, combined with the different impact of treatment with NS1643 identified that it is not so much about the hERG channel kinetics, but more about the disruption of membrane potential that potentially has detrimental effects on the cells. NS1643 inhibited cell proliferation in both cell lines, it also initiated apoptosis instead of necrosis in both cell lines, but NS1643 appears to agonise hERG channels in MDA-MB-231 cells, while antagonising hERG channels in MCF-7 cells.

Immunohistochemistry has confirmed the expression of hERG channels in two different breast cancer cell lines, MCF-7 and MDA-MB-231, but revealed different expression patterns particularly associated with the ER. In both MCF-7 and MDA-MB-231 breast cancer cell lines there is specific colocalization to the nucleus and the mitochondria. Discrete staining around the nucleus, and possibly the ER, was only observed in the MCF-7 cells. Previous immunohistochemistry studies to localise hERG channels, only reported a diffuse staining pattern in the melanoma cell line MDA-MB-435S (Afrasiabi et al. 2010) and ovarian cancer cell line SK-OV-3 (Asher et al. 2011) with no reference to specific intracellular membranes or organelles.

Previously, hERG channel expression in MCF-7 (Roy et al. 2008) and MDA-MB-231 (Hammadi et al. 2012) breast cancer cell lines have only been conducted using western blot analysis and mRNA, with different length hERG channels being expressed in each. The full length hERG channel transcript was identified in MCF-7 cells while the shorter transcript was reported in MDA-MB-231 cells. The smaller transcripts generally lack part of or most of the NH2 terminus of the hERG channel and functionally have faster inactivation kinetics (Bianchi et al. 1998). This difference in transcript expression, along with localisation to mitochondria in both cell lines, and MCF-7 expression in endoplasmic reticulum, could contribute to the different function that hERG channels appear to have in different cancers. Localisation to the mitochondria in both cell lines, MCF-7 and MDA-MB-231, is potentially significant since the mitochondrial membrane potential in cancer cells is more hyperpolarised than in normal cells. The presence of potassium channels in the mitochondrial membrane was confirmed in A549 human lung carcinoma cells by using small molecule dichloroacetate (DCA) which alters the activity of the mitochondria in glucose oxidation which is believed to result in increased expression of K_v potassium channels by inhibiting nuclear factor of activated T lymphocytes (NFAT) responsible for the regulation of cell differentiation (Bonnet, Archer, Allalunis-Turner, Haromy, Beaulieu, Thompson, Lee, Lopaschuk, Puttagunta, Bonnet, et al. 2007). From the results presented here hERG channels could be one class of channels with increased

expression on mitochondria membranes contributing to a more hyperpolarized mitochondrial membrane potential. The apparent expression of hERG in mitochondria opens the question whether the effects of the hERG activators could be related at least in part to the binding of the molecules to the intracellular target. As NS1643 may bind to the S5-S6 domain in cardiomyocytes, it may also with prolonged exposure diffuse into the cancer cells and affect an intracellular site. This could be on the truncated amino end or at the carboxylic end of the channel complex.

Previous studies on MDA-MB-231 breast cancer cells used 50µM NS1643 to significantly reduce cell number monitored with the Trypan Blue assay (Lansu and Gentile 2013) but NS1643 had not previously been investigated on MCF-7 cells. An initial experiment was conducted to investigate inhibition of proliferation in both cell lines using the colorimetric Sulforhodamine B (SRB) assay which is more sensitive than the Trypan Blue and has no time sensitive constraints (Longo-Sorbello et al. 2006). The concentrations of NS1643 used were 1, 5 and 10µM for each cell line. MCF-7 cells were more sensitive to NS1643, with significantly reduced cell number for all concentrations used compared with the control. Conversely in MDA-MD-231 cells proliferation was only significantly reduced in the presence of 10µM NS1643. Since both cell lines were sensitive to 10µM NS1643 this was used in all other experiments.

NS1643 can act as a hERG channel agonist in MDA-MB-231 cells (Lansu and Gentile 2013) and cardiomyocytes (Hansen, Diness, et al. 2006) where Kv11.1 is expressed, but it is also known to be a partial antagonist in Chinese hamster ovary cells (CHO) stably transfected with the Kv11.3 hERG subtype (Bilet and Bauer 2012). To test that NS1643 was acting as an agonist in this study a simple membrane potential assay was used whereby an indicator dye will enter cells when channels are opened increasing relative fluorescence. This assay did not distinguish between channels nor provide actual membrane potential values, rather relative fluorescence would change under experimental conditions used to open or close specific channels. The dye does not fluoresce until it is inside the cells, and so relative fluorescence will only increase when channels open to allow it to diffuse inside. Thus, by using specific hERG channels modulators (agonists or antagonists) one should be able to record a difference in relative fluorescence from control conditions.

In MCF-7 cells, relative fluorescence decreased in the presence of 10µM NS1643 indicating that hERG channels had been blocked. The opposite effect was observed in MDA-MB-231 cells, with increasing relative fluorescence, indicating that NS1643 was opening hERG channels. The difference in the activity of NS1643 in each cell line, could be associated with different transcripts being expressed. It is also feasible that this assay was not detecting only

the activity of hERG channels and a more sensitive assay should be used to confirm these observations.

Previously, the membrane potential in MCF-7 cells has been monitored throughout the cell cycle with more cells being hyperpolarized in G1/S or G2/M but more depolarized when arrested in G0/G1 (Wonderlin, Woodfork, and Strobl 1995) with significant decrease in overall proliferation. Using the SRB assay to detect cell number an initial experiment demonstrated that MCF-7 cell number was significantly reduced after exposure to 10μM NS1643. To further investigate whether hERG channels were being activated or inactivated by NS1643, this experiment was repeated in the presence of 2μM terfenadine which is a known antagonist. Cell number was also reduced significantly after exposure to terfenadine. So, it appeared that agonising or antagonizing hERG channels could reduce cell number in MCF-7 cells. If NS1643 and terfenadine were having opposite actions on hERG channels, when used together, there should be a diminished effect, so that cell number should return toward control conditions. However, when MCF-7 were exposed to them in combination, cell number was significantly reduced even more than for each alone. These results confirm the initial findings from the membrane potential assay earlier that NS1643 was acting as an antagonist rather than an agonist under these experimental conditions. When this approach was repeated with MDA-MB-231 cells however, 2μM terfenadine predictably decreased cell number by antagonizing hERG channels, but when NS1643 and terfenadine were introduced in combination, there was no significant reduction in cell number than for when they were used independently. In this case, the results suggest that NS1643 was acting as an agonist in MDA-MB-231 cells as expected. Further, proliferation was significantly inhibited in each cell line by 10μM NS1643, so changing the membrane potential in the cells to either chronically more depolarized or hyperpolarized prevented cell growth.

From the early observations that MCF-7 cells would not progress through the cell cycle if the membrane potential was changed to either a more depolarized or more hyperpolarized state (Wonderlin, Woodfork, and Strobl 1995) it was investigated how cell cycle progression would be affected in MCF-7 cells after exposure to 10μM NS1643. The cell cycle was arrested in MCF-7 cells with cells accumulating in G1 phase indicating they could not progress through to S phase. This is consistent with reports that hERG channels are only active in G1 to S phase and not involved in G2 and M phases (Urrego et al. 2014; Rao et al. 2015). These data also confirm that NS1643 was blocking hERG channels in MCF-7 cells in this study and are consistent with the effect of the experimental hERG channel antagonist E-4301 also arresting cells at G1 phase in the SDF-1a stimulated leukaemia cell line HL-60 (Zheng et al. 2011). So, by blocking the hERG channels, the membrane potential would remain more depolarized as

cells left G1 phase and the membrane potential drop required for progression to S phase would be inhibited.

When the cell cycle was investigated in MDA-MB-231 cells however, NS1643 acting as an agonist, had no effect. Since in this case NS1643 was causing hyperpolarization of the membrane potential it was expected that the cells would progress through G1 and S phases but depending on how critical a hyperpolarized membrane potential is for transition to G2 and M phases, may accumulate. In MDA-MB-231 cells no such accumulation was observed, but hERG channel expression is less in these cells than MCF-7 cells. Agonising hERG channels in the SKBR3 breast cancer cell line did cause cell cycle arrest in G1 phase, but 50µM NS1643 was used (Lansu and Gentile 2013).

It is well known that cell cycle progression relies on the rhythmic changes in membrane potential from more hyperpolarized to more depolarized. Interruption of this will not only arrest the cell cycle, but can induce apoptosis if cells cannot progress to mitosis, resulting in reduced proliferation (Ouadid-Ahidouch and Ahidouch 2013). Since proliferation was affected in both cell lines by 10µM NS1643, but cell cycle progression was only affected in MCF-7 cells, it was of interest to determine whether apoptosis and or necrosis was increased. Using the Annexin V / Propidium iodide assay which distinguishes between early apoptosis, late apoptosis and necrosis, cell death was recorded for both MCF-7 and MDA-MB-231 cells after exposure to 10µM NS1643 for 18 hours. Apoptosis was increased, and necrosis was decreased in both cell lines, demonstrating that cell death was more programmed. The intrinsic apoptotic process is reliant on changes to the mitochondrial membrane potential allowing Ca^{2+} fluxes to initiate apoptotic factors entering the cytoplasm activating the degradative processes characteristic of apoptosis. Altering the membrane potential may have had a downstream effect on mitochondrial membrane potential, or NS1643 which is lipophilic may have had time to diffuse into the cells and affect hERG channels directly on the mitochondrial membrane.

The apoptosis membrane array was used as a preliminary analysis tool to assess the impact of hERG channel modulator NS1643 on the induction of apoptosis through either the extrinsic or intrinsic pathway. Due to time and financial constraints the apoptosis microarray was only conducted once, with 2 replicates for each sample. Given this lack of statistical strength only results where there was 2-fold change were reported. In MCF-7 cells (Figure 26), only a decrease in HTRA, a mitochondrial pro-apoptotic molecule, was observed in cells treated with NS1643. This molecule is associated with the intrinsic pathway. However, caspase 3, the executioner caspase, did not show changes in levels as a downstream consequence of HTRA decrease, but HTRA is known to also initiate apoptosis independently of caspase which needs to be further explored. In contrast, in MDA-MB-231 cells (Figure 26) treatment with NS1643,

increasing apoptosis, was associated with a decrease in the anti-apoptosis proteins, bcl2 and bcl-xl, and the pro-apoptotic proteins, Bad and Bax. Given the interaction between the molecules in determining cell fate, a decrease in both doesn't clearly identify how the change favours apoptosis stimulation. But results do suggest that the intrinsic pathway is the more favoured process. Similarly, in MCF-7 cells, there was no change in caspase 8 or 3, but there are at least 10 known cascades involved in apoptosis that could be involved and not assessed here. Further research is required to assess the mechanisms involved in enhancing apoptosis following treatment with NS1643.
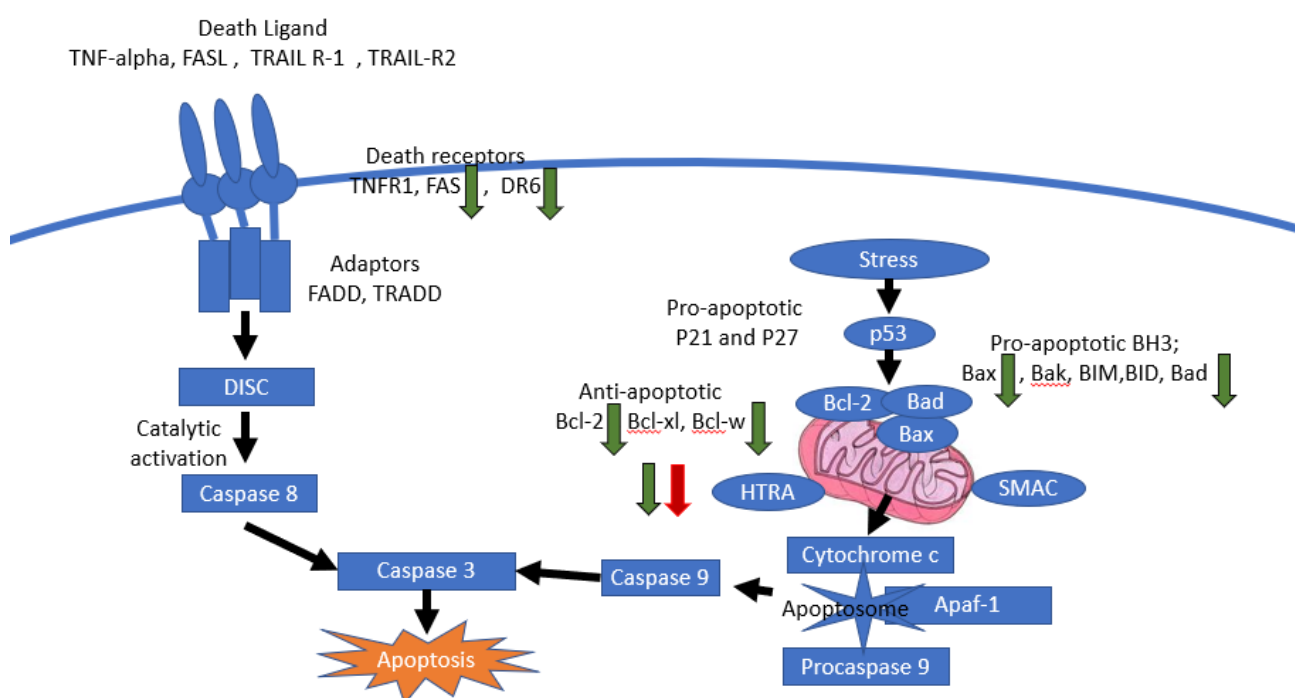
Figure 26. Impact on apoptotic markers involved in the activation of the extrinsic and intrinsic pathways after 18 hours exposure to 10μM NS1643 in MCF-7 cells (red arrow), and MDA-MB-231 cells (green arrows).

In this study, it appears that when NS1643 acted as an antagonist in MCF-7 cells, it caused decreased proliferation, inhibited the cell cycle with accumulation of cells at G1 phase with induction of apoptosis and reduced necrosis. While acting as an agonist in MDA-MB-231 cells NS1643 decreased proliferation but did not affect the cell cycle, yet increased apoptosis and reduced cell death by necrosis.

Regardless of whether channels are open or closed, the disruption to membrane potential is deleterious to cell survival by inhibiting proliferation, stimulating apoptosis, although the mechanisms need to be further explored. But the potential as an alternative therapy for cancer treatment would be benefical as it would reduce the cardiotoxicities.

Chapter 4 - Modulation of hERG channels by urea and thiourea quinazolin-4-one compounds as potential anti-cancer agents in hormone positive and hormone negative breast cancer cells MCF-7 and MDA-MB-231

4.1 Introduction

The abnormal expression of hERG channels in cancers, and its association with poor prognosis makes it a good therapeutic target. NS1643, a known modulator of hERG channel function, has varying effects in different cancer cell populations. As an antagonist in MCF-7 cells, NS1643 caused decreased proliferation, inhibited the cell cycle with accumulation of cells at G1 phase with induction of apoptosis, which was accompanied by a predictable decrease in necrosis. While acting as an agonist in MDA-MB-231 cells, NS1643 decreased proliferation without changing the cell cycle, yet increased apoptosis, with less necrosis occurring. Regardless of the mechanisms, disruption to membrane potential had deleterious effects on cell survival, which is an important feature in cancer therapy. The structure of NS1643 seen in Figure 27, chemically known as 1,3-bis-(2-hydroxy-5-trifluoromethyl-phenyl)-urea (NS1643), is an acyclic diphenyl urea with tri-fluoromethyl (CF_3) at C5 position of the compound.

It has been previously reported that the presence of fluorine atoms enhances the lipophilicity, absorption and bioavailability of quinazoline-sulphonamide small molecules that have shown anti-cancer activity in various cancer cell lines including cervical cancer (Hela), lung (A549) and colorectal (LoVo) cell lines (Ghorab et al. 2016). The urea substitution enhances the anti-cancer effects in cell lines such as liver cancer cells (HepG2), stomach cancer cells (MGC-803) and lung cancer (A549) cells with some anti-proliferative effects seen in all cell lines (Chen et al. 2016). Thiourea modified quinazolines (thiourea-modified 3-chloro-4-fluoroanilino-quinazoline derivatives) have also been found to inhibit the epidermal growth receptor (EGFR) in NCI-H460 and NCI-H1975 lung cancer cells with potency as low as 1.7 µM which is equal to that of the known inhibitor Gefitinib (Yang et al. 2015).
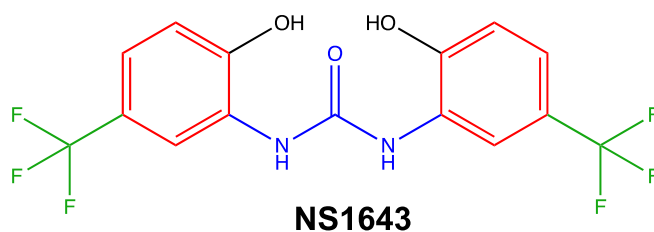
NS1643

Figure 27 The structure of hERG channel modulator NS1643 (highlighted structures; red; di-phenyl groups, blue; acyclic urea, green; the fluorine atom substitutions).

The responses of both MCF-7 and MDA-MB-231 cells to NS1643, inspired further investigation into how its structure might be associated with its various anti-cancer actions observed in this study. The class of molecules selected to assist in the investigation was the quinazolin-4-one compounds. The quinazolin-4-one structure (Figure 28) includes an aromatic benzopyrimidine (made up of aromatic rings benzene and pyrimidine) containing two

fused six member rings and two nitrogen atoms (Saurav et al. 2011). This quinazoline derivative has many pharmacological properties, including antimicrobial (Panneerselvam et al. 2009), antimalarial (Verhaeghe et al. 2008), anti-inflammatory (Saravanan, Pannerselvam, and Prakash 2010), anticonvulsant (Georgey, Abdel-Gawad, and Abbas 2008), anti-hypertensive (Ismail et al. 2006) and anti-viral (Krishnan et al. 2011) actions.
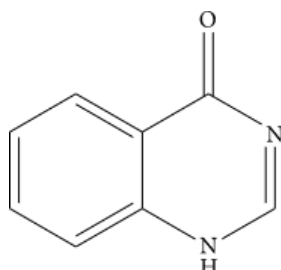
Figure 28. Structural representation of quinazoline-4-one (Faraj et al. 2014)

The selection of the quinazolin-4-one compounds used in this study was based on structural similarity to NS1643 which includes; the presence of cyclic thioxo-(S) or oxo-(O) and fluorine side chains. Synthesis and NMRA spectra of these derivatives has been confirmed (Heppell and Al-Rawi 2015), and they are known as cyclic thioureas (LTUJH06B, LTUJH18B and LTUJH28B) having a thioxo (S) and cyclic ureas (LTUJH37B, LTUJH47B and LTUJH51B) with an oxo (O) at C2, and an ester or amide functional group attached to N3 (Table 7).

Compound LTUJH06B is a cyclic quinazolin-4-one that contains a thioxo at C2 and at N3 there is a methylene (CH$_2$) spacer between the quinazolin-4-one and the ester functional group. There is also a fluorine atom attached at C7 and C8. Compound LTUJH18B is a cyclic quinazolin-4-one with a thioxo attached at C2 and an ester group attached to N3 with fluorine atoms attached to C7 and C8. Compound LTUJH28B is a cyclic quinazolin-4-one with a thioxo attached at C2 that comprises an N,N-dimethyl amide group attached to N3 and fluorine atoms attached to C7 and C8. Compound LTUJH37B is a cyclic quinazolin-4-one with an oxo attached at C2 that lacks an ester/amide functional group at N3 but has fluorine atoms attached to C7 and C8. While compound LTUJH47B is a cyclic quinazolin-4-one with an oxo attached at C2, an ester group attached at N3, a fluorine atom attached at C8 and a morpholino group attached at C7. The final compound LTUJH51B is a cyclic quinazolin-4-one with an oxo attached at C2 an N, N-dimethyl amide group attached to N3 and fluorine atoms attached at C7 and C8.
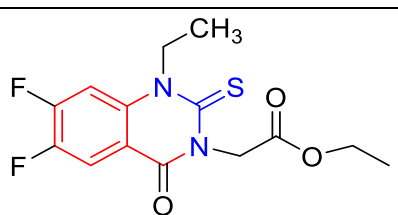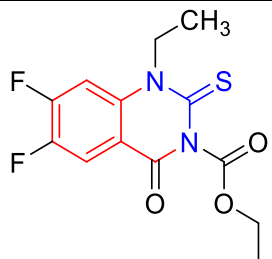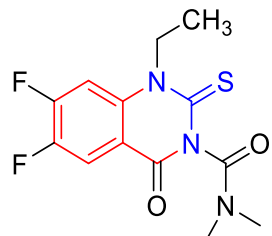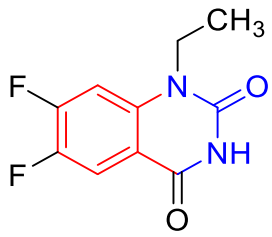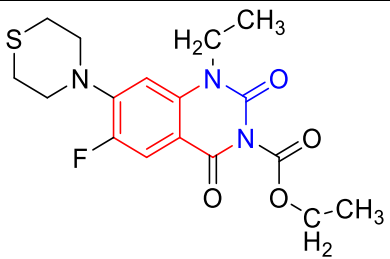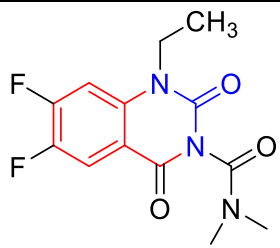
Quinazolin-4-one compounds (Generic name)	Structure and chemical name
LTUJH06B*	ethyl 2-(1-ethyl-6,7-difluoro-4-oxo-2-thioxo-1,4-dihydroquinazolin-3(2*H*)-yl)acetate
LTUJH18B*	ethyl 1-ethyl-6,7-difluoro-4-oxo-2-thioxo-1,4-dihydroquinazoline-3(2*H*)-carboxylate
LTUJH28B*	1-ethyl-6,7-difluoro-*N*,*N*-dimethyl-4-oxo-2-thioxo-1,4-dihydroquinazoline-3(2*H*)-carboxamide
LTUJH37B**	1-ethyl-6,7-difluoroquinazoline-2,4(1*H*,3*H*)-dione
LTUJH47B**	ethyl 1-ethyl-6-fluoro-2,4-dioxo-7-thiomorpholino-1,4-dihydroquinazoline-3(2*H*)-carboxylate
LTUJH51B**	1-ethyl-6,7-difluoro-*N*,*N*-dimethyl-2,4-dioxo-1,4-dihydroquinazoline-3(2*H*)-carboxamide

Table 7 Quinazolin-4-ones tested in this study (red highlighted structure = quinazoline unit, blue highlighted stucture = thioxo- or oxo- subitution) *cyclic thiourea, **cyclic urea.

The compounds were screened for hERG channel modulation in MCF-7 and MDA-MB-231 breast cancer cell lines using the same assays for cell growth and cell death as described in Chapter 3. The results were compared not only with the control conditions but also the results obtained for NS1643 from the previous chapter. This provided the opportunity to screen for potentially better hERG channel modulators than NS1643 and later to consider some structure activity relationships based on any differences in their effects on these breast cancer cell lines.

4.2 Results

4.2.1 Cell proliferation inhibition-NS1643 versus Quinazolin-4-one compounds

The Sulforhodamine B (SRB) assay was used to determine cell density (indicative of cell proliferation) in both MCF-7 and MDA-MB-231 cell lines after 72 hours exposure to 10µM LTUJH06B, LTUJH18B, LTUJH28B, LTUJH37B, LTUJH47B or LTUJH51B. The results were compared with those obtained for NS1643 as well as the control conditions (media only).

All the compounds significantly reduced cell proliferation in MCF-7 cells (Figure 29). The average cell number (relative to control) for each compound was: LTUJH06B (96.18 ± 0.62, p<0.0001), LTUJH18B (96.50 ± 0.68, p<0.0001), LTUJH28B (96.38 ± 0.83, p<0.0001), LTUJH37B (95.02 ± 0.95, p<0.0001), LTUJH47B (95.79 ± 0.14, p<0.0001) and LTUJH51B (94.07 ± 1.39, p<0.0001), respectively. However, all compounds were significantly less potent when compared with NS1643 (87.66 ± 0.89, p<0.0001).
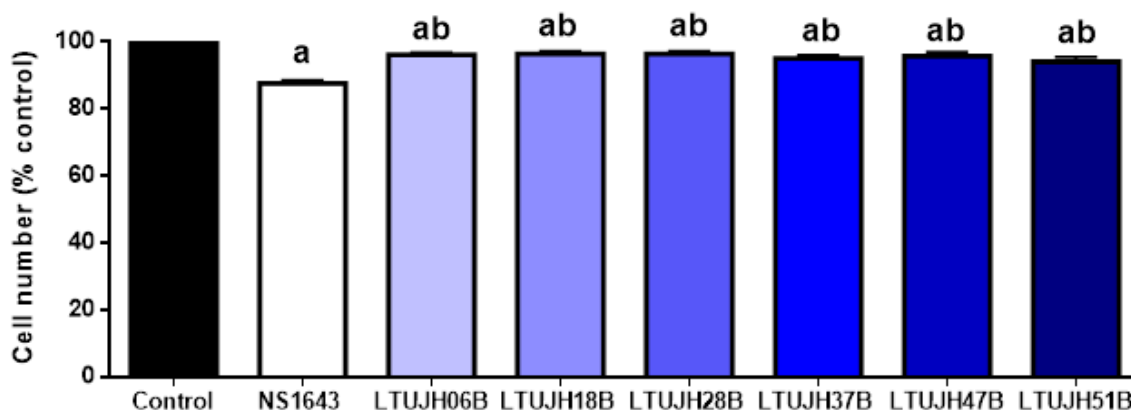
Figure 29 Sulforhodamine B analysis of cell density in the MCF-7 breast cancer cell line, following treatment with 10µM NS1643, LTUJH06B, LTUJH18B, LTUJH28B, LTUJH37B, LTUJH47B and LTUJH51B for 72 hours. Data expressed as mean ± SEM, No. of replicates = 12 from 3 individual experiments. Statistical analysis; one-way ANOVA (Newman-Keuls) a - compound significantly different from control, b - compound significantly different from NS1643.

Exposing the MDA-MB-231 cell line to 10µM of each quinazolin-4-one compounds for 72 hours caused varied responses (refer to Figure 30). Cell proliferation was significantly reduced compared with the control for LTUJH28B (92.92 ± 1.44, p<0.01) and LTUJH37B (87.04 ± 4.32, p<0.0001), while exposure to LTUJH06B (95.98 ± 2.65), LTUJH18B (97.58 ± 1.612), LTUJH47B (99.71 ± 0.39) and LTUJH51B (98.29 ± 0.35) did not significantly reduce cell number compared with control. None of the quinazolin-4-one compounds tested was more potent than NS1643 (85.09 ± 3.24) but LTUJH37B reduced cell number more than any of the other quinazolin-4-one compounds.
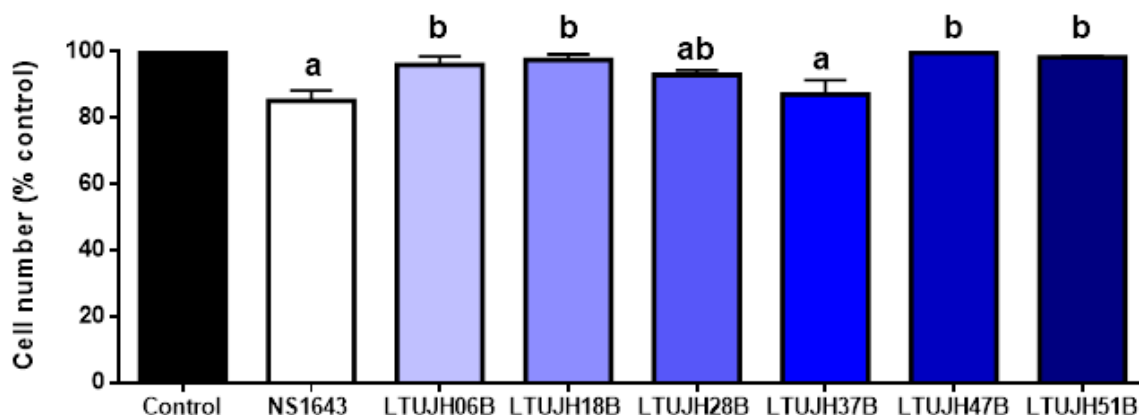
Figure 30. Sulforhodamine B analysis of cell density in MDA-MB-231 breast cancer cell line, following exposure to 10µM NS1643, LTUJH06B, LTUJH18B, LTUJH28B, LTUJH37B, LTUJH47B and LTUJH51B for 72 hours. Data expressed as mean ± SEM, No. of replicates = 12 from 3 individual experiments. Statistical analysis; one-way ANOVA (Newman-Keuls) a – compound significantly different from control, b - compound significantly different from NS1643.

4.2.2 Impact of quinazolin-4-one compounds on membrane potential in breast cancer cells

To confirm that quinazolin-4-one compounds were modulating hERG channels, the same membrane potential assay (permeability to K^+) was used as in Chapter 3. For details of this assay please refer to section 2.9 (Materials and Methods). Comparing the results for NS1643 with those of the quinazolin-4-one compounds provided an opportunity to explore some basic structure-activity relationships and to allow a preliminary assessment of their mode of action. Among the quinazolin-4-one compounds, it was decided to focus on three of them in depth for this assay and later in the microarray assay. Compounds LTUJH18B, LTUJH28B and LTUJH37B were chosen because they showed the largest change in cell number. Each compound was tested at a single concentration (10µM) in all assays described below.

In MCF-7 cells (Figure 31a), 50mM KCl (positive control) stimulated a significant increase in relative fluorescence (1.12 ± 0.03, $p<0.0001$) above control, indicating channels being opened (potentially potassium channels). All the test compounds significantly reduced relative fluorescence, suggesting that channels were being blocked acting as potential antagonists. The decrease in the presence of 10µM LTUJH18B (0.85 ± 0.02, $p<0.0001$) was the most significant among the quinazolin-4-ones, and equally potent as NS1643 (0.88 ± 0.02, $p<0.0001$). Exposure to 10µM LTUJH28B and LTUJH37B also significantly reduced relative fluorescence to (0.92 ± 0.01, $p< 0.01$) and (0.94 ± 0.01, $p<0.01$), respectively compared with control.
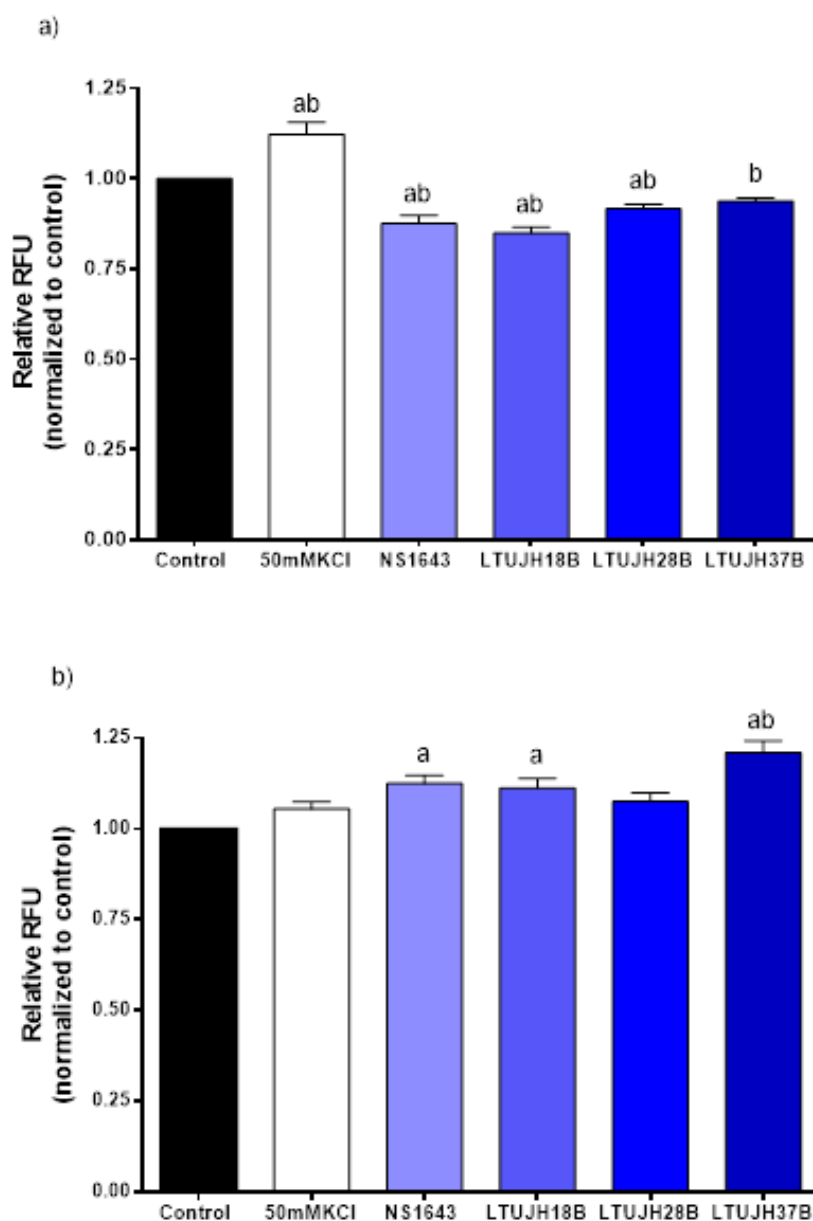
Figure 31. Changes in membrane potential in a) MCF-7 and b) MDA-MB-231 breast cancer cell lines following exposure to variable conditions including; in the presence of growth media only (negative control), 50mM of KCl (positive control) and 10µM NS1643, LTUJH18B, LTUJH28B or LTUJH37B. Data expressed as mean ± SEM (n=4). Statistical analysis; Newman-Keuls one-way analysis of variance, a - compound significantly different from positive control, b - compound significantly different from NS1643.

In MDA-MB-231 cells (Figure 31b), exposure to 50mM KCl slightly increased relative fluorescence, KCl (1.06 ± 0.02) but this was not significant from control. In the presence of 10µM NS1643 relative fluorescence significantly increased (1.13 ± 0.02, p<0.01) compared to control, suggesting hERG channels were being opened. Among the quinazolin-4-ones, LTUJH28B did not increase relative fluorescence above control (1.11 ± 0.03), but both LTUJH18B (1.11 ± 0.03, p<0.01) and LTUJH37B (1.21 ± 0.03, p<0.0001) did significantly

relative fluorescence compared to control. All these compounds acted as agonists, potentially to hERG channels in MDA-MB-231 cells.

4.2.3 Impact on cell cycle progression: NS1643 versus quinazolin-4-one compounds

The DNA specific dye, Propidium Iodide, was used to assess the effect of urea and thiourea quinazolin-4-one compounds on cell cycle progression by measuring the change in the number of cells in each phase (G1, S and G2/M) compared with cells growing in normal media (control conditions). The effect of the quinazolin-4-one compounds LTUJH06B, LTUJH18B, LTUJH28B, LTUJH37B, LTUJH47B and LTUJH51B on the cell cycle phases was also compared to the results for NS1643.

The percentage of MCF-7 cells (Figure 32) in each phase of the cell cycle cultured in media only (control conditions) was 51.94 ± 3.66 (G1), 35.32 ± 3.45 (S) and 12.74 ± 2.03 (G2/M), respectively. When cells were exposed to 10µM NS1643 the number of cells in G1 phase increased significantly (76.67 ± 9.03, $p<0.001$), with a corresponding decrease of cells in S phase (18.95 ± 6.43) and G2/M phase (4.37 ± 3.60) compared with control conditions. This indicated cell cycle arrest at the transition between G1 and S phase.

The number of cells in each phase of the cell cycle after 72 hours exposure to 10µM LTUJH06B was: G1 (62.09 ± 4.53), S (8.56 ± 2.61) and G2/M (19.34 ± 4.09). For LTUJH47B the number of cells in each phase were G1 (57.67 ± 6.71), S (28.43 ± 5.18) and G2/M (13.90 ± 3.75) while for LTUJH51B the number of cells in each phase were G1 (57.04 ± 8.62), S (31.65 ± 6.65) and G2/M (11.31 ± 3.55), none of which were significantly different from control. However, after exposure to 10µM LTUJH18B (G1: 45.13 ± 2.36, S: 31.35 ± 4.09 and G2/M: 23.52 ± 3.12, $p<0.05$), LTUJH28B (G1: 47.79 ± 4.43, S: 27.85 ± 5.78 and G2/M: 24.36 ± 4.03, $p<0.05$) and LTUJH37B (G1: 49.30 ± 5.54, S: 24.25 ± 5.93 and G2/M: 26.47 ± 4.67, $p<0.05$) there was a significantly increased percentage of cells in G2/M and decreased percentage of cells in S phase with no change in the percentage of cells in G1 phase compared with the control.
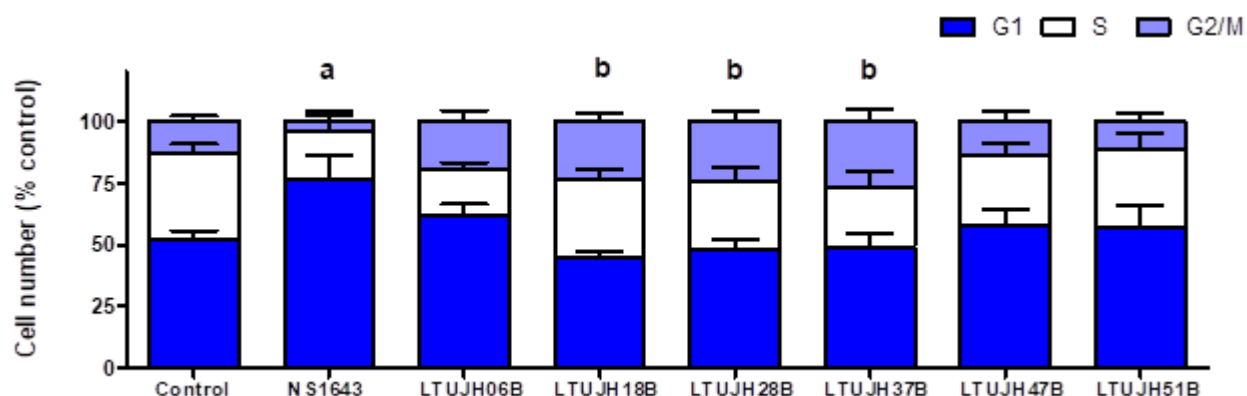
Figure 32. Cell cycle analysis measuring cell number (relative to control) at G1 phase, S phase and G2/M phase in breast cancer cell line MCF-7, following exposure to 10µM NS1643, LTUJH06B, LTUJH18B, LTUJH28B, LTUJH37B, LTUJH47B and LTUJH51B for 72 hours. Data expressed as mean ± SEM. No. of replicates =12 from 3 individual experiments. Statistical analysis; one-way ANOVA (Newman-Keuls). a - compound significantly different from control, b - compound significantly different from NS1643.

In the MDA-MB-231 cell line (Figure 33), there was no significant change in the percentage cells in any of the phases of the cell cycle after 72 hours exposure to any of the compounds tested. The percentage of cells in each phase of the cell cycle was: LTJH06B, 31.44 ± 8.45 (G1), 61.25 ± 8.79 (S), 7.31 ± 2.49 (G2/M); LTUJH18B 43.96 ± 4.25 (G1), 38.32 ± 4.54 (S) 17.73 ± 4.02 (G2/M); LTUJH28B 42.29 ± 6.12 (G1), 46.35 ± 7.02 (S), 11.36 ± 3.80 (G2/M); LTUJH37B 32.05 ± 5.98 (G1), 47.54 ± 8.13 (S), 20.41 ± 3.94 (G2/M); LTUJH47B 47.98 ± 3.35 (G1), 35.22 ± 2.75 (S),16.65 ± 2.52 (G/2M); and LTUJH51B 50.92 ± 2.03 (G1), 38.30 ± 3.83 (S) 18.95 ± 2.30(G2/M), respectively.
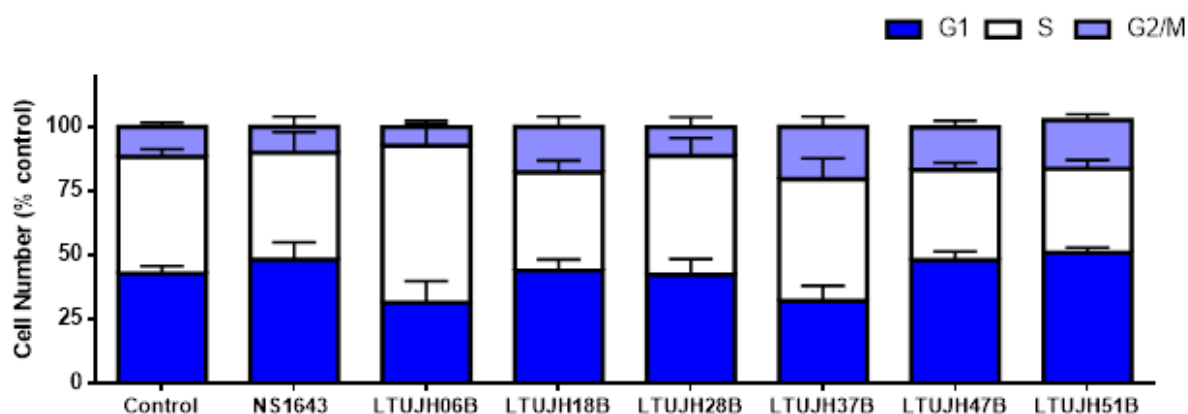
Figure 33. Cell cycle analysis to measure the percentage of cells at G1 phase, S phase and G2/M phase in breast cancer cell line MDA-MB-231, following treatment with 10 µM hERG channel modulator NS1643, and quinazolin-4-one compounds; LTUJH06B, LTUJH18B, LTUJH28B, LTUJH37B, LTUJH47B and LTUJH51B for 72 hours. Statistically analysis; One-way ANOVA (Newman-Keuls), data expressed as mean ± SEM, No. of replicates =12 from 3 individual experiments.

4.2.4 Comparing the impact of quinazolin-4-one compounds on apoptosis and necrosis

Since there was a significant increase in apoptotic events with concomitant significant decrease in the necrotic events in the presence of NS1643, it was of interest to see how each of the quinazolin-4-one compounds affected cell death in the two breast cancer cell lines. The Annexin V/Propidium assay was used to assess which of the cell death pathways, apoptosis (regulated cell death) versus necrosis (unregulated, less desired form of cell death) was preferentially activated following exposure to quinazolin-4-one compounds LTUJH06B, LTUJH18B, LTUJH28B, LTUJH37B, LTUJH47B and LTUJH51B. Results were compared to effects seen following exposure to NS1643.

4.2.4.1 MCF-7

In MCF-7 cells (Figure 34a), 72 hours exposure to 10μM LTUJH51B (3.61± 0.46, p<0.001) and LTUJH28B (3.79 ± 0.38, p<0.001) doubled the percentage of apoptotic cells when compared to cells growing in control media (2.36 ± 0.19) and the results were comparable to NS1643 (3.83 ± 0.33). After 72 hours exposure to 10μM LTUJH06B (1.31 ± 0.20), LTUJH37B (2.63 ± 0.31) LTUJH18B (2.28 ± 0.47), and LTUJH47B (2.08 ± 0.25), there was no significant increase in apoptotic cells compared with those recorded for cells in control media.

The quinazolin-4-one compounds were also assessed for their induction of necrosis (Figure 34b). Following 72 hours exposure to 10μM LTUJH06B (6.9 ± 0.73, p<0.01) and LTUJH18B (10.74 ± 1.10, p<0.05), there were significantly less necrotic cells than control media (13.70 ± 1.39), which was similar to the results for NS1643 (9.86 ± 0.89). Whereas LTUJH28B (15.64 ± 1.74) and LTUJH37B (17.38 ± 2.10) did not cause a significant increase in necrotic cells compared with control, however LTUJH37B generated more necrotic events than NS1643 (p<0.05). LTUJH47B (23.59 ± 1.14, p<0.0001) and LTUJH51B (22.19 ± 1.40, p<0.0001) also produced significantly more necrotic cells compared with control and NS1643.

Finally, while NS1643 increased apoptosis and correspondingly decreased necrosis, this did not occur for all the quinazolin-4-one compounds. Neither LTUJH06B nor LTUJH18B had any effect on apoptosis but decreased necrosis, while LTUJH28B and LTUJH37B increased apoptosis without a corresponding decrease in necrosis. LTUJH47B only increased necrosis, while LTUJH51B increased both apoptosis and necrosis.

a)
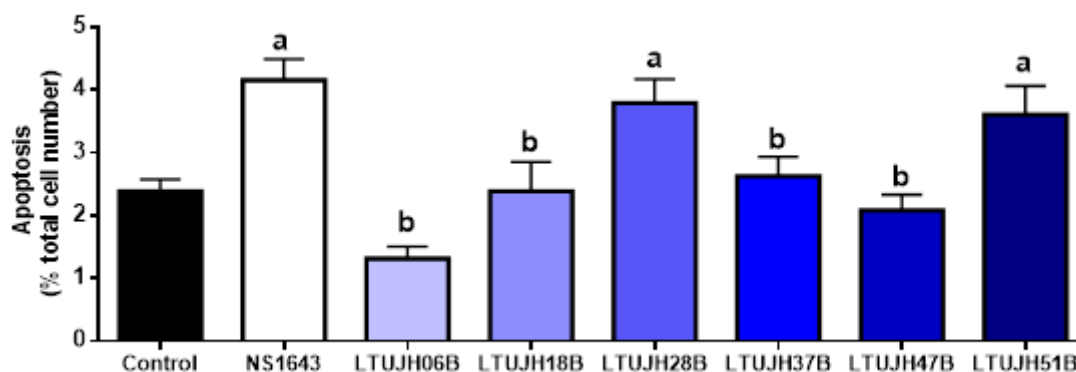
b)
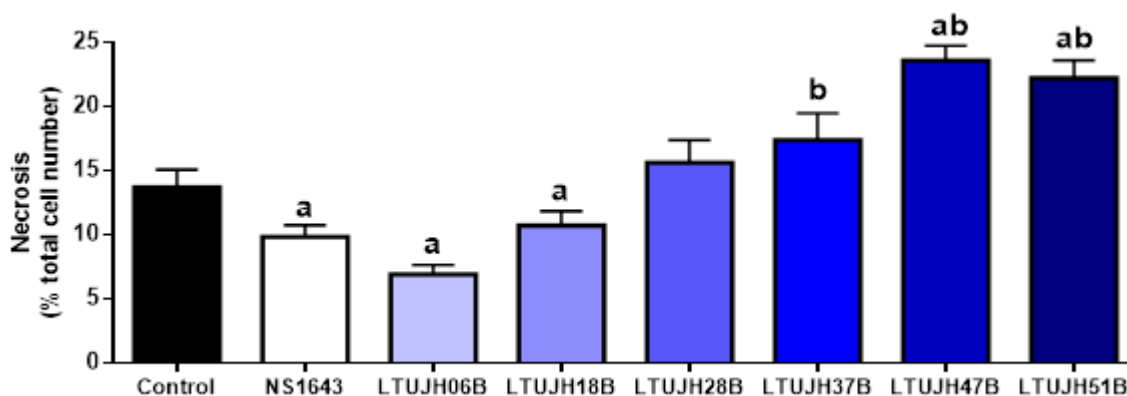
Figure 34. Analysis of apoptosis (a) and necrosis (b) using Annexin V assay, for MCF-7 cells after 72 hours exposure to 10µM quinazolin-4-one compounds LTUJH06B, LTUJH18B, LTUJH28B, LTUJH37B, LTUJH47B, LTUJH51B and NS1643. Data expressed as mean ± SEM, No. of replicates = 12 from 3 individual experiments. Statistical analysis; one-way ANOVA (Newman-Keuls), a - compound significantly different from control, b - compound significantly different from NS1643.

4.2.4.2 MDA-MB-231

In the MDA-MB-231 cell line (Figure 35a), there was significant increase in the percentage of apoptotic cells following 72 hours exposure to 10µM LTUJH06B (12.79 ± 1.4, $p<0.001$), LTUJH18B (8.9 ± 1.05, $p<0.05$), LTUJH28B (9.62 ± 0.98, $p<0.05$), LTUJH47B (12.72 ± 1.36, $p<0.001$) and LTUJH51B (9.36 ± 0.97, $p<0.05$) compared with the control. Among the quinazolin-4-one compounds, only LTUJH37B (14.44 ± 1.52, $p<0.05$) increased the number of apoptotic events above control and NS1643.

The quinazolin-4-one compounds were also assessed for their induction of necrosis and compared with the effect of NS1643 (Figure 35b). Following exposure for 72 hours to 10µM NS1643 and the quinazolin-4-one compounds, the percentage of cells undergoing necrosis was: NS1643 (2.88 ± 0.48, $p<0.01$), LTUJH06B (1.15 ± 0.13, $p<0.001$), LTUJH28B (1.94 ± 0.46, $p<0.01$) and LTUJH51B (1.80 ± 0.26, $p<0.001$), all of which were significantly less

compared with the control (4.88 ± 0.37). LTUJH18B (4.64 ± 0.50, p<0.01) and LTUJH47B (3.86 ± 0.57, p<0.001) however, showed no effect on the percentage of necrotic cells. Finally, in MDA-MB-231 cells, most of the compounds increased apoptosis with a corresponding decrease in necrosis, except for LTUJH18B and LTUJH51B which showed an increase in apoptosis without any change in necrosis.

a)
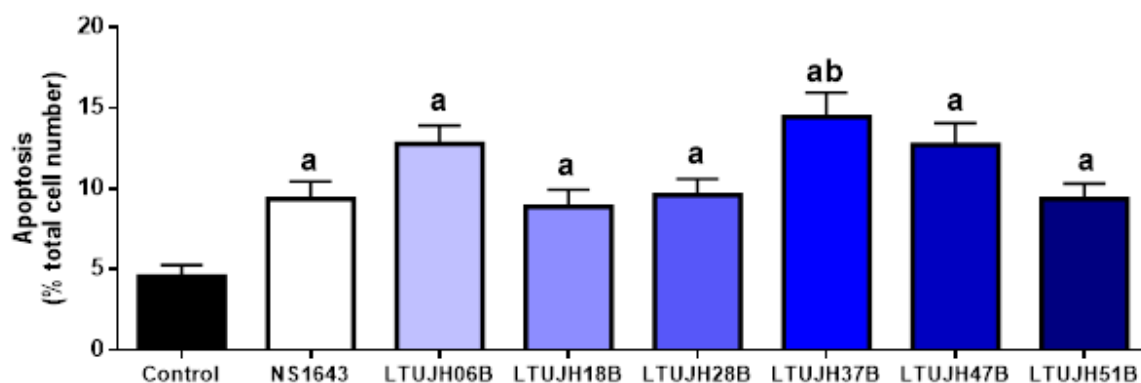
b)
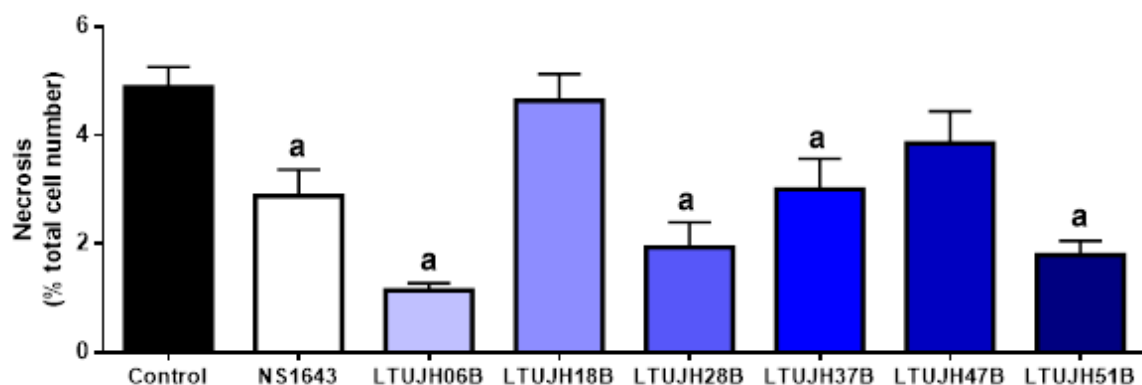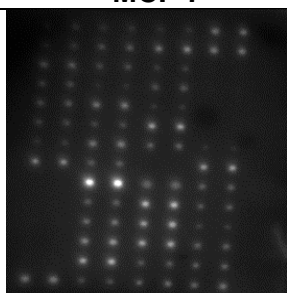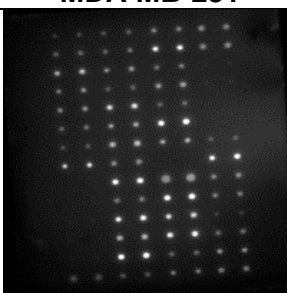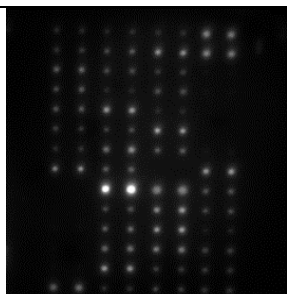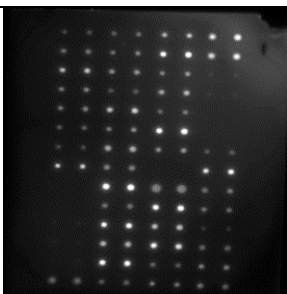
Figure 35. Analysis of apoptosis (a) and necrosis (b) using Annexin V assay, for MDA-MB-231 cells exposed for 72 hours to 10µM LTUJH06B, LTUJH18B, LTUJH28B, LTUJH37B, LTUJH47B, LTUJH51B and NS1643. Data expressed as mean ± SEM, No. of replicates = 12 from 3 individual experiments. a - compound significantly different from control.

4.2.5 Human Apoptosis Antibody Membrane Array

The commercial hERG channel modulator, NS1643 and quinazolin-4-one compounds LTUJH18B, LTUJH28B and LTUJH37B were selected due to their varying actions on cell proliferation and the cell cycle resulting in apoptosis in both MCF-7 and MDA-MB-231 cell lines.

The Abcam Human Apoptosis Antibody Array was used to investigate the induction of both apoptotic pathways (intrinsic and extrinsic) utilised by each of the cell lines MCF-7 and MDA-MB-231 following treatment with 10µM of each of the compounds by changes in the protein levels of 43 known apoptosis markers. Changes were assessed after 18 hours treatment with each of the compounds. Only select proteins involved in the intrinsic or extrinsic pathways were analysed. The array membranes are represented in Figure 36.a, and the corresponding map of apoptosis markers are in Figure 36.b. The results show relative change in respective markers compared with values obtained in the absence of any compounds (normal growth media only).

a)

Treatment	MCF-7	MDA-MB-231
Control (no treatment)		
Cells treated with NS1643		

b)

sTNF-R2	sTNF-R2	IGFBP-1	IGFBP-1	CD40	CD40	Pos	Pos
TNF-α	TNF-α	IGFBP-2	IGFBP-2	CD40L	CD40L	Pos	Pos
TNF-β	TNF-β	IGFBP-3	IGFBP-3	cIAP-2	cIAP-2	Neg	Neg
TRAILR-1	TRAILR-1	IGFBP-4	IGFBP-4	cytoC	cytoC	Neg	Neg
TRAILR-2	TRAILR-2	IGFBP-5	IGFBP-5	DR6	DR6	BLANK	
TRAILR-3	TRAILR-3	IGFBP-6	IGFBP-6	Fas	Fas	BLANK	
TRAILR-4	TRAILR-4	IGF-1sR	IGF-1sR	FasL	FasL	Bad	Bad
XIAP	XIAP	Livin	Livin	BLANK		Bax	Bax
BLANK	BLANK	P21	P21	HSP27	HSP27	Bcl-2	Bcl-2
BLANK	BLANK	P27	P27	HSP60	HSP60	Bcl-w	Bcl-w
Neg	Neg	P53	P53	HSP70	HSP70	BID	BID
Neg	Neg	SMAC	SMAC	HTRA	HTRA	BIM	BIM
Neg	Neg	Survivin	Survivin	IGF-I	IGF-I	Caspase 3	Caspase 3
Pos	Pos	sTNF-R1	sTNF-R1	IGF-II	IGF-II	Caspase 8	Caspase 8

Figure 36. a) A representation of chemiluminescence detection of Abcam Human Apoptosis Antibody Array membranes in cell lines MCF-7 and MDA-MB-231 exposed to 10µM test compound and without treatment (control), and b) is the corresponding map of apoptosis markers.

The results in Table 8 show trends seen following 18 hours exposure to 10µM quinazolin-4-one compounds LTUJH18B, LTUJH28B and LTUJH37B on the expression of both pro and anti-apoptotic markers involved in the intrinsic pathway of apoptosis. The arrow is indicative of a change more than 2-fold above control values.

MCF-7 cells treated with LTUJH18B displayed a similar change as cells treated with NS1643, with no change in the expression of the extrinsic apoptotic markers except for a 2-fold decrease in HTRA. While in MDA-MB-231 cells there was 2-fold decrease in pro-apoptotic markers Bad and Bax, as well as the anti-apoptotic marker Bcl-2. There was also a change in receptor expression, DR6 and Fas decreased levels, while sTNF-R2 increased.

MCF-7 cells treated with LTUJH28B displayed a similar change as cells treated with NS1643, being no change in the expression of the extrinsic apoptotic markers except for a 2-fold decrease in HTRA. While in MDA-MB-231 cells there was no change in proteins associated with the intrinsic pathway, but changes in the levels of receptors (TRAILR-2, Fas, sTNF-R1 and sTNF-R2) and ligands (TNF-α) of the extrinsic pathway.

Cells treated with LTUJH37B displayed changes in the levels of proteins in both cell lines for both the extrinsic and intrinsic pathway. In MCF-7 cells the levels of FasL (ligand) and TRAIL-1 and TRAIL-2 increased in the extrinsic pathway, while the pro-apoptotic Bax increased in the intrinsic pathway. A different pattern was observed in MDA-MB-231 cells, with a decrease in the receptors DR6 and Fas, while there was increased TNF-R1 and sTNF-R2. Further, there was 2-fold decrease in pro-apoptotic markers Bad, Bax and HTRA, as well as the anti-apoptotic marker Bcl-2.

Apoptosis marker		LTUJH18B		LTUJH28B		LTUJH37B	
		MCF-7	MDA-MB-231	MCF-7	MDA-MB-231	MCF-7	MDA-MB-231
Extrinsic Pathway	*TNF-α*	-	-	-	↑	-	-
	FasL	-	-	-	-	↑	-
	TRAILR-1	-	-	-	-	↑	-
	TRAILR-2	-	-	-	↑	↑	-
	TRAILR-3	-	-	-	-	-	-
	TRAILR-4	-	-	-	-	-	-
	DR6	-	↓	-	-	-	↓
	Fas	-	↓	-	↓	-	↓
	sTNF-R1	-	↑	-	↓	-	↑
	sTNF-R2	-	-	-	↑	-	↑
Intrinsic Pathway	*P53*	-	-	-	-	-	-
	Bad	-	↓	-	-	-	↓
	Bax	-	↓	-	-	↑	↓
	BID	-	-	-	-	-	-
	BIM	-	-	-	-	-	-
	SMAC	-	-	-	-	-	-
	HTRA	↓	-	↓	-	-	↓
	CytoC	-	-	-	-	↑	-
	XIAP	-	-	-	-	-	-
	Bcl-2	-	↓	-	-	-	↓
	Bcl-w	-	-	-	-	-	-
Caspases	*Caspase 8*	-	-	-	-	-	-
	Caspase 3	-	-	-	-	-	-

Table 8. Impact of quinazolin-4-one compounds LTUJH18B, LTUJH28B and LTUJH37B on the extrinsic and intrinsic apoptosis pathways in breast cancer cell lines MCF-7 and MDA-MB-231 (arrows are indicative of 2-fold increase/decrease in the expression of the respective apoptotic marker).

4.3 Discussion

The development of small molecule cancer agents is one of the tools currently employed to better understand the mechanism of cancer progression leading of the development of a more targeted therapy with reduced side effects to ultimately achieve a more personalised medicine strategy where anticancer agents can be designed in accordance with the abnormal biology and genetic characteristics of each cancer (Hoelder, Clarke, and Workman 2012). The urea and thiourea quinazolin-4-one compounds investigated in this study were selected for their structural similarity to NS1643 with the presence of cyclic urea and thiourea substitutions as well as the presence of fluorine atoms which as previously discussed may increase lipophilicity. This enables the compounds to cross the plasma membrane to act on intracellular organelles such as the mitochondria, which have increased activity in G1 phase of the cell cycle (Martínez-Diez et al. 2006), proliferation, and apoptotic cell death in cancer (Vyas, Zaganjor, and Haigis 2016). Further the presence of an amide or ester substitution which is different from NS1643 was of interest to see whether there were any differences in the compound's actions on MCF-7 and MDA-MB-231 breast cancer cell lines that might allude to their mode of action.

A summary of the effects of the quinazolin-4-one compounds on proliferation, cell cycle progression, apoptosis and necrosis in MCF-7 and MDA-MB-231 breast cancer cell lines is shown in Table 9. Also, their properties as hERG channel agonists or antagonists is provided.

Quinazolin-4-one compounds	hERG channel action		Cell proliferation		Cell cycle phase (Accumulation)		Apoptosis		Necrosis	
	MCF-7	MDA	MCF-7	MDA	MCF-7	MDA	MCF-7	MDA	MCF-7	MDA
NS1643	Antagonist	Agonist	↓	↓	G1	-	↑	↑	↓	↓
LTUJH06B	ND	ND	↓	-	-	-	↓	↑	↓	↓
LTUJH18B	Antagonist	Agonist	↓	-	G2/M	-	-	↑	↓	-
LTUJH28B	Antagonist	Weak Agonist	↓	↓	G2/M	-	↑	↑	-	↓
LTUJH37B	Antagonist	Agonist	↓	↓	G2/M	-	-	↑	↑	↓
LTUJH47B	ND	ND	↓	-	-	-	-	↑	↑	-
LTUJH51B	ND	ND	↓	-	-	-	↑	↑	↑	↓

Table 9. Summary of the results following exposing MCF-7 and MDA-MB-231 cells to NS1643 and six quinazolin-4-ones. *ND - not done, MDA-refers to MDA-MB-231cells, '-' No change

Since the quinazolin-4-ones were previously untested as potential hERG channel modulators, a membrane potential assay was conducted revealing that unexpectedly NS1643 acted as an antagonist in MCF-7 cells and so did LTUJH18B, LTUJH28B and LTUJH37B. Yet, in MDA-MB-231 cells NS1643 was confirmed as an agonist and the same quinazolin-4-one derivatives were also agonists. The modest rise in response to KCl was not entirely surprising since less hERG channels are expressed in MDA-MB-231 cells (refer section 3.2.1) and the average transmembrane potential is more depolarized (average Vm ~ -20mV) than in MCF-7 cells (average Vm ~ -38mV)(Yang and Brackenbury 2013a). Therefore, the 50mM KCl solution may not have produced as much of a voltage step in MDA-MB-231 cells as it did in MCF-7 cells. From these results it appears that in MDA-MB-231 cells the full transcript of hERG channels is expressed, but in MCF-7 cells a shorter transcript may be present. Notably, none of the quinazolin-4-one compounds were stronger agonists or antagonists than NS1643, except for LTUJH37B in MDA-MB-231 cells. Compound LTUJH37B is a cyclic urea with no functional group at N3, while LTUJH18B and LTUJH28B are thioureas with an ester or an amide at N3, respectively. It doesn't appear to matter whether they are urea or thiourea compounds, but the presence of these functional groups at N3 may be contributing to their reduced potency as agonists in MDA-MB-231 cells. Further, LTUJH18B was slightly more potent with an ester at N3 than LTUJH28B having an amide at N3. In the MCF-7 cells, LTUJH37B was the weakest antagonist, followed by LTUJH28B and LTUJH18B which were significantly different from NS1643. Further studies into where these compounds bind to hERG channels will help to better understand these observations.

With respect to the anti-proliferative effect of the quinazolin-4-one compounds on MCF-7 cells, all reduced cell number significantly from control, but they were all much weaker than NS1643. Quinazoline derivative PVHD121 (which has a 1-hydroxyethyl group at position C4) caused significant anti-proliferative activity against a variety of tumours cell lines including MCF-7 breast cancer cell line, by binding to the colchicine binding site of tubulin (Kuroiwa et al. 2015). In the MDA-MB-231 cell line, only the LTUJH37B (a urea with no functional group on position N3) and LTUJH28B (a thiourea with an amide at position N3) inhibited proliferation significantly from control conditions. It is noted that LTUJH51B which only differs from LTUJH37B by the presence of an amide functional group at N3, was one of the weakest antiproliferative compounds. This is the first time the presence of a thiourea was better than a urea in the compounds. Again, NS1643 was more effective than either quinazoline-4-one compounds. A similar trend was seen with quinazoline derivatives (with substitutions at N1 and C2) significantly inhibiting proliferation in MCF-7 cells but not MDA-MB-231 cells (Zahedifard et al. 2015). In this study, substitutions at N3 and the presence of a thiourea rather than a urea,

alter anti-proliferative effect in the MDA-MB-231 cell line. These differences begin to unravel the specificity for anti-proliferative activity among different cancer cell lines.

Cell cycle progression was affected differently in each cell line in part because all the compounds (NS1643 and the quinazolin-4-one compounds) were hERG channel antagonists in MCF-7 cells and agonists in MDA-MB-231 cells. Since hERG channels are most active in the G1 to S phase of the cell cycle (Rao et al. 2015), antagonizing them would prevent the required membrane potential drop (towards more hyperpolarizing levels) early in G1. NS1643 caused a significant increase in cells at G1, while all the quinazolin-4-one compounds (LTUJH18B, LTUJH28B, LTUJH37B) caused cell accumulation at G2/M phase. One explanation for this result is that because they are weaker antagonists than NS1643, they may not have prevented the membrane potential from hyperpolarizing sufficiently to stall the cell cycle at G1, so cells progressed through S phase, but could not enter G2 phase. It would be interesting to see whether a higher concentration of these compounds would arrest the cell cycle at G1.

In the MDA-MB-231 cells, cell cycle progression was not affected by any of the compounds tested. Since both NS1643 and the three quinazolin-4-one compounds tested were all hERG channel agonists, they would enhance the membrane potential moving to a more hyperpolarized state which would easily allow cell to progress through G1 to S phase. Further hERG channel activity is not important in the transition between G2 and M phase (Rao et al. 2015), so modulating their activity would not be expected to arrest cell cycle progression. Yet these compounds did effectively inhibit proliferation in MDA-MB-231 cells, so they may be initiating apoptosis or a senescence pathway, particularly if they impede the membrane potential becoming more depolarized during transition from S phase to G2/M phase. Cells that cannot successfully undergo mitosis will often undergo apoptosis (Yang and Brackenbury 2013a) .

Initial investigation on the induction of cell death via apoptosis revealed more apoptotic activity in MDA-MB-231 cells than MCF-7 cells overall. All the quinazolin-4-one compounds caused apoptotic events in MCF-7 cells but in the presence of thiourea compound LTUJH28B and urea compound LTUJH51B this was comparable to NS1643. This is consistent with reports that exposure to quinazoline derivatives produce significant apoptotic activity in MCF-7 cells overexpressing HER2 factor (Wu et al. 2010). While in MDA-MB-231 cells all the quinazolines increased apoptosis but only LTUJH37B was significantly higher than NS1643.

When investigating necrosis, the secondary cell death pathway, only urea quinazolin-4-one compounds LTUJH37B, LTUJH47B and LTUJH51B increased necrosis in MCF-7cells while

all quinazolin-4-one compounds either did not produce a significant change or significantly reduced necrotic activity in MDA-MB-231 cells.

From the limited structure activity study it can be seen that although the compounds selected for this study have a central quinazolin-4-one moiety, the presence or lack of an amide or ester group or a cyclic urea or cyclic thiourea altered the activity of the compounds with respect to proliferation, cell cycle progression and programmed cell death. Comparing the action of the quinazolin-4-one compounds to NS1643 activity, those containing a urea (LTUJH37B, LTUJH47B and LTUJH51B) could have contriubted to the enhanced potency of these compounds in inducing apoptosis rather than those with a thiourea (LTUJH06B, LTUJH18B and LTUJH28B).

Investigating the anti-cancer effect of quinazolin-4-one compounds through the modulation of hERG channels in MCF-7 and MDA-MB-231 cells revealed that quinzolin-4-one compounds are potential anticancer agents at a relatively low concentration (10µM). Both urea and thiourea compounds inhibited proliferation in MCF-7 cells which is a representative of the hormone positive breast cancer cells, with some inhibition was seen in the hormone negative MDA-MB-231 cells which is traditionally difficult to treat.

Chapter 5- Investigating the off-target side effects of quinazolin-4-one urea and thiourea compounds in non-cancerous tissue models

5.1 Introduction

One of the major challenges of chemotherapy administration is that the cell killing properties of the cytotoxic agent is not selective to cancer cells (Nygren 2001), with chemotherapy affecting every organ in the body producing either acute or delayed manifestations often with debilitating effects. The most affected cells by chemotherapy are those that are highly dividing including cells of the bone marrow and gastrointestinal (GI) mucosa, hair follicles and the gonads (Goodman 1989).

Significant consideration needs to be taken when developing new anti-cancer compounds, including their toxicity in normal tissues which may lead to organ failure (Curigliano et al. 2009) and whether their activity is reversible or permanent (Goodman 1989). To expedite the process of drug development, a few key components may be considered in the early screening of new compounds. One of the first tests for any new compound is a cytotoxicity assay to determine whether the compound is toxic to normal tissues and over what concentration range. Ideally this should be done in many cell types, to give broader representation of the possible systemic implications.

Chemotherapeutics can cause significant liver toxicity (Sharma et al. 2014) especially to the cytochrome P450 enzymes. The cytochrome P450 family of enzymes is responsible for the metabolism of xenobiotics. Some of these enzymes are found in tissues like the lung, kidney and small intestine, although 70% of CYP450 enzymes, responsible for 90% of drug metabolism, are found in the liver, including CYP450 2E1, CYP450 3A4/5, CYP450 2C9, CYP450 2C19 and CYP450 2D6 (Tanaka 1998). Factors that can influence the expression and subsequently the drug metabolism activity of these enzymes include; environmental factors, stress, drugs and disease (Furukawa et al. 2004).

Since the liver is responsible for the metabolism and clearance of drugs, including many chemotherapeutics, there can be a profound impact on the well characterised cytochrome P450 (CYP450) enzyme system. Simple bioassays can be completed to screen key CYP450 enzymes to determine if a new compound is potentially toxic to the liver or if a specific enzyme may be affected that should be identified for any potential drug interactions in patients. As part of a general introductory screening process the key CYP450 isoenzymes 2E1 and 3A4 should be tested since many anticancer agents used for the treatment of solid tumours are substrates for those isoenzymes (Scripture, Sparreboom, and Figg 2005). Deeper analysis of liver toxicity may be performed with cultured hepatocytes before moving to whole animal models. At the end of the screening process of a new novel compound, cytotoxicity, and CYP450 metabolism should be identified as a first step in understanding the potential for toxicity in living systems.

One of the most significant side effects associated with cytotoxic agents (which may become fatal) is cardiotoxicity (Albini et al. 2010). The definition of cardiotoxicity according to the American National Cancer Institute, is the toxic effect to the heart following the administration of chemotherapeutics agents, radiation therapy, and molecular targeted therapies (NIH 2018). There are three class of cardiotoxicity identified; subacute, acute and chronic. Among the subacute and acute classes, cardiac arrhythmia is most common, often associated with abnormalities in ventricular repolarization particularly in the QT interval. These can manifest at variable times ranging from the initiation of treatment up to 2 weeks following the cessation of treatment. Chronic cardiotoxicity is divided into two subtypes; one occurring 1 year after termination of treatment, and the second occurring more than 1 year after treatment cessation (Dolci et al. 2008).

The potential for a drug to adversely affect the QT interval of the cardiac action potential, specifically associated with hERG channels, deserves investigation since it is well documented that many chemotherapeutic agents (e.g. anthracyclines) are cardiotoxic and increase the risk of patients developing fatal arrhythmias or even heart failure (Yeh and Bickford 2009). Some initial screening for the potential effects of new compounds on hERG channel conductance should be completed to determine whether they may produce long QT syndrome. Later the impact of the new compounds on targeted chemotherapy for cancer treatments will need to be weighed against their potential for cardiotoxicity.

Further, from the results in chapter 4, the quinazolin-4-one compounds appeared to be antagonists in the MCF-7 cell line but agonists in the MDA-MB-231 cell line. Also, NS1643 a commercially hERG channel agonist (with some weak antagonist effects in some cell types) appeared to be an antagonist in MCF-7 cells but an agonist in MDA-MB-231 cells. This raises the question whether different hERG channel transcripts are expressed in these two different breast cancer cell lines. It has been reported previously that NS1643 was an agonist in MDA-MB-231 (Lansu and Gentile 2013). Therefore, another reason for checking the effect on hERG channels was to test their activity in a cell line known to express the full transcript. All mammalian adult cardiomyocytes express $K_V11.1$ or hERG potassium channels in high amounts, with hERG channel found in the plasma membrane of cardiac myocytes (Balse et al.2012)(Vandenberg et al. 2012). Sheep cardiomyocytes were used for cardiotoxicity studies at this time.

5.2 Results

5.2.1 CellTox Green Assay

Initial cell toxicity screening was conducted for all the quinazolin-4-one compounds (LTUJH06B, LTUJH18B, LTUJH28B, LTUJH37B, LTUJH47B and LTUJH51B) using the CellTox Green Assay (Promega, Australia) in sheep cardiomyocytes. The basic principle of the assay is that the green dye will fluoresce if there is free DNA in the solution indicating cell lysis and cell death (further details of this assay is available in materials and methods (chapter 2.11). Cardiomyocytes were exposed to each quinazolin-4-one compound over the concentration range 10^{-8} to 10^{-4} M for 24 hours. The amount of cytotoxicity was compared to natural cell death under control conditions (in normal cell media). It was expected that the adult cardiomyocytes would be relatively fragile since they do not undergo mitosis and would have a higher natural cell death rate than typically seen in immortalized cell lines.

Neither compound LTUJH06B (Figure 37a) nor LTUJH28B (Figure 37c) increased cell lysis in sheep cardiomyocytes after 24 hours exposure, for any of the concentrations tested (10^{-8} to 10^{-4} M). There was a slight increase in cell lysis in the presence of LTUJH06B at 10^{-6} M (83.02 $\pm$ 11.02, p=0.09) and 10^{-5} M (71.16 $\pm$ 20.34, p=0.62) while there was a slight decrease in cell lysis in the presence of LTUJH28B at 10^{-6} M (53.90 $\pm$ 7.07, p=0.19) and 10^{-5} M (62.77 $\pm$ 11.29, p=0.55), but they were not significantly different from that observed in control conditions (64.67 $\pm$ 4.32).

When sheep cardiomyocytes were exposed to 10^{-5} M of LTUJH18B (Figure 37b) for 24 hours, cell lysis increased significantly above those observed under control conditions (64.67 $\pm$ 4.32) (81.39 $\pm$ 5.53, p=0.039). LTUJH47B (Figure 37e) showed significantly increased lysis at 10^{-5} M (77.43 $\pm$ 4.89, p = 0.04) while LTUJH51B (Figure 37f) only significantly increased lysis at 10^{-6} M (84.07 $\pm$ 7.40, p= 0.04), compared with control conditions (64.67 $\pm$ 4.32), respectively.

Finally, both LTUJH37B (Figure 37d) and LTUJH47B (Figure 37e) showed significantly decreased lysis at 10^{-4} M compared with control conditions. The average responses for LTUJH37B (33.95 $\pm$ 12.97, p=0.014) and LTUJH47B (40.76 $\pm$ 3.24, p= 0.003), were both significantly less than for control conditions (64.67 $\pm$ 4.32), respectively.
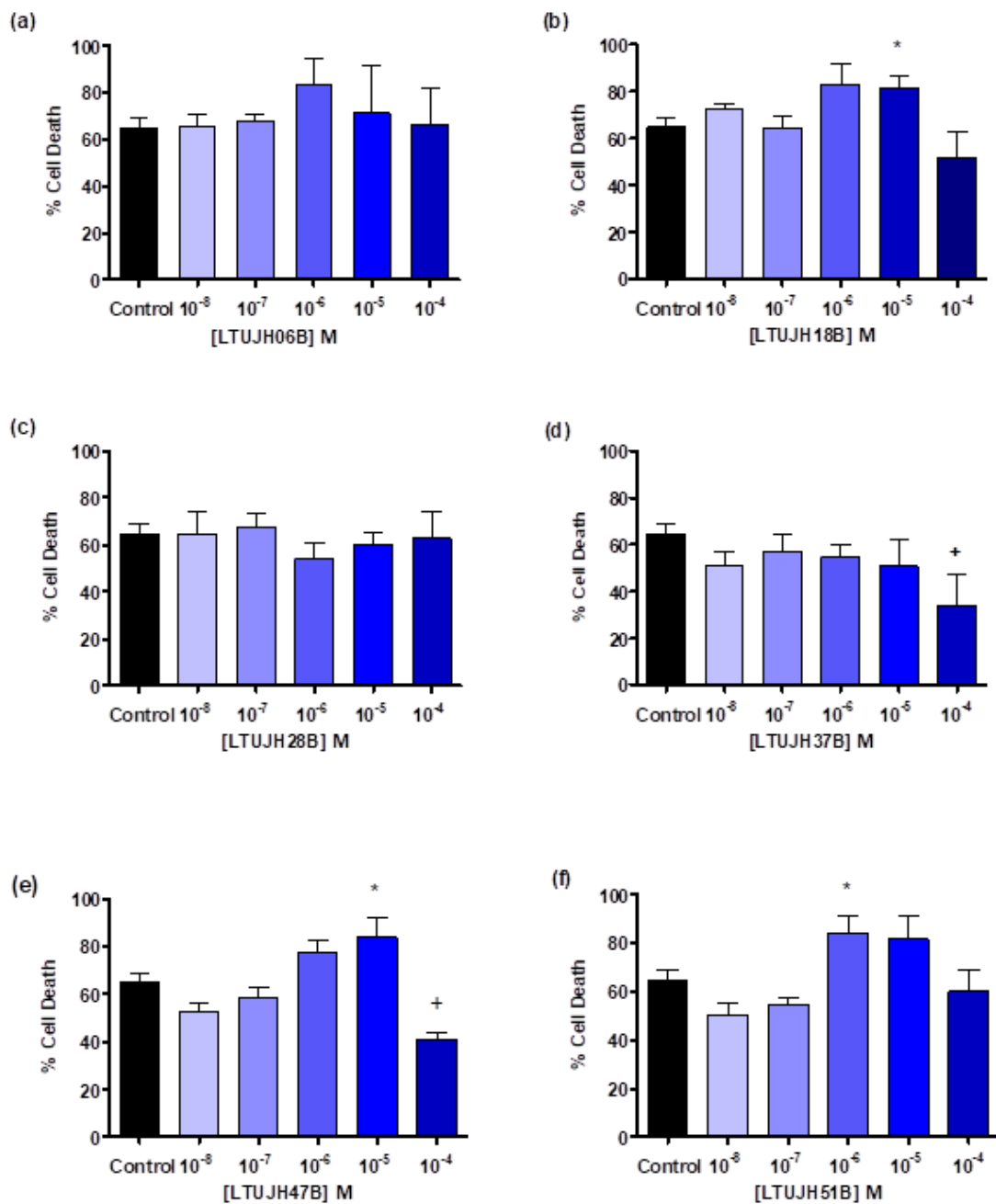
Figure 37. Cytotoxicity analysis using CellTox green after exposing sheep cardiomyocytes to quinazolin-4-one derivatives for 24 hours at varying concentrations. (a) LTUJH06B, (b) LTUJH18B, (c) LTUJH28B, (d) LTUJH37B, (e) LTUJH47B and (f) LTUJH51B. Graph indicates mean of 3 to 6 replicates ± SEM, from 2 individual experiments (* compound significantly more toxic than control, + compound significantly less toxic than control, $p < 0.05$).

5.2.2 Vivid CYP450 screening assay

The liver toxicity potential of all quinazolin-4-one derivatives (LTUJH06B, LTUJH18B, LTUJH28B, LTUJH37B, LTUJH47B and LTUJH51B) on two major CYPP450 isoenzymes, CYP450 2E1 and CYP450 3A4 was screened using the Vivid CYP450 Assay (Life Technologies) over the concentration range 10^{-6} to 1.25×10^{-4} M. Since there is no information available regarding the CYP450 profile of the commercial hERG channel modulator, NS1643, it was included in this assay. The principle of the assay is that when the vivid substrates are metabolized by the CYP450 enzymes, the resulting metabolites are highly fluorescent due to the release of the fluorescent dye from the substrate. If a compound inhibits a CYP450 enzyme, there will be a decrease in fluorescence. Conversely, if the compound does not inhibit the activity of the CYP450 enzyme, then the substrate will be broken down emitting high fluorescence (LifeTechnologies 2012).

The only quinazolin-4-one compound that could not be assessed was LTUJH18B since it had an emission peak in the middle of the emission wavelength for the Vivid CYP450 assay. The average results for the effect of each compound on CYP450 2E1 is shown in Figure 38. Each graph has two curves, one for the known inhibitor, cupral, and the other for the quinazolin-4-one compounds being tested. The data were fitted to Hill equations see materials and methods (chapter 2.11.1) and the effect of each quinazolin-4-one compound was measured against the known inhibitor curve. As this is an inhibition assay, enzyme activity decreased in a dose-dependent manner for the known inhibitor over the concentration range 10^{-6} to 1.25×10^{-4} M (shown as $-\log_{10}$ [compound] on the x-axis, range 6.05 to 3.9).

5.2.2.1 Vivid CYP450 screening assay (CYP450 2E1)

When CYP450 2E1 was exposed to the commercially available hERG channel agonist NS1643 (Figure 38a), it was inhibited as potently and completely as for the known inhibitor, cupral. The average IC_{50} for cupral was (5.06 ± 0.02) and for NS1643 (5.10 ± 0.04, p=0.30), which were not statistically significantly different. Also, there was no significant difference, in the Hill coefficient for cupral (2.11 ± 0.21) and NS1643 (2.55 ± 0.13, p=0.11), respectively. Similarly, there was no significant difference in the inhibition of CYP450 2E1 in the presence of LTUJH06B, LTUJH28B, LTUJH37B or LTUJH47B (Figures 38 b, c, d and e) compared with the standard inhibitor cupral. All these compounds were complete inhibitors of CYP450 2E1 over the concentration range tested. The average IC_{50} and Hill coefficients were: LTUJH06B (IC_{50}, 5.19 ± 0.09, p=0.18; Hill coefficient, 2.02 ± 0.26, p=0.80), LTUJH28B (IC_{50}, 5.15 ± 0.07, p=0.19, Hill coefficient, 1.85 ± 0.15, p=0.33), LTUJH37B (IC_{50}, 5.05 ± 0.06, p=0.94, Hill coefficient, 1.84 ± 0.11, p=0.27) and LTUJH47B (IC_{50}, 5.14 ± 0.06, p=0.15, Hill coefficient, 1.98 ± 0.15, p=0.63). Compound LTUJH51B (Figure 38f) did show increased inhibition

between 1.9 x 10^{-6} and 7.8 x 10^{-6} M with a significant shift in IC_{50} (5.25 ± 0.09, p=0.046) and Hill coefficient (1.46 ± 0.14, P=0.03).

Figure 38. Relative fluorescence (%inhibition) of CYP450 2E1 after exposure to compounds (a) NS1634, (b) LTUJH06B, (c) LTUJH28B, (d) LTUJH37B, (e) LTUJH47B and (f) LTUJH51B over the concentration range 10^{-6} to 1.25 x 10^{-4} M (-$\log_{10}$ 6.05 to 3.90) compared with the standard inhibitor, cupral. Data expressed as mean of 6 replicates ± SEM, 3 individual experiments.

5.2.2.2 Vivid CYP450 screening assay (CYP450 3A4)

The effect of the quinazolin-4-one derivatives was also tested on the activity of CYP450 3A4, another important cytochrome P450 isoenzyme in the liver. The commercial modulator, NS1643 caused complete inhibition of the enzyme with similar potency to the standard inhibitor, ketoconazole (Figure 39a). There was a slight but insignificant (p=0.12) shift to the right of the curve in the presence of NS1643, indicating that it was slightly less potent than ketoconazole. Average IC_{50} values were 4.75 ± 0.03 (ketoconazole) and 4.56 ± 0.10 (NS1643). Similarly, there was no shift in the Hill coefficient; ketoconazole (2.27 ± 0.35) and NS1643 (2.07 ± 022, p=0.66), respectively. LTUJH06B (Figure 39b) also had a slightly shifted inhibition profile to the right of the standard inhibitor ketoconazole. The average IC_{50} value was 4.52 ± 0.04, p=0.87 and similarly. there was no significant change in the Hill coefficient; 2.19 ± 0.25. LTUJH37B (Figure 39d) also completely inhibited CYP3A4 but was not different from the effect of ketoconazole. Average IC_{50} values were 4.73 ± 0.08, p=0.83 and the average Hill coefficient was 2.11 ± 0.65, p=0.83.

Compound LTUJH47B (Figure 39e) also completely inhibited CYP450 3A4 but was less potent than Ketoconazole. The average IC_{50} was (4.41 ± 0.14, p=0.04), but there was no change in the Hill coefficient (1.48 ± 0.15, p=0.09). Finally, compound LTUJH28B (Figure 39c) and LTUJH51B (Figure 39f) completely inhibited CYP3A4, with significant decreases in the IC_{50} and Hill coefficient. Both compounds were weaker inhibitors. Average IC_{50} values for LTUJH28B (4.44 ± 0.09, p=0.01) and LTUJH51B (4.33 ± 0.14, p=0.02), which were significantly different from Ketoconazole respectively. The average Hill coefficients were also significantly reduced with LTUJH28B (1.17 ± 0.13, p=0.01) and LTUJH51B (1.22 ± 0.23, p=0.03), respectively.

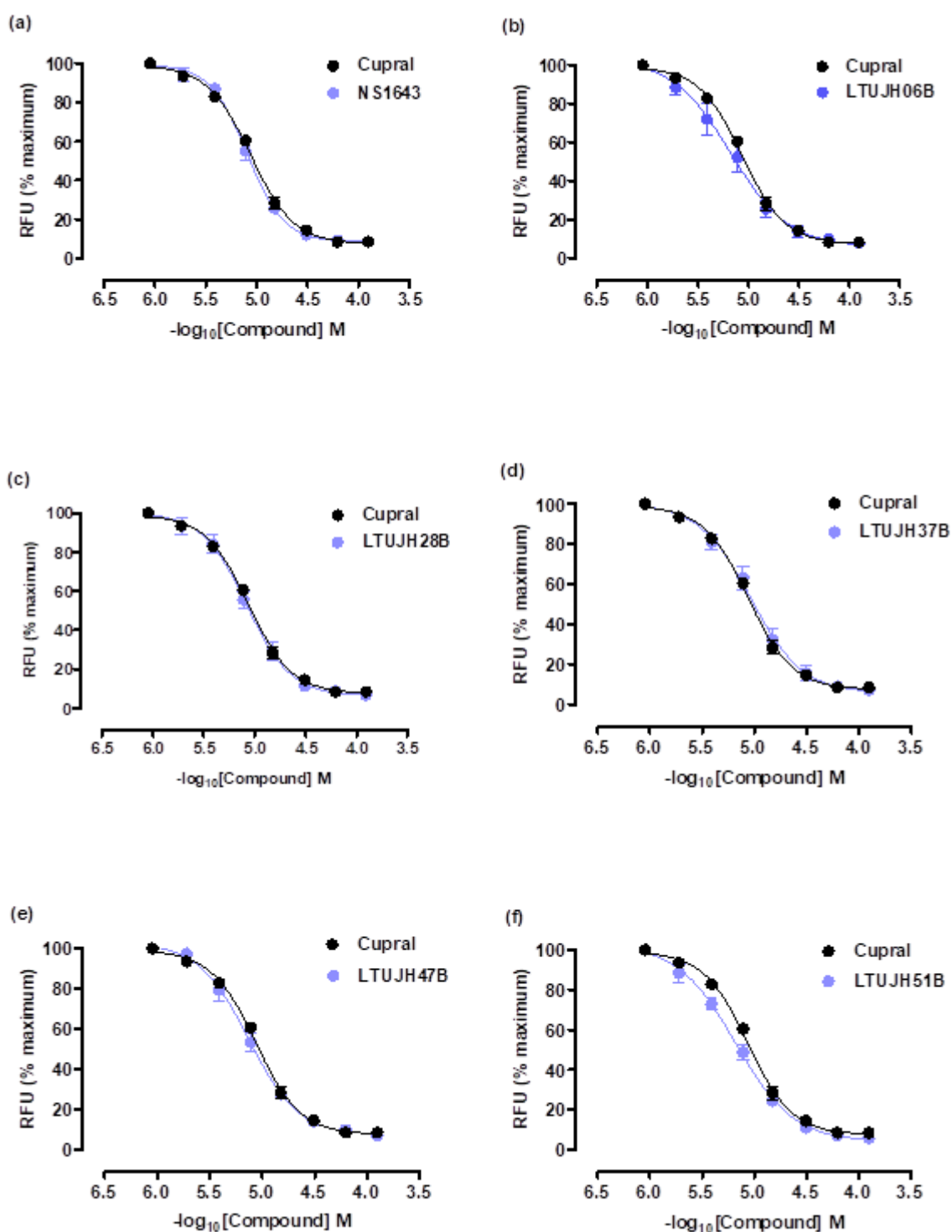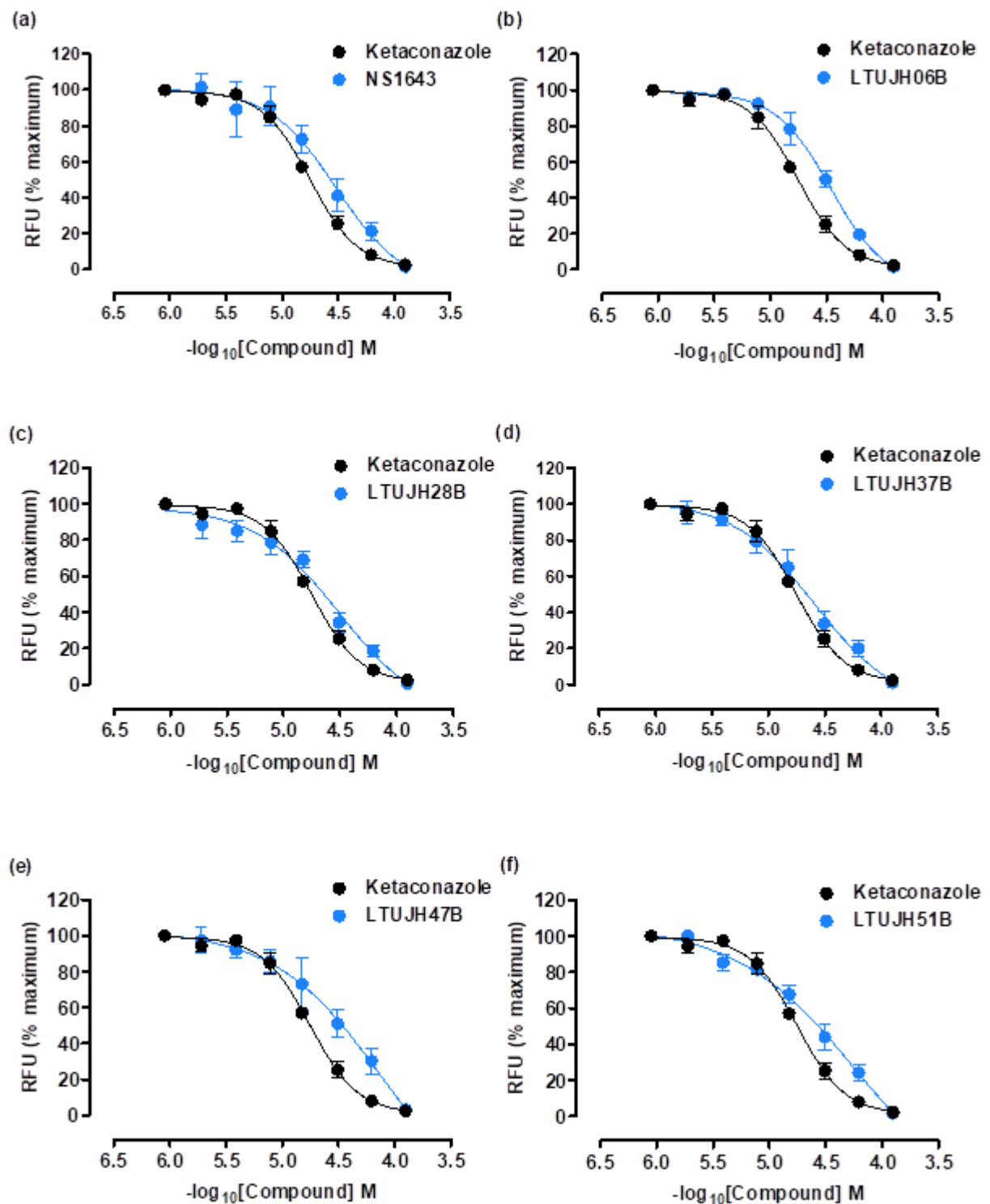Figure 39. Relative fluorescence (% inhibition) of CYP450 3A4 after exposure to compounds (a) NS1634, (b) LTUJH06B, (c) LTUJH28B, (d) LTUJH37B, (e) LTUJH47B, and (f) LTUJH51B over the concentration range 10^{-6} to 1.25×10^{-4} M (-$\log_{10}$ 6.05 to 3.90) compared with the standard inhibitor, ketoconazole. Data expressed as mean of 6 replicates ± SEM, from 3 individual experiments.

5.2.3 FluxOR potassium ion channel assay

Investigation into the impact of the commercially available hERG channel modulator, NS1643 and all of the quinazolin-4-one compounds (LTUJH06B, LTUJH18B, LTUJH28B, LTUJH37B, LTUJH47B and LTUJH51B) on the modulation of hERG channel currents was conducted in the absence and presence of terfenadine, the commercially available hERG channel antagonist. The principle of the assay is to use thallium (Tl^+) permeability to potassium channels. A thallium solution outside the cells will move down its concentration gradient (into the cells) when potassium channels are stimulated to open. Once inside the cells, thallium binds with a preloaded dye increasing fluorescence. This assay was conducted in sheep cardiomyocytes. A concentration of 10μM of each compound was used, with cells exposed to compounds in the presence of potassium where the induction of current through hERG channels would occur, and absence of potassium where no current is expected (apart from some background drift). If current is detected in the potassium negative conditions, this may indicate a ligand gated channel opening (e.g. Ca^{2+}-activated K^+ channel) since no depolarizing signal is available to stimulate voltage gated K^+ channels (LifeTechnologies 2014).

After equilibrating cardiomyocytes in the Flexstation 3 for 20 seconds, the stimulus buffer was added to the wells. For negative control (± compound) there was no added potassium in the buffer (potassium negative, or K^-), while for positive control (± compound) 50mM K_2SO_4 was included in the stimulus buffer (potassium positive, or K^+). It was expected that the response in the presence of compound would be close to that under positive control (potassium positive) conditions for an agonist or reduced for an antagonist. Similarly, little if any current would be seen under negative control (potassium negative) conditions in the absence and presence of compound, since hERG channels are voltage gated. Further details of the FluxOR potassium ion channel assay is provided in the material & methods chapter 2 (section 2.10).

The first compound investigated using the FluxOR assay was the known hERG channel modulator, NS1643. The results are shown in Figure 4 below, where the relative fluorescence units (RFU) has been normalized to the initial fluorescence (t=0) in each case ($\Delta F/F_0$) and plotted over the time course of the experiment (180 s). In both potassium negative conditions there was an initial drop in signal and a slow climb which is typical of this assay and is regarded as background 'noise'. The positive control response was significantly higher than the negative control response both in the absence and presence of NS1643 (p=0.006 and p=0.002, respectively). Under positive control conditions, RFU increased rapidly reaching a plateau by 50 seconds with a maximum response of 0.18 ± 0.02. In the presence of 10μM NS1643 as seen in Figure 40a, the RFU also rapidly increased reaching a maximum of 0.18 ± 0.05 which was not significantly different from the positive control (p > 0.05). In the negative control conditions, little change in the RFU was observed 0.04 ± 0.05). In the presence of

10µM NS1643 (see Figure 40a), a similar trend was seen with the maximum response being 0.04 ± 0.02.
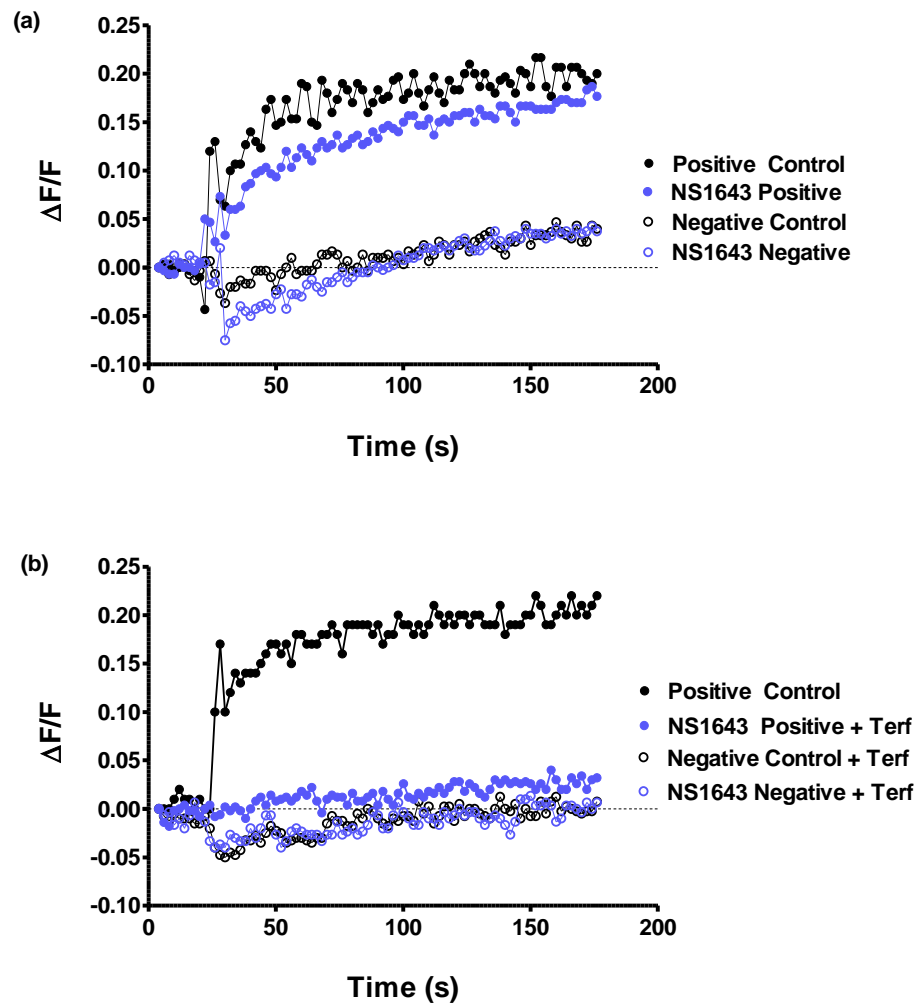
Figure 40. Relative fluorescence versus time relations in the presence of 10µM NS1643 (a) and 1µM terfenadine (b). Positive control solution was added to the cells after 20 seconds equilibration, to stimulate opening of hERG potassium channels. Note this solution did not contain terfenadine in (b) to ensure the assay was working. Data expressed as mean only for clarity. Results are from 4 individual experiments in (a) and (b), respectively.

To ensure that the potassium stimulating conditions (50mM K_2SO_4) were activating hERG channels, the above experiment was repeated in the presence of 1μM terfenadine, the well-known hERG channel antagonist. It is expected that if only hERG channels were being activated, then terfenadine should prevent any increase in RFU in the potassium positive stimulating conditions (in the absence and presence of NS1643). The results for this experiment are shown in Figure 40b, with the average positive control (no terfenadine) response being 0.21 ± 0.01. In the presence of 1μM terfenadine however, the positive potassium response in the presence of 10μM NS1643 was reduced to that recorded in potassium negative conditions 0.04 ± 0.01.

The effects of LTUJH06B on hERG channel activity are shown in Figure 41 in the absence (a) and presence of 1μM terfenadine (b). In the first experiment (absence of terfenadine), 10μM LTUJH06B did not affect the K^+ (depolarizing) stimulus; neither increasing it nor decreasing it from the control response, positive control (0.14 ± 0.03), LTUJH06B (0.16 ± 0.04). There was, however, a significantly increased RFU recorded under the K^- (non-depolarizing) conditions in the presence of LTUJH06B; negative control (0.02 ± 0.01), LTUJH06B (0.12 ± 0.02, p= 0.006), which was approximately 85% of the K^+ response. Activation in the potassium negative conditions suggests that LTUJH06B may be acting as a ligand on the normally voltage gated channels or activating a different ligand-gated ion channel. When the experiment was repeated in the presence of 1μM terfenadine, all the results were reduced to almost zero (see Figure 41(b)). Average maximum responses in the presence of terfenadine were: positive control (0.06 ± 0.02), LTUJH06B positive (0.05 ± 0.01), negative control (0.07 ± 0.26) and LTUJH06B negative (0.05 ± 0.006), all of which were not significantly different from each other (p>0.05). From these results, it appears that the effect of LTUJH06B is removed in the presence of terfenadine. Since terfenadine is a specific antagonist for hERG channels, and it completely inhibited the effect of LTUJH06B, this suggests that LTUJH06B may be an agonist of hERG channels and works in a voltage-independent manner.

When the effects of LTUJH18B were investigated, the results were like those for LTUJH06B. There was no stimulatory effect on the K^+ response, but the rate of rise was slightly less for up to 55 seconds, after which the maximum response was the same. There was a significantly increased (p= 1.85×10^{-5}) response under K^- conditions in the presence of LTUJH18B compared with the negative control ending up as large as the K^+ response, as shown in Figure 42a. Average maximum responses were: positive control (0.15 ± 0.02), in response to LTUJH18B presence (0.14 ± 0.01), negative control (0.03 ± 0.01), and K^- with LTUJH18B (0.136 ± 0.011). In the presence of 1μM terfenadine, all the responses were reduced to basal levels in non-depolarizing conditions (K^- solution) as shown in Figure 42b. Average responses in the presence of 1μM terfenadine were: positive control (0.07 ± 0.01), K^+ with LTUJH18B

(0.05 ± 0.01), negative control (0.06 ± 0.02), and K$^-$ with LTUJH18B (0.052 ± 0.005),
respectively. None of these were significantly different from each other ($p > 0.05$).

Figure 41 Relative fluorescence versus time relations in the presence of 10µM LTUJH06B (a) and
1µM terfenadine (b). Positive control solution was added to the cells after 20 seconds equilibration, to
stimulate opening of hERG potassium channels. Note both K$^+$ responses (± 1µM terfenadine) are
shown to confirm hERG channel inhibition under our depolarizing conditions. Data expressed as
mean only for clarity. Results are from 6 and 4 individual experiments in (a) and (b), respectively.

Figure 42. Relative fluorescence versus time relations in the presence of 10µM LTUJH18B (a) and 1µM terfenadine (b). Positive control solution was added to the cells after 20 seconds equilibration, to stimulate opening of hERG potassium channels. Note both K$^+$ responses (± 1µM terfenadine) are shown to confirm hERG channel inhibition under depolarizing conditions. Data expressed as mean only for clarity. Results are from 6 and 4 individual experiments in (a) and (b), respectively.

When compound LTUJH28B was investigated, the results were less conclusive as seen in Figure 43. Generally, under depolarizing conditions (K^+ stimulating solution), there was no significant difference seen ($p > 0.05$) in the absence or presence of compound as shown in Figure 43a; positive control (0.10 ± 0.01), in presence of LTUJH28B (0.12 ± 0.02). Under non-depolarizing conditions as seen in Figure 43a, the presence of 10µM LTUJH28B did produce a slight increase in RFU compared with the corresponding negative control; negative control (0.04 ± 0.01) and in presence of LTUJH28B (0.05 ± 0.01), however, it was not statistically significant ($p > 0.05$). From these results it appears that LTUJH28B does not affect hERG channels.

In the presence of 1µM Terfenadine, to block hERG channels, all traces were less than in its absence (Figure 43b). Average maximum responses were for positive control (0.10 ± 0.01) and positive control with terfenadine (0.06 ± 0.01, p=0.013), the decrease in positive control (with terfenadine) compared with the positive control (no terfenadine) was significantly different. Under non-depolarizing conditions shown in Figure 43b, there was no difference between the absence and presence of 1µM terfenadine confirming that LTUJH28B had no effect on hERG channels. Average maximum responses were for negative control (0.040 ± 0.006) negative control with terfenadine (0.04 ± 0.02). These were not statistically significantly different ($p > 0.05$).

(a)

(b)

Figure 43. Relative fluorescence versus time relations in the presence of 10µM LTUJH28B (a) and 1µM terfenadine (b). Positive control solution was added to the cells after 20 seconds equilibration, to stimulate opening of hERG potassium channels. Note both K^+ responses (± 1µM terfenadine) are shown to confirm hERG channel inhibition under depolarizing conditions. Data expressed as mean only for clarity. Results are from 5 individual experiments in (a) and (b), respectively.

Compound LTUJH37B as seen in Figure 44a caused slight stimulation of hERG channel conductance under depolarizing conditions (K^+ stimulation) with the average maximum responses for positive control and (0.13 ± 0.02), and in response to LTU37B (0.12 ± 0.01), but it was not significantly different (p > 0.05). Under non-depolarizing (K^- stimulation) conditions shown in Figure 44a, LTUJH37B caused a very large increase in RFU compared with the negative control. The average maximum responses were, for negative control (0.04 ± 0.01) and K- with LTUJH37B (0.11 ± 0.01, p = 6.28×10^{-5}) respectively which were significantly different.

Terfenadine (1µM) caused a 31% drop in the response to LTUJH37B (Figure 44b) under depolarizing conditions when compared with a 63% drop in the positive control conditions. Average maximum responses were (0.05 ± 0.01) for positive control with terfenadine and (0.09 ± 0.01, P = 0.15) for K^+ stimulation with both terfenadine and LTUJH37B, which were not significantly different. From these results it appears that LTUJH37B is stimulating a current that is only partly associated with hERG channels, and other currents are being activated under depolarizing conditions. Further, under non-depolarizing conditions shown in Figure 44b, the addition of 1µM terfenadine only reduced the K^- simulation in the presence of LTUJH37B by 30%. Average maximum responses were 0.11 ± 0.01, (LTUJH37B K^- stimulation) and 0.08 ± 0.02 (LTUJH37B K^- stimulation with 1µM terfenadine), which were not statistically significantly different (p=0.183).

When compound LTUJH47B was investigated as seen Figure 45a, there was a slight decrease in the K^+ stimulating conditions, compared with the positive control (p>0.05). Average maximum responses were: for positive control (0.19 ± 0.01) and in presence of LTUJH47B (0.15 ± 0.03, P=0.31) which were not significantly different. Under non-depolarizing conditions (K^- stimulation) the RFU increased to slightly more than the positive control shown in Figure 45a. This was like the response seen for LTUJH37B in the depolarising conditions. Average maximum responses for negative control 0.03 ± 0.01, and K^- with 10µM LTUJH47B (0.24 ± 0.04, p=$6.57x10^{-4}$) which were significantly different. Unlike LTUJH37B however, both K^+ and K^- responses in the presence of LTUJH47B and 1µM terfenadine, were reduced back to negative control values (Figure 45b). Under K^- stimulation conditions, LTUJH47B appears to be directly activating hERG channels in a voltage independent manner which is largely blocked by terfenadine. Average maximum responses in the presence of 1µM terfenadine for positive control (0.07 ± 0.01), K^+ with LTUJH47B (0.06 ± 0.01), negative control (0.05 ± 0.01), and K^- with LTUJH47B (0.03 ± 0.01), respectively.
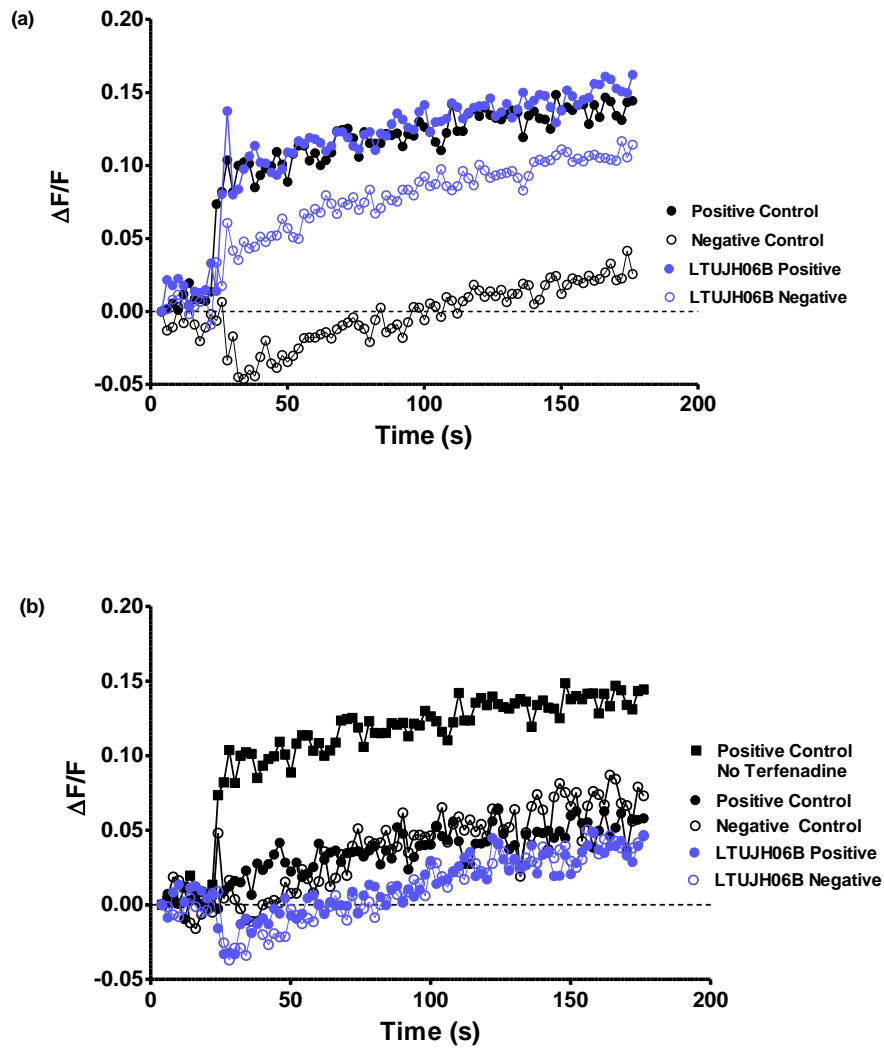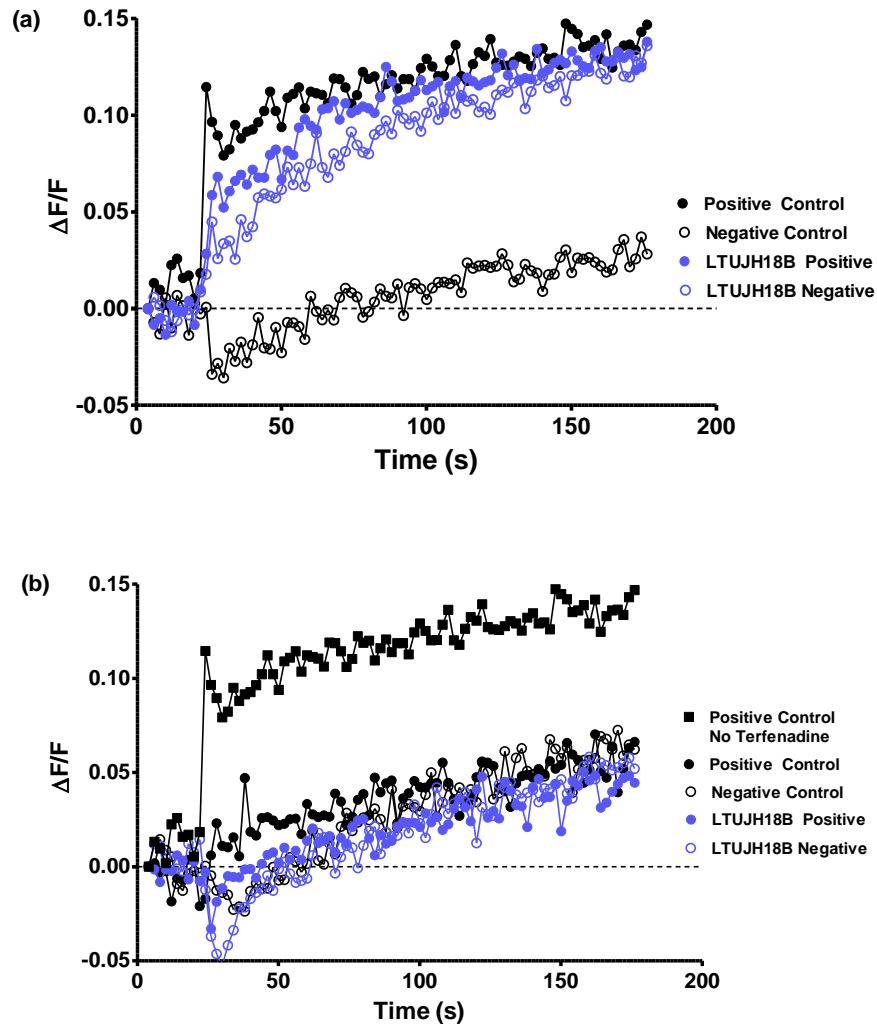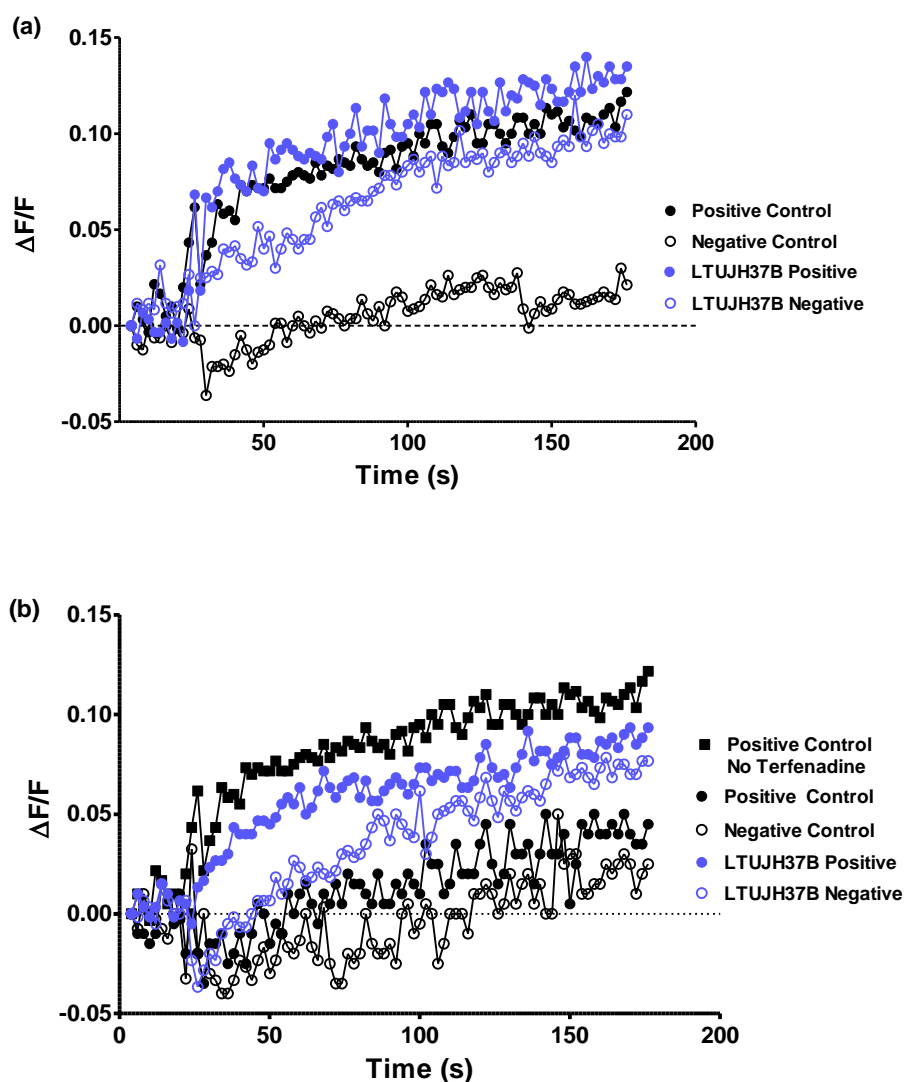
Figure 44. Relative fluorescence versus time relations in the presence of 10µM LTUJH37B (a) and 1µM terfenadine (b). Positive control solution was added to the cells after 20 seconds equilibration, to stimulate opening of hERG potassium channels. Note both K^+ responses (± 1µM terfenadine) are shown to confirm hERG channel inhibition under depolarizing conditions. Data expressed as mean only for clarity. Results are from 6 individual experiments in (a) and (b), respectively.

The final quinazolin-4-one compound LTUJH51B produced results similar to LTUJH47B. Under depolarizing conditions, 10µM LTUJH51B caused a rapid increase in RFU which remained higher than the positive control and was not significantly different (p=0.22) as shown in Figure 46a. Average maximum responses for positive control (0.19 ± 0.02) and K^+ with LTUJH51B (0.22 ± 0.01). In the nondepolarizing conditions as shown in Figure 46a, (K^- stimulation) there was a slower but steady rise in RFU to the same maximum as the K^+ with LTUJH51B. Maximum responses for negative control (0.03 ± 0.01) and K- with LTUJH51B (0.18 ± 0.01, p=6.79×10^{-7}) which were significantly different.
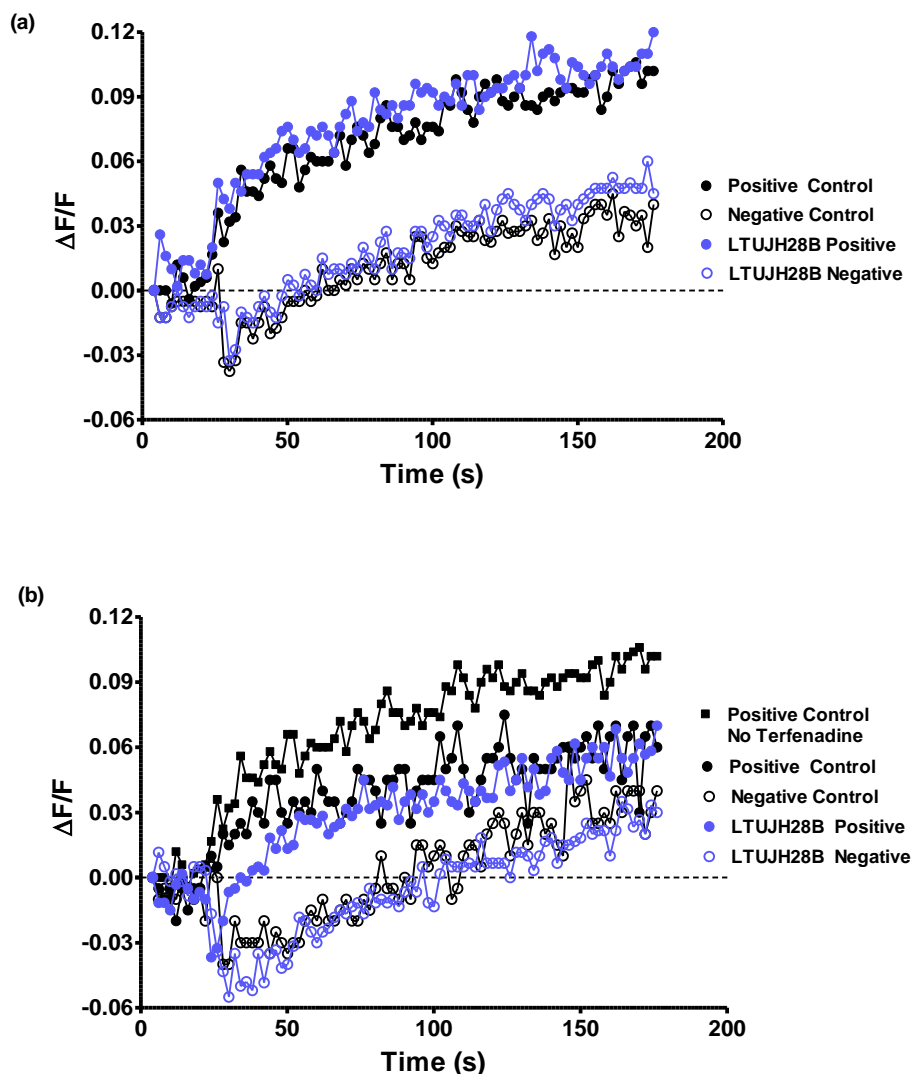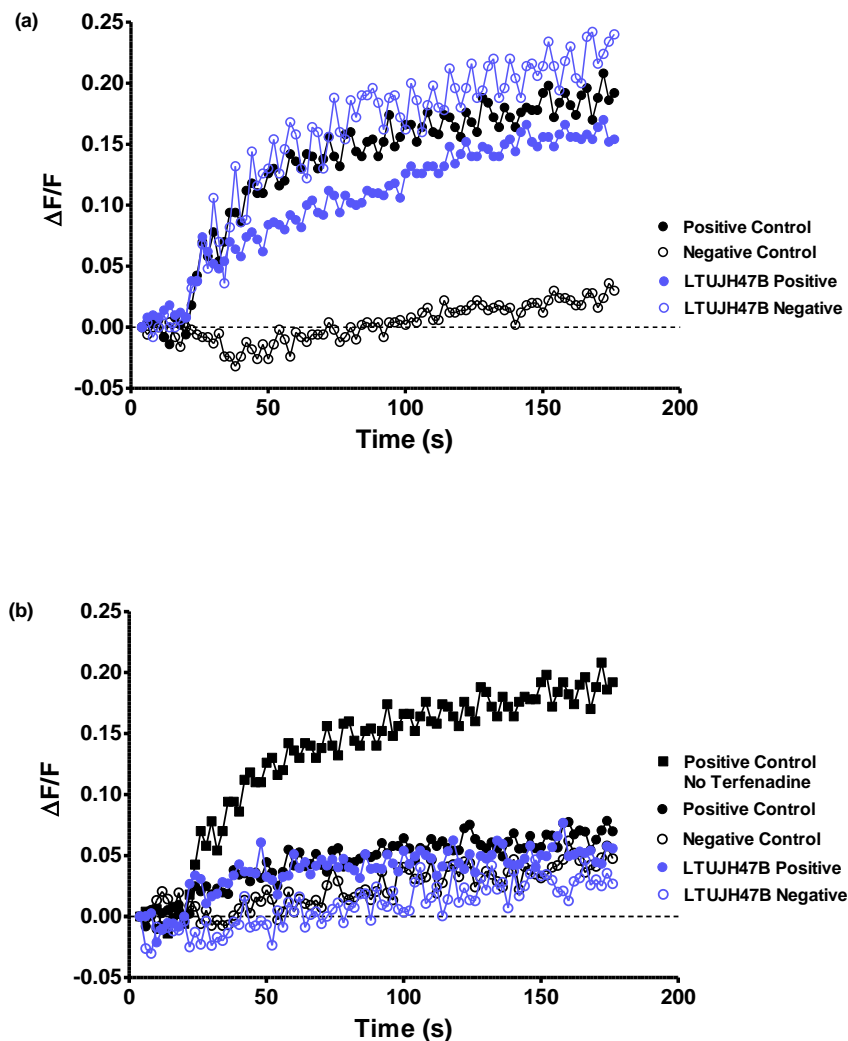
Figure 45. Relative fluorescence versus time relations in the presence of 10µM LTUJH47B (a) and 1µM terfenadine (b). Positive control solution was added to the cells after 20 seconds equilibration, to stimulate opening of hERG potassium channels. Note both K+ responses (± 1µM terfenadine) are shown to confirm hERG channel inhibition under depolarizing conditions. Data expressed as mean only for clarity. Results are from 6 and 4 individual experiments in (a) and (b), respectively.

In the presence of 1µM terfenadine, again all of the responses were reduced to that of the negative control (Figure 46b), indicating that LTUJH51B was acting as a ligand to activate hERG channels under non-depolarizing conditions, as well as being a weak agonist (increasing K+ response) under depolarizing conditions.
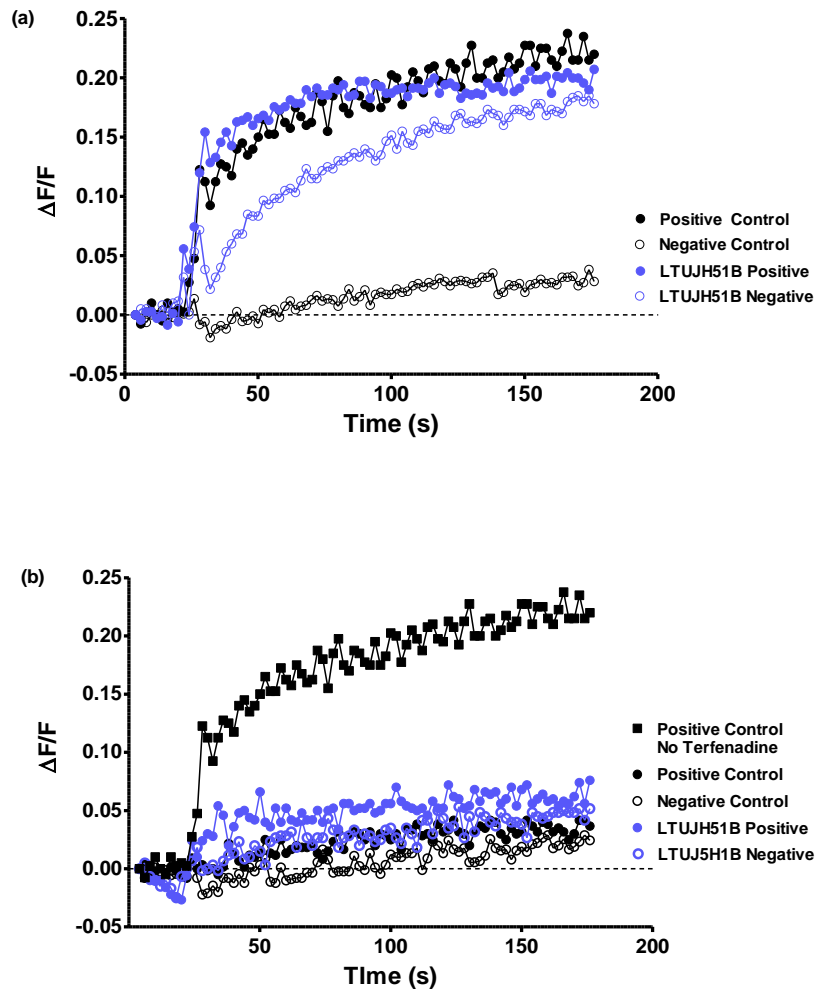
Figure 46 Relative fluorescence versus time relations in the presence of 10µM LTUJH51B (a) and 1µM terfenadine (b). Positive control solution was added to the cells after 20 seconds equilibration, to stimulate opening of hERG potassium channels. Note both K+ responses (± 1µM terfenadine) are shown to confirm hERG channel inhibition under depolarizing conditions. Data expressed as mean only for clarity. Results are from 6 individual experiments in (a) and (b), respectively.

5.2.4 Kinetic Analysis of FluxOR Responses

From the FluxOR results so far, some of the quinazolin-4-one compounds do activate hERG channels. In some cases, this is voltage-dependent but in others it appears to be voltage-independent or ligand gating. To further evaluate how the quinazolin-4-one compounds were affecting hERG channel activation, each trace was normalized to the respective B_{max} so that the rate of rise (Hill coefficient, η) and the binding affinity (K_D) for each could be determined after fitting the data with a one-site binding hyperbola (see materials and methods chapter 2.10 for details). Changes in the Hill coefficient (η) indicate how many ligands need to be bound to the channel to affect its activation, while changes in K_D normally indicate the apparent sensitivity of the channels over a range of compound concentrations. However, in this case, K_D refers to the time required for 50% activation of the channels. In the absence of potassium in the stimulating solution, K_D indicates how long it takes for the quinazolin-4-one derivative to directly activate the channels under non-depolarizing conditions.

The compiled data are given in Table 10 below. Initial difference among the groups (positive control, K^+ in the presence of the quinazolin-4-one derivative and K^+neg in presence of the quinazolin-4-one compound) were tested for any difference among the mean responses for the Hill coefficient (η) and K_D. The data were then subjected to an unpaired Student's t-test between 2 groups with unequal variances (determined by F-test): (a) positive control versus K^+ in the presence of the quinazolin-4-one derivative, (b) positive control versus K^+neg in the presence of the quinazolin-4-one derivative, and finally (c) between K^+ and K^+neg in the presence of the quinazolin-4-one compound. Data were considered significantly different when $P < 0.05$ (two-tailed).

There were no significant changes in either the rate of activation of the channels nor the K_D for NS1643 and LTUJH28B. Further, these were the only two compounds that did not open the channels under nondepolarizing conditions (K^- or K^+neg in the presence of the respective compound). All the other quinazolin-4-one compounds did cause a rise in RFU in the absence of K^+ in the stimulating buffer (nondepolarizing conditions). There was no significant difference in the Hill coefficient for any of the compounds tested so the activation kinetics were the same in the absence and presence of K^+ as well as the absence and presence of the quinazolin-4-one compounds. From the range of Hill coefficients shown in Table 10, it appears that only 1 molecule of compound is required to bind per channel for activation to occur, whether in a depolarizing step or directly as ligand gating. The values for K_D were different for some of the quinazolin-4-one derivative compared with the positive controls. LTUJH18B had a significantly increased K_D (47.67 ± 5.84, P=0.006) from both the positive control and the K^+ in the presence of LTUJH18B responses (see Table 10).

Compound	Stimulating Solution	Hill Coefficient (n) Mean ± s.e.m.	N		P=	K_D Mean ± s.e.m.	N		P=
NS1643	K$^+$ control	1.106 ± 0.036	3	a	0.252	17.42 ± 2.34	3	a	0.288
	K$^+$ + NS1643	1.777 ± 0.419	3	b	-	30.83 ± 9.06	3	b	-
	K$^-$ + NS1643	-	-	c	-	-	-	c	-
LTUJH06B	K$^+$ control	1.499 ± 0.280	4	a	0.746	20.34 ± 5.54	4	a	0.474
	K$^+$ + JH06B	1.381 ± 0.198	4	b	0.612	30.00 ± 10.92	4	b	0.134
	K$^-$ + JH06B	1.293 ± 0.264	4	c	0.797	38.77 ± 8.70	4	c	0.553
LTUJH18B	K$^+$ control	1.077 ± 0.122	5	a	0.278	20.55 ± 3.17	5	a	0.939
	K$^+$ + JH18B	1.263 ± 0.103	5	b	0.069	20.88 ± 2.79	5	b	0.007
	K$^-$ + JH18B	1.885 ± 0.329	5	c	0.131	47.67 ± 5.89	5	c	0.006
LTUJH28B	K$^+$ control	1.214 ± 0.081	5	a	0.683	30.95 ± 2.12	5	a	0.912
	K$^+$ + JH28B	1.296 ± 0.174	5	b	-	31.99 ± 8.65	5	b	-
	K$^-$ + JH28B	-	-	c	-	-	-	c	-
LTUJH37B	K$^+$ control	1.124 ± 0.124	4	a	0.331	25.65 ± 3.93	4	a	0.304
	K$^+$ + JH37B	1.368 ± 0.190	4	b	0.074	36.44 ± 8.28	4	b	0.004
	K$^-$ + JH37B	1.679 ± 0.213	4	c	0.317	54.31 ± 5.10	4	c	0.125
LTUJH47B	K$^+$ control	1.389 ± 0.364	4	a	0.925	17.91 ± 2.14	4	a	0.459
	K$^+$ + JH47B	1.350 ± 0.097	4	b	0.934	22.99 ± 5.83	4	b	0.004
	K$^-$ + JH47B	1.352 ± 0.214	4	c	0.995	40.20 ± 3.96	4	c	0.059
LTUJH51B	K$^+$ control	1.556 ± 0.225	4	a	0.795	19.99 ± 7.41	4	a	0.388
	K$^+$ + JH51B	1.731 ± 0.587	4	b	0.257	12.33 ± 2.79	4	b	0.078
	K$^-$ + JH51B	1.777 ± 0.419	4	c	0.722	38.57 ± 2.73	4	c	0.001

Table 10. Statistical analysis of changes in the Hill coefficient (η) and K_D of FluxOR traces under positive control conditions and in the presence of NS1643 and each of the quinazolin-4-one derivative. (a) positive control versus K$^+$ in the presence of quinazolin-4-one derivatives, (b) positive control versus K$^-$ in the presence of quinazolin-4-one derivative, and finally (c) between K$^+$ and K$^-$ in the presence of the quinazolin-4-one derivative.

Under nondepolarizing conditions, the K_D was more than twice that required under depolarizing conditions. LTUJH37B showed a similar trend to LTUJH18B with an increased K_D (54.31 ± 5.10, p=0.004) under nondepolarizing conditions compared with the positive control (25.65 ± 3.93). Under depolarizing conditions (K$^+$ with LTUJH37B) the K_D was shifted to the right (36.44 ± 8.28, P=0.304) but this was not significantly different from the positive control. Similarly, LTUJH47B had a significantly increased K_D in nondepolarizing conditions approximately twice that determined under depolarizing conditions. Finally, LTUJH51B had a significantly larger K_D (38.57 ± 2.73, p=0.001) under depolarizing conditions in its presence compared with the K_D for nondepolarizing conditions in this presence (12.33 ± 2.79) but this was not significantly different from the K_D in the positive control (19.99 ± 7.4, P=0.078). Invariably the K_D was larger under nondepolarizing conditions in the presence of the quinazolin-4-one compounds, than under depolarizing conditions. This is not surprising given that normally hERG channels require a voltage step for activation, but the quinazolin-4-one compounds appear to open these channels directly in a voltage-independent manner.

5.3 Discussion

Any new potential drug must be tested for its effects not only on the desired target tissue, but for side effects including cardiotoxicity and cytochrome P450 profile. This is a tedious, time consuming and expensive process. From a toxicological viewpoint, some basic testing of each new compound can be done at the outset. There is no point investigating a new compound if it kills normal tissue cells. One of the first tests for any new compound is a cytotoxicity assay to determine whether the compound is toxic and over what concentration range. To determine if the quinazolin-4-one compounds had any toxic effect on a cardiac model using sheep cardiomyocytes, the CellTox green assay was used. The green dye in this assay is excluded from intact cells while they bind to DNA in lysed cells, which allows for quantification of cell integrity following exposure to compounds. Out of the 5 the quinazolin-4-one compounds tested only compounds LTUJH18B (Figure 37b) and LTUJH47B (Figure 37e) showed toxic effect at 10^{-5} M. Compound LTUJH51B also caused significant toxicity at 10^{-6} M (Figure 37f). While there was decreased cell lysis following exposure to 10^{-4}M of compounds LTUJH37B (Figure 37d) and LTUJH47B (Figure 37e).

The sheep cardiomyocytes were used to test whether the quinazolin-4-one compounds was toxic to a sensitive normal tissue cell model. From a clinical view, toxicity in normal tissue cells provides an indication of how important dosage selection is when developing novel anti-cancer drugs. While this initial assay in sheep cardiomyocytes was useful (particularly with the focus on hERG channel modulation in this project), further investigation in a range of normal tissue cells should occur. In general, none of the quinazolin-4-one compounds was particularly toxic to the cardiomyocytes (see Figure 37).

Identifying the quinazolin-4-one compounds inhibition profile of CYP450 2E1 and 3A4 enzymes is essential, as they are key enzymes responsible for a majority of drug metabolism in the liver. While CYP450 2E1 is only responsible for 4% of all xenobiotic metabolism (Lewis 2003) it is important for the metabolism of drugs such as paracetamol, angiotensin II converting enzyme (ACE) inhibitors and alcohol (Vaglini et al. 2013) which are commonly used in society. CYP450 2E1 is also responsible for the metabolism of several substrates that are toxins, established carcinogens or suspected carcinogens (Lee et al. 1996) so its inhibition can increase the risk of cancer developing. Overexpression of CYP450 2E1 has also been implicated in nephrotoxicity and liver toxicity in patients receiving cancer treatment for solid tumours with Cisplatin (Lu and Cederbaum 2005) in part by increasing ROS in normal cells (Santos et al. 2007), CYP450 2E1 is involved in etoposide 3'-demethylation, though its activity in minor when compared to the metabolism activity of CYP450 3A4 (Kawashiro et al. 1998).

CYP450 3A4 however, is responsible for more than 19% of all xenobiotic metabolism (Lewis 2003). This certainly indicates the importance of potential drug interactions if the quinazolin-4-one derivatives were used clinically, since many known medicines are metabolised by CYP450 3A4 including some used in cancer therapy. Nifedipine, erythromycin and terfenadine are all CYP450 3A4 substrates (Lewis 2003). Of particular interest is that terfenadine is known to induce long QT syndrome in patients because it is a hERG channel antagonist even though it is prescribed for seasonal allergic rhinitis (Paakkari 2002). Among cancer medicines, etoposide and tamoxifen are also metabolised by CYP450 3A4. With respect to breast cancer the metabolism of tamoxifen by CYP450 3A4 is very important since any other medication that inhibits CYP450 3A4 will reduce the efficacy of tamoxifen in patients. This is of more concern in patients with oestrogen receptor positive forms of breast cancer than those with the triple negative forms (Yang et al. 2012).

The Vivid CYP450 assay (Life Technologies, Australia) was used to record the inhibition profiles of CYP450 2E1 and 3A4 enzymes in the presence of each of the quinazolin-4-one derivatives and the commercial hERG modulator, NS1643. In general, all the compounds investigated were complete inhibitors of both CYP450 2E1 and CYP450 3A4. Only LTUJH51B showed a significant decrease in the IC_{50} compared with the known inhibitors, cupral and ketoconazole, respectively (see Figure 38 and 39).

The potential for a drug to adversely affect the QT interval; specifically associated with hERG channels is of paramount importance in the current climate and should be investigated. Naturally much more rigorous testing by many investigators is necessary before any new compound can become commercially available. Here though, the first steps in evaluating the potential cardiac effects of new novel compounds can be undertaken and documented for the next level of scrutiny to build upon.

The effect of NS1643 and the quinazolin-4-one compounds on hERG channel modulation was investigated in sheep cardiomyocytes. True hERG channels ($K_V11.1$) are normally expressed in high amounts in cardiac muscle (Vandenberg et al. 2012) in all mammalian species. Sheep cardiomyocytes offered a convenient alternative to genetically engineered human cardiomyocytes which tend to have properties more like neonatal heart than adult heart (Fijnvandraat et al. 2003). The aim in these experiments was to determine how the compounds affected native hERG channels *in situ* in cardiomyocytes.

NS1643 is marketed as a hERG channel agonist but is also recognized that it can have weak antagonist effects in some cases (Casis, Olesen, and Sanguinetti 2005). From the membrane potential assay conducted in chapter 3 (see Figure 21) NS1643 appeared to be an antagonist in MCF7 cells but an agonist in MDA-MB-231 cells. This could be in part attributed to different

hERG channel transcript expressions that have been identified in these two different breast adenocarcinoma cell lines (Roy et al. 2008; Williams, Bateman, and O'Kelly 2013).

In sheep cardiomyocytes, NS1643 was at best a weak agonist that could be argued had little if any effect on the voltage-gated activation of native hERG channels. Indeed, the slower rate of rise could suggest that is acting as a weak antagonist. The rate of rise appeared slower than for the positive control conditions (see Figure 40a and 40b) but when the Bmax was normalized in the kinetic analysis, there was no significant difference in the either Hill coefficient or the K_D, so the curves were essentially identical. This could also be interpreted that NS1643 had no effect on the hERG channels, so the experiment was repeated in the presence of the known hERG antagonist, terfenadine. In the presence of 1 µM terfenadine, there was no response to K+ stimulation in the presence of NS1643. From these results it was concluded that NS1643 was acting as an agonist in the sheep cardiomyocytes.

The FluxOR assay is particularly insensitive for the investigation of agonists of voltage-gated channels like hERG because such channels open quickly and completely only when a specific depolarizing step is provided to them. After several attempts to vary the K+ concentration to vary the depolarization step failed, it was decided to use the most successful K+ conditions (50mM K_2SO_4) for all experiments. Increasing to 300mM K_2SO_4 (increments of 100, 150, 200, 250 mM) did not produce any variation in the results. Clearly hERG channels were being activated in the sheep cardiomyocytes, but NS1643 was at best a weak agonist.

This approach was repeated for the quinazolin-4-one derivatives with some interesting results. Since the quinazolin-4-one compounds and NS1643 appeared to act as antagonists in MCF-7 cells, but agonists in MDA-MB-231 cells it was considered that different hERG transcripts may be present in the two breast cancer cell lines. Testing them in sheep cardiomyocytes might clarify the situation.

The first quinazolin-4-one compound tested was LTUJH06B which produced a slightly higher response under depolarizing conditions than the positive control (though not significantly different). This trace was better than for NS1643, but the Hill coefficient and K_D were not significantly from positive control (see Table 10). Surprisingly, under non-depolarizing conditions (K+ neg stimulation) where no activation was expected, LTUJH06B produced a trace almost as big as for the positive control conditions. In fact, there was no significant difference in the Hill coefficient or the K_D when the data were normalized (as shown in Table 10). For the first time there appeared to be a voltage-independent ligand for hERG channels identified. Again, this was tested in the presence of 1µM terfenadine and the effect of LTUJH06B was completely blocked in the non-depolarizing conditions, confirming it was activating hERG channels. Similar observations were made for LTUJH18B, LTUJH47B and

LTUJH51B. The results from LTUJH28B and LTUJH37B were less convincing since they were not completely inhibited by 1μM terfenadine. Further, LTUJH47B did increase the signal above the positive control and was much more convincing as a true agonist under both voltage-gated and ligand-gated conditions. While LTUJH18B, LTUJH47B and LTUJH51B were all voltage independent agonists, the hERG channels were significantly slower to activate (see Table 10).

Finally, if the structural differences of the quinazolin-4-one compounds is considered for the FluxOR results (shown in Table 11), it can be seen, at least in part, why LTUJH28B and LTUJH37B appeared to be less specific than the rest of the compounds. LTUJH37B is a urea containing quinazolin-4-one with no substitutions at position N3, whereas LTUJH28B is a thiourea with an amide at position N3. The effect of these compounds was not blocked by terfenadine indicating that they are not hERG channel specific. This is interesting to note because LTUJH51B was a strong agonist that was terfenadine sensitive and only differed from LTUJH28B by being a urea rather than a thiourea compound. The presence of the thiourea may affect hERG channel selectivity in these compounds. Even though LTUJH37B is a urea containing quinazolin-4-one, the lack of a functional group at N3 (its only difference from LTUJH51B) appears to reduce its specificity for hERG channels. Knowing that LTUJH28B and LTU37B are not specifically activating hERG channels in cardiomyocytes raises questions regarding their activation or inhibition of hERG channels in the breast cancer cell lines. It appears that these two compounds have other effects yet to be elucidated.

Quinazolin-4-one properties	Structure and chemical name
LTUJH06B	
Voltage gating	
Ligand gating	
Terfenadine Sensitive	ethyl 2-(1-ethyl-6,7-difluoro-4-oxo-2-thioxo-1,4-dihydroquinazolin-3(2H)-yl)acetate
LTUJH18B	
Voltage gating	
Ligand gating	
Terfenadine Sensitive	ethyl 1-ethyl-6,7-difluoro-4-oxo-2-thioxo-1,4-dihydroquinazoline-3(2H)-carboxylate
LTUJH28B	
Voltage gating	
Ligand gating	
Terfenadine Insensitive	1-ethyl-6,7-difluoro-N,N-dimethyl-4-oxo-2-thioxo-1,4-dihydroquinazoline-3(2H)-carboxamide
LTUJH37B	
Voltage gating	
Ligand gating	
Terfenadine Insensitive	1-ethyl-6,7-difluoroquinazoline-2,4(1H,3H)-dione
LTUJH47B	
Voltage gating	
Ligand gating	
Terfenadine Sensitive	ethyl 1-ethyl-6-fluoro-2,4-dioxo-7-thiomorpholino-1,4-dihydroquinazoline-3(2H)-carboxylate
LTUJH51B	
Voltage gating	
Ligand gating	
Terfenadine Sensitive	1-ethyl-6,7-difluoro-N,N-dimethyl-2,4-dioxo-1,4-dihydroquinazoline-3(2H)-carboxamide

Table 11.Summary of the structures and gating properties and hERG channel specificity of the quinazolin-4-one derivatives.

127

Chapter 6- General discussion

Breast cancer, as with all types of cancers, is a very heterogeneous disease, mostly associated with varying histopathology and receptor and oncogene expression (i.e. oestrogen, progesterone and HER2) which affects cancer development, progression, metastasis and patient prognosis (Burstein 2005; Park, Kim, Kim, et al. 2005; Weigelt and Reis-Filho 2009). Therapeutic approaches are complex, varied and often very uncomfortable for the patients and involve a combination of biopsies, surgery, radiotherapy and chemotherapy (Osborne 1998; Bartsch and Bergen 2016). Today patient outcomes are much better than in the past, but breast cancer can still kill patients either from the disease itself metastasizing, or from side effects associated with the complex chemotherapy required to arrest disease progression. In cancer research the development of more targeted therapies to treat the disease while minimizing the side effects is a serious and important challenge to improve the health outcomes of patients.

Among the chemotherapeutic strategies used in breast cancer treatment, hormone therapy depends in part on the presence of oestrogen receptors which is very variable not only in different types of breast cancer (Manna and Holz 2016), but also throughout progression of the disease; being more expressed in early stages and decreasing in advanced cancer (Welsh 2013). Efficacy of this approach depends on the presence of oestrogen receptors so declines in advanced breast cancer. In some aggressive forms of breast cancer, there is little or no expression of these proteins or genes known as triple negative and patient prognosis is poor. While many cytotoxic agents are effectively used to inhibit the progression of breast cancer (e.g. anthracyclines, taxanes, antimetabolites and monoclonal antibodies) they have serious side effects in normal body tissues and can often lead to very serious diseases unrelated to the initial breast cancer (e.g. heart failure, cardiac arrhythmia, renal failure).

Prevention of disease progression is one major approach to breast cancer treatment with many drugs used to arrest the cell cycle and induce apoptosis (rather than necrosis and associated inflammation). Many drugs are very effective in doing this (e.g. doxorubicin, docetaxel, gemcitabine and cyclophosphamide) but again they also affect the cell cycle of normal tissues, particularly epithelia, hair follicles and bone marrow (Pérez-Herrero and Fernández-Medarde 2015). Further, many of these drugs (e.g. doxorubicin) are known to induce cardiovascular symptoms in patients which can be life threatening (i.e. cardiac arrhythmia, long QT syndrome and heart failure) (Senkus and Jassem 2011; Kumar et al. 2012). Traditionally these cardiac side effects have been attributed to a range of metabolic changes occurring in cardiac cells such as production of reactive oxygen species (ROS) or triggering apoptosis (Takemura and Fujiwara 2007; Shi et al. 2011; Octavia et al. 2012). More recently doxorubicin has been identified to not only affect hERG potassium channels in the heart (Becker and Yeung 2010; Ducroq et al. 2010; Tamargo, Caballero, and Delpón 2015),

predisposing patients to long QT syndrome and cardiac arrhythmia, but it also blocks ryanodine receptors (RyR_2) and reduces Ca^{2+} availability in the heart for contraction (Park, Kim, Park, et al. 2005; Hanna et al. 2017). Many chemotherapeutic agents are known to induce such cardiovascular abnormalities including 1) alkylating agents and tyrosine kinase inhibitors, 2) antitumor antibiotics and topoisomerase inhibitors, 3) anthracyclines and 4) cyclophosphamide and cytarabine, to name a few (Thomas 2017; Tromp et al. 2017). Now it is better understood that in part their accidental blockage of hERG channels in the heart is part of the cause (Kim and Ewer 2014; Moudgil and Yeh 2016).

While considerable advances have been made by investigating how to arrest the cell cycle and promote or inhibit specific regulatory proteins in cell proliferation, or stimulating apoptosis via the intrinsic apoptotic pathway, attention has shifted toward better understanding ion channels in cancer and how they may be manipulated to arrest disease progression. It has long been recognized that cancer cells have less negative membrane potentials (ranging from -40mV to -10mV) than normal tissue cells (ranging from -90mV to +20mV) (Yang and Brackenbury 2013a). Indeed, it is now recognized that cancer cells (as with all proliferating cells) undergo a cyclic change of membrane potential as they progress through the cell cycle(Cone 1969; Sachs, Stambrook, and Ebert 1974). Further, there are key changes in membrane potential that must occur in cancer cells corresponding to the cell cycle checkpoints. In general, cells (normal or cancerous) undergo cell cycle phases (G1, S and G2/M) before proliferating. Many of the ionic currents and channels responsible for this variation in the membrane potential during the cell cycle have been identified. There are many different potassium channels involved in the regulation of the cell cycle, tend to make the membrane potential more negative (hyperpolarizing). There is increased hERG conductance between M and G1 phases which allows the cells to enter G1 phase by bringing the membrane potential to more negative values prior to S phase (Rao et al. 2015), while there is no hERG channel activity in S and G2 phase (Ouadid-Ahidouch et al. 2004; Arcangeli and Yuan 2011). Cancerous cells have a less negative (more depolarized) Vm than non-proliferating cells which is bought about by elevations in intracellular Na^+, Ca^{2+}, and may be associated with reduced intracellular Cl^- concentrations.   Any alteration in channel conductance that affects the rhythmic cycle in cancerous cells (alternating hyperpolarized and depolarized Vm states) will likely disrupt proliferation and arrest the cell cycle (Rao et al. 2015).

Today the participation of ion channels in cancer cells in the progression of the cyclic changes in membrane potential that in part regulate cell cycle progression has been established. As seen in (Figure 9 in chapter 1) there are various ion channels that maintain the oscillating membrane potential of cancer cells to allow progression through the cell cycle phases (G1, S and G2) until reaching mitosis. Calcium channels impact the cell cycle mechanisms directly

by regulating cytokinesis and the mitotic spindle (Chandy et al. 2004). The L-type calcium channel (Cav1) is expressed in the non-proliferative phase of the cell cycle (G0) which allows cells to move from G0 to G1, while the expression of T-type calcium channels (Ca_v3) is expressed in the proliferative S phase of the cell cycle (Panner and Wurster 2006). Blocking Cav1 channels by specific inhibitors such as nifedipine or verapamil does not inhibit proliferation rather proliferation and metastasis was enhanced in MCF-7 and MDA-MB-231 breast cancer cells both *in vitro* and *in vivo* (Guo et al. 2014). Yet overexpression of full length Cav3.1 inhibits the proliferation of MCF-7 cells (Ohkubo and Yamazaki 2012). Expression of potassium channels Kv1.3 and Kv1.5 increases during G1 phase to initiate and maintain hyperpolarisation, with inhibition of Kv1.3 preventing cells from entering S phase (Chittajallu et al. 2002). The expression of Kv10.1 is increased in G1 phase and is involved in not only the hyperpolarization state of the membrane potential but also enhances calcium influx leading to activation of calcium activated channels (KCa 3.1) in both S and G2 phase (Becchetti 2011). The Kv11.1 (hERG) channels also increases in expression between M and G1 phase and contribute to the transient hyperpolarized state of the membrane potential, while the activity of these channels decreases during the S and G2 phases. Inhibition of Kv11.1 has been linked with inhibition of proliferation (Rao et al. 2015). Chloride conductance through CLC3 channels in the M phase, regulate the pre-mitotic condensation, a process including changes in cell volume resulting in cytoplasmic condensation/shrinkage, which is important for cell cycle progression into M phase. Inhibition of the CLC3 channel have been associated with increased duration of the cell cycle which delays cells reaching to mitosis (Xu et al. 2010; Li, Wu, and Wang 2013)

Cancer is now regarded (in part) as a channelopathy, since the expression of some channels is clearly associated with the cancer (see Table 12) but not normal tissue of the same type (Preußat et al. 2003; Bielanska et al. 2009; Choi et al. 2011; Williams, Bateman, and O'Kelly 2013; Pardo and Stühmer 2014; Than et al. 2014; Prevarskaya, Skryma, and Shuba 2018). One important example of these is hERG channels typically expressed in high amounts in the central nervous system (Shi et al. 1997; Emmi et al. 2000; Papa et al. 2003) and cardiac muscle (Vandenberg et al. 2012), but much less in other tissues such as smooth muscle (Farrelly et al. 2003; Greenwood et al. 2009) and endocrine cells (Schäfer et al. 1999). There is now evidence that overexpression of hERG channels occurs in many solid forms of cancers including breast cancer (Thomas et al. 2003; Lansu and Gentile 2013), endometrial cancer (Cherubini, Taddei, Crociani, Paglierani, Buccoliero, Fontana, Noci, Borri, Borrani, and Giachi 2000), ovarian cancer (Asher et al. 2010), oesophageal cancer (Lastraioli, Taddei, Messerini, Comin, Festini, Giannelli, Tomezzoli, Paglierani, Mugnai, and De Manzoni 2006; Ding et al.

2008), gastric cancer (Crociani, Lastraioli, Boni, Pillozzi, Romoli, D'Amico, Stefanini, Crescioli, Taddei, and Bencini 2014) and colorectal cancer (Lastraioli et al. 2004).

Cancer type	Kv1.1 KCNA1	Kv1.3 KCNA3	Kv1.5 KCNA5	Kv3.4 KCNC4	Kv4.1 KCND1	Kv7.1 KCNQ1	Kv10.1 KCNH1	Kv10.2 KCNH5	Kv11.1 KCNH2	KCa1.1 KCNMA1	KCa2.3 SK3	KCa3.1 IK1	Kir2.2 KCNJ12	Kir3.1 KCNJ3	Kir3.4 KCNJ5	Kir4.1 KCNJ10	Kir6.1 KCNJ8	Kir6.2 KCNJ11	K2P2.1 KCNK2	K2P3.1 KCNK3	K2P5.1 KCNK5	K2P9.1 KCNK9
Adrenal															B					R		
Blood			G				R		R													
Bone							R			R												
Brain	R		G				R	R	R		R					R	R	R				
Breast		R			R		R		R	R	R	R				R	R	R		R	R	R
Cervix																						R
GI tract					R	G	R		R		R	R										R
Head and neck				R					R													
Kidney							R															
Lung		R							R					R								R
Lymphoma		R																				
Melanoma									R		R			R		R	R					R
Ovary							R		R													
Pancreas		R					R															
Prostate		R							R	R		R						R				
Sarcoma							R															
Thyroid									R													
Uterine																R	R					

Table 12. Expression of potassium channels including hERG channels in various cancers (red box: indicative of overexpression of channel in the cancer, green box : indicative of channel expression correlated with tumour malignancy, blue box: somatic mutation associated with channel action in the tumour cell) (Huang and Jan 2014).

The focus of this study was to investigate how manipulation of hERG channels in two breast cancer cell lines would affect proliferation, cell cycle progression and apoptosis. The two breast cancer cell models chosen for this study were MCF-7 which is an example of a less aggressive breast cancer positive for oestrogen and progesterone receptors as well as the HER2 oncogene (Welsh 2013) and MDA-MB-231 which has none of these receptors or gene expression and is known as "triple negative" which in patients is a very aggressive form of breast cancer often with very poor prognosis. Both cell lines have been previously reported to have higher than normal expression of hERG channels, but more so in the MCF-7 cell line (Jung 2016). This provided an excellent experimental model to test how hERG channel modulation would affect breast cancer in two extreme models under the same experimental conditions.

Previous work has demonstrated that hERG channels may exist not only on the plasma membrane of cancer cells (Cherubini, Taddei, Crociani, Paglierani, Buccoliero, Fontana, Noci, Borri, Borrani, and Giachi 2000), but also inside cancer cells, particularly the mitochondria (Bonnet, Archer, Allalunis-Turner, Haromy, Beaulieu, Thompson, Lee, Lopaschuk, Puttagunta, and Bonnet 2007). The results have not been conclusive for MCF-7 or MDA-MD-231 cell lines, with only diffuse staining of hERG protein intracellularly when investigated by immunohistochemistry(Afrasiabi et al. 2010; Asher et al. 2011; Jung 2016). Therefore, the first experiment conducted in this study was to determine where hERG channels are located

within these two breast cancer cell lines to determine whether they were in fact associated with mitochondrial membranes. Since it has already been established that they exist on the plasma membrane, an immunohistochemical analysis using KCNH2 primary antibody to stain hERG protein inside the cells was conducted. Breast cancer cells were counterstained with Hoechst blue (for nuclei) and Mitotracker red (for mitochondria). From this staining, where green fluorescence from the KCNH2 stain overlapped the Hoechst blue and Mitotracker red, the presence of hERG channels could be confirmed. Results for MCF-7 cells showed more staining than MDA-MB-231 cells (see Figures 17d and 18d in chapter 3) indicating that there was more hERG protein expression in the former. There was little diffuse staining in the cytosol for either cell line, indicating that the hERG protein was localized to cell membranes associated with these organelles. hERG channels expression has previously been shown to be present in and its gating directly impacted by plasma membrane stability (Massaeli et al. 2010). However, there was no attempt to stain hERG protein on the plasma membrane of these cells which would have been removed after the Triton X100 treatment to allow the KCNH2 antibody access to the cytosol, a technique that has been previously shown to improve antibody access when staining adult newt spinal cords (Zukor, Kent, and Odelberg 2010). This was then followed by several washed that may have removed any remnants of plasma membrane and hence hERG protein expression.

To investigate the effect of hERG channels in proliferation, cell cycle progression and apoptosis in the two breast cancer cell lines, hERG channels modulators needed to be selected. From cardiovascular research, the notion of using hERG agonists to reverse long QT syndrome in patients has attracted attention in oncology research. One fairly new hERG channel agonist, NS1643, has been shown to inhibit cell cycle progression in breast cancer lines SKBr3 and MDA-MB-231 (Breuer et al. 2019). The cell cycle in MDA-MB-231 and SKBr3 cells was arrested at G1 phase following exposure to 50µM NS1643 (Lansu and Gentile 2013).

Prior to using NS1643 for proliferation or apoptosis experiments, a membrane potential (or permeability) assay was conducted to confirm its effect in each cell line. If the presence of NS1643 enhanced the current through potassium channel in cells compared to normal growth conditions, then it was considered an agonist while if the current was inhibited then it was considered an antagonist. Results showed that in MCF-7 cells NS1643 was an antagonist, while in MDA-MD-231 cells it was an agonist (see Figures 21a and 21b, chapter 3). To ensure NS1643 was interacting with hERG channels, the commercial antagonist, terfenadine was used to block the channels. In MCF-7 cells, the combination of NS1643 and terfenadine was additive (more inhibition than either agent alone) confirming that NS1643 was in fact an antagonist (see Figure 20a, chapter 3). In MDA-MB-231 cells however, when NS1643 and terfenadine were combined their respective effects were largely cancelled out because

NS1643 was behaving as an agonist in this cell line (see Figure 20b, chapter 3). Similar action was reported by (Lansu and Gentile 2013) where the application of a hERG channel inhibitor E4031 in the presence of NS1643 in MDA-MB-231 and SKBr3 cells preserved the cell cycle arrest activity of NS1643 alone and they also proposed that this confirms that hERG channels determine the agonist-dependent inhibition of proliferation (Lansu and Gentile 2013).

Normally hERG channels (Kv11.1) have a full transcript of 4.4kb in cardiomyocytes (London et al. 1997), but often in cancer cells this is much shorter. In various cancer cell lines, multiple mRNA transcripts exist ranging in size from 2.2kb to the full size 4.4kb, suggesting alternative splicing of hERG mRNA may occur in different cancer phenotypes (Bianchi et al. 1998). Since it is the amino end of the channel that is truncated, corresponding to the voltage sensor domain (S1 to S4), this might explain why different effects are seen in different cell lines (and perhaps experimental conditions). Certainly, it is known that when shorter transcripts are expressed the inactivation kinetics of the hERG channels is much shorter than normal, but there have been no reports that the activation kinetics have been affected, since the potassium pore filter is associated with the carboxyl end of the channel between S5 and S6 (refer to Figure 7 in Chapter 1) which is usually considered to be well conserved (Perry, Sanguinetti, and Mitcheson 2010). Another explanation for the response to NS1643 may be associated with its lipid solubility. It has been previously reported that the presence of fluorine atoms enhances the lipophilicity, absorption and bioavailability of quinazoline-sulphonamide small molecules that have shown anti-cancer activity in various cancer cell lines including cervical cancer (Hela), lung (A549) and colorectal (LoVo) cell lines (Ghorab et al. 2016).

While NS1643 may bind to the S5-S6 domain in cardiomyocytes, it may also with prolonged exposure diffuse into the cancer cells and affect an intracellular site. This could be on the truncated amino end or at the carboxylic end of the channel complex. Since the breast cancer cells were exposed to 10µM NS1643 for 72 hours prior to assay, it would certainly have had time to diffuse into the cells and affect the channels intracellularly. Further experimentation would need to be done to verify this possibility. Also, hERG channels require a less negative membrane potential (more depolarized) that is beginning to drop toward more negative potential to reactivate after an initial voltage step. Since MDA-MB-231 cells have a resting Vm ~ -20mV but MCF-7 cells are on average ~ -30mV (Yang and Brackenbury 2013b), the conditions may have not been appropriate to activate hERG channels in the MCF-7 cells. At -20mV hERG channels may be more responsive to an agonist binding than at -30mV, since in the normal cardiac action potential, hERG channels are stimulated to open initially at about 0 to +20mV, inactivate and then reactivate at about -20mV (Vandenberg et al. 2012). But in cardiomyocytes, hERG channels usually remain open until the membrane potential reaches as low as -70mV. Perhaps in the MCF-7 cells, the hERG channels failed to activate, but it is

also possible that they were simply inhibited by NS1643 under the experimental conditions used.

Knowing that NS1643 was acting as an antagonist in MCF-7 cells, it would be expected to block the cell cycle at G1 (refer to Figure 47), since hERG channels normally open to produce the hyperpolarization step required to move beyond G1 phase into S phase (Rao et al. 2015).
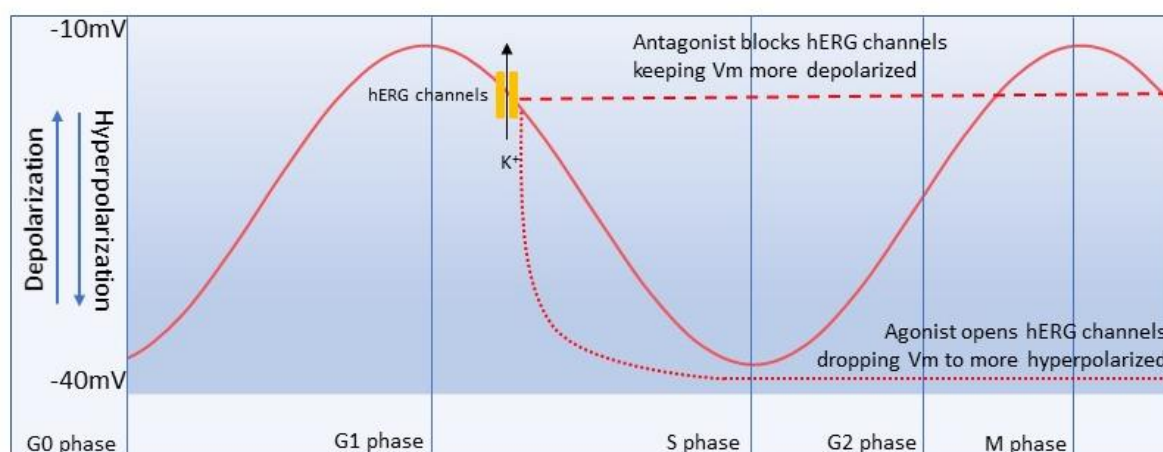
Figure 47. Diagram showing how membrane potential (Vm) changes normally throughout the cell cycle (solid red line). Blocking hERG channels, keeping Vm more depolarized prevents the hyperpolarizing step required for progression through S phase leading to cells accumulating at G1 phase (dashed red line). Opening hERG channels drops Vm more quickly to hyperpolarizing levels allowing S phase to progress and perhaps the beginning of G2 phase, leading to cells accumulating in G2/M. If cells are not found in G2/M apoptosis may have been triggered. (Adapted from (Rao et al. 2015).

Blocking the hERG channels would keep the membrane potential more depolarized and prevent cells moving into S phase. Indeed, from Figure 22a the cell cycle in MCF-7 cells did show accumulation of cells at G1 after exposure to 10µM NS1643 for 72 hours. In the MDA-MB-231 cells (Figure 22b) however, with NS1643 acting as an agonist, it would bring the membrane potential down more quickly to allow progression from G1 phase to S phase. Since the cells were chronically exposed to NS1643 for 72 hours, the membrane potential would not be able to become more depolarized during S phase to trigger G2 phase. It was expected that the cells might show accumulation at G2 or M phase, but this did not occur. However, it is feasible that the cells were stalled at G2 and could not enter mitosis, which would trigger apoptosis. Indeed, apoptosis was increased in both cell lines (with concomitant decrease in necrosis), but more so in the MDA-MD-231 cell line (see Figures 24a and 24b, chapter 3). Another explanation for this is that 10µM NS1643 was not enough a high enough concentrations to affect the MDA-MB-231 cells. (Lansu and Gentile 2013) used 50µM NS1643 to show cell cycle arrest at G1 phase in this cell line. Further, since MDA-MB-231 cells express fewer hERG channels perhaps they were not very sensitive to modulation of this channel class.

Similarly, proliferation of MCF-7 cells and MDA-MB-231 cells was comparably inhibited by 10µM NS1643. When apoptosis and necrosis was monitored in both cell lines each of them showed an increase in apoptosis which the preferred cell death pathway (reducing inflammatory side effects *in vivo*) and a decrease in necrosis. MCF-7 cells as well as MDA-MB-231 cells were sensitive to the presence of NS1643, whether it was acting as an agonist or an antagonist. Since there was no clear explanation from the cell cycle results, an apoptosis array for 43 different markers in the extrinsic and intrinsic apoptosis pathways was used to see whether this agonism versus antagonism would lead to different apoptosis induction. While the results are only preliminary, in MCF-7 cells it appears that markers associated with the intrinsic pathway are inhibited as HTRA decrease, but in MDA-MB-231 cells the markers associated with both pathways changed, in the intrinsic pathway markers decreased while in extrinsic pathway, some markers increase and other decreased. (refer Figure 26, chapter 3). These results should be investigated in more detail in future.

It appears that when NS1643 acted as an antagonist in MCF-7 cells, it caused decreased proliferation, inhibited the cell cycle with accumulation of cells at G1 phase with induction of apoptosis, probably via the intrinsic pathway with reduced necrosis. While acting as an agonist in MDA-MB-231 cells NS1643 decreased proliferation but did not affect the cell cycle, yet increased apoptosis, probably via the extrinsic pathway and reduced cell death by necrosis as well.

Discovering new and novel treatments for cancer is important to not only better target cancer cells but to reduce side effects by normal tissue cells being affected. There is a host of bioactive molecules scanned or their effects as novel anti-cancer therapies worldwide and one class is centred around the heterocyclic molecule quinazoline (see Figure 48).
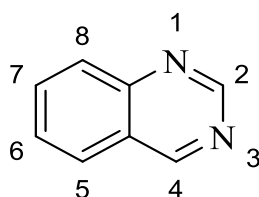
Figure 48. Structural representation of quinazoline

Many quinazoline derivatives have been synthesized with substitutions in many places on their ring structure. Among the successful finds that are now FDA approved are Gefitinib, Lapatinib and Afatinib (see their structures with the quinazoline parent molecule highlighted in red in Figure 49 below). Gefitinib inhibits the growth of MDA-MB-231 breast cancer cells by causing dephosphorylation of EGFR leading to loss of telomerase activity promoting cell death (Moon et al. 2009). In oesophageal tumours that contain multiple copies of the EGFE gene, Gefitinib

has been very successful (Ismail et al. 2016). Lapatinib has also been used to treat HER-2 positive advanced or metastatic breast cancer, again by inhibiting EGFR but it also affects HER2/neu pathways (Higa and Abraham 2007). Finally, Afatinib, is an irreversible covalent inhibitor of the receptor tyrosine kinases, epidermal growth factor receptor (EGFR) and HER2 receptors that has been used in phase II trials in with HER2-positive breast cancer patients with metastases treatment with Trastuzumab. It is a promising monotherapy associated with the pre-treated hER2-positive breast cancer in patients (Ismail et al. 2016). Gefitinib has substitutions at C1, C6 and C7, Lapatinib at C1, C7 and Afatinib at C1, C3 and C4. All of them have at least one fluorine to improve lipid solubility since all of them work inside the cancer cells.

Gefitinib

Lapatinib
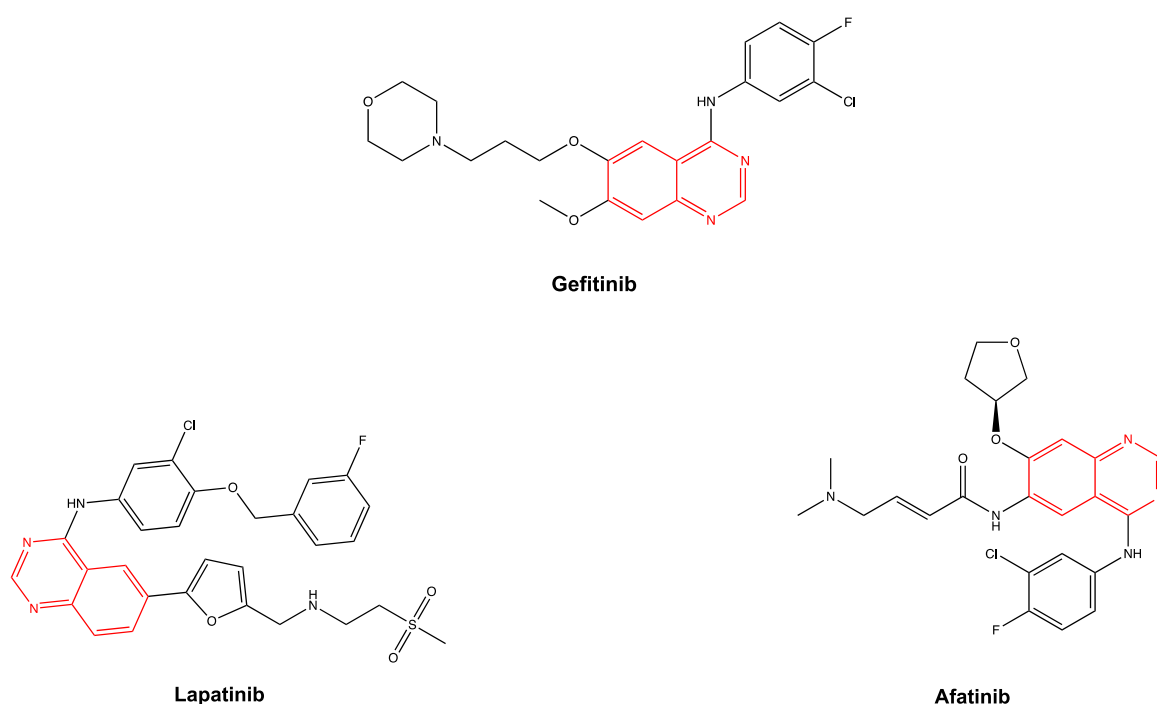
Afatinib

Figure 49.Structures of Gefitinib, Lapatinib and Afatinib.(Ismail et al. 2016)

Doxazosin (Figure 50a) and Prazosin (Figure 50b) are clinically used α_1 adrenergic receptor antagonists that have been investigated for a possible role as anti-cancer theraputics. Doxazosin (>10µM) has been shown to activate apoptosis in prostate cancel cells lines (PC-3 and DU-145) by inducing TGF-β signalling and Iк-β signalling (Kyprianou and Benning 2000). On breast cancer cell lines (MCF-7 and MDA-MB-231). Doxazosin (20-30 µM for 72 hours) significantly inhibited proliferation, increased apoptosis 10-15 fold, and caused a 2-3 fold increase in cells at G0/G1 phase with a slight decrease in cells at S phase in MCF-7 cells (Hui, Fernando, and Heaney 2008). Prazosin is also effective at inhibiting proliferation in a

range of cancer cell lines (PC3, DU-145 and LNCap) at concentrations between 7.5 and 16.7μM which caused cell cycle arrest at G2 phase and an increase in apoptotic events, the latter being mediated by activation mitochondrial associated caspase executioner pathways (Lin et al. 2007). The substitions on the quinazoline backbone for both Doxazosin and Prazosin are on C1, C3, C6 and C7, with no fluorines attached but they are still lipophilic since they affect intracellular apoptotic pathways.

a)   b)
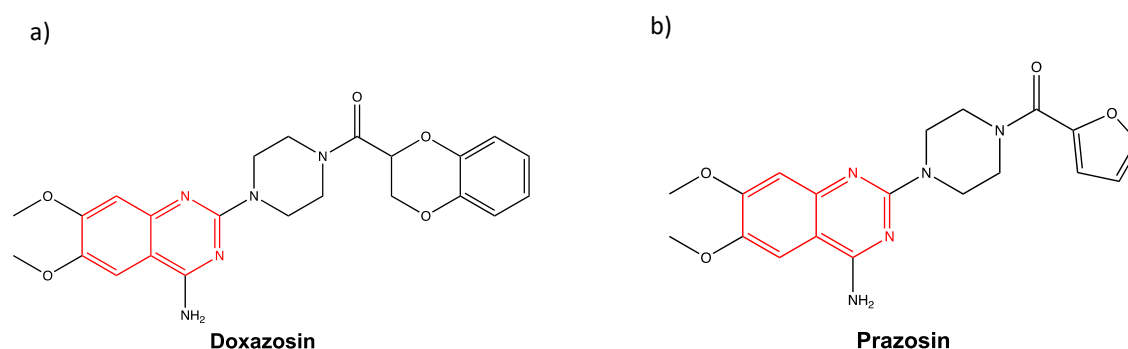
Figure 50. Structures of the α1 adrenergic receptor antagonists a) Doxazosin and b) Prazosin (red highlighted stucture: quinazoline unit of the compound)(Desiniotis and Kyprianou 2011)

The evasion of apoptotic signalling is one of the hallmarks of cancer, a key apoptotic regulator p53 is inactivated due to mutation in many cancer types. This inactivation causes cells to bypass intrinsic apoptosis as well as apoptosis initiation due DNA damage following traditional anti-cancer treatment. This has prompted interest in finding agents that can regulate apoptosis in cancer cells which would ultimately eliminated these cells from the body (Lee and Bernstein 1995).

There has been significant research into developing small molecules that regulate the apoptotic pathways. Some of the targets that has been investigated includes the development of small molecules inhibitors of the anti-apoptotic Bcl-2/Bcl-xl such as compound HA1A-1 which interferes with the binding of Bcl-2/Bak binding (Wang et al. 2000). Through nuclear magnetic resonance (NMR) screening, the small molecule ABT-737 was found to inhibit anti-apoptotic proteins Bcl-s, Bcl-X_L and Bcl-w in lymphoma and small cell lung cancer cells as well with adjuvant with chemotherapy and radiation (Oltersdorf et al. 2005). The small novel compound Embelin was found to inhibit the anti-apoptotic X-linked inhibitor of apoptosis (XIAP) that is expressed highly in prostate cancer cells PC-3, LNCap, CL-1 and DU-145 via modulating the BIR3 domain of XIAP with minimal effect seen in normal prostate epithelium and fibroblast with low XIAP. Embelin was also found to overcome the anti-apoptotic effect of XIAP in XIAP-transfected Jurkat cells when used in conjugation with etoposide (Nikolovska-Coleska et al. 2004).

A more recent approach to treating cancers has been to investigate modulation of hERG channels more directly and then determine whether apoptotic signalling is affected. Several quinazoline derivatives that are used clinically have been investigated for their effect on a range of voltage gated channels. For example, two analogues of Prazosin (Alfuzosin and Bunazosin, structures shown in figure 51 below) are also used to treat prostate disease (Lacerda et al. 2008; Lee and Su 2008) and have been investigated in cardiac myocytes for their impact on the cardiac action potential.

a)   b)
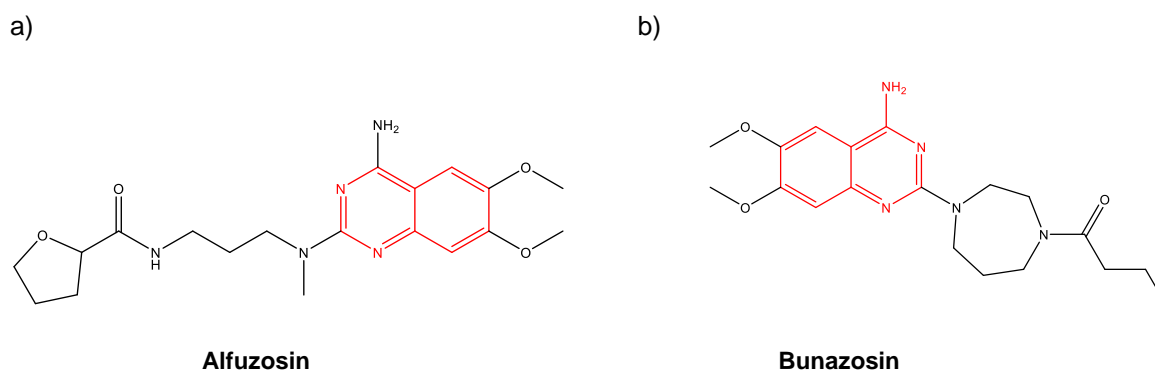
Figure 51. Structures of the α₁ adrenergic receptor antagonists a) Alfuzosin and b) Bunazosin (Lacerda et al. 2008; Lee and Su 2008). Red highlighted stucture is the quinazoline unit of the compound.

Alfuzosin, (N-[3-[(4-amino-6,7-dimethoxy-quinazolin-2-yl)-methyl-amino] propyl] oxolane-2-carboxamide) is a selective postsynaptic α₁ adrenergic receptor antagonist used to treat benign prostatic hyperplasia (Selvam and Kumar 2011) that prolongs the QT interval in rabbit heart. It did not block K_v11.1 or K_v7.1 channels nor affect L type Ca^{2+} channels ($I_{ca,L}$) but significantly increased Na^+ current (Nav 1.5) (Lacerda et al. 2008). Bunazosin (1-(4-(4-amino-6,7-dimethoxyquinazolin-2-yl)-1,4-diazepan-1-yl) butan-1-one) is also an α₁ ‑ adrenoceptor antagonist Prazosin analogue inhibited L-type calcium channel ($I_{ca,L}$) with no effect on any of the channels investigated (potassium outward current (I_{to}) or I_{K1}) in rat ventricular myocytes yet it did prolong repolarisation of the action potential (Lee and Su 2008). It is interesting that the only difference between these compounds is the substitution at N3, with the same substitutions at C6 and C7, and while they prolonged the cardiac action potential, it was not by blocking hERG channels.

From cardiovascular research, hERG channel activators have been developed and tested in part to use as experimental tools, but also to test for their ability to reverse drug-induced long QT syndrome. None of these compounds are quinazoline analogues but they are small organic molecules that not only activate hERG channels but have anti-cancer properties.

NS1643 and NS3623 (an analogue of NS1643 shown in Figure 52 below) are both di-phenyl ureas that increase hERG currents in cardiomyocytes. In fact, NS3623 has also been shown to bind to closed hERG channels, while NS1643 requires the S5-S6 area to be open(Hansen, Diness, Christ, Wettwer, et al. 2006; Xu et al. 2008). So, while NS1643 is truly a voltage-dependent agonist, NS3623 is both a voltage-gated and ligand-gated agonist of (Kv11.1) hERG channels. Presently there are reports of NS3623 impact on volume regulated Anion channel (VRAC) in HEK293 cells and was found to be a potent VRAC blocker (IC$_{50}$ 1.8µM) enhancing channel inactivation at positive potential. Inhibition of VRAC channel is believed to be of therapeutic value in cancer treatment as it causes anti-angiogenic effects.(Helix et al. 2003).However, no studies to date have reporting impact of NS3623 on proliferation and cell death of cancer cell lines.

a)

b)
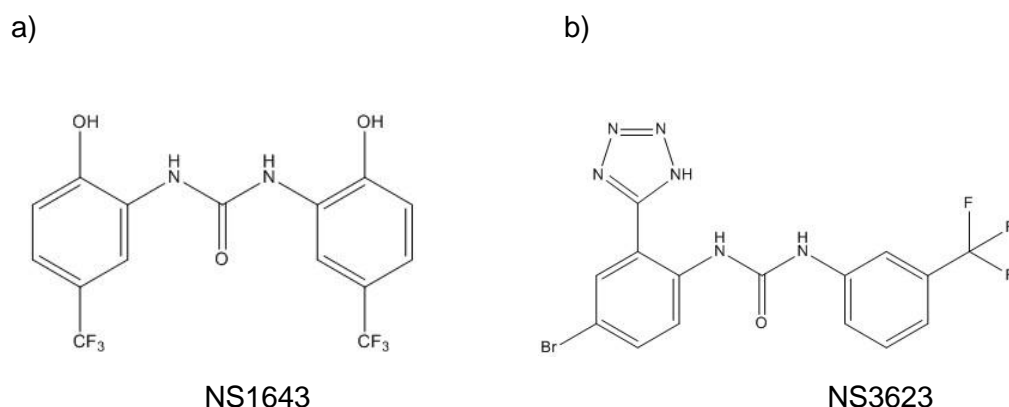
NS1643

NS3623

Figure 52. Structures of the di-subsituted a) NS1643 and b) NS3623 (Hansen, Diness, et al. 2006; Hansen, Diness, Christ, Wettwer, et al. 2006).

NS1643 has been investigated in breast cancer cell lines (SKBr3 and MDA-MB-231) and irreversible inhibition of cell proliferation (Lansu and Gentile 2013). They also used hERG channel agonist PD118057 (2-(4-[2-(3,4-dichloro-phenyl)-ethyl]-phenylamino)-benzoic acid) a 2-subsituted benzoic acid (see structure figure 53 below) which also significantly reduced proliferation in these cell lines. From molecular docking studies, the benzoic acid end of PD118057 interacts with the F619 residue of the selectivity pore on the hERG channel and there are hydrophobic interactions between the central phenyl group and S6 helix residues (Perry et al. 2009). Further, PD118057 strongly increased hERG currents in HEK-293 cells and shortened the action potential in guinea-pig ventricular myocytes but did not appear to alter the activation or inactivation kinetics of hERG channels (Zhou et al. 2005; Perry et al. 2009).
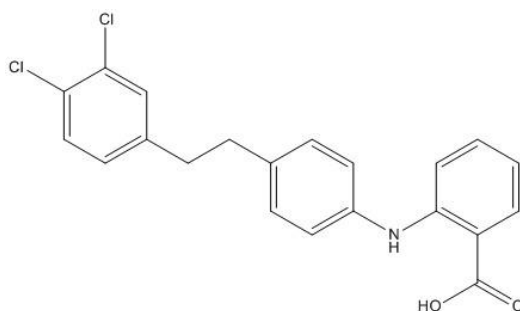
Figure 53. Structure of PD118057 (2-(4-[2-(3,4-dichloro-phenyl)-ethyl]-phenylamino)-benzoic acid) (Zhou et al. 2005).

In this project six untested quinazoline-4-one compounds were investigated for their effects on hERG channel modulation and how this would impair grown in two breast cancer cell lines, MCF-7 and MDA-MB-231. In a recent review (see (Ahmad 2017)), quinazoline derivatives have shown enormous promise and anti-cancer compounds. Among their properties are significant inhibition of protein kinases, tubulin polymerization, protein lysine methyltransferase, topoisomerase I, PI3K/Akt/mTOR, poly (ADP-ribose) and polymerase-1(PARP-1). Two quinazolinone Schiff base derivatives synthesized and tested by (Zahedifard et al. 2015),   (3-(5-chloro-2 hydroxybenzylidene amino)-2-(5-chloro-2-hydroxyphenyl)-2,3-dihydroquinazolin-4IJ1H)-one   and   3-(5-nitro-2-hydroxybenzylideneamino)-2-(5-nitro-2-hydr oxyphenyl)-2,3-dihydroquinazolin-4IJ1H)-one) proved to induce apoptosis in many cancers including MCF-7 and MDA-MB-231 breast cancer cell lines. Similar compounds have been shown to inhibit purified DNAPK and PI3K enzymes and are being developed as potential anticancer drugs (Heppell and Al-Rawi 2015). To date, however, it appears that very few quinazolin-4-one compounds have been investigated for their potential to modulate hERG channels.

After reviewing a range of quinazolin-4-ones available for this project, it was decided to select those with either a urea or thiourea as well as fluorine attached which enhances lipophilicity, absorption and bioavailability (Ahmad 2017). Since both NS1643 and NS3623 (both di-substituted urea compounds) have shown promise as anti-cancer agents that activate hERG channels, it was of interest to see whether any of the quinazolin-4 one compounds (LTUJH06B, LTUJH18B, LTUJH28B, LTUJH37B, LTUJH47B, LTUJH51B) could firstly affect hERG channels and secondly alter growth and cell death in MCF-7 and MDA-MB-231 breast cancer cell lines.

All the quinazoline-4-one compounds acted as hERG antagonists in MCF-7 cells which was unexpected because they acted as agonists in MDA-MB-231 cells. The commercial hERG agonist NS1643 also acted as an antagonist in the MCF-7 cells which have not been

previously reported in literature. The membrane potential was not very reliable and so the compounds were subsequently tested in sheep cardiomyocytes using the FluxOR assay where it was confirmed that they were agonist of native hERG channels and their activation was inhibited by the known antagonist, terfenadine. The only compounds that were not terfenadine sensitive were LTUJH28B and LTUJH37B, but they did not increase Ca^{2+} influx (from a simple fluorescence test with Fluo4AM). These compounds may well be affecting ion channels not yet identified.

One of the only quinazolines derivatives already reported to cause significant anti-proliferative activity in a variety of tumour cell lines including breast (MCF-7), HCT116 (colon), Hela (cervical), PC3 (prostate) and A549 (lung) is PVHD121 (1-Phenyl-1(quinazolin-4-yl)ethanol) (Kuroiwa et al. 2015). All the quinazolin-4one compounds in this study significantly inhibited proliferation in MCF-7 cells (see Figure 29 chapter 4), but in the MDA-MB-231 cell line only the thiourea containing LTUJH37B and the urea containing LTUJH28B had any anti-proliferative effect (Figure 30 chapter 4). This was similar to results for the quinazolinone Schiff base derivatives synthesized by(Zahedifard et al. 2015).

Cell cycle analysis in MCF-7 cells demonstrated that LTUJH37B (urea containing), LTUJH18B and LTUJH28B (both thiourea containing) cause cells to accumulate at G2/M suggesting that these compounds maybe acting on a checkpoint between S phase and G2/M phases. There was no effect on cell cycle progression in the MDA-MB-231 cells. Quinazolines derivatives have also been reported to cause accumulation in lung cancer cells (A549), prostate cancer cells (DU145) and epidermoid carcinoma of the mouth (KB) in the G2/M phase (Wang et al. 2013).

Initial investigating on the induction of cell death via apoptosis revealed more apoptotic activity in MDA-MB-231 compared with MCF-7 cells. All of the quinazolin-4-one compounds caused significantly increased apoptotic events only in MDA-MB-231 cells (Figure 35a chapter 4) while only LTUJH28B (thiourea) and LTUJH51B (urea) caused significantly increased apoptotic events in MCF-7 cells (Figure 34a chapter 4). This contradicts the reported effect of Gefitinib analogues (4-benzothienyl amino quinazolines) inducing significant apoptotic activity in MCF-7 cells overexpressing HER2 factor (Wu et al. 2010). When investigating necrosis, the secondary cell death pathway, again only LTUJH37B, LTUJH47B and LTUJH51B (all urea containing) increased necrosis in MCF-7cells (Figure 34b chapter 4) while all quinazolin-4-one compounds either did not produce a significant change or significantly reduced the necrotic activity in MDA-MB-231 cells (Figure 35b chapter 4).

Overall these six previously untested quinazolin-4-one compounds with either urea or thiourea in their structure did affect hERG channels, decreased proliferation and induced apoptosis or

necrosis in two breast cancer lines, MCF-7 cells and MDA-MB-231 cells. Further work should be done to clarify how these compounds affect hERG channels as well as more specific assays for various enzyme systems to inhibit cancer growth. As an initial study, these compounds show promise in both future cancer and cardiovascular research.

6.1 Conclusion, limitations and future studies

The role of hERG channel modulation to inhibit proliferation, arrest the cell cycle and induce cell death (by apoptosis or necrosis) was investigated in two extreme forms of breast cancer. The MCF-7 cell line representing an early form which is positive for HER2, oestrogen and progesterone receptors, and therefore easier to treat responses were compared with those of the MDA-MB-231 cell line also known as the triple negative and more aggressive form of breast cancer with significantly poorer patient prognosis. The commercial hERG channel agonist, NS1643, was effective in reducing cell growth and promoting cell death in both cell lines, but in MCF-7 cells it appeared to be acting as an antagonist, which was not expected. In fact, NS1643 was confirmed to be an agonist in sheep cardiomyocytes which express the native Kv11.1 (hERG channels). Perhaps different transcripts of the hERG channels were being expressed in MCF-7 cells.

One aim in this project was to investigate how, six previously untested quinazolin-4-one compounds would affect firstly, hERG channels and secondly, proliferation, cell cycle progression and cell death in the two breast cancer cell lines (MCF-7 and MDA-MB-231). All the quinazoline-4-one compounds altered hERG channel activity. In MCF-7 cells they acted as antagonists, but in MDA-MB-231 cells and cardiomyocytes, they were all agonists. Further, some of these compounds did not require a voltage step to open hERG channels (LTUJH18B, LTUJH47B and LTUJH51B) and acted as direct ligands. Among those compounds, LTUJH28B and LTUJH37B, were less hERG channel specific (terfenadine insensitive), but had more pronounced effects on retarding cell growth and inducing apoptosis in the cancer cells. It is expected that these compounds are activating different voltage or ligand channels as well as hERG channels, since their effect could not be blocked completely by terfenadine. Further investigation into which channels they may be affecting is required to clarify this situation. When the effects of the quinazolin-4-one compounds was compared with that of NS1643, none of them was more potent, but they did have different effects to NS1643.

Limited structure activity relationship was conducted to shed some light on the mode of action of the compounds used. LTUJH06B is a thio-urea quinazolin-4-one that is different from all the compounds as it contains a methylene(CH_2) spacer between the quinazolin-4-one and the ester functional group caused minimal effect in MCF-7 cells causing inhibition of proliferation only in MCF-7 and enhanced apoptosis in MDA-MB-231 cells. The direct link of the ester functional to the quinazolin-4-one in LTUJH18B, may have contributed the significant activity in MCF-7 cells, such as cell cycle arrest at G2/M and subsequent inhibition of proliferation. Though not seen with Annexin V assay, the investigation of the cell death pathway induction following exposure to LTUJH18B caused an increase in the expression of TNF-R1 apoptotic marker indicating that this compound may have a proapoptotic activity in MDA-MB-231 cells.

The difference between compounds LTUJH18B and LTUJH28B is the presence of an N,N-dimethyl amide group attached to N3 in LTUJH28B while there is an ester group attached to N3 in LTUJH18B. This difference may be responsible for compound LTUJH28B induction of apoptosis in MDA-MB-231 cells possibly through the induction of the extrinsic apoptotic pathway marked by an increase in the apoptotic markers TNF- α, TRAIL-R2 and TNF-R2 , while LTUJH18B did not have this activity. The presence of the N, N-dimethyl amide group on N3 in LTUJH28B appear to have also contributed to the inhibition of the MCF-7 cell proliferation, while the presence of an ester group on N3 in LTUJH18B influenced the MCF-7 cells more significantly as it caused G2/M cell cycle arrest with subsequent inhibition of cell proliferation. The only difference between the compounds LTUJH28B and LTUJH51B is the presence of a thio-urea at C2 in LTUJH28B and a urea at C2 in LTUJH51B. This difference may contribute to compound LTUJH28B inhibition of cell proliferation is due to the G2/M cell cycle, while LTUJH51B inhibition of proliferation through the induction of cell death via apoptosis and necrosis in MCF-7. Both compounds only induced apoptosis in MDA-MB-231 cells, possibly contributing to compound LTUJH28B inhibition of proliferation.

Compound LTUJH37B does not have an ester/amide functional groups and a thio-urea group attached to C2. The lack of an ester or amide functional group at N3 may have contributed to LTUJH37B inhibition of MCF-7 cell proliferation which is likely to have occurred consequently to G2/M cell cycle arrest with enhance cell death via the necrotic pathway. The inhibition of proliferation may be due to the induction of the intrinsic pathway which is marked by the increased expression of apoptotic markers such as CytoC, and Bax, as well as increased expression of extrinsic apoptosis pathway markers FasL, TRAIL-R1 and TRAIL-R2. While in MDA-MB-231 cells, compound LTUJH37B caused inhibition of proliferation due to the induction of the extrinsic apoptotic pathway marked by the increase in the expression of apoptotic markers TNF-R1 and TNF-R2.

Compound LTUJH47B have a urea at C2 , and ester group at N3 . The presence of a morpholino- group at C7 makes it different to the rest of the compounds tested. The presence of the morpholino- group may have contributed the biological activity of LTUJH47B with inhibition proliferation of MCF-7 cells occurring through the induction of necrosis, while inducing apoptosis in MDA-MB-231 cells. Each of these compounds had a different mode of action through the modulation of the hERG channel in MCF-7 and MDA-MB-231 cancer cells.

If the structural differences of the quinazolin-4-one compounds is considered for the FluxOR results (shown in Table 11), it can be seen, at least in part, why LTUJH28B and LTUJH37B appeared to be less specific than the rest of the compounds. LTUJH37B is a urea containing quinazolin-4-one with no substitutions at position N3, whereas LTUJH28B is a thiourea with

an amide at position N3. These compounds were not inhibited by terfenadine indicating that they are not hERG channel specific. Yet, LTUJH51B was a strong agonist that was terfenadine sensitive and only differed from LTUJH28B by being a urea rather than a thiourea compound. The presence of the thiourea may affect hERG channel selectivity in these compounds. Even though LTUJH37B is a urea containing quinazolin-4-one, the lack of a functional group at N3 (its only difference from LTUJH51B) appears to reduce its specificity for hERG channels. Knowing that LTUJH28B and LTU37B are not specifically activating hERG channels in cardiomyocytes raises questions regarding their activation or inhibition of hERG channels in the breast cancer cell lines. It appears that these two compounds have other effects yet to be elucidated.

Also, since all the quinazolin-4-one compounds were lipophilic, it was expected that with prolonged exposure they would diffuse into cells and exert their effects on intracellular sites. Among these could be hERG channels that appear to be present on the mitochondrial and nuclear membranes and associated with the endoplasmic reticulum. Also, quinazolin-4-one compounds appear to have many intracellular effects (e.g. tyrosine kinase inhibitors, list a few others). Since the properties of compounds tested in this study were previously unknown in breast cancer cells, it would be important to follow up their potential effects on some of these key systems involved in proliferation and determine whether they were effective inhibitors. Conducting experimentations using non transformed cells such as MCF10A as a control could have significantly improved the rigor of the experimentation. However, information obtained in this study provides a foundation for such work to build on. Unfortunately, such investigations were outside the scope of this project.

In an ideal world there would be unlimited funding, time and access to equipment and technical expertise. Among the limitations of this study were the inability to more rigorously investigate hERG channel activation and inactivation kinetics using electrophysiology technique such as patch clamp experiments to study ion channels as it would provide a better understanding of the biophysics of the hERG channel that can improve the understanding of limitation and confounding factors that are inherent of other techniques as well as the experimental outcome. While the FluxOR assay was useful it is relatively insensitive and only really allows for activation of hERG channels to be recorded. Since the inactivation kinetics are so important in long QT syndrome, it is recommended that these compounds be investigated more thoroughly. Another approach that could have been used to assess hERG Ion channel activity present in the plasma membrane of breast cancer cells was to use voltage sensitive oxonol dyes to monitor membrane potential changes using real time confocal microscopy to show channel activity. Further, since these compounds did not necessarily require a voltage step to activate hERG channels, it would be useful to know if they could potentially induce short

QT syndrome in cardiac cells. While not as clinically significant, prolonged exposure to these quinazolin-4-one compounds may shorten the action potential and be a source of cardiac arrhythmia.

Finally, while preliminary toxicological studies were undertaken showing that the quinazolin-4-one compounds were not toxic to cardiomyocytes, it was shown that these compounds were metabolised by two important cytochrome P450 enzymes (2E1 and 3A4). This is significant because many cancer drugs are also metabolized by these enzymes. Should any of the quinazolin-4-one compounds be taken further in medical research, they could be a source of drug interactions or toxicity, particularly if used as adjuvants or neoadjuvant. However, these problems exist for many of the cancer chemotherapeutic agents used clinically already.

Appendix

Effects of novel urea analogues of NS1643 on potassium and calcium fluxes in cardiac muscle
cells

S. Al Rawi, J.T. Heppell, J. Al Rawi and L.M. Gibson, Department of Pharmacy and Applied Science, La Trobe
Institute for Molecular Sciences, La Trobe University, Bendigo, VIC 3550, Australia..

NS1643 is a commercially available urea compound that enhances IK_r current in hERG transfected *Xenopus laevis* oocytes at concentrations ranging from 3 to 30µM (Casis *et al.*, 2006). It is a "type 1" HERG channel partial agonist binding to residue Y652A on the α S6 subunit of the HERG channel (Grunnet *et al.*,2011). Several analogues have been synthesized to investigate their effects on ion currents and contractility in cardiac muscle. Here we report the effects of two novel urea compounds LTUJH47B and LTUJH51B (Heppell and Al-Rawi, 2015).

Sheep hearts were purchased from Hardwick's Abattoirs (Kyneton, Victoria), transported back to the laboratory on ice and the right ventricle was enzymatically digested to produce single cardiac cells. Changes in potassium fluxes were investigated using the FluxOR assay (Life Technologies) on isolated sheep cardiomyocytes dispensed (10^4 cells per well) into 96-well micro-array plates and the resultant fluorescence was read using a Flexstation 3 (Molecular Devices). The FluxOR assay uses thallium as an indicator activating a fluorescent dye that has been loaded into the cells. When potassium channels are opened fluorescence increases.
In potassium negative stimulus buffer, no current is expected while in potassium positive stimulus buffer, a depolarization step is introduced that will open hERG channels and fluorescence is observed.

When isolated sheep cardiomyocytes were exposed to 10 µM NS1643 we confirmed that hERG channels were opened with increased fluorescence in the potassium positive conditions. In the presence of 10 µM LTUJH47B and LTUJH51B a smaller current was observed in the potassium containing stimulus buffer, but there was also an increase in the potassium negative stimulus conditions. This suggested that another current was being activated by these novel compounds. To test whether a calcium current was being activated sheep cardiomyocytes were loaded with calcium sensitive probe Fluo4AM (Life Technologies) and using the same buffering conditions in the FluxOR assay for depolarization including the addition of 1mM calcium chloride. In the potassium free conditions there was a significant increase in fluorescence in the presence of LTUJH51B but not with LTUJH47B. In the potassium positive conditions there was no increase in fluorescence associated with calcium. These results suggest that LTUJH51B may be opening voltage dependent calcium channels in sheep cardiomyocytes.

Finally using isolated snail hearts (*Helix aspersa*) mounted onto an isometric force recording apparatus (PowerLab, AD Instruments), changes in heart rate and contractility were recorded. NS1643 had little effect on spontaneous heart rate or force production ($CaCl_2$ range 0 to 10mM). Both LTUJH47B and LTUJH51B decreased heart rate by 18% at 100⌈M but only LTUJH51B increased control force by 142%. It appears that both of these novel compounds exhibit weak hERG channel activity and LTUJH51B increases calcium fluxes in cardiac muscle.

Casis O, Olesen SP, Sanguinetti MC. (2006) *Mol Pharm* **69**, 658-665.
Grunnet M, Abbruzzese J, Sachse FB, Sanguinetti MC. (2011) *Mol Pharm* **79**, 1-9.
Heppell JT, Al-Rawi JM. (2015) *Med Chem Res* **24**, 2756-2769.

Exploring the role of hERG channels in breast cancers, using novel urea compounds that modulate hERG function

Sara Al-Rawi, Terri Meehan-Andrews and Jasim Al-Rawi

Increasing evidence indicates that ion channels are involved in the pathophysiology of cancer. The human ether-á-go-go-related gene (hERG) can be considered one of the most critical ion-channel encoding genes involved in the establishment, maintenance and progression of neoplastic growth. A benefit of focusing on modulation of ion channels in the biology of cancer cells is, that ion channel proteins can be easily accessed from extracellular environment which allows for lower drug doses which subsequently reduced side effects. Modulation of hERG channels, using a commercially available hERG channel modulator NS1643, inhibits proliferation and migration in breast cancer cells (MDA-MB-231 and MCF-7). Similar compounds have been developed, with varying levels of specificity to hERG channel function. Using in vitro breast cancer cell lines, we have explored the function of these compounds as potential anti-neoplastic therapeutics. The hERG channel activator NS1643 (1,3-bis-(2-hydroxy-5-trifluoromethyl-phenyl)-urea) caused inhibition of proliferation at concentration 10uM. Though it seems that the effect of the compound is more significant in MCF-7 cell line with gradual inhibition on cell number as the concentration increased [1]. Comparing the effect of these new compounds to NS1643, all compounds inhibited cell growth in MCF-7, and initiated cell cycle arrest at the G1 phase. But 2 compounds (JH28B and JH37B) also displayed this toxic effect in MDA cells, which was more significant than NS1643. Further exploration of these novel compounds is important as they appear to have higher efficacy and having similar benefits in different cancer types.

1. Perez-Neut, M., V.R. Rao, and S. Gentile, hERG1/Kv11.1 activation stimulates transcription of p21 (waf/cip) in breast cancer cells via a calcineurin-dependent mechanism. Oncotarget, 2016. 7(37): p. 58893-58902.

References

Afrasiabi, Emad, Marika Hietamäki, Tero Viitanen, Pramod Sukumaran, Nina Bergelin, and Kid Törnquist. 2010. 'Expression and significance of HERG (KCNH2) potassium channels in the regulation of MDA-MB-435S melanoma cell proliferation and migration', *Cellular Signalling*, 22: 57-64.

Ahmad, Irshad. 2017. 'An insight into the therapeutic potential of quinazoline derivatives as anticancer agents', *MedChemComm*, 8: 871-85.

Albini, Adriana, Giuseppina Pennesi, Francesco Donatelli, Rosaria Cammarota, Silvio De Flora, and Douglas M. Noonan. 2010. 'Cardiotoxicity of Anticancer Drugs: The Need for Cardio-Oncology and Cardio-Oncological Prevention', *JNCI: Journal of the National Cancer Institute*, 102: 14-25.

Alexander, S. P. H., A. Mathie, and J. A. Peters. 2011. 'ION CHANNELS', *British Journal of Pharmacology*, 164: S137-S74.

Alexander, Stephen PH, Jörg Striessnig, Eamonn Kelly, Neil V Marrion, John A Peters, Elena Faccenda, Simon D Harding, Adam J Pawson, Joanna L Sharman, Christopher Southan, Jamie A Davies, and CGTP Collaborators. 2017. 'THE CONCISE GUIDE TO PHARMACOLOGY 2017/18: Voltage-gated ion channels', British Journal of Pharmacology, 174: S160-S94.

An, Ki-Chan. 2016. 'Selective Estrogen Receptor Modulators', *Asian Spine Journal*, 10: 787-91.

Anderson, James D, Todd P Hansen, Paul W Lenkowski, Alison M Walls, Indrani M Choudhury, Hilary A Schenck, Mati Friehling, Genevieve M Höll, Manoj K Patel, and Robert A Sikes. 2003. 'Voltage-gated sodium channel blockers as cytostatic inhibitors of the androgen-independent prostate cancer cell line PC-3', *Molecular Cancer Therapeutics*, 2: 1149-54.

Andrews, Paul L. R., and John A. Rudd. 2016. 'The Physiology and Pharmacology of Nausea and Vomiting Induced by Anticancer Chemotherapy in Humans.' in Rudolph M. Navari (ed.), *Management of Chemotherapy-Induced Nausea and Vomiting: New Agents and New Uses of Current Agents* (Springer International Publishing: Cham).

Arcangeli, Annarosa, and Jason X. J. Yuan. 2011. 'American Journal of Physiology-Cell Physiology theme: ion channels and transporters in cancer', *American Journal of Physiology-Cell Physiology*, 301: C253-C54.

Asher, Viren, Raheela Khan, Averil Warren, Robert Shaw, Gerhard V Schalkwyk, Anish Bali, and Heidi M Sowter. 2010. 'The Eag potassium channel as a new prognostic marker in ovarian cancer', *Diagnostic Pathology*, 5: 78.

Asher, Viren, Averil Warren, Robert Shaw, Heidi Sowter, Anish Bali, and Raheela Khan. 2011. 'The role of Eag and HERG channels in cell proliferation and apoptotic cell death in SK-OV-3 ovarian cancer cell line', *Cancer Cell International*, 11: 6.

Azimi, I, S J Roberts-Thomson, and G R Monteith. 2014. 'Calcium influx pathways in breast cancer: opportunities for pharmacological intervention', British Journal of Pharmacology, 171: 945-60

B.C.NAustralia. 2019. 'Current Breast Cancer Statistics in Australia'. https://www.bcna.org.au/media/7111/bcna-2019-current-breast-cancer-statistics-in-australia-11jan2019.pdf.

Bane, Anita. 2013. 'Ductal carcinoma in situ: what the pathologist needs to know and why', *International Journal of Breast Cancer*, 2013: 914053-53.

Balse, Elise, David F. Steele, Hugues Abriel, Alain Coulombe, David Fedida, and Stéphane N. Hatem. 2012. 'Dynamic of Ion Channel Expression at the Plasma Membrane of Cardiomyocytes', Physiological reviews, 92: 1317-58.

Barnes, Nicholas M, Tim G Hales, Sarah CR Lummis, and John A Peters. 2009. 'The 5-HT3 receptor–the relationship between structure and function', *Neuropharmacology*, 56: 273-84.

Bartek, Jiri, and Jiri Lukas. 2001. 'Mammalian G1- and S-phase checkpoints in response to DNA damage', *Current Opinion in Cell Biology*, 13: 738-47.

Bartsch, Rupert, and Elisabeth Bergen. 2016. 'ASCO 2016: highlights in breast cancer', *memo-Magazine of European Medical Oncology*, 9: 211-14.

Becchetti, Andrea. 2011. 'Ion channels and transporters in cancer. 1. Ion channels and cell proliferation in cancer', *American Journal of Physiology-Cell Physiology*, 301: C255-C65.

Becker, Torben K., and Sai-Ching J. Yeung. 2010. 'Drug-induced QT interval prolongation in cancer patients', *Oncology Reviews*, 4: 223-32.

Belelli, Delia, Neil L Harrison, Jamie Maguire, Robert L Macdonald, Matthew C Walker, and David W Cope. 2009. 'Extrasynaptic GABAA receptors: form, pharmacology, and function', *Journal of Neuroscience*, 29: 12757-63.

Berridge, Michael J, Martin D Bootman, and H Llewelyn Roderick. 2003. 'Calcium: calcium signalling: dynamics, homeostasis and remodelling', *Nature Reviews Molecular Cell Biology*, 4: 517.

Bianchi, Laura, Barbara Wible, Annarosa Arcangeli, Maurizio Taglialatela, Ferdinando Morra, Pasqualina Castaldo, Olivia Crociani, Barbara Rosati, Laura Faravelli, Massimo Olivotto, and Enzo Wanke. 1998. 'herg Encodes a K+ Current Highly Conserved in Tumors of Different Histogenesis: A Selective Advantage for Cancer Cells?', *Cancer Research*, 58: 815-22.

Bielanska, J, J Hernandez-Losa, M Perez-Verdaguer, T Moline, R Somoza, S Cajal, E Condom, JC Ferreres, and A Felipe. 2009. 'Voltage-dependent potassium channels Kv1. 3 and Kv1. 5 in human cancer', *Current Cancer Drug Targets*, 9: 904-14.

Bilet, Arne, and Christiane K Bauer. 2012. 'Effects of the small molecule HERG activator NS1643 on Kv11. 3 channels', *PloS one*, 7: e50886.

Biolegends. 2018. "FITC Annexin V Apoptosis Detection Kit with PI.".

Biosciences, BD. 2011. "Detection of Apoptosis Using the BD Annexin V FITC Assay on the BD FACSVerse™ System.".

Blackiston, Douglas J, Kelly A McLaughlin, and Michael Levin. 2009. 'Bioelectric controls of cell proliferation: ion channels, membrane voltage and the cell cycle', *Cell Cycle*, 8: 3527-36.

Bonnet, Sébastien, Stephen L Archer, Joan Allalunis-Turner, Alois Haromy, Christian Beaulieu, Richard Thompson, Christopher T Lee, Gary D Lopaschuk, Lakshmi Puttagunta, and Sandra Bonnet. 2007. 'A mitochondria-K+ channel axis is suppressed in cancer and its normalization promotes apoptosis and inhibits cancer growth', *Cancer Cell*, 11: 37-51.

Bonnet, Sébastien, Stephen L. Archer, Joan Allalunis-Turner, Alois Haromy, Christian Beaulieu, Richard Thompson, Christopher T. Lee, Gary D. Lopaschuk, Lakshmi Puttagunta, Sandra Bonnet, Gwyneth Harry, Kyoko Hashimoto, Christopher J. Porter, Miguel A. Andrade, Bernard Thebaud, and Evangelos D. Michelakis. 2007. 'A Mitochondria-K+ Channel Axis Is Suppressed in Cancer and Its Normalization Promotes Apoptosis and Inhibits Cancer Growth', *Cancer Cell*, 11: 37-51.

Bortner, Carl D, and John A Cidlowski. 2007. 'Cell shrinkage and monovalent cation fluxes: role in apoptosis', *Archives of Biochemistry and Biophysics*, 462: 176-88.

Brackenbury, William J, Athina-Myrto Chioni, James KJ Diss, and Mustafa BA Djamgoz. 2007. 'The neonatal splice variant of Nav1. 5 potentiates in vitro invasive behaviour of MDA-MB-231 human breast cancer cells', *Breast Cancer Research and Treatment*, 101: 149-60.

Breuer, Eun-Kyoung, Daniela Fukushiro-Lopes, Annika Dalheim, Miranda Burnette, Jeremiah Zartman, Simon Kaja, Claire Wells, Loredana Campo, Kimberly J. Curtis, Ricardo Romero-Moreno, Laurie E. Littlepage, Glen L. Niebur, Kent Hoskins, Michael I. Nishimura, and Saverio Gentile. 2019. 'Potassium channel activity controls breast cancer metastasis by affecting β-catenin signaling', *Cell Death & Disease*, 10: 180.

Brito, Daniela A, Zhenye Yang, and Conly L Rieder. 2008. 'Microtubules do not promote mitotic slippage when the spindle assembly checkpoint cannot be satisfied', *The Journal of Cell Biology*, 182: 623-29.

Burstein, Harold J. 2005. 'The distinctive nature of HER2-positive breast cancers', *New England Journal of Medicine*, 353: 1652-54.

Casis, Oscar, Soren Peter Olesen, and Michael C Sanguinetti. 2005. 'Mechanism of action of NS1643, a novel hERG channel activator', *Molecular Pharmacology*.

Chandy, K George, Heike Wulff, Christine Beeton, Michael Pennington, George A Gutman, and Michael D Cahalan. 2004. 'K+ channels as targets for specific immunomodulation', *Trends in Pharmacological Sciences*, 25: 280-89.

Changeux, Jean-Pierre. 2010. 'Allosteric receptors: from electric organ to cognition', *Annual Review of Pharmacology and Toxicology*, 50: 1-38.

Chen, Jia-Nian, Xian-Fu Wang, Ting Li, De-Wen Wu, Xiao-Bo Fu, Guang-Ji Zhang, Xing-Can Shen, and Heng-Shan Wang. 2016. 'Design, synthesis, and biological evaluation of novel quinazolinyl-diaryl urea derivatives as potential anticancer agents', *European Journal of Medicinal Chemistry*, 107: 12-25.

Chen, Min, Huaping He, Shixing Zhan, Stan Krajewski, John C Reed, and Roberta A Gottlieb. 2001. 'Bid is cleaved by calpain to an active fragment in vitro and during myocardial ischemia/reperfusion', *Journal of Biological Chemistry*, 276: 30724-28.

Chen, Shu-zhen, Min Jiang, and Yong-su Zhen. 2005. 'HERG K+ channel expression-related chemosensitivity in cancer cells and its modulation by erythromycin', *Cancer Chemotherapy and Pharmacology*, 56: 212-20.

Cheng, Emily H-Y, Tatiana V Sheiko, Jill K Fisher, William J Craigen, and Stanley J Korsmeyer. 2003. 'VDAC2 inhibits BAK activation and mitochondrial apoptosis', *Science*, 301: 513-17.

Cherubini, A, GL Taddei, O Crociani, M Paglierani, AM Buccoliero, L Fontana, I Noci, P Borri, E Borrani, and M Giachi. 2000. 'HERG potassium channels are more frequently expressed in human endometrial cancer as compared to non-cancerous endometrium', *British Journal Of Cancer*, 83: 1722.

Cherubini, A., G. L. Taddei, O. Crociani, M. Paglierani, A. M. Buccoliero, L. Fontana, I. Noci, P. Borri, E. Borrani, M. Giachi, A. Becchetti, B. Rosati, E. Wanke, M. Olivotto, and A. Arcangeli. 2000. 'HERG potassium channels are more frequently expressed in human endometrial cancer as compared to non-cancerous endometrium', *British Journal Of Cancer*, 83: 1722.

Chittajallu, R, Y Chen, H Wang, X Yuan, CA Ghiani, T Heckman, CJ McBain, and V Gallo. 2002. 'Regulation of Kv1 subunit expression in oligodendrocyte progenitor cells and their role in G1/S phase progression of the cell cycle', *Proceedings of the National Academy of Sciences*, 99: 2350-55.

Choi, Murim, Ute I Scholl, Peng Yue, Peyman Björklund, Bixiao Zhao, Carol Nelson-Williams, Weizhen Ji, Yoonsang Cho, Aniruddh Patel, and Clara J Men. 2011. 'K+ channel mutations in adrenal aldosterone-producing adenomas and hereditary hypertension', *Science*, 331: 768-72.

Comes, Nuria, Antonio Serrano-Albarrás, Jesusa Capera, Clara Serrano-Novillo, Enric Condom, Santiago Ramón y Cajal, Joan Carles Ferreres, and Antonio Felipe. 2015. 'Involvement of potassium channels in the progression of cancer to a more malignant phenotype', *Biochimica et Biophysica Acta (BBA) - Biomembranes*, 1848: 2477-92.

Cone, Clarence D. 1969. 'SECTION OF BIOLOGICAL AND MEDICAL SCIENCES: ELECTROOSMOTIC INTERACTIONS ACCOMPANYING MITOSIS INITIATION IN SARCOMA CELLS IN VITRO', *Transactions of the New York Academy of Sciences*, 31: 404-27.

Crociani, Olivia, Leonardo Guasti, Manuela Balzi, Andrea Becchetti, Enzo Wanke, Massimo Olivotto, Randy S Wymore, and Annarosa Arcangeli. 2003. 'Cell cycle-dependent expression of HERG1 and HERG1B isoforms in tumor cells', *Journal of Biological Chemistry*, 278: 2947-55.

Crociani, Olivia, Elena Lastraioli, Luca Boni, Serena Pillozzi, Maria Raffaella Romoli, Massimo D'Amico, Matteo Stefanini, Silvia Crescioli, Antonio Taddei, and Lapo Bencini. 2014. 'hERG1 channels regulate VEGF-A secretion in human gastric cancer: clinicopatholgial correlations and therapeutical implications', *Clinical Cancer Research*: clincanres. 2633.013.

Crociani, Olivia, Elena Lastraioli, Luca Boni, Serena Pillozzi, Maria Raffaella Romoli, Massimo D'Amico, Matteo Stefanini, Silvia Crescioli, Antonio Taddei, Lapo Bencini, Marco Bernini, Marco Farsi, Stefania Beghelli, Aldo Scarpa, Luca Messerini, Anna Tomezzoli, Carla Vindigni, Paolo Morgagni, Luca Saragoni, Elisa Giommoni, Silvia Gasperoni, Francesco Di Costanzo, Franco Roviello, Giovanni De Manzoni, Paolo Bechi, and Annarosa Arcangeli. 2014. 'hERG1 Channels

Regulate VEGF-A Secretion in Human Gastric Cancer: Clinicopathological Correlations and Therapeutical Implications', *Clinical Cancer Research*, 20: 1502-12.

Csapo, Melinda, and Liviu Lazar. 2014. 'Chemotherapy-induced cardiotoxicity: Pathophysiology and prevention', *Clujul Medical*, 87: 135.

Cui, Guohui, Wenxiu Shu, Qing Wu, and Yan Chen. 2009. 'Effect of Gambogic acid on the regulation of hERG channel in K562 cells in vitro', *Journal of Huazhong University of Science and Technology [Medical Sciences]*, 29: 540-45.

Curigliano, G., G. Spitaleri, F. de Braud, D. Cardinale, C. Cipolla, M. Civelli, N. Colombo, A. Colombo, M. Locatelli, and A. Goldhirsch. 2009. 'QTc prolongation assessment in anticancer drug development: clinical and methodological issues', *Ecancermedicalscience*, 3: 130-30.

Curry, Merril C, Amelia A Peters, Paraic A Kenny, Sarah J Roberts-Thomson, and Gregory R Monteith. 2013. 'Mitochondrial calcium uniporter silencing potentiates caspase-independent cell death in MDA-MB-231 breast cancer cells', *Biochemical and Biophysical Research Communications*, 434: 695-700.

Davies, Eleri Lloyd. 2016. 'Breast cancer', *Medicine*, 44: 42-46.

Davis, Gary C, Yali Kong, Mikell Paige, Zhang Li, Ellen C Merrick, Todd Hansen, Simeng Suy, Kan Wang, Sivanesan Dakshanamurthy, and Antoinette Cordova. 2012. 'Asymmetric synthesis and evaluation of a hydroxyphenylamide voltage-gated sodium channel blocker in human prostate cancer xenografts', *Bioorganic & Medicinal Chemistry*, 20: 2180-88.

de Bakker, Jacques MT, and Harold VM van Rijen. 2010. 'Cardiac Action Potentials, Ion Channels, and Gap Junctions.' in, *Cardiac Electrophysiology Methods and Models* (Springer).

Desiniotis, Andreas, and Natasha Kyprianou. 2011. 'Advances in the design and synthesis of prazosin derivatives over the last ten years', *Expert Opinion on Therapeutic Targets*, 15: 1405-18.

Devita Jr, Vincent T, Theodore S Lawrence, and Steven A Rosenberg. 2015. *DeVita, Hellman, and Rosenberg's cancer: principles & practice of oncology* (Lippincott Williams & Wilkins).

Ding, Xiang-Wu, Wen-Bin Yang, Shan Gao, Wei Wang, Zheng Li, Wang-Ming Hu, Jian-Jun Li, and He-Sheng Luo. 2010. 'Prognostic significance of hERG1 expression in gastric cancer', *Digestive Diseases and Sciences*, 55: 1004-10.

Ding, Xiang-Wu, He-Sheng Luo, Bing Luo, Dong-Qiang Xu, and Shan Gao. 2008. 'Overexpression of hERG1 in resected esophageal squamous cell carcinomas: a marker for poor prognosis', *Journal of Surgical Oncology*, 97: 57-62.

Djamgoz, Mustafa B. A., R. Charles Coombes, and Albrecht Schwab. 2014. 'Ion transport and cancer: from initiation to metastasis', *Philosophical Transactions of the Royal Society B: Biological Sciences*, 369.

Dolci, Alberto, Roberto Dominici, Daniela Cardinale, Maria T Sandri, and Mauro Panteghini. 2008. 'Biochemical markers for prediction of chemotherapy-induced cardiotoxicity: systematic review of the literature and recommendations for use', *American Journal of Clinical Pathology*, 130: 688-95.

Downward, Julian. 2003. 'Targeting RAS signalling pathways in cancer therapy', *Nature Reviews Cancer*, 3: 11-22.

Ducroq, Joffrey, H Moha ou Maati, S Guilbot, S Dilly, E Laemmel, C Pons-Himbert, JF Faivre, P Bois, O Stücker, and M Le Grand. 2010. 'Dexrazoxane protects the heart from acute doxorubicin-induced QT prolongation: a key role for IKs', *British Journal of Pharmacology*, 159: 93-101.

Duprez, Linde, Ellen Wirawan, Tom Vanden Berghe, and Peter Vandenabeele. 2009. 'Major cell death pathways at a glance', *Microbes and infection*, 11: 1050-62.

Ellis, Paul A, Gloria Saccani-Jotti, Robert Clarke, Stephen RD Johnston, Elizabeth Anderson, Anthony Howell, Roger A'hern, Janine Salter, Simone Detre, and Robert Nicholson. 1997. 'Induction of apoptosis by tamoxifen and ICI 182780 in primary breast cancer', *International Journal of Cancer*, 72: 608-13.

Emmi, Adriana, H Jurgen Wenzel, Philip A Schwartzkroin, Maurizio Taglialatela, Pasqualina Castaldo, Laura Bianchi, Jeanne Nerbonne, Gail A Robertson, and Damir Janigro. 2000. 'Do Glia Have

Heart? Expression and Functional Role forEther-A-Go-Go Currents in Hippocampal Astrocytes', *Journal of Neuroscience*, 20: 3915-25.

Evan, Gerard, and Trevor Littlewood. 1998. 'A matter of life and cell death', *Science*, 281: 1317-22.

Fabiato, Alexandre. 1985. 'Simulated calcium current can both cause calcium loading in and trigger calcium release from the sarcoplasmic reticulum of a skinned canine cardiac Purkinje cell', *The Journal of General Physiology*, 85: 291-320.

Faraj, Fadhil Lafta, Maryam Zahedifard, Mohammadjavad Paydar, Chung Yeng Looi, Nazia Abdul Majid, Hapipah Mohd Ali, Noraini Ahmad, Nura Suleiman Gwaram, and Mahmood Ameen Abdulla. 2014. 'Synthesis, Characterization, and Anticancer Activity of New Quinazoline Derivatives against MCF-7 Cells', *The Scientific World Journal*, 2014: 15.

Farrelly, AM, S Ro, BP Callaghan, MA Khoyi, Neal Fleming, B Horowitz, KM Sanders, and KD Keef. 2003. 'Expression and function of KCNH2 (HERG) in the human jejunum', *American Journal of Physiology-Gastrointestinal and Liver Physiology*, 284: G883-G95.

Fearon, Eric R. 1997. 'Human cancer syndromes: clues to the origin and nature of cancer', *Science*, 278: 1043-50.

Feng, Jin, Junbo Yu, Xiaolin Pan, Zengliang Li, Zheng Chen, Wenjie Zhang, Bin Wang, Li Yang, Hao Xu, and Guoxin Zhang. 2014. 'HERG1 functions as an oncogene in pancreatic cancer and is downregulated by miR-96', *Oncotarget*, 5: 5832.

Fijnvandraat, Arnoud C, Antoni CG van Ginneken, Piet AJ de Boer, Jan M Ruijter, Vincent M Christoffels, Antoon FM Moorman, and Ronald H Lekanne Deprez. 2003. 'Cardiomyocytes derived from embryonic stem cells resemble cardiomyocytes of the embryonic heart tube', *Cardiovascular Research*, 58: 399-409.

Fornari, Frank A, Joyce K Randolph, Jack C Yalowich, Mary K Ritke, and David A Gewirtz. 1994. 'Interference by doxorubicin with DNA unwinding in MCF-7 breast tumor cells', *Molecular Pharmacology*, 45: 649-56.

Foster, Irene. 2008. 'Cancer: A cell cycle defect', *Radiography*, 14: 144-49.

Fraser, Scott P, James KJ Diss, Athina-Myrto Chioni, Maria E Mycielska, Huiyan Pan, Rezan F Yamaci, Filippo Pani, Zuzanna Siwy, Monika Krasowska, and Zbigniew Grzywna. 2005. 'Voltage-gated sodium channel expression and potentiation of human breast cancer metastasis', *Clinical Cancer Research*, 11: 5381-89.

Fraser, Scott P, Iley Ozerlat-Gunduz, William J Brackenbury, Elizabeth M Fitzgerald, Thomas M Campbell, R Charles Coombes, and Mustafa BA Djamgoz. 2014. 'Regulation of voltage-gated sodium channel expression in cancer: hormones, growth factors and auto-regulation', *Philosophical Transactions of the Royal Society B: Biological Sciences*, 369: 20130105.

Freedman, B. D., M. A. Price, and C. J. Deutsch. 1992. 'Evidence for voltage modulation of IL-2 production in mitogen-stimulated human peripheral blood lymphocytes', *The Journal of Immunology*, 149: 3784.

Fuentes-Prior, Pablo, and Guy S Salvesen. 2004. 'The protein structures that shape caspase activity, specificity, activation and inhibition', *Biochemical Journal*, 384: 201-32.

Fukushiro-Lopes, Daniela F, Alexandra D Hegel, Vidhya Rao, Debra Wyatt, Andrew Baker, Eun-Kyoung Breuer, Clodia Osipo, Jeremiah J Zartman, Miranda Burnette, and Simon Kaja. 2018. 'Preclinical study of a Kv11. 1 potassium channel activator as antineoplastic approach for breast cancer', *Oncotarget*, 9: 3321.

Furukawa, Motonobu, Masuhiro Nishimura, Daisuke Ogino, Ryoji Chiba, Iwao Ikai, Nobuhiko Ueda, Shinsaku Naito, Shunji Kuribayashi, Mohsen A Moustafa, and Takafumi Uchida. 2004. 'Cytochrome p450 gene expression levels in peripheral blood mononuclear cells in comparison with the liver', *Cancer Science*, 95: 520-29.

Ganapathi, Sindura B, Mark Kester, and Keith S Elmslie. 2009. 'State-dependent block of HERG potassium channels by R-roscovitine: implications for cancer therapy', *American Journal of Physiology-Cell Physiology*, 296: C701-C10.

Gavrilova-Ruch, O, K Schönherr, G Gessner, R Schönherr, T Klapperstück, W Wohlrab, and SH Heinemann. 2002. 'Effects of imipramine on ion channels and proliferation of IGR1 melanoma cells', *The Journal of Membrane Biology*, 188: 137-49.

Georgey, Hanan, Nagwa Abdel-Gawad, and Safinaz Abbas. 2008. 'Synthesis and anticonvulsant activity of some quinazolin-4-(3H)-one derivatives', *Molecules*, 13: 2557-69.

Gewies, Andreas. 2003. 'Introduction to apoptosis', *Apo Review*, 3: 1-26.

Ghorab, Mostafa, Mansour Alsaid, Mohammed Al-Dosari, Marwa El-Gazzar, and Mohammad Parvez. 2016. 'Design, synthesis and anticancer evaluation of novel quinazoline-sulfonamide hybrids', *Molecules*, 21: 189.

Gil-Parrado, Shirley, Amaury Fernández-Montalván, Irmgard Assfalg-Machleidt, Oliver Popp, Felix Bestvater, Andreas Holloschi, Tobias A Knoch, Ennes A Auerswald, Katherine Welsh, and John C Reed. 2002. 'Ionomycin-activated calpain triggers apoptosis A probable role for Bcl-2 family members', *Journal of Biological Chemistry*, 277: 27217-26.

Giorgi, Carlotta, Federica Baldassari, Angela Bononi, Massimo Bonora, Elena De Marchi, Saverio Marchi, Sonia Missiroli, Simone Patergnani, Alessandro Rimessi, and Jan M Suski. 2012. 'Mitochondrial Ca2+ and apoptosis', *Cell Calcium*, 52: 36-43.

Glassmeier, Günter, Kathrin Hempel, Iris Wulfsen, Christiane K Bauer, Udo Schumacher, and Jürgen R Schwarz. 2012. 'Inhibition of HERG1 K+ channel protein expression decreases cell proliferation of human small cell lung cancer cells', *Pflügers Archiv-European Journal of Physiology*, 463: 365-76.

Goh, Chih Wan, Jiayi Wu, Shuning Ding, Caijin Lin, Xiaosong Chen, Ou Huang, Weiguo Chen, Yafen Li, Kunwei Shen, and Li Zhu. 2019. 'Invasive ductal carcinoma with coexisting ductal carcinoma in situ (IDC/DCIS) versus pure invasive ductal carcinoma (IDC): a comparison of clinicopathological characteristics, molecular subtypes, and clinical outcomes', *Journal of Cancer Research and Clinical Oncology*.

Gong, Jian-Hua, Xiu-Jun Liu, Bo-Yang Shang, Shu-Zhen Chen, and Yong-Su Zhen. 2010. 'HERG K+ channel related chemosensitivity to sparfloxacin in colon cancer cells', *Oncology Reports*, 23: 1747-56.

Goodman, Michelle. 1989. "Managing the side effects of chemotherapy." In *Seminars in Oncology Nursing*, 29-52.

Greenwood, Iain A, SY Yeung, RM Tribe, and S Ohya. 2009. 'Loss of functional K+ channels encoded by ether-a-go-go-related genes in mouse myometrium prior to labour onset', *The Journal of Physiology*, 587: 2313-26.

Guasti, Leonardo, Olivia Crociani, Elisa Redaelli, Serena Pillozzi, Simone Polvani, Marika Masselli, Tommaso Mello, Andrea Galli, Amedeo Amedei, and Randy S Wymore. 2008. 'Identification of a posttranslational mechanism for the regulation of hERG1 K+ channel expression and hERG1 current density in tumor cells', *Molecular and Cellular Biology*, 28: 5043-60.

Guo, D. Q., H. Zhang, S. J. Tan, and Y. C. Gu. 2014. 'Nifedipine promotes the proliferation and migration of breast cancer cells', *PloS one*, 9: e113649.

Habela, Christa W, Nola Jean Ernest, Amanda F Swindall, and Harald Sontheimer. 2009. 'Chloride accumulation drives volume dynamics underlying cell proliferation and migration', *Journal of Neurophysiology*, 101: 750-57.

Habela, Christa W, and Harald Sontheimer. 2007. 'Cytoplasmic volume condensation is an integral part of mitosis', *Cell Cycle*, 6: 1613-20.

Hajnóczky, György, György Csordás, Sudipto Das, Cecilia Garcia-Perez, Masao Saotome, Soumya Sinha Roy, and Muqing Yi. 2006. 'Mitochondrial calcium signalling and cell death: approaches for assessing the role of mitochondrial Ca2+ uptake in apoptosis', *Cell Calcium*, 40: 553-60.

Hall, AG, and MJ Tilby. 1992. 'Mechanisms of action of, and modes of resistance to, alkylating agents used in the treatment of haematological malignancies', *Blood Reviews*, 6: 163-73.

Hammadi, Mehdi, Valérie Chopin, Fabrice Matifat, Isabelle Dhennin-Duthille, Maud Chasseraud, Henri Sevestre, and Halima Ouadid-Ahidouch. 2012. 'Human ether à-gogo K+ channel 1

(hEag1) regulates MDA-MB-231 breast cancer cell migration through Orai1-dependent calcium entry', *Journal of Cellular Physiology*, 227: 3837-46.

Hanahan, Douglas, and Robert A Weinberg. 2000. 'The hallmarks of cancer', *Cell*, 100: 57-70.

Hanna, Amy D, Alexander Lam, Chris Thekkedam, Hermia Willemse, Angela F Dulhunty, and Nicole A Beard. 2017. 'The anthracycline metabolite doxorubicinol abolishes RyR2 sensitivity to physiological changes in luminal Ca2+ through an interaction with calsequestrin', *Molecular Pharmacology*, 92: 576-87.

Hansen, Rie Schultz, Thomas Goldin Diness, Torsten Christ, Joachim Demnitz, Ursula Ravens, Søren-Peter Olesen, and Morten Grunnet. 2006. 'Activation of Human ether-a-go-go-Related Gene Potassium Channels by the Diphenylurea 1,3-Bis-(2-hydroxy-5-trifluoromethyl-phenyl)-urea (NS1643)', *Molecular Pharmacology*, 69: 266-77.

Hansen, Rie Schultz, Thomas Goldin Diness, Torsten Christ, Erich Wettwer, Ursula Ravens, Søren-Peter Olesen, and Morten Grunnet. 2006. 'Biophysical characterization of the new human ether-a-go-go-related gene channel opener NS3623 [N-(4-bromo-2-(1H-tetrazol-5-yl)-phenyl)-N'-(3'-trifluoromethylphenyl) urea]', *Molecular Pharmacology*, 70: 1319-29.

Hartwell, Leland H, and Michael B Kastan. 1994. 'Cell cycle control and cancer', *Science*, 266: 1821-28.

Hattori, Hiroyuki, Masahiko Kuroda, Tsuyoshi Ishida, Koutarou Shinmura, Shuzou Nagai, Kiyoshi Mukai, and Atsuhiro Imakiire. 2004. 'Human DNA damage checkpoints and their relevance to soft tissue sarcoma', *Pathology International*, 54: 26-31.

Helix, N, D Strøbaek, BH Dahl, and P Christophersen. 2003. 'Inhibition of the endogenous volume-regulated anion channel (VRAC) in HEK293 cells by acidic di-aryl-ureas', *The Journal of Membrane Biology*, 196: 83-94.

Hemmerlein, Bernhard, Rüdiger M Weseloh, Fernanda Mello de Queiroz, Hendrik Knötgen, Araceli Sánchez, María E Rubio, Sabine Martin, Tessa Schliephacke, Marc Jenke, and Walter Stühmer. 2006. 'Overexpression of Eag1 potassium channels in clinical tumours', *Molecular Cancer*, 5: 41.

Heppell, Jacob T, and Jasim MA Al-Rawi. 2015. 'Synthesis, antibacterial, and DNA-PK evaluation of some novel 6-fluoro-7-(cyclic amino)-2-(thioxo or oxo)-3-substituted quinazolin-4-ones as structural analogues of quinolone and quinazolin-2, 4-dione antibiotics', *Medicinal Chemistry Research*, 24: 2756-69.

Higa, Gerald M., and Jame Abraham. 2007. 'Lapatinib in the treatment of breast cancer', *Expert Review of Anticancer Therapy*, 7: 1183-92.

Hille, Bertil. 2001. *Ion channels of excitable membranes* (Sinauer Sunderland, MA).

Hoelder, Swen, Paul A. Clarke, and Paul Workman. 2012. 'Discovery of small molecule cancer drugs: Successes, challenges and opportunities', *Molecular Oncology*, 6: 155-76.

Hong, Sen, Miaomiao Bi, Lei Wang, Zhenhua Kang, Limian Ling, and Chunyan Zhao. 2015. 'CLC-3 channels in cancer', *Oncology Reports*, 33: 507-14.

Huang, Hai, Michael K. Pugsley, Bernard Fermini, Michael J. Curtis, John Koerner, Michael Accardi, and Simon Authier. 2017. 'Cardiac voltage-gated ion channels in safety pharmacology: Review of the landscape leading to the CiPA initiative', *Journal of Pharmacological and Toxicological Methods*, 87: 11-23.

Huang, Xi, and Lily Yeh Jan. 2014. 'Targeting potassium channels in cancer', *The Journal of Cell Biology*, 206: 151-62.

Hui, Hongxiang, Manory A Fernando, and Anthony P Heaney. 2008. 'The α1-adrenergic receptor antagonist doxazosin inhibits EGFR and NF-κB signalling to induce breast cancer cell apoptosis', *European Journal of Cancer*, 44: 160-66.

Iorio, Jessica, Icro Meattini, Simonetta Bianchi, Marco Bernini, Virginia Maragna, Luca Dominici, Donato Casella, Vania Vezzosi, Lorenzo Orzalesi, Jacopo Nori, Lorenzo Livi, Annarosa Arcangeli, and Elena Lastraioli. 2018. 'hERG1 channel expression associates with molecular subtypes and prognosis in breast cancer', *Cancer Cell International*, 18: 93.

Ismail, Mohamed AH, Stewart Barker, Dalal A Abou El Ella, Khaled AM Abouzid, Rabab A Toubar, and Matthew H Todd. 2006. 'Design and synthesis of new tetrazolyl-and carboxy-biphenylylmethyl-quinazolin-4-one derivatives as angiotensin II AT1 receptor antagonists', *Journal of Medicinal Chemistry*, 49: 1526-35.

Ismail, Rania S. M., Nasser S. M. Ismail, Sahar Abuserii, and Dalal A. Abou El Ella. 2016. 'Recent advances in 4-aminoquinazoline based scaffold derivatives targeting EGFR kinases as anticancer agents', *Future Journal of Pharmaceutical Sciences*, 2: 9-19.

Jahchan, Nadine S, Joel T Dudley, Pawel K Mazur, Natasha Flores, Dian Yang, Alec Palmerton, Anne-Flore Zmoos, Dedeepya Vaka, Kim QT Tran, and Margaret Zhou. 2013. 'A drug repositioning approach identifies tricyclic antidepressants as inhibitors of small cell lung cancer and other neuroendocrine tumors', *Cancer Discovery*, 3: 1364-77.

Jarvis, Michael F, and Baljit S Khakh. 2009. 'ATP-gated P2X cation-channels', *Neuropharmacology*, 56: 208-15.

Jehle, J, PA Schweizer, HA Katus, and D Thomas. 2011. 'Novel roles for hERG K+ channels in cell proliferation and apoptosis', *Cell Death & Disease*, 2: e193.

Jentsch, Thomas J., Christian A. Hübner, and Jens C. Fuhrmann. 2004. 'Ion channels: Function unravelled by dysfunction', *Nature Cell Biology*, 6: 1039.

Jia, Xiaoling, Jingyun Yang, Wei Song, Ping Li, Xia Wang, Changdong Guan, Liu Yang, Yan Huang, Xianghui Gong, Meili Liu, Lisha Zheng, and Yubo Fan. 2013. 'Involvement of large conductance Ca2+-activated K+ channel in laminar shear stress-induced inhibition of vascular smooth muscle cell proliferation', *Pflügers Archiv - European Journal of Physiology*, 465: 221-32.

Jung, Min-Yong. 2016. 'HERG and STAT1 Interactions in Estrogen Receptor Positive and Estrogen Receptor Negative Human Breast Cancers', University of Saskatchewan.

Kale, Vijay Pralhad, Shantu G. Amin, and Manoj K. Pandey. 2015. 'Targeting ion channels for cancer therapy by repurposing the approved drugs', *Biochimica et Biophysica Acta (BBA) - Biomembranes*, 1848: 2747-55.

Katz, Arnold M. 2010. *Physiology of the Heart* (Lippincott Williams & Wilkins).

Kawashiro, Takashi, Kouwa Yamashita, Xue-Jun Zhao, Eriko Koyama, Masayoshi Tani, Kan Chiba, and Takashi Ishizaki. 1998. 'A Study on the Metabolism of Etoposide and Possible Interactions with Antitumor or Supporting Agents by Human Liver Microsomes', *Journal of Pharmacology and Experimental Therapeutics*, 286: 1294.

Kim, Peter Y., and Michael S. Ewer. 2014. 'Chemotherapy and QT Prolongation: Overview With Clinical Perspective', *Current Treatment Options in Cardiovascular Medicine*, 16: 303.

Klabunde, Richard. 2011. *Cardiovascular physiology concepts* (Lippincott Williams & Wilkins).

Kleger, Alexander, and Stefan Liebau. 2011. 'Calcium-Activated Potassium Channels, Cardiogenesis of Pluripotent Stem Cells, and Enrichment of Pacemaker-Like Cells', *Trends in Cardiovascular Medicine*, 21: 74-83.

Kondratskyi, Artem, Kateryna Kondratska, Roman Skryma, and Natalia Prevarskaya. 2015. 'Ion channels in the regulation of apoptosis', *Biochimica et Biophysica Acta (BBA)-Biomembranes*, 1848: 2532-46.

Krishnan, SK, S Ganguly, R Veerasamy, and B Jan. 2011. 'Synthesis, antiviral and cytotoxic investigation of 2-phenyl-3-substituted quinazolin-4 (3H)-ones', *Eur Rev Med Pharmacol Sci*, 15: 673-81.

Kroemer, Guido, Lorenzo Galluzzi, and Catherine Brenner. 2007. 'Mitochondrial membrane permeabilization in cell death', *Physiological Reviews*, 87: 99-163.

Krysko, DV, and Peter Vandenabeele. 2008. 'From regulation of dying cell engulfment to development of anti-cancer therapy', *Cell Death and Differentiation*, 15: 29.

Kumar, Simi, Ravi Marfatia, Susan Tannenbaum, Clifford Yang, and Erick Avelar. 2012. 'Doxorubicin-induced cardiomyopathy 17 years after chemotherapy', *Texas Heart Institute Journal*, 39: 424.

Kunzelmann, Karl. 2005. 'Ion channels and cancer', *The Journal of Membrane Biology*, 205: 159.

Kuroiwa, Kenta, Hirosuke Ishii, Kenji Matsuno, Akira Asai, and Yumiko Suzuki. 2015. 'Synthesis and structure–activity relationship study of 1-phenyl-1-(quinazolin-4-yl) ethanols as anticancer agents', *ACS medicinal chemistry letters*, 6: 287-91.

Kurokawa, Junko, Masaji Tamagawa, Nobuhiro Harada, Shin-Ichiro Honda, Chang-Xi Bai, Haruaki Nakaya, and Tetsushi Furukawa. 2008. 'Acute effects of oestrogen on the guinea pig and human IKr channels and drug-induced prolongation of cardiac repolarization', *The Journal of Physiology*, 586: 2961-73.

Kwon, Youngjoo. 2016. 'Mechanism-based management for mucositis: option for treating side effects without compromising the efficacy of cancer therapy', *OncoTargets and therapy*, 9: 2007-16.

Kyprianou, Natasha, and Cynthia M Benning. 2000. 'Suppression of human prostate cancer cell growth by α1-adrenoceptor antagonists doxazosin and terazosin via induction of apoptosis', *Cancer Research*, 60: 4550-55.

LaCasse, E. C., D. J. Mahoney, H. H. Cheung, S. Plenchette, S. Baird, and R. G. Korneluk. 2008. 'IAP-targeted therapies for cancer', *Oncogene*, 27: 6252.

Lacerda, Antonio E, Yuri A Kuryshev, Yuan Chen, Muthukrishnan Renganathan, Heather Eng, Sanjay J Danthi, James W Kramer, Tianen Yang, and Arthur M Brown. 2008. 'Alfuzosin delays cardiac repolarization by a novel mechanism', *Journal of Pharmacology and Experimental Therapeutics*, 324: 427-33.

Lansu, K, and S Gentile. 2013. 'Potassium channel activation inhibits proliferation of breast cancer cells by activating a senescence program', *Cell Death & Disease*, 4: e652.

Laskey, RA, MP Fairman, and JJ Blow. 1989. 'S phase of the cell cycle', *Science*, 246: 609-14.

Lastraioli, E, G Perrone, A Sette, A Fiore, O Crociani, S Manoli, M D'amico, M Masselli, J Iorio, and M Callea. 2015. 'hERG1 channels drive tumour malignancy and may serve as prognostic factor in pancreatic ductal adenocarcinoma', *British Journal Of Cancer*, 112: 1076.

Lastraioli, E., A. Taddei, L. Messerini, C. E. Comin, M. Festini, M. Giannelli, A. Tomezzoli, M. Paglierani, G. Mugnai, G. De Manzoni, P. Bechi, and A. Arcangeli. 2006. 'hERG1 channels in human esophagus: Evidence for their aberrant expression in the malignant progression of Barrett's esophagus', *Journal of Cellular Physiology*, 209: 398-404.

Lastraioli, Elena, Lapo Bencini, Elisa Bianchini, Maria Raffaella Romoli, Olivia Crociani, Elisa Giommoni, Luca Messerini, Silvia Gasperoni, Renato Moretti, and Francesco Di Costanzo. 2012. 'hERG1 channels and Glut-1 as independent prognostic indicators of worse outcome in stage I and II colorectal cancer: a pilot study', *Translational Oncology*, 5: 105-12.

Lastraioli, Elena, Leonardo Guasti, Olivia Crociani, Simone Polvani, Giovanna Hofmann, Harry Witchel, Lapo Bencini, Massimo Calistri, Luca Messerini, and Marco Scatizzi. 2004. 'herg1 gene and HERG1 protein are overexpressed in colorectal cancers and regulate cell invasion of tumor cells', *Cancer Research*, 64: 606-11.

Lastraioli, Elena, Jessica Iorio, and Annarosa Arcangeli. 2015. 'Ion channel expression as promising cancer biomarker', *Biochimica et Biophysica Acta (BBA) - Biomembranes*, 1848: 2685-702.

Lastraioli, Elena, Antonio Taddei, Luca Messerini, Camilla E Comin, Mara Festini, Matteo Giannelli, Anna Tomezzoli, Milena Paglierani, Gabriele Mugnai, and Giovanni De Manzoni. 2006. 'hERG1 channels in human esophagus: evidence for their aberrant expression in the malignant progression of Barrett's esophagus', *Journal of Cellular Physiology*, 209: 398-404.

Le, Xiao-Feng, Franz Pruefer, and Robert C Bast. 2005. 'HER2-targeting antibodies modulate the cyclin-dependent kinase inhibitor p27Kip1 via multiple signaling pathways', *Cell Cycle*, 4: 87-95.

Leanza, L., M. Zoratti, E. Gulbins, and I. Szabo. 2014. 'Mitochondrial ion channels as oncological targets', *Oncogene*, 33: 5569.

Lee, An-Sheng, and Ming-Jai Su. 2008. 'Comparison of the cardiac effects between quinazoline-based α 1-adrenoceptor antagonists on occlusion–reperfusion injury', *Journal of Biomedical Science*, 15: 239-49.

Lee, Jonathan M, and Alan Bernstein. 1995. 'Apoptosis, cancer and the p53 tumour suppressor gene', *Cancer and Metastasis Reviews*, 14: 149-61.

Lee, Susanna ST, Jeroen TM Buters, Thierry Pineau, Pedro Fernandez-Salguero, and Frank J Gonzalez. 1996. 'Role of CYP2E1 in the hepatotoxicity of acetaminophen', *Journal of Biological Chemistry*, 271: 12063-67.

Lewis, David FV. 2003. 'Human cytochromes P450 associated with the phase 1 metabolism of drugs and other xenobiotics: a compilation of substrates and inhibitors of the CYP1, CYP2 and CYP3 families', *Current Medicinal Chemistry*, 10: 1955-72.

Li, M, B Wang, and W Lin. 2008. 'Cl-channel blockers inhibit cell proliferation and arrest the cell cycle of human ovarian cancer cells', *European Journal of Gynaecological Oncology*, 29: 267.

Li, M, DB Wu, and J Wang. 2013. 'Effects of volume-activated chloride channels on the invasion and migration of human endometrial cancer cells', *European Journal of Gynaecological Oncology*, 34: 60-64.

LifeTechnologies. 2012. "Vivid CYP450 Screening Kits User Guide ".

LifeTechnologies. 2014. "FluxOR™ Potassium Ion Channel Assay." .

Lin, Ssu-Chia, Shih-Chieh Chueht, Che-Jen Hsiao, Tsia-Kun Li, Tzu-Hsuan Chen, Cho-Hwa Liao, Ping-Chiang Lyu, and Jih-Hwa Guh. 2007. 'Prazosin displays anticancer activity against human prostate cancers: targeting DNA, cell cycle', *Neoplasia*, 9: 830-39.

Litan, Alisa, and Sigrid A. Langhans. 2015. "Cancer as a channelopathy: ion channels and pumps in tumor development and progression." In *Frontiers in Cellular Neuroscience*, 86.

Lodge, David. 2009. 'The history of the pharmacology and cloning of ionotropic glutamate receptors and the development of idiosyncratic nomenclature', *Neuropharmacology*, 56: 6-21.

London, Barry, Matthew C Trudeau, Kimberly P Newton, Anita K Beyer, Neal G Copeland, Debra J Gilbert, Nancy A J enkins, Carol A Satler, and Gail A Robertson. 1997. 'Two isoforms of the mouse ether-a-go-go–related gene coassemble to form channels with properties similar to the rapidly activating component of the cardiac delayed rectifier K+ current', *Circulation Research*, 81: 870-78.

Longley, Daniel B, D Paul Harkin, and Patrick G Johnston. 2003. '5-fluorouracil: mechanisms of action and clinical strategies', *Nature Reviews Cancer*, 3: 330.

Longo-Sorbello, Giuseppe SA, Guray Saydam, Debabrata Banerjee, and Joseph R Bertino. 2006. 'Cytotoxicity and cell growth assays.' in, *Cell Biology* (Elsevier).

Loreto, Carla, Giampiero La Rocca, Rita Anzalone, Rosario Caltabiano, Giuseppe Vespasiani, Sergio Castorina, David J Ralph, Selim Cellek, Giuseppe Musumeci, and Salvatore Giunta. 2014. 'The role of intrinsic pathway in apoptosis activation and progression in Peyronie's disease', *BioMed Research International*, 2014.

Lu, Yongke, and Arthur I Cederbaum. 2005. 'Cisplatin-induced hepatotoxicity is enhanced by elevated expression of cytochrome P450 2E1', *Toxicological Sciences*, 89: 515-23.

Lynch, Joseph W. 2009. 'Native glycine receptor subtypes and their physiological roles', *Neuropharmacology*, 56: 303-09.

Lyseng-Williamson, Katherine A, and Caroline Fenton. 2005. 'Docetaxel', *Drugs*, 65: 2513-31.

Macheret, Morgane, and Thanos D Halazonetis. 2015. 'DNA replication stress as a hallmark of cancer', *Annual Review of Pathology: Mechanisms of Disease*, 10: 425-48.

Malhotra, Gautam K., Xiangshan Zhao, Hamid Band, and Vimla Band. 2010. 'Histological, molecular and functional subtypes of breast cancers', *Cancer Biology & Therapy*, 10: 955-60.

Manna, Subrata, and Marina K. Holz. 2016a. 'Tamoxifen Action in ER-Negative Breast Cancer', *Signal Transduction Insights*, 5: STI.S29901.

Marchi, Saverio, Laura Lupini, Simone Patergnani, Alessandro Rimessi, Sonia Missiroli, Massimo Bonora, Angela Bononi, Fabio Corrà, Carlotta Giorgi, and Elena De Marchi. 2013.

'Downregulation of the mitochondrial calcium uniporter by cancer-related miR-25', *Current Biology*, 23: 58-63.

Martínez-Diez, Marta, Gema Santamaría, Alvaro D. Ortega, and José M. Cuezva. 2006. 'Biogenesis and dynamics of mitochondria during the cell cycle: significance of 3'UTRs', *PloS one*, 1: e107-e07.

Massaeli, Hamid, Jun Guo, Jianmin Xu, and Shetuan Zhang. 2010. 'Extracellular K+ is a prerequisite for the function and plasma membrane stability of HERG channels', Circulation research, 106: 1072.

Mastyugin, Vladimir, Elizabeth McWhinnie, Mark Labow, and Frank Buxton. 2004. 'A Quantitative High-Throughput Endothelial Cell Migration Assay', *Journal of Biomolecular Screening*, 9: 712-18.

McCormick, David A. 2014. 'Membrane potential and action potential.' in, From Molecules to Networks (Elsevier)

McGowan, John V, Robin Chung, Angshuman Maulik, Izabela Piotrowska, J Malcolm Walker, and Derek M Yellon. 2017. 'Anthracycline chemotherapy and cardiotoxicity', Cardiovascular Drugs and Therapy, 31: 63-75

Millar, Neil S, and Cecilia Gotti. 2009. 'Diversity of vertebrate nicotinic acetylcholine receptors', *Neuropharmacology*, 56: 237-46.

Mindell, Joe, and Merritt Maduke. 2001. 'ClC chloride channels', *Genome Biol*, 2: reviews3003.1.

Mini, E, SFAU Nobili, BFAU Caciagli, I Landini, and T Mazzei. 2006. 'Cellular pharmacology of gemcitabine', *Annals of Oncology*, 17: v7-v12.

Molinari, M. 2000. 'Cell cycle checkpoints and their inactivation in human cancer', *Cell Proliferation*, 33: 261-74.

Monteith, Gregory R, Felicity M Davis, and Sarah J Roberts-Thomson. 2012. 'Calcium channels and pumps in cancer: changes and consequences', Journal of Biological Chemistry, 287: 31666-73.

Moon, Dong-Oh, Mun-Ock Kim, Moon-Soo Heo, Jae-Dong Lee, Yung Hyun Choi, and Gi-Young Kim. 2009. 'Gefitinib induces apoptosis and decreases telomerase activity in MDA-MB-231 human breast cancer cells', *Archives of Pharmacal Research*, 32: 1351.

Moudgil, Rohit, and Edward T. H. Yeh. 2016. 'Mechanisms of Cardiotoxicity of Cancer Chemotherapeutic Agents: Cardiomyopathy and Beyond', *Canadian Journal of Cardiology*, 32: 863-70.e5.

Nahta, Rita, Gabriel N. Hortobágyi, and Francisco J. Esteva. 2003. 'Growth Factor Receptors in Breast Cancer: Potential for Therapeutic Intervention', *The Oncologist*, 8: 5-17.

Nakajima, T, N Kubota, T Tsutsumi, A Oguri, H Imuta, T Jo, H Oonuma, M Soma, K Meguro, and H Takano. 2009. 'Eicosapentaenoic acid inhibits voltage-gated sodium channels and invasiveness in prostate cancer cells', *British Journal of Pharmacology*, 156: 420-31.

Nakayama, Kei-ichi, and Keiko Nakayama. 1998. 'Cip/Kip cyclin-dependent kinase inhibitors: brakes of the cell cycle engine during development', *BioEssays*, 20: 1020-29.

Negrini, Simona, Vassilis G. Gorgoulis, and Thanos D. Halazonetis. 2010. 'Genomic instability — an evolving hallmark of cancer', *Nature reviews Molecular Cell Biology*, 11: 220.

Nekouzadeh, Ali, and Yoram Rudy. 2016. 'Conformational changes of an ion-channel during gating and emerging electrophysiologic properties: Application of a computational approach to cardiac Kv7.1', Progress in Biophysics and Molecular Biology, 120: 18-27.

Nelson, Michael H, and Christian R Dolder. 2006. 'Lapatinib: a novel dual tyrosine kinase inhibitor with activity in solid tumors', *Annals of Pharmacotherapy*, 40: 261-69.

Nelson, Michaela, Ming Yang, Adam A Dowle, Jerry R Thomas, and William J Brackenbury. 2015. 'The sodium channel-blocking antiepileptic drug phenytoin inhibits breast tumour growth and metastasis', *Molecular Cancer*, 14: 13.

NIH. 2018. 'Cardiotoxicity'. https://www.cancer.gov/search/results.

Nikolovska-Coleska, Zaneta, Liang Xu, Zengjian Hu, York Tomita, Peng Li, Peter P. Roller, Renxiao Wang, Xueliang Fang, Ribo Guo, Manchao Zhang, Marc E. Lippman, Dajun Yang, and Shaomeng Wang. 2004. 'Discovery of Embelin as a Cell-Permeable, Small-Molecular Weight Inhibitor of XIAP through Structure-Based Computational Screening of a Traditional Herbal Medicine Three-Dimensional Structure Database', *Journal of Medicinal Chemistry*, 47: 2430-40.

Nygren, Peter. 2001. 'What is cancer chemotherapy?', *Acta Oncologica*, 40: 166-74.

Octavia, Yanti, Carlo G Tocchetti, Kathleen L Gabrielson, Stefan Janssens, Harry J Crijns, and An L Moens. 2012. 'Doxorubicin-induced cardiomyopathy: from molecular mechanisms to therapeutic strategies', *Journal of Molecular and Cellular Cardiology*, 52: 1213-25.

Ohkubo, T., and J. Yamazaki. 2012. 'T-type voltage-activated calcium channel Cav3.1, but not Cav3.2, is involved in the inhibition of proliferation and apoptosis in MCF-7 human breast cancer cells', *Int J Oncol*, 41: 267-75.

Olsen, Richard W, and Werner Sieghart. 2008. 'International Union of Pharmacology. LXX. Subtypes of γ-aminobutyric acidA receptors: classification on the basis of subunit composition, pharmacology, and function. Update', *Pharmacological Reviews*.

Oltersdorf, Tilman, Steven W. Elmore, Alexander R. Shoemaker, Robert C. Armstrong, David J. Augeri, Barbara A. Belli, Milan Bruncko, Thomas L. Deckwerth, Jurgen Dinges, Philip J. Hajduk, Mary K. Joseph, Shinichi Kitada, Stanley J. Korsmeyer, Aaron R. Kunzer, Anthony Letai, Chi Li, Michael J. Mitten, David G. Nettesheim, ShiChung Ng, Paul M. Nimmer, Jacqueline M. O'Connor, Anatol Oleksijew, Andrew M. Petros, John C. Reed, Wang Shen, Stephen K. Tahir, Craig B. Thompson, Kevin J. Tomaselli, Baole Wang, Michael D. Wendt, Haichao Zhang, Stephen W. Fesik, and Saul H. Rosenberg. 2005. 'An inhibitor of Bcl-2 family proteins induces regression of solid tumours', *Nature*, 435: 677-81.

Orrenius, Sten, Boris Zhivotovsky, and Pierluigi Nicotera. 2003. 'Calcium: Regulation of cell death: the calcium–apoptosis link', *Nature reviews Molecular Cell Biology*, 4: 552.

Osborne, C. Kent. 1998. 'Tamoxifen in the Treatment of Breast Cancer', *New England Journal of Medicine*, 339: 1609-18.

Osborne, Cynthia, Paschal Wilson, and Debu Tripathy. 2004. 'Oncogenes and Tumor Suppressor Genes in Breast Cancer: Potential Diagnostic and Therapeutic Applications', *The Oncologist*, 9: 361-77.

Ouadid-Ahidouch, Halima, and Ahmed Ahidouch. 2013. 'K+ channels and cell cycle progression in tumor cells', *Frontiers in Physiology*, 4: 220.

Ouadid-Ahidouch, Halima, Morad Roudbaraki, Philippe Delcourt, Ahmed Ahidouch, Nathalie Joury, and Natalia Prevarskaya. 2004. 'Functional and molecular identification of intermediate-conductance Ca2+-activated K+ channels in breast cancer cells: association with cell cycle progression', *American Journal of Physiology-Cell Physiology*, 287: C125-C34.

Oved, Shlomo, and Yosef Yarden. 2002. 'Molecular ticket to enter cells', *Nature*, 416: 133-36.

Paakkari, Ilari. 2002. 'Cardiotoxicity of new antihistamines and cisapride', *Toxicology Letters*, 127: 279-84.

Panneerselvam, Perumal, Bilal Ahmad Rather, Dontireddy Ravi Sankar Reddy, and Natesh Ramesh Kumar. 2009. 'Synthesis and anti-microbial screening of some Schiff bases of 3-amino-6,8-dibromo-2-phenylquinazolin-4(3H)-ones', *European Journal of Medicinal Chemistry*, 44: 2328-33.

Panner, Amith, and Robert D Wurster. 2006. 'T-type calcium channels and tumor proliferation', *Cell Calcium*, 40: 253-59.

Papa, Michele, Francesca Boscia, Adriana Canitano, Pasqualina Castaldo, Stefania Sellitti, Lucio Annunziato, and Maurizio Taglialatela. 2003. 'Expression pattern of the ether-a-gogo-related (ERG) K+ channel-encoding genes ERG1, ERG2, and ERG3 in the adult rat central nervous system', *Journal of Comparative Neurology*, 466: 119-35.

Pardo, Luis A, and Walter Stühmer. 2014. 'The roles of K+ channels in cancer', *Nature Reviews Cancer*, 14: 39.

Pardo, Luis A. 2004. 'Voltage-Gated Potassium Channels in Cell Proliferation', *Physiology*, 19: 285-92.

Parise, Carol A, Katrina R Bauer, Monica M Brown, and Vincent Caggiano. 2009. 'Breast cancer subtypes as defined by the estrogen receptor (ER), progesterone receptor (PR), and the human epidermal growth factor receptor 2 (HER2) among women with invasive breast cancer in California, 1999–2004', *The Breast Journal*, 15: 593-602.

Park, Il Yeong, Eun Jung Kim, HaJeung Park, Kelly Fields, A Keith Dunker, and ChulHee Kang. 2005. 'Interaction between cardiac calsequestrin and drugs with known cardiotoxicity', *Molecular Pharmacology*, 67: 97-104.

Park, S. S., J. E. Kim, Y. A. Kim, Y. C. Kim, and S. W. Kim. 2005. 'Caveolin-1 is down-regulated and inversely correlated with HER2 and EGFR expression status in invasive ductal carcinoma of the breast', *Histopathology*, 47: 625-30.

Parrales, Alejandro, and Tomoo Iwakuma. 2015. 'Targeting Oncogenic Mutant p53 for Cancer Therapy', *Frontiers in Oncology*, 5.

Pedersen, Stine Falsig, and Christian Stock. 2013. 'Ion Channels and Transporters in Cancer: Pathophysiology, Regulation, and Clinical Potential', *Cancer Research*, 73: 1658.

Pérez-Herrero, Edgar, and Alberto Fernández-Medarde. 2015. 'Advanced targeted therapies in cancer: Drug nanocarriers, the future of chemotherapy', *European Journal of Pharmaceutics and Biopharmaceutics*, 93: 52-79.

Perez-Neut, Mathew, Lauren Haar, Vidhya Rao, Sreevidya Santha, Katherine Lansu, Basabi Rana, Walter K Jones, and Saverio Gentile. 2016. 'Activation of hERG3 channel stimulates autophagy and promotes cellular senescence in melanoma', *Oncotarget*, 7: 21991.

Perry, Matthew, Frank B Sachse, Jennifer Abbruzzese, and Michael C Sanguinetti. 2009. 'PD-118057 contacts the pore helix of hERG1 channels to attenuate inactivation and enhance K+ conductance', *Proceedings of the National Academy of Sciences*, 106: 20075-80.

Perry, Matthew, Michael Sanguinetti, and John Mitcheson. 2010. 'Revealing the structural basis of action of hERG potassium channel activators and blockers', *The Journal of Physiology*, 588: 3157-67.

Peter, M El, and PH Krammer. 2003. 'The CD95 (APO-1/Fas) DISC and beyond', *Cell Death and Differentiation*, 10: 26.

Pillozzi, S, MF Brizzi, M Balzi, O Crociani, A Cherubini, L Guasti, B Bartolozzi, A Becchetti, E Wanke, and PA Bernabei. 2002. 'HERG potassium channels are constitutively expressed in primary human acute myeloid leukemias and regulate cell proliferation of normal and leukemic hemopoietic progenitors', *Leukemia*, 16: 1791.

Pillozzi, Serena, Marika Masselli, Emanuele De Lorenzo, Benedetta Accordi, Emanuele Cilia, Olivia Crociani, Amedeo Amedei, Marinella Veltroni, Massimo D'Amico, and Giuseppe Basso. 2011. 'Chemotherapy resistance in acute lymphoblastic leukemia requires hERG1 channels and is overcome by hERG1 blockers', *Blood*, 117: 902-14.

Pinton, Paolo, Carlotta Giorgi, Roberta Siviero, Erika Zecchini, and Rosario Rizzuto. 2008. 'Calcium and apoptosis: ER-mitochondria Ca $^{2+}$ transfer in the control of apoptosis', *Oncogene*, 27: 6407.

Plenderleith, Ian H. 1990. 'Treating the treatment: toxicity of cancer chemotherapy', *Canadian Family Physician*, 36: 1827.

Podda, Maria Vittoria, Roberto Piacentini, Saviana Antonella Barbati, Alessia Mastrodonato, Daniela Puzzo, Marcello D'Ascenzo, Lucia Leone, and Claudio Grassi. 2013. 'Role of Cyclic Nucleotide-Gated Channels in the Modulation of Mouse Hippocampal Neurogenesis', *PLoS one*, 8: e73246.

Pommier, Yves, Elisabetta Leo, HongLiang Zhang, and Christophe Marchand. 2010. 'DNA topoisomerases and their poisoning by anticancer and antibacterial drugs', *Chemistry & Biology*, 17: 421-33.

Preußat, Katja, Christian Beetz, Michael Schrey, Robert Kraft, Stefan Wölfl, Rolf Kalff, and Stephan Patt. 2003. 'Expression of voltage-gated potassium channels Kv1. 3 and Kv1. 5 in human gliomas', *Neuroscience Letters*, 346: 33-36.

Prevarskaya, Natalia, Roman Skryma, and Yaroslav Shuba. 2018. 'Ion Channels in Cancer: Are Cancer Hallmarks Oncochannelopathies?', *Physiological Reviews*, 98: 559-621.

Promega. 2016. 'CellTox Green Cytotoxicity Assay Technical Manual '. http://au.promega.com/media/files/resources/protocols/technicalmanuals/101/celltoxgreencytotoxicityassayprotocol.pdf.

Rakha, Emad A., Jorge S. Reis-Filho, Frederick Baehner, David J. Dabbs, Thomas Decker, Vincenzo Eusebi, Stephen B. Fox, Shu Ichihara, Jocelyne Jacquemier, Sunil R. Lakhani, José Palacios, Andrea L. Richardson, Stuart J. Schnitt, Fernando C. Schmitt, Puay-Hoon Tan, Gary M. Tse, Sunil Badve, and Ian O. Ellis. 2010. 'Breast cancer prognostic classification in the molecular era: the role of histological grade', *Breast Cancer Research*, 12: 207.

Rampe, David, and Arthur M. Brown. 2013. 'A history of the role of the hERG channel in cardiac risk assessment', *Journal of Pharmacological and Toxicological Methods*, 68: 13-22.

Rampe, David, Michael K Murawsky, Jessica Grau, and Eric W Lewis. 1998. 'The antipsychotic agent sertindole is a high affinity antagonist of the human cardiac potassium channel HERG', *Journal of Pharmacology and Experimental Therapeutics*, 286: 788-93.

Rao, R. Vidhya, Mathew Perez-Neut, Simon Kaja, and Saverio Gentile. 2015. 'Voltage-Gated Ion Channels in Cancer Cell Proliferation', *Cancers*, 7.

Reed, Amy E. McCart, Jamie R. Kutasovic, Sunil R. Lakhani, and Peter T. Simpson. 2015. 'Invasive lobular carcinoma of the breast: morphology, biomarkers and 'omics', *Breast Cancer Research*, 17: 12.

Riedl, Stefan J, and Guy S Salvesen. 2007. 'The apoptosome: signalling platform of cell death', *Nature Reviews Molecular Cell Biology*, 8: 405.

Ring, Karen L, Leslie M Tong, Maureen E Balestra, Robyn Javier, Yaisa Andrews-Zwilling, Gang Li, David Walker, William R Zhang, Anatol C Kreitzer, and Yadong Huang. 2012. 'Direct Reprogramming of Mouse and Human Fibroblasts into Multipotent Neural Stem Cells with a Single Factor', *Cell Stem Cell*, 11: 100-09.

Rizzuto, Rosario, Diego De Stefani, Anna Raffaello, and Cristina Mammucari. 2012. 'Mitochondria as sensors and regulators of calcium signalling', *Nature reviews Molecular Cell Biology*, 13: 566.

Rock, Kenneth L., and Hajime Kono. 2008. 'The inflammatory response to cell death', *Annual Review of Pathology*, 3: 99-126.

Roger, Sébastien, Pierre Besson, and Jean-Yves Le Guennec. 2003. 'Involvement of a novel fast inward sodium current in the invasion capacity of a breast cancer cell line', *Biochimica et Biophysica Acta (BBA)-Biomembranes*, 1616: 107-11.

Roger, Sébastien, Marie Potier, Christophe Vandier, Pierre Besson, and Jean-Yves Le Guennec. 2006. 'Voltage-gated sodium channels: new targets in cancer therapy?', *Current pharmaceutical design*, 12: 3681-95.

Rostovtseva, Tatiana K, and Sergey M Bezrukov. 2008. 'VDAC regulation: role of cytosolic proteins and mitochondrial lipids', *Journal of Bioenergetics and Biomembranes*, 40: 163.

Roy, Jeremy, Brenna Vantol, Elizabeth A Cowley, Jonathan Blay, and Paul Linsdell. 2008. 'Pharmacological separation of hEAG and hERG K+ channel function in the human mammary carcinoma cell line MCF-7', *Oncology Reports*, 19: 1511-16.

Ruddon, Raymond W. 2007. *Cancer biology* (Oxford University Press).

Sachs, H. G., P. J. Stambrook, and J. D. Ebert. 1974. 'Changes in membrane potential during the cell cycle', *Exp Cell Res*, 83: 362-6.

Salvesen, Guy S, and Colin S Duckett. 2002. 'Apoptosis: IAP proteins: blocking the road to death's door', *Nature Reviews Molecular Cell Biology*, 3: 401.

Sanguinetti, Michael C., and Martin Tristani-Firouzi. 2006. 'hERG potassium channels and cardiac arrhythmia', *Nature*, 440: 463-69.

Santos, NAG, CS Catao, NM Martins, C Curti, MLP Bianchi, and AC Santos. 2007. 'Cisplatin-induced nephrotoxicity is associated with oxidative stress, redox state unbalance, impairment of energetic metabolism and apoptosis in rat kidney mitochondria', *Archives of Toxicology*, 81: 495-504.

Saravanan, Govindaraj, Perumal Pannerselvam, and Chinnasamy Rajaram Prakash. 2010. 'Synthesis and anti-microbial screening of novel schiff bases of 3-amino-2-methyl quinazolin 4-(3H)-one', *Journal of Advanced Pharmaceutical Technology & Research*, 1: 320.

Saurav, K, M Garima, S Pradeep, KK Jha, RL Khosa, and SK Gupta. 2011. 'Quinazoline-4-one: a highly important hetrocycle with diverse biological activities', *Der Chemica Sinica*, 2: 36-58.

Schäfer, Roland, Iris Wulfsen, Susanne Behrens, Frank Weinsberg, Christiane K Bauer, and Jürgen R Schwarz. 1999. 'The erg-like potassium current in rat lactotrophs', *The Journal of Physiology*, 518: 401-16.

Schmitt, Nicole, Morten Grunnet, and Søren-Peter Olesen. 2014. 'Cardiac potassium channel subtypes: new roles in repolarization and arrhythmia', *Physiological Reviews*, 94: 609-53.

Scripture, Charity D., Alex Sparreboom, and William D. Figg. 2005. 'Modulation of cytochrome P450 activity: implications for cancer therapy', *The Lancet Oncology*, 6: 780-89.

Selvam, Theivendren Panneer, and Palanirajan Vijayaraj Kumar. 2011. 'Quinazoline marketed drugs', *Research in Pharmacy*, 1.

Senkus, Elżbieta, and Jacek Jassem. 2011. 'Cardiovascular effects of systemic cancer treatment', *Cancer Treatment Reviews*, 37: 300-11.

Seyfried, Thomas N, and Laura M Shelton. 2010. 'Cancer as a metabolic disease', *Nutrition & Metabolism*, 7: 7.

Shao, Xiao-Dong, Kai-Chun Wu, Xiao-Zhong Guo, Man-Jiang Xie, Jing Zhang, and Dai-Ming Fan. 2008. 'Expression and significance of HERG protein in gastric cancer', *Cancer Biology & Therapy*, 7: 45-50.

Shao, Xiao-Dong, Kaichun Wu, Zhi-Ming Hao, Liu Hong, Jiang Zhang, and Daiming Fan. 2005. 'The potent inhibitory effects of cisapride, a specific blocker for human ether-a-go-go-related gene (HERG) channel, on gastric cancer cells', *Cancer Biology & Therapy*, 4: 295-301.

Sharma, Ankush, Roozbeh Houshyar, Priya Bhosale, Joon-Il Choi, Rajesh Gulati, and Chandana Lall. 2014. 'Chemotherapy induced liver abnormalities: an imaging perspective', *Clinical and Molecular Hepatology*, 20: 317-26.

Shi, Bianhua, Jiayu Bao, Yongbin Liu, and Juan Shi. 2018. 'Death receptor 6 promotes ovarian cancer cell migration through KIF 11', *FEBS open bio*, 8: 1497-507.

Shi, Wenmei, Randy S Wymore, Hong-Sheng Wang, Zongming Pan, Ira S Cohen, David McKinnon, and Jane E Dixon. 1997. 'Identification of Two Nervous System-Specific Members of theerg Potassium Channel Gene Family', *Journal of Neuroscience*, 17: 9423-32.

Shi, Y., M. Moon, S. Dawood, B. McManus, and P. P. Liu. 2011. 'Mechanisms and management of doxorubicin cardiotoxicity', *Herz*, 36: 296-305.

Shih, Ted, and Celeste Lindley. 2006. 'Bevacizumab: an angiogenesis inhibitor for the treatment of solid malignancies', *Clinical Therapeutics*, 28: 1779-802.

Shin, Sejeong, Byung-Je Sung, Yong-Soon Cho, Hyun-Ju Kim, Nam-Chul Ha, Jong-Ik Hwang, Chul-Woong Chung, Yong-Keun Jung, and Byung-Ha Oh. 2001. 'An anti-apoptotic protein human survivin is a direct inhibitor of caspase-3 and-7', *Biochemistry*, 40: 1117-23.

Shou, Jiang, Suleiman Massarweh, C Kent Osborne, Alan E Wakeling, Simale Ali, Heidi Weiss, and Rachel Schiff. 2004. 'Mechanisms of tamoxifen resistance: increased estrogen receptor-HER2/neu cross-talk in ER/HER2–positive breast cancer', *Journal of the National Cancer Institute*, 96: 926-35.

Slamon, D. J., G. M. Clark, S. G. Wong, W. J. Levin, A. Ullrich, and W. L. McGuire. 1987. 'Human breast cancer: correlation of relapse and survival with amplification of the HER-2/neu oncogene', *Science*, 235: 177.

Smith, Garth A. M., Hing-Wo Tsui, Evan W. Newell, Xinpo Jiang, Xiao-Ping Zhu, Florence W. L. Tsui, and Lyanne C. Schlichter. 2002. 'Functional Up-regulation of HERG K+ Channels in Neoplastic Hematopoietic Cells', *Journal of Biological Chemistry*, 277: 18528-34.

Snyders, Dirk J. 1999. 'Structure and function of cardiac potassium channels', *Cardiovascular Research*, 42: 377-90.

Staudacher, Ingo, Julian Jehle, Kathrin Staudacher, Hans-Werner Pledl, Dieter Lemke, Patrick A Schweizer, Rüdiger Becker, Hugo A Katus, and Dierk Thomas. 2014. 'HERG K+ channel-dependent apoptosis and cell cycle arrest in human glioblastoma cells', *PloS one*, 9: e88164.

Subik, Kristina, Jin-Feng Lee, Laurie Baxter, Tamera Strzepek, Dawn Costello, Patti Crowley, Lianping Xing, Mien-Chie Hung, Thomas Bonfiglio, David G. Hicks, and Ping Tang. 2010. 'The Expression Patterns of ER, PR, HER2, CK5/6, EGFR, Ki-67 and AR by Immunohistochemical Analysis in Breast Cancer Cell Lines', *Breast Cancer: Basic and Clinical Research*, 4: 117822341000400004.

Sundelacruz, Sarah, Michael Levin, and David L Kaplan. 2013. 'Depolarization alters phenotype, maintains plasticity of predifferentiated mesenchymal stem cells', *Tissue Engineering Part A*, 19: 1889-908.

Surprenant, Annmarie, and R Alan North. 2009. 'Signaling at purinergic P2X receptors', *Annual Review of Physiology*, 71: 333-59.

Suzuki, Yoshihiro, Toshio Inoue, Mayumi Murai, Miki Suzuki-Karasaki, Toyoko Ochiai, and Chisei Ra. 2012. 'Depolarization potentiates TRAIL-induced apoptosis in human melanoma cells: role for ATP-sensitive K+ channels and endoplasmic reticulum stress', *Int J Oncol*, 41: 465-75.

Szabadkai, György, Katiuscia Bianchi, Péter Várnai, Diego De Stefani, Mariusz R Wieckowski, Dario Cavagna, Anikó I Nagy, Tamás Balla, and Rosario Rizzuto. 2006. 'Chaperone-mediated coupling of endoplasmic reticulum and mitochondrial Ca2+ channels', *J Cell Biol*, 175: 901-11.

Szabò, Ildikò, Jurgen Bock, Andreas Jekle, Matthias Soddemann, Constantin Adams, Florian Lang, Mario Zoratti, and Erich Gulbins. 2005. 'A novel potassium channel in lymphocyte mitochondria', *Journal of Biological Chemistry*, 280: 12790-98.

Tait, Stephen WG, and Douglas R Green. 2010. 'Mitochondria and cell death: outer membrane permeabilization and beyond', *Nature Reviews Molecular Cell Biology*, 11: 621.

Tajeddine, Nicolas, L Galluzzi, O Kepp, E Hangen, E Morselli, L Senovilla, N Araujo, G Pinna, N Larochette, and N Zamzami. 2008. 'Hierarchical involvement of Bak, VDAC1 and Bax in cisplatin-induced cell death', *Oncogene*, 27: 4221.

Takemura, Genzou, and Hisayoshi Fujiwara. 2007. 'Doxorubicin-Induced Cardiomyopathy: From the Cardiotoxic Mechanisms to Management', *Progress in Cardiovascular Diseases*, 49: 330-52.

Tamargo, Juan, Ricardo Caballero, and Eva Delpón. 2015. 'Cancer chemotherapy and cardiac arrhythmias: a review', *Drug Safety*, 38: 129-52.

Tamargo, Juan, Ricardo Caballero, Ricardo Gómez, Carmen Valenzuela, and Eva Delpón. 2004. 'Pharmacology of cardiac potassium channels', *Cardiovascular Research*, 62: 9-33.

Tan, Wenzhi, and Marco Colombini. 2007. 'VDAC closure increases calcium ion flux', *Biochimica et Biophysica Acta (BBA)-Biomembranes*, 1768: 2510-15.

Tanaka, E. 1998. 'Clinically important pharmacokinetic drug–drug interactions: role of cytochrome P450 enzymes', *Journal of clinical Pharmacy and Therapeutics*, 23: 403-16.

Than, BLN, JACM Goos, Aaron L Sarver, MG O'sullivan, A Rod, TK Starr, RJA Fijneman, GA Meijer, L Zhao, and Y Zhang. 2014. 'The role of KCNQ1 in mouse and human gastrointestinal cancers', *Oncogene*, 33: 3861.

Thomas, Dierk, Ramona Bloehs, Ronald Koschny, Eckhard Ficker, Jaromir Sykora, Johann Kiehn, Kathrin Schlömer, Jakob Gierten, Sven Kathöfer, and Edgar Zitron. 2008. 'Doxazosin induces apoptosis of cells expressing hERG K+ channels', *European Journal of Pharmacology*, 579: 98-103.

Thomas, Dierk, Bernd Gut, Syrus Karsai, Anna-Britt Wimmer, Kezhong Wu, Gunnar Wendt-Nordahl, Wei Zhang, Sven Kathöfer, Wolfgang Schoels, and Hugo A Katus. 2003. 'Inhibition of cloned HERG potassium channels by the antiestrogen tamoxifen', *Naunyn-Schmiedeberg's Archives of Pharmacology*, 368: 41-48.

Thomas, Sonia Amin. 2017. 'Chemotherapy Agents That Cause Cardiotoxicity', *US Pharmacist*, 42: HS24.

Thompson, A. M., and S. L. Moulder-Thompson. 2012. 'Neoadjuvant treatment of breast cancer', *Annals of Oncology*, 23: x231-x36.

Thor, Ann D., Dan H. Moore, II, Susan M. Edgerton, Ernest S. Kawasaki, Ellen Reihsaus, Henry T. Lynch, Joseph N. Marcus, Laurent Schwartz, Ling-Chun Chen, Brian H. Mayall, and Helene S. Smith. 1992. 'Accumulation of p53 Tumor Suppressor Gene Protein: An Independent Marker of Prognosis in Breast Cancers', *JNCI: Journal of the National Cancer Institute*, 84: 845-55.

Traynelis, Stephen F, Lonnie P Wollmuth, Chris J McBain, Frank S Menniti, Katie M Vance, Kevin K Ogden, Kasper B Hansen, Hongjie Yuan, Scott J Myers, and Ray Dingledine. 2010. 'Glutamate receptor ion channels: structure, regulation, and function', *Pharmacological Reviews*, 62: 405-96.

Tromp, J, LC Steggink, DJ Van Veldhuisen, JA Gietema, and P Van der Meer. 2017. 'Cardio-oncology: progress in diagnosis and treatment of cardiac dysfunction', *Clinical Pharmacology & Therapeutics*, 101: 481-90.

Uriu-Adams, Janet Y., and Carl L. Keen. 2010. 'Zinc and reproduction: effects of zinc deficiency on prenatal and early postnatal development', *Birth Defects Research Part B: Developmental and Reproductive Toxicology*, 89: 313-25.

Urrego, Diana, Adam P Tomczak, Farrah Zahed, Walter Stühmer, and Luis A Pardo. 2014. 'Potassium channels in cell cycle and cell proliferation', *Philosophical Transactions of the Royal Society B: Biological Sciences*, 369: 20130094.

Vaglini, Francesca, Cristina Viaggi, Valentina Piro, Carla Pardini, Claudio Gerace, Marco Scarselli, and Giovanni Umberto Corsini. 2013. 'Acetaldehyde and parkinsonism: role of CYP450 2E1', *Frontiers in Behavioral Neuroscience*, 7: 71.

van de Graaf, Stan FJ, Joost GJ Hoenderop, and René JM Bindels. 2006. 'Regulation of TRPV5 and TRPV6 by associated proteins', American Journal of Physiology-Renal Physiology, 290: F1295-F302.

van Kerrebroeck, M. J. A., A. van Ginneken, I. de Grijs, N. A. M. Mutsaers, T. Opthof, H. J. Jongsma, and M. A. G. van der Heyden. 2003. 'Expression of the Electrophysiological System During Murine Embryonic Stem Cell Cardiac Differentiation', *Cellular Physiology and Biochemistry*, 13: 263-70.

van Vliet, Patrick, Teun P. de Boer, Marcel A. G. van der Heyden, Mazen K. El Tamer, Joost P. G. Sluijter, Pieter A. Doevendans, and Marie-José Goumans. 2010. 'Hyperpolarization Induces Differentiation in Human Cardiomyocyte Progenitor Cells', *Stem Cell Reviews and Reports*, 6: 178-85.

Vandenberg, Jamie I, Matthew D Perry, Mark J Perrin, Stefan A Mann, Ying Ke, and Adam P Hill. 2012. 'hERG K+ channels: structure, function, and clinical significance', *Physiological reviews*, 92: 1393-478.

Vander Heiden, Matthew G, Navdeep S Chandel, Xiao Xian Li, Paul T Schumacker, Marco Colombini, and Craig B Thompson. 2000. 'Outer mitochondrial membrane permeability can regulate coupled respiration and cell survival', *Proceedings of the National Academy of Sciences*, 97: 4666-71.

Verhaeghe, Pierre, Nadine Azas, Monique Gasquet, Sébastien Hutter, Christophe Ducros, Michèle Laget, Sylvain Rault, Pascal Rathelot, and Patrice Vanelle. 2008. 'Synthesis and antiplasmodial activity of new 4-aryl-2-trichloromethylquinazolines', *Bioorganic & Medicinal Chemistry Letters*, 18: 396-401.

Vermeulen, Katrien, Zwi N Berneman, and Dirk R Van Bockstaele. 2003. 'Cell cycle and apoptosis', *Cell Proliferation*, 36: 165-75.

Vermeulen, Katrien, Dirk R. Van Bockstaele, and Zwi N. Berneman. 2003. 'The cell cycle: a review of regulation, deregulation and therapeutic targets in cancer', *Cell Proliferation*, 36: 131-49.

Vichai, Vanicha, and Kanyawim Kirtikara. 2006. 'Sulforhodamine B colorimetric assay for cytotoxicity screening', *Nature Protocols*, 1: 1112.

Viola, Helena M., Abbie M. Adams, Stefan M. K. Davies, Susan Fletcher, Aleksandra Filipovska, and Livia C. Hool. 2014. 'Impaired functional communication between the L-type calcium channel and mitochondria contributes to metabolic inhibition in the *mdx* heart', *Proceedings of the National Academy of Sciences*, 111: E2905.

Vogelstein, Bert, and Kenneth W Kinzler. 1993. 'The multistep nature of cancer', *Trends in Genetics*, 9: 138-41.

Vyas, Sejal, Elma Zaganjor, and Marcia C. Haigis. 2016. 'Mitochondria and Cancer', *Cell*, 166: 555-66.

Wallach, David, Tae-Bong Kang, Christopher P Dillon, and Douglas R Green. 2016. 'Programmed necrosis in inflammation: Toward identification of the effector molecules', *Science*, 352: aaf2154.

Walstab, Jutta, Gudrun Rappold, and Beate Niesler. 2010. '5-HT3 receptors: role in disease and target of drugs', *Pharmacology & Therapeutics*, 128: 146-69.

Walweel, K, and DR Laver. 2015. 'Mechanisms of SR calcium release in healthy and failing human hearts', *Biophysical Reviews*, 7: 33-41.

Wang, Huizhen, Yiqiang Zhang, Liwen Cao, Hong Han, Jingxiong Wang, Baofeng Yang, Stanley Nattel, and Zhiguo Wang. 2002. 'HERG K+ channel, a regulator of tumor cell apoptosis and proliferation', *Cancer Research*, 62: 4843-48.

Wang, Jia-Lun, Dongxiang Liu, Zhi-Jia Zhang, Simei Shan, Xiaobing Han, Srinivasa M Srinivasula, Carlo M Croce, Emad S Alnemri, and Ziwei Huang. 2000. 'Structure-based discovery of an organic compound that binds Bcl-2 protein and induces apoptosis of tumor cells', *Proceedings of the National Academy of Sciences*, 97: 7124-29.

Wang, Xiao-Feng, Sheng-Biao Wang, Emika Ohkoshi, Li-Ting Wang, Ernest Hamel, Keduo Qian, Susan L Morris-Natschke, Kuo-Hsiung Lee, and Lan Xie. 2013. 'N-Aryl-6-methoxy-1, 2, 3, 4-tetrahydroquinolines: A novel class of antitumor agents targeting the colchicine site on tubulin', *European journal of Medicinal Chemistry*, 67: 196-207.

Weigelt, Britta, Felipe C Geyer, and Jorge S Reis-Filho. 2010. 'Histological types of breast cancer: how special are they?', *Molecular Oncology*, 4: 192-208.

Weigelt, Britta, and Jorge S Reis-Filho. 2009. 'Histological and molecular types of breast cancer: is there a unifying taxonomy?', *Nature Reviews Clinical Oncology*, 6: 718.

Weinberg, Robert A. 1996. 'How cancer arises', *Scientific American*, 275: 62-70.

Weinzierl, Elizabeth P., and Daniel A. Arber. 2013. 'The Differential Diagnosis and Bone Marrow Evaluation of New-Onset Pancytopenia', *American Journal of Clinical Pathology*, 139: 9-29.

Welfare, Australian Institute of Health an. 2018. 'Cancer compendium: information and trends by cancer type'. https://www.aihw.gov.au/reports/cancer/cancer-compendium-information-trends-by-cancer/report-contents/breast-cancer.

Welsh, JoEllen. 2013.'Chapter 40 - Animal Models for Studying Prevention and Treatment of Breast Cancer.' in P. Michael Conn (ed.), *Animal Models for the Study of Human Disease* (Academic Press: Boston).

Williams, Sarah, Andrew Bateman, and Ita O'Kelly. 2013. 'Altered Expression of Two-Pore Domain Potassium (K2P) Channels in Cancer', *PloS one*, 8: e74589.

Wilson, Nicholas S, Vishva Dixit, and Avi Ashkenazi. 2009. 'Death receptor signal transducers: nodes of coordination in immune signaling networks', *Nature Immunology*, 10: 348.

Witton, Caroline J., Jonathan R. Reeves, James J. Going, Timothy G. Cooke, and John M. S. Bartlett. 2003. 'Expression of the HER1–4 family of receptor tyrosine kinases in breast cancer', *The Journal of Pathology*, 200: 290-97.

Wonderlin, William F., Karen A. Woodfork, and Jeannine S. Strobl. 1995. 'Changes in membrane potential during the progression of MCF-7 human mammary tumor cells through the cell cycle', *Journal of Cellular Physiology*, 165: 177-85.

Wong E., Chaudhry S. and Rossi M. 2018. 'Breast Cancer'.

Wong, Rebecca S. Y. 2011. 'Apoptosis in cancer: from pathogenesis to treatment', *Journal of Experimental & Clinical Cancer Research*, 30: 87.

Wu, Xiaoqing, Mingdong Li, Yang Qu, Wenhua Tang, Youguang Zheng, Jiqin Lian, Min Ji, and Liang Xu. 2010. 'Design and synthesis of novel Gefitinib analogues with improved anti-tumor activity', *Bioorganic & Medicinal Chemistry*, 18: 3812-22.

Wu, Xinyu, Daixing Zhong, Bin Lin, Wenliang Zhai, Zhenqi Ding, and Jin Wu. 2013. 'p38 MAPK regulates the expression of ether a go-go potassium channel in human osteosarcoma cells', *Radiology and Oncology*, 47: 42-49.

Wulff, Heike, Neil A. Castle, and Luis A. Pardo. 2009. 'Voltage-gated potassium channels as therapeutic targets', *Nature Reviews Drug Discovery*, 8: 982.

Xu, Bin, Jianwen Mao, Liwei Wang, Linyan Zhu, Hongzhi Li, Weizhang Wang, Xiaobao Jin, Jiayong Zhu, and Lixin Chen. 2010. 'ClC-3 chloride channels are essential for cell proliferation and cell cycle progression in nasopharyngeal carcinoma cells', *Acta Biochim Biophys Sin*, 42: 370-80.

Xu, Xulin, Maurizio Recanatini, Marinella Roberti, and Gea-Ny Tseng. 2008. 'Probing the binding sites and mechanisms of action of two hERG channel activators, NS1643 and PD307243', *Molecular Pharmacology*.

Yang, Li-Heng, Hsin-Shun Tseng, Che Lin, Li-Sheng Chen, Shou-Tung Chen, Shou-Jen Kuo, and Dar-Ren Chen. 2012. 'Survival benefit of tamoxifen in estrogen receptor-negative and progesterone receptor-positive low grade breast cancer patients', *Journal of Breast Cancer*, 15: 288-95.

Yang, Ming, and William Brackenbury. 2013a. 'Membrane potential and cancer progression', *Frontiers in Physiology*, 4.

Yang, Ming, and William J Brackenbury. 2013b. 'Membrane potential and cancer progression', *Frontiers in Physiology*, 4: 185.

Yang, Mu, Amanda J. Pickard, Xin Qiao, Matthew J. Gueble, Cynthia S. Day, Gregory L. Kucera, and Ulrich Bierbach. 2015. 'Synthesis, Reactivity, and Biological Activity of Gold(I) Complexes Modified with Thiourea-Functionalized Tyrosine Kinase Inhibitors', *Inorganic Chemistry*, 54: 3316-24.

Yeh, Edward T.H., and Courtney L. Bickford. 2009. 'Cardiovascular Complications of Cancer Therapy', *Incidence, Pathogenesis, Diagnosis, and Management*, 53: 2231-47.

Yevenes, Gonzalo E, and Hanns Ulrich Zeilhofer. 2011. 'Allosteric modulation of glycine receptors', *British Journal of Pharmacology*, 164: 224-36.

Yoon, Ji-Seon, Mira Choi, Chang Yup Shin, Seung Hwan Paik, Kyu Han Kim, and Ohsang Kwon. 2016. 'Development of a Model for Chemotherapy-Induced Alopecia: Profiling of Histological Changes in Human Hair Follicles after Chemotherapy', *Journal of Investigative Dermatology*, 136: 584-92.

Youle, Richard J, and Andreas Strasser. 2008. 'The BCL-2 protein family: opposing activities that mediate cell death', *Nature Reviews Molecular Cell Biology*, 9: 47.

Yu, F. H., and W. A. Catterall. 2003. 'Overview of the voltage-gated sodium channel family', *Genome Biol*, 4: 207.

Zahedifard, Maryam, Fadhil Lafta Faraj, Mohammadjavad Paydar, Chung Yeng Looi, Maryam Hajrezaei, Mohadeseh Hasanpourghadi, Behnam Kamalidehghan, Nazia Abdul Majid, Hapipah Mohd Ali, and Mahmood Ameen Abdulla. 2015. 'Synthesis, characterization and apoptotic activity of quinazolinone Schiff base derivatives toward MCF-7 cells via intrinsic and extrinsic apoptosis pathways', *Scientific Reports*, 5: 11544.

Zhang, Han-Zhong, Shailaja Kasibhatla, Yan Wang, John Herich, John Guastella, Ben Tseng, John Drewe, and Sui Xiong Cai. 2004. 'Discovery, characterization and SAR of gambogic acid as a potent apoptosis inducer by a HTS assay', *Bioorganic & Medicinal Chemistry*, 12: 309-17.

Zhang, Mei, Jie Liu, and Gea-Ny Tseng. 2004. 'Gating Charges in the Activation and Inactivation Processes of the hERG Channel', *The Journal of General Physiology*, 124: 703.

Zhao, Jie, Xiao-Li Wei, Yong-Sheng Jia, and Jian-Quan Zheng. 2008. 'Silencing of herg gene by shRNA inhibits SH-SY5Y cell growth in vitro and in vivo', *European Journal of Pharmacology*, 579: 50-57.

Zheng, Fang, Huiyu Li, Wen Du, and Shiang Huang. 2011. 'Role of hERG1 K+ channels in leukemia cells as a positive regulator in SDF-1a-induced proliferation', *Hematology*, 16: 177-84.

Zhou, Jun, Corinne E Augelli-Szafran, Jenifer A Bradley, Xian Chen, Bryan J Koci, Walter A Volberg, Zhuoqian Sun, and Jason S Cordes. 2005. 'Novel potent human ether-a-go-go-related gene (hERG) potassium channel enhancers and their in vitro antiarrhythmic activity', *Molecular Pharmacology*, 68: 876-84.

Zhou, Ping-zheng, Joseph Babcock, Lian-qing Liu, Min Li, and Zhao-bing Gao. 2011. 'Activation of human ether-a-go-go related gene (hERG) potassium channels by small molecules', *Acta Pharmacol Sin*, 32: 781-88.

Zou, Zhiqiang, Chunling Gao, Akhilesh K. Nagaich, Theresa Connell, Shin'ichi Saito, Judd W. Moul, Prem Seth, Ettore Appella, and Shiv Srivastava. 2000. 'p53 Regulates the Expression of the Tumor Suppressor Gene Maspin', *Journal of Biological Chemistry*, 275: 6051-54.

Zukor, K. A., Kent, D. T. and Odelberg, S. J. (2010), Fluorescent whole-mount method for visualizing three-dimensional relationships in intact and regenerating adult newt spinal cords. Dev. Dyn., 239: 3048-3057.

Zurawa-Janicka, Dorota, Joanna Skorko-Glonek, and Barbara Lipinska. 2010. 'HtrA proteins as targets in therapy of cancer and other diseases', *Expert Opinion on Therapeutic Targets*, 14: 665-79.